

COMPONENT INTERACTIONS OF THE PRIME NUMBERS

by

Ernest G. Hibbs

A Dissertation Presented in Partial Fulfillment

of the Requirements for the Degree

Doctor of Technology

CAPITOL TECHNOLOGY UNIVERSITY

January 2022

© 2022 by Ernest G. Hibbs
ALL RIGHTS RESERVED

COMPONENT INTERACTIONS OF THE PRIME NUMBERS

Approved:

Ian R. McAndrew, Ph.D. FRAeS, Chair

Allen H. Exner, BSEET, Committee Member (Ex officio)

Richard E. Baker, Ph.D. FRAeS, Committee Member (External)

Accepted and Signed:

Ian McAndrew

Ian R. McAndrew

11 February, 2022

Date

Allen H. Exner

Allen H. Exner

February 11, 2022

Date

Richard E. Baker

Richard E. Baker

February 11, 2022

Date

Ian McAndrew

Dr Ian R. McAndrew
Dean of Doctoral Programs
Capitol Technology University

11 February, 2022

Date

ABSTRACT

This research used the standard system modeling techniques of normal vectors, Doppler vectors, trigonometric relationships, and growth ratios to evaluate the systemic interactions and component related derivatives of the prime number increments in their own coordinate system.

A prime number growth model was developed by using each $6n\pm 1$ transition as a cardinal heading. The multiples of 6 that occur on the axis headings and in the quadrants between each axis were treated as one $6z$ system with an assumed harmonic influence over the structure. Vectors were created from the $6z$ rate of growth in each quadrant and on each axis intersection. System relationships between those vectors were examined in two models, a magnitude model that revealed integrated modes with the raw values and an inverse squared model that captured directional forces as with a horizontally expanding wave property.

The results revealed the integrated harmonic balancing of growth and field effects that aligned with system properties of vibration, electromagnetics, force, gravity, and quantum-like angular velocity and acceleration. The recommendations were to apply the intrinsic dynamically balancing properties of this prime number structure as a framework for controlling systems through the displacement or absorption of energy and force. The framework also reveals possible research in multiple areas. Suggested contributions of this framework were also directed to rethinking some foundational approaches to the Millennium Prize Problems.

Keywords: Harmonic, Electromagnetic and Doppler.

DEDICATION

To my wife, Meridith, for her encouragement, faith, and vision.

ACKNOWLEDGMENT

This accomplishment could not have been possible without my family's support and encouragement through all the weekends of study and listening to my wild ramblings of abstract models of prime number growth in their own dimension. Through all the advanced arm-waving sessions describing the system's dynamic and self-balancing interactions, their patience and intense belief made the difference in what felt like an uphill struggle introducing an entirely new approach.

This type of research would also not be possible without the educational vision of Capitol Technology University, which endorsed a practical system engineering approach to describe problems that many deemed strictly theoretical and far-reaching. The hours of mentoring, guidance, and discussions provided by my advisor, Dr. Ian McAndrew, were essential in integrating the characteristics between the system models.

Acknowledgement and thanks are probably overdue to some people who have taken of their own personal time to provide a solid academic starting point for others in the field of prime numbers. One specific effort to provide prime number data with academic integrity has benefitted many in this area of research. Many thanks to Dr. Chris Caldwell in the University of Tennessee for his tireless and exacting work in establishing validated prime number sets for the purpose of research and education.

Looking back, I also see the close friends and role models who have humbly demonstrated that making a significant difference means looking for the needs not being met, and that the meaning of success "is not about me".

TABLE OF CONTENTS

LIST OF TABLES	VII
LIST OF FIGURES	VIII
CHAPTER 1: INTRODUCTION	1
Background of Study	3
Problem Statement.....	6
Purpose of Dissertation Study.....	7
Significance of the Study	8
Nature of Study	9
Hypotheses/Research Questions	11
Conceptual or Theoretical Framework	13
Definitions.....	18
Assumptions.....	19
Scope, Limitations, and Delimitations.....	21
Chapter Summary	22
CHAPTER 2: LITERATURE REVIEW	23
Chapter Conclusion.....	43
Chapter Summary	44
CHAPTER 3: METHOD	45
Research Method and Design Appropriateness	45
Population, Sampling, and Data Collection Procedures and Rationale	47
Validity: Internal and External.....	48
Data Analysis	49

Organization and Clarity	51
Chapter Summary	51
CHAPTER 4: RESULTS	53
Pilot Study.....	53
Findings.....	95
Summary	97
CHAPTER 5: FINDINGS AND RECOMMENDATIONS	99
Limitations	99
Findings and Interpretations	101
Study Taxonomy	107
Recommendations.....	109
Recommendations for Future Research.....	110
Chapter Summary	121
REFERENCES	122
APPENDIX A: ANALYSIS GRAPHS	142
APPENDIX B: EQUILIBRIUM AND VIBRATION GRAPHS	178

LIST OF TABLES

Table 1 Research design for comparison of component interactions	9
Table 2 Summary of references by date and principal areas	26
Table 3 Summary of comprehensive validation references.....	27
Table 4 Examples of prime number types by group	33
Table 5 What reference literature was found for similar systems	42
Table 6 Sample of capturing data points and activity compass	59
Table 7 Post zeta(2) area values by quadrant.....	79
Table 8 Original 90-degree vector products	88
Table 9 Concepts and Common Formal Equations	102
Table 10 Findings from Magnitude Analysis	103
Table 11 Findings from Post-Zeta Analysis	104
Table 12 Translating findings to known systems	109
Table 13 Possible contributions to Millennium Prize Problem efforts.....	111

LIST OF FIGURES

Figure 1 Harmonic 6z influence on 2-4 threads.....	3
Figure 2 Defining a component-driven coordinate system for harmonic behavior	6
Figure 3 The harmonic field effect of the 90-degree component vectors.....	8
Figure 4 Creating quadrant dimensions from components	14
Figure 5 Normal and Doppler vectors for first 200 coils.....	15
Figure 6 Comparing the vertical and horizontal physical models	16
Figure 7 System of literature questions and expected results	23
Figure 8 Resonant frequency destroying Tacoma Narrows Bridge.....	29
Figure 9 Activities being done with prime numbers.....	30
Figure 10 When model reference literature for similar systems is gathered	40
Figure 11 How model reference literature for similar systems is gathered	41
Figure 12 Allocating multiples of 6z into the coordinate system	46
Figure 13 Quadrant data to build vectors.....	47
Figure 14 Validating and entering data.....	48
Figure 15 Plans for analysis with magnitude models.	49
Figure 16 Plans for analysis with inverse-squared models.....	50
Figure 17 Magnitude models and their contribution.....	55
Figure 18 Distribution package versus component magnitude growth	56
Figure 19 Systematic logarithmic magnitude 6z growth	58
Figure 20 Sample of color-coded 90-vector activity compass.....	60
Figure 21 Sample of event analysis performed with vector graphs, activity compasses..	61
Figure 22 Grouping of all diagrams for event trace.....	62

Figure 23 Even trace of all vector properties.....	63
Figure 24 Sample of sine and cosine events marked	65
Figure 25 Sine partials reveal two systems.....	66
Figure 26 Upper and lower plane 90-degree field vectors.....	68
Figure 27 Lower Q2 and Q4 comparison	69
Figure 28 Lower to upper tensor products.....	71
Figure 29 Upper and lower plane Doppler vectors	73
Figure 30 Process used to find an exact solution.....	75
Figure 31 Adjustments and accuracy of estimated function.....	76
Figure 32 Resulting translation of growth rate into Euler form.....	77
Figure 33 Updated magnitude growth model	78
Figure 34 Resulting magnitude vector model.....	81
Figure 35 Quadrant balancing and off-center gravity.....	82
Figure 36 Post-zeta sines and cosines.....	83
Figure 37 Post-zeta field vector sums.....	85
Figure 38 Applying angular velocity to previous vector products	87
Figure 39 Post-zeta Doppler relationships.....	89
Figure 40 Balancing growth and centers of gravity.....	91
Figure 41 Tornado-like gravity balancing behavior	92
Figure 42 Centers of gravity balancing in magnitude growth model	93
Figure 43 Adjusting the earth-tilt of the conical growth model.....	94
Figure 44 Storyboard summary of findings	97
Figure 45 Taxonomy of progressive data analysis	108

CHAPTER 1: INTRODUCTION

Prime numbers have been characterized as a complicated self-referential system with the potential to unleash hidden information about core relationships in natural and harmonic systems (Hibbs, 2008). Yet, mathematical studies continue to use external measurement approaches, such as the number line, to understand this supposedly self-referential system. The goal of this research is to discover internally focused vector and system relationships that will reveal potential designs for optimizing and advancing technology. This study will examine the component interactions of the prime numbers with a quadrant-based self-referential system. Previous studies have revealed a consistent harmonic and electromagnetic pattern influence of the multiples of 6 over a physical double-thread structure (Hibbs, 2010).

Components from that harmonic influence and structure will be used to define a self-referential coordinate system. Activities between the quadrant components will be used to define system relationships and models. Those relationships and models will be compared to physical system behaviors and correlated to technical systems. From initial studies with limited data, the expectation is that the relationships will reveal properties of harmonic convergence and of dynamical self-balancing systems. Current challenges from the Clay Mathematical Institute Millennium Prize Problems will also be used for comparing the potential contribution and applicability of the prime number component behavior (Bombieri, 2000; Fefferman, 2000; Wiles, 2000; Deligne, 2000; Jaffe & Witten, 2000).

This introductory chapter will provide a background of the paradigm shift that will be necessary to understand the prime numbers in a different structure, based strictly on their double-threaded growth pattern. A problem statement covers the task to consider the prime number components as representing different dimensions, with goal of producing system models for

practical engineering designs. An intentional axis alignment of component configurations for new system model(s) is described as necessary to meet the purpose of understanding the internal system behaviors. The introduction continues by addressing two concepts that will show the unique significance of this approach: using the two-pole physical harmonic system to define a component and coordinate system and defining specific harmonic influence between the components of that system.

Prior to a summary of the hypotheses to be proven, the study's purely quantitative nature will be described in terms of comparing and synchronizing models. The main hypothesis of how self-referential components will reveal harmonic properties is immediately followed by the proposed components, models, vectors, relationships, and derivative rates in the section that will address the conceptual or theoretical framework. The core assumptions, which drove the hypothesis and the theoretical framework, will then be discussed.

This introductory chapter closes by covering the planned scope for the study of the 100,000 prime number increments followed by definitive amounts of model permutations and combinations possible in the study's limitations and delimitations, with suggested boundaries limited to future research and current application to Millennium Prize Problems.

Background of Study

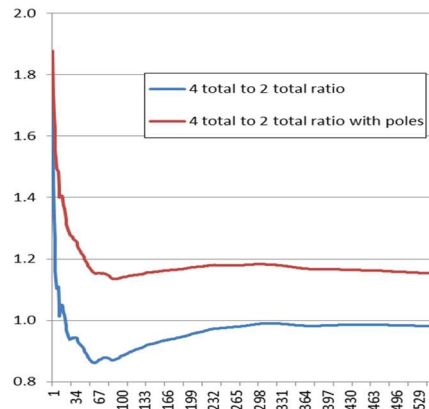
Can the sequence of prime numbers reveal hidden behavior essential to the optimization of systems? What if the behavior of the prime numbers only appears hidden because everything in the prime number sequence is self-referential? If so, fully understanding the prime numbers will need to be strictly according to their terms and dimensions. This study will use the previously discovered double-thread structure, which aligns the repetitive oscillation of prime number increments between two poles, as the foundational self-referential model (Hibbs, 2008). Figure 1 shows the reliable double-threaded structure, which previously revealed the harmonic underdamped behavior from the ratio comparing the multiples of 6 in reverse movement (4 to 2) to forward movement (2 to 4), shown in Figure 1.b (Hibbs, 2012).

Figure 1

Harmonic 6z influence on 2-4 threads

#	2	2 to 4	4	4 to 2
1	2		4	
2	2		4	
3	2		4	6
4	2	6	4	
5	2		4	6
6	2	6	4	
7	2		6	4
8	8		4	
9	2		4	
10	2		4	
11	14		4	6
12	2		10	
13	2	6	6	4
			6	6

1.a. Double thread components



1.b. Underdamped forward/reverse ratio

The threads of this structure will be the axis used to direct a quadrant-oriented, component-focused approach. The quadrant components will be separated into two categories: continuous harmonic poles and harmonic system influence. The continuous harmonic poles will

be from the alignment of the continuous “2” and “4” thread, or axis, values remaining after a modulo 6 operation is performed on all prime number increments (Hibbs, 2012). (The modulo 6 operation divides a number by 6 and only keeps the remainder.) The harmonic system influence will be created from the overlay effect of replacing multiples of “6” back on that two-pole structure. Those component categories will declare the framework and the coordinate system for evaluating, defining, and understanding of the prime number electromagnetic or harmonic behavior and properties.

This new concept will require a large paradigm shift from all historical efforts in understanding prime numbers. The change will be from considering methods to factor prime numbers to considering the prime numbers as a complete system that combines functions growing together over time. Three abstract concepts will be maintained throughout the study as a discipline required to limit the model variation while expanding prime numbers in a different perspective.

First, the number line will not be the reference framework by which growth is measured. The repeating coils in the coordinate systems derived from the double-threaded structure will be the conceptual reference framework. Second, the models will not contain negative coordinates. The positive integer increments and the relationships between their component groupings will drive the definition of systemic behavior. Third, the self-referential model has intrinsic harmonic behaviors that can only be analyzed in abstract dimensions. This third concept will challenge engineers and scientists to look beyond the current elementary understanding of prime numbers as merely foundational factors and to look at the prime number components as a structural framework of synchronized harmonic activity.

Unfortunately, the popular interest in prime numbers as a source for obfuscating cryptographic deciphering of data has clouded the significance of understanding the integer-based harmonic behavior. Outside the cryptographic implementation, and even without this component framework, earlier discoveries of prime number quadratic roots point to distinct elliptical and nonlinear system behavior (Socrates, 1993). Theoretical prime number integer correlation to inherently physical harmonic systems has also been considered, yet the integer and harmonic concepts have not been tied together into one framework (Deninger, 1998).

The cryptographic contribution of primes may also be a hindrance to appreciating the importance of the Riemann Hypothesis. The significance of the Riemann Hypothesis is its connection to a potential common zeta dynamic system, which makes it “probably today the most important open problem in pure mathematics” (Bombieri, 2000). Focusing on their cryptographic utility misses the multidimensional potential of prime numbers. Although the Clay Mathematical Institute (CMI) of the Massachusetts Institute of Technology (MIT) has stated the significance of the Riemann Hypothesis, the proving or disproving the Riemann Hypothesis will not be the goal of this research. Why? This research will be based on a different structure.

The goal of this research will be to use the prime number’s own structure and components to align with an understanding the dynamics of prime numbers. Models derived from this study will describe properties that lead to harmonic convergence and variations to harmonic convergence. These models will provide not only an understanding of the prime number behavior but suggested correlations between the system of prime numbers and existing systems that could stabilize, optimize, and advance technology. As such, this approach should be deemed a parallel, or complementary, approach to the Riemann Hypothesis.

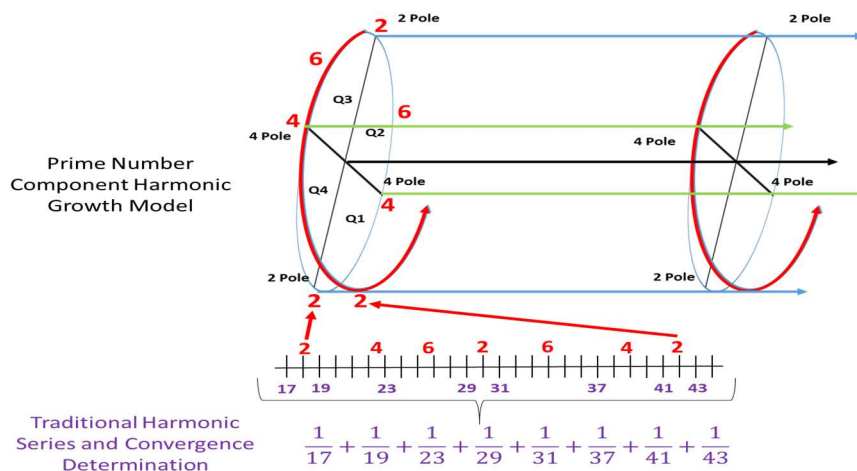
Problem Statement

Deriving a new technical contribution from prime numbers will require a practical and disciplined modeling approach that translates the system of prime numbers into recognized system engineering properties. While traditional approaches focus on complexity of factoring each prime number (Socrates, 1993), considering each prime number as an atomic element overcomplicates discovering systematic behavior. Instead, this study will use the additive nature of prime number increments to build components that represent different dimensions.

Vector relationships between these components will be the source for practical engineering models. Figure 2 denotes the difference between this component-driven approach compared to the traditional approach using the sums of the reciprocal values, an approach of Euler and still consistent for determining infinite growth (Jara-Vera & Sánchez-Ávila, 2020). To facilitate describing the harmonic interactions of internal components, the first 100,000 prime number increments (UTM, 2020) will be placed into the component-driven quadrant coordinate system in the upper part of Figure 2, which is conducive to defining vector-based relationships.

Figure 2

Defining a component-driven coordinate system for harmonic behavior



Purpose of Dissertation Study

This dissertation will investigate the systemic characteristics of prime number growth to define models and relationships. These models will demonstrate how the harmonic growth behavior of primes align with current systems with the purpose of understanding the internal prime number system behaviors and finding practical corollaries from using the prime number coordinate system.

An intentional alignment of component configurations for new system model(s) will be necessary to meet the stated purpose. The analysis of behaviors will be aligned with the two component coordinate system models; one for only the $6z$ harmonic behavior and another one with the 2-4 pole values added to the $6z$ harmonic behavior. Each model will have two possible physical growth dynamics: a horizontal growth model like a radiated wave area intensity and a vertical growth model like a helical volume or DNA structure.

The research variables are the vector values and relationship ratios and derivatives of growth and distribution for the first 100,000 prime number increments, two orders of magnitude above the stabilization that happened at the first 1,000 prime number increments. The research design for comparing derivatives and ratios will reveal significant behavior, and as such, will be the essential method for correlating prime number behavior to existing systems.

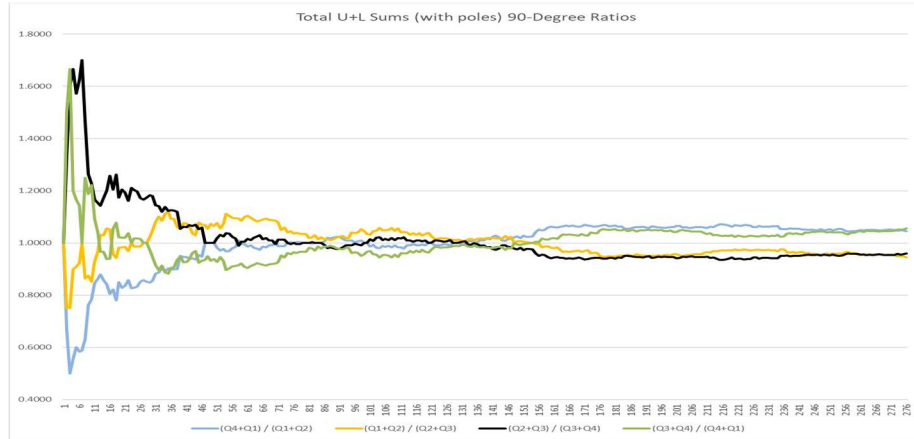
The research will have three key phases. Phase one will transpose the 100,000 prime number increments from the double-pole structure into their quadrant components and coordinates with initial trigonometric vectors. Phase two will describe the harmonic activity from the trigonometric and differential vector relationships. Phase three will correlate the unique behaviors to known natural system properties; those descriptions will be used to frame and to recommend further research opportunities.

Significance of the Study

Using the two-pole physical harmonic system as an axis to define a component and coordinate system will reveal internal relationships in the prime number structure that have only been captured on the surface through traditional methods. Within that structure, the $6z$ oscillatory harmonic distribution over the two consistent poles (2-pole and 4-pole) will dictate a behavioral model unable to be viewed otherwise. Traditional methods defining behavior though complex roots are limited by the approaches of a linear coordinate system external to the significant inner relationships of the prime number components. Using merely 2% of the planned set of 100,000 for data analysis, the sample in Figure 3 reveals the complicated intertwined properties involved.

Figure 3

The harmonic field effect of the 90-degree component vectors



While Figure 3 is a high-level summary of the 90-degree quadrant vector relationships, it also demonstrates potential success in taming the wild nature of prime numbers into a stable harmonic system.

Nature of Study

Models and model comparisons will drive this analytical effort. Due to the $6z$ harmonic influence as a total integrated effect, two separate models will be the source of comparison for quantitative and systemic behavior. One behavioral model with only the harmonic influence of the $6z$ components will be examined for the behavior of both upper and lower planes against typical quadrant relationships and physical system vector interactions. Unique 90-degree and 180-degree relationships will be generated from combining quadrant data into vector form. After the core vector relationships and comparisons are established, the pole values (2 and 4) that occur per oscillation will be added to the respective quadrant component. Values from component relationship comparisons will be repeated after the addition of the pole values. Table 1 is a summary of vectors comparisons and the systematic behavior justification for the attempting this form of modeling. The main model difference between the models is that the $6z$ only model will be focused on a circular behavior while the $6z$ with poles will be focused on an elliptical behavior caused by the major and minor axis of the poles.

Table 1

Research design for comparison of component interactions

Component Characteristics	6z Influence with 2-4 Pole Values Included	6z Harmonic Influence Only
Single Plane with Quadrants	Elliptical quadrants with 4 Field Effect "total" System State changes correlated to combined Single Plane Harmonic E-W, N-S Transitions	Circular quadrants with 4 Field Effect "total" System State changes correlated to combined Single Plane Harmonic E-W, N-S Transitions
Double Plane with Quadrants	Elliptical quadrants with 8 Field Effect "total" System State changes correlated to each different Plane's Harmonic E-W, N-S Transitions	Circular quadrants with 8 Field Effect "total" System State changes correlated to each different Plane's Harmonic E-W, N-S Transitions
90-degree E-M flow field effect	Stabilizing effect on Wave Emission on upper plane and lower plane; Combined U + L	Wave Emission on upper plane and lower plane; Combined U + L
180-degree reversal quantity	Stabilizing effect on North/South flow; West/East flow, Combined U + L	North/South flow; West/East flow, Combined U + L

The component comparison data staged by the 90-degree and 180-degree vectors is the start of several other parameters for comparison. Those parameters will also be ones expected to fully describe any electromagnetic or physical wave behavior. The derivative growth rates for the hypotenuse, tangent, sine, cosine, Doppler (180-degree vectors), right hand rule, field effects (90-degree vectors), and wave intensity (by area and by coil) distribution will be compared. Consistency and variation in behavior will be considered in potential mode shifts of a system.

Data points from different behavior models will be correlated (based on occurrence in elliptical time) to provide an integrated summary of major transitions. Relational data comes from comparing upper plane to lower plane behavior, correlating field effects with Doppler effects, and comparing the $6z$ harmonic influence to the total harmonic influence that includes the 2-4 poles. Packaging and describing these relationships into a form that translates to current physical systems will require correlation of concepts, models, and system state transitions.

This component vector research method will meet a research need for prime number behavior definition in a system engineering perspective. This perspective will reference a framework purely internal to the prime numbers and tie to theoretical mathematical challenges. It will open new approaches to the integer-only Diophantine nature of the prime numbers, apart from historical combinations of real and imaginary roots. In the realm of mathematics, the Diophantine equations with unique integer only solutions are of special interest due to the simplicity of roots and structure. Behaviors from these component integer values will be considered as being generated from a Diophantine form with the prime number increments. The typical searching for “roots” will not be part of this study. Comparing and synchronizing these models will show how the component increments of the prime numbers can provide structures and designs for harmonically stabilizing forces, forces either generated or absorbed.

Hypotheses/Research Questions

While a new framework revealing the tightly coupled components of the prime numbers can easily excite the conceptual and theoretical possibilities, the practical application of prime number behavior as a system is also the challenge of this study. This research effort will focus on the methods to understand the self-referring, harmonic, dynamical, and systematic behavior of the prime numbers. Significant quantitative evidence will be sought to prove those properties exist in this unique prime number component structure.

Self-Referential System

The first research hypothesis (H_A1) is that the prime number components will reveal the self-referential systemic behavior of the prime numbers. This would be demonstrated by the consistent system behavior of the vector relationships for the hypotenuse, tangent, sine, cosine, Doppler, and normal vector field effects.

The corresponding null hypothesis (H_01) is that the prime number components will not reveal the self-referential systemic behavior of the prime numbers. This would be demonstrated by the inconsistent and systematically inexplicable behavior of the vector relationships for the hypotenuse, tangent, sine, cosine, Doppler, and normal vector field effects.

Harmonic and Dynamical Behavior

The second research hypothesis (H_A2) is that the specific components of this prime number growth model consistently maintain a harmonic and dynamically balanced behavior throughout the first 100,000 prime number increments. This would be demonstrated by continuously self-balancing reciprocal values between interdependent diagonal quadrant components, related to a zeta function dynamic.

The corresponding null hypothesis (H_02) is that the specific components of this prime number growth model do not consistently maintain a harmonic and dynamically balanced behavior throughout the first 100,000 prime number increments. This would be demonstrated by uncontrolled drifting of the derivative relationships, thereby showing either a gradual or a reactive unbalanced behavior between interdependent diagonal quadrant components.

Reproducible System Model

The third research hypothesis (H_A3) is that the prime number growth can be defined in a system model with this component coordinate system and vector relationships that align with natural or manufactured system behaviors. This would be demonstrated by the ability to define the system's specific phases and relationships that mirror behaviors of currently known systems, such as electromagnetic fields, force, or acceleration.

The corresponding null hypothesis (H_03) is that the prime number growth cannot be defined in a system model with this component coordinate system and vector relationships that align with natural or manufactured system behaviors. This would be demonstrated by the inability to define the system's specific phases and relationships that mirror behaviors of currently known systems, such as electromagnetic fields, force, or acceleration.

Hypotheses to Concept

From a practical perspective of reusing the component relationships, the generic concept and summary of this set of hypotheses would be an existing elastic-like potential growth behavior. This would be a new concept of prime number flexibility allowing them to conform to different object coordinate structures and balance dynamic force vectors, much like wrapping the surface of an object in a rubber band under a certain tension would maintain surface tension vectors.

Conceptual or Theoretical Framework

The main concept of the component model is the alignment of the prime number increments with their own reference axis. Within the continuous harmonic poles and the harmonic system influence as the two main categories of components, the harmonic system influence is further decomposed into four separate components. These four harmonic influence components of $6z$ are the additive multiples of $6z$ on the 2-pole, between the 2 and 4 poles, on the 4-pole, and between the 4 and 2 poles. As a result, six total components exist including the two continuously harmonic poles. No other studies have been identified that require a focus on the harmonic influence of $6z$, which would have required fully removing the multiples of $6z$ by performing a modulo 6 operation as if peeling back a transparent overlay of $6z$ occurrences.

Although the 2-pole, 4-pole, and $6z$ properties are referenced by Johansen (2012), the application of possible components and interactions were not discussed. Ironically, with the immense desire amongst the mathematical community to prove the “Twin Prime Conjecture” how the gap of “2” between continues throughout the prime number sequences, many have failed to see the significance of a modulo 6 operation that can literally form a perfectly repeating 2-4 sequence (Baibekov & Durmagambetov, 2016). Continuing to treat prime numbers as discrete incompressible events and their increments as unrelated values has not helped understand the potential interactions between components of prime numbers. Future models need to accommodate an expected total system behavior of the prime numbers versus isolated items.

As this study considers the interaction of what was previously determined a core underdamped behavior by Hibbs (2012), a coordinate system will be built from the poles that maintains a self-referential model containing vector relationships that would most likely reveal any intrinsic harmonic properties. Figure 4 introduces the concept that will become the main

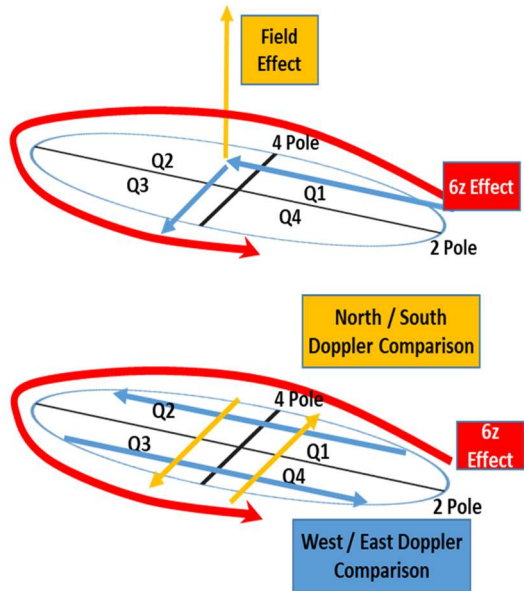
theme for all models compared in this study. The concept of applying the original two-pole structure to define a quadrant coordinate system based on the six components (the four harmonic influence components of $6z$ along with the 2 and 4 poles).

Figure 4

Creating quadrant dimensions from components

Ellipse Coil	Original Coils	North				South			
		Q1		Q2		Q3		Q4	
		Lower Plane	Upper Plane	Lower Plane	Upper Plane	Lower Plane	Upper Plane	Lower Plane	Upper Plane
2	2	2	2 to 4	4	4 to 2	2	2 to 4	4	4 to 2
1, 2	1, 2	2		4		2		4	
2, 3, 4	2, 3, 4	2		4	6	2	6	4	
3, 5, 6	3, 5, 6	2		4	6, 6	2	6	4	
4, 7, 8	4, 7, 8	2	6	4	6	8		4	
5, 9, 10	5, 9, 10	2		4		2		4	
6, 11, 12	6, 11, 12	14		4	6	2		10	
7, 13, 14	7, 13, 14	2	6, 6	4	6, 6	2		10	
8, 15, 16	8, 15, 16	2		4		2	12, 12	4	

4.a. From double-thread coils to quadrants



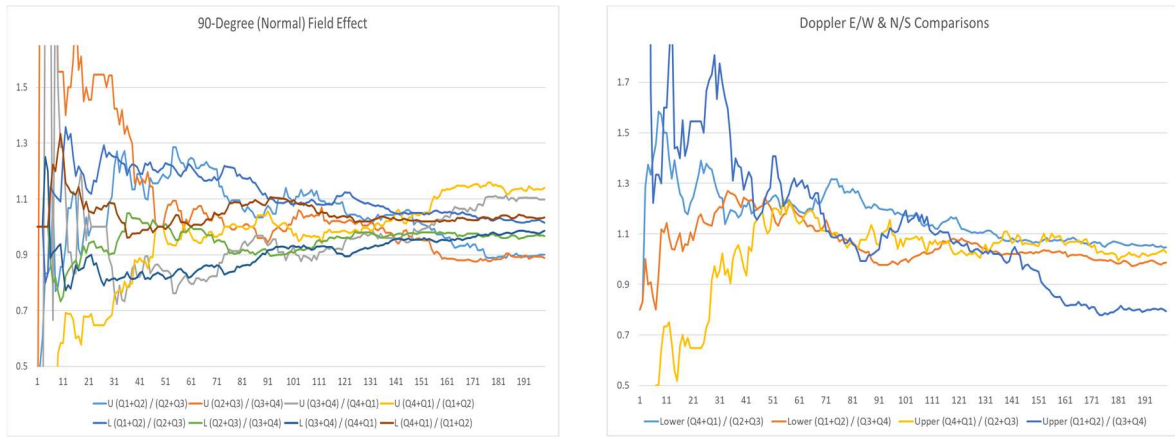
4.b. Normal vector and Doppler vector development

The proposed vectors, relationships, and derivative rates are based on translating the previously introduced double-pole structure to this quadrant coordinate system. Each elliptical coil contains two consecutive sets of the transition data from the original 2-4 pole model. Values occurring on an axis (2 or 4) are assigned the title of lower plane values, being bound to a specific location. The $6z$ values in the open quadrant field are assigned the title of upper plane values because there can be zero, one, two, or several occurrences with an undefined path in transition to the next pole. There is no guarantee that the upper plane unbound values of $6z$ will

behave the same as the lower plane values. The rightmost portion (Figure 4.b) of Figure 4 reveals the practical intent of this coordinate system that allows building 90-degree and 180-degree vectors from the quadrant values. The quadrant vector values from this component model show the potential for revealing balanced self-referential harmonic behavior. Figure 5 shows sample results for the 90-degree normal field vectors and the 180-degree Doppler comparison vectors for less than 2% of the data.

Figure 5

Normal and Doppler vectors for first 200 coils



5.a. Upper and lower normal vectors at 90-degrees

5.b. Doppler vectors: West/East, North/South

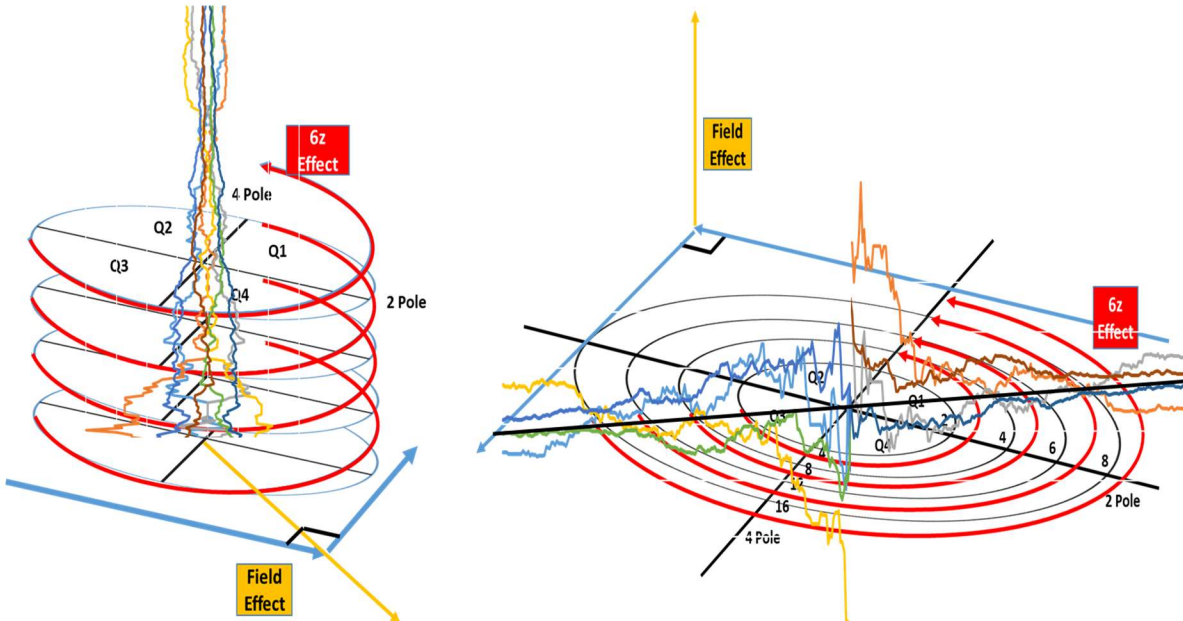
These sample sets of vector relationships already display a balanced transition of harmonic activity and frequency (Doppler) shifts. This component approach provides a more in-depth decomposition related to other research of the suggested harmonic activity associated with control systems (Marshall & Smith, 2013) that might reside inside the prime number behavior. Marshall's suggestion also aligns well with actual results for underdamped harmonic prime number growth (Hibbs, 2012). Figure 5 should be considered as the first glimpse into what will

possibly provide a definitive answer to the question of the self-referential nature of the prime numbers as a system.

In Figure 6, applying the sample set of 90-degree vector results onto the vertical and the horizontal physical growth models illustrates the connection to other potential research. Overlaying the normal vectors from Figure 5.a by aligning it with the vertical progression over time (Figure 6.a), a possible correlation to research in helical structures and angular velocity could be made. Separating the reciprocal normal vectors from Figure 5.a. into two sections offset horizontally by 180-degrees (Figure 6.b), a possible correlation to research in zeta functions and dynamical Lorentz systems could be made.

Figure 6

Comparing the vertical and horizontal physical models



6.a. Vertical helical angular acceleration

6.b. Horizontal zeta and Lorentz dynamics

Applying the prime number coordinate system might open new dimensions in system modeling and number theory. Considering prime number increments to have components with dimensional properties could provide a unique contribution by using a format easily comprehended and modeled. Current approaches stand in contrast; they require a complex plane for understanding the systemic behavior of prime numbers (Andrianov, 2012). Treating the prime number components as pliable elements could also provide a future method for modeling harmonic systems in an integer format, without a complex plane or imaginary numbers. The logical extension of this method would be new abstract dimensional approaches to redescribe quantum behavior, dynamical systems, or dipole effects.

Definitions

Component Coordinate system: Quadrant-based reference system based on the sequential locations of the multiples of $6z$ over the 2-axis and 4-axis.

Components: Prime number increments in designated quadrants between poles or on designated poles.

Cousin Primes: Consecutive prime numbers with a gap of four. These are increments on the 4-axis without an additional harmonic influence of $6z$.

Lower plane: Increments of prime numbers occurring an axis (2 or 4 axis). If there is a $6z$ value on that physical axis, it is assigned as a lower plane $6z$ value tied to (or intersecting with) that axis.

Upper plane: Increments of prime numbers occurring in the open quadrant field between two poles (or axis). They are assigned the title of upper plane $6z$ values. Due to being between poles/axis, they can be zero, one, two, or several occurrences of $6z$ with a nonlinear or undefined path in transition to the next pole.

Sextuplets: Consecutive prime numbers with a gap of a multiple of 6. These are $6z$ increments in the upper plane.

Twin Primes: Consecutive prime numbers with a gap of two. These are increments on the 2-axis without an additional harmonic influence of $6z$.

Assumptions

The assumptions associated with this study are focused on the statistical consistency of the framework, the existence of a fundamental harmonic behavior, and that the computational community is receptive to a clearer conceptual model and approach to understanding the prime numbers.

Statistical Consistency

Assumption: The double pole structure that produced the six components is a consistent structure throughout the first 100,000 increments used on this study.

Rationale: Statistical assurance of continuity is provided from the initial harmonic studies based on the double pole structure with 550 coils for the first 2000 prime number increments. The 550 coils were created by the 1,100 nonzero occurrences from the post modulo 6 operation (Hibbs, 2012). With “2” and “4” as the only possible nonzero result of a post modulo 6 of an even number, the probability of the occurrence of “4” is one of two options, or $\frac{1}{2}$. With 1,100 nonzero selections in the 550 coils, the probability of the perfectly alternating “2-4” is $[1 - (\frac{1}{2})^{1,100}]$, or 7.7×10^{-340} , also known in reliability terms as being in excess of 337 “nines” of reliability.

Fundamental Harmonic Behavior

Assumption: A core harmonic behavior exists between the relationships of components or dimensions of the prime number increments.

Rationale: From the previous work of Hibbs (2012), the result shown in Figure1.b, there is at a minimum an overall balanced harmonic relationship between the forward and backward movement of the contiguous multiples of $6z$.

Common Desire for Clearer Models

Assumption: The cumulative extensive work by mathematicians using imaginary roots, zeta functions, and dynamical system behavioral models has made even the description of the prime number behavior difficult to understand. The assumption is that a new perspective would be welcome if it could provide more straightforward integer-based approach.

Rationale: Publishing the exact challenges of Millennium Prize Problems by the Clay Mathematical Institute expressed the sincere search for a new approach to understanding the prime numbers. The overall plea from the publication and associated rewards of these problems appears to be an honest desire to consider efforts “working towards a solution of the deepest, most difficult problems” (CMI, 2000).

Scope, Limitations, and Delimitations

The focus of this study's information will be the first 100,000 prime number increments and data derived from vector and systematic behavior. The scope of model comparison will be focused on translating data and rates in the vertical models and the horizontal models (in Figure 6) to properties of flow dynamics, elliptical behavior, geometric growth, and wave properties. The potential multidisciplinary impact of a new component coordinate approach could be far-reaching. This scope will be limited to gather enough parametric data to describe the potential flexibility of the framework.

Because the models facilitate an approach with relational growth derivatives with respect to the prime numbers' own components, most ratios (or rates) will be dimensionless. Dimensionless numbers are the result of comparing two forms of the same type of rate, a real-life example would be miles per gallon (mpg) compared to mpg downhill to show relative fuel consumption. These types of ratios are essential for translating and aligning system behavior with geometric and trigonometric forms.

Due to the component relationships having properties of elliptical, current flow, wave dynamics, harmonic activity, and self-balancing dynamical systems, the comparison of actual or theoretical system properties will also address potential future research. The application of the derived models will be used for concepts that could contribute to rethinking the foundational solutions to some Millennium Prize Problems, such as the Navier Stokes Equations (Fefferman, 2000), the Birch-Swinnerton-Dyer Conjecture (Wiles, 2000), Hodge's Conjecture (Deligne, 2000), and the Quantum Yang-Mills Mass Gap Theory (Jaffe & Witten, 2000).

Chapter Summary

This chapter has introduced several new concepts for understanding the behavior of prime numbers in preparation for applying engineering modeling disciplines to current and future products. It introduced a necessary paradigm shift to consider the double-threaded growth pattern as a reference for describing a new set of prime number components, key to a new coordinate system representing different dimensions. Engineering models and alignment of component configurations were discussed as they will be essential to understanding the internal system behaviors. This two-pole physical harmonic approach will clearly be a unique significant modeling contribution.

As a model-driven study, an assumed self-referential system is foundational to the hypotheses of harmonic properties between components in the relationships of the conceptual framework. The planned model combinations in 100,000 prime number increment scope will potentially provide interdisciplinary foundations for future research and application to Millennium Prize Problems.

The topics for the proposed literature research of Chapter 2 will be derived from the system properties revealed through the earlier samples of component interactions and applying the different concepts (Table 1) to the vertical and horizontal two growth models (Figure 6).

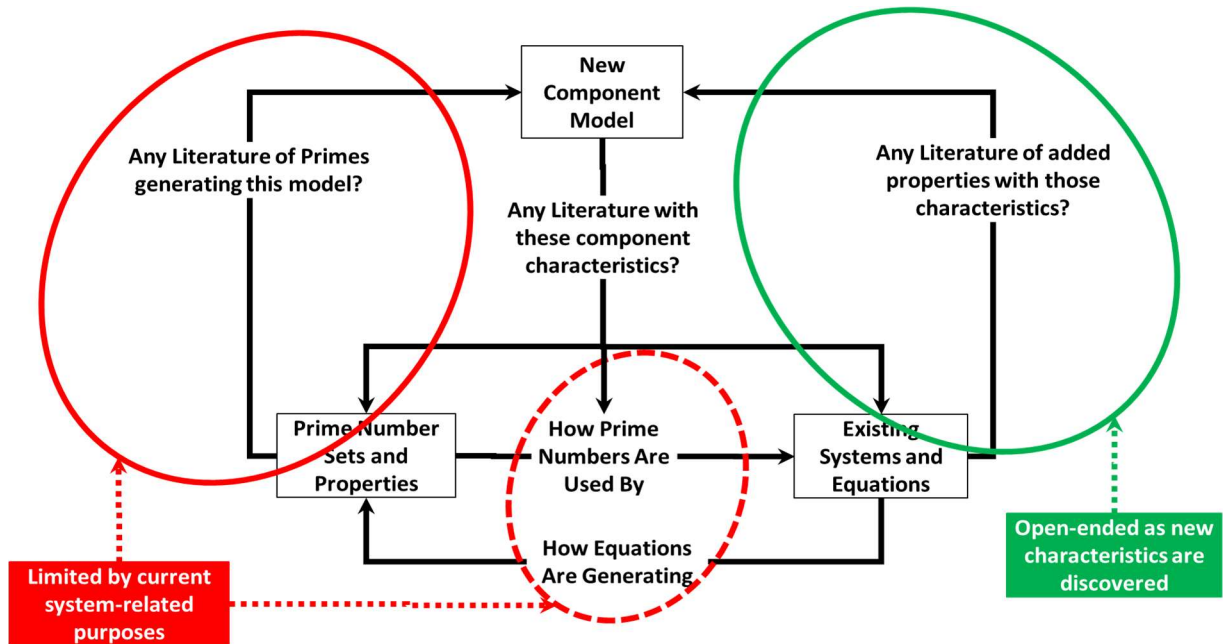
CHAPTER 2: LITERATURE REVIEW

Introduction to Review Structure

While there is no shortage of academic literature and information on prime numbers, whether it contributes to the description, modification, or implementation of the proposed component model is a much different story. Is there any literature with the characteristics of this new component model? The center of Figure 7 shows the distribution of that main question across three topics: prime number sets and properties, how prime numbers are used in systems, and existing systems (with or without the use of prime numbers). Due to the utilitarian purpose of prime numbers in engineering, those three topics will contain most of the literature.

Figure 7

System of literature questions and expected results



Discovering two types of literature can be expected. The first type will determine what literature exists that demonstrates prime numbers generating characteristics of this model.

Limited, if any, results are expected due to the current system-related use of prime numbers. The second type of literature will describe characteristics of existing systems that can provide an added property to the new model. Those characteristics will be not just from the systems that use prime numbers but any system that has some property of the new component model. Open-ended results can be expected as more characteristics are discovered in the new prime number component model. With the threat of potentially reproducing variations without limit, careful bounding of this research is essential. Literature for multiple model characteristics will be reviewed, but a principal set of characteristics will be selected to represent and bound this research.

The artifacts will be covered in three main sections: historical overview, conflicting views, and current findings. The historical overview of literature will be a summary of how prime numbers have been used and any current work being done with prime numbers. It will group the literature into several categories that will help determine its relevancy. Conflicting views will be summarized as part of the historical overview before discussing the current findings.

The current findings section will discuss the relevancy of publications placed in those categories. After findings are discussed from literature for relevant prime number models, findings from literature for models of known systems will be addressed. The last part of the current findings section will present the process for investigating literature in the principal areas of science and mathematics. Those principal areas will be selections from a more comprehensive list of literature search parameters. That comprehensive list will demonstrate the possible open-ended situation that could occur due to the continuing discovery of new characteristics in the component model.

Journal and Research Documents

The search for documents started with the current use of prime numbers and the most recent research examined for relevancy to the new component model. A more comprehensive list of research topics and system behaviors were used in the process described in the current findings section. The totals for number of times a type of journal or source was used in each topic area is included in Table 2, along with a mapping to literature in the principal areas. Table 3 provides an equivalent mapping to literature in the comprehensive list of sources used in validating model behavior and characteristics. Literature published greater than seven years is used only if it provides core concepts or represents a pinnacle point in research information. Reference checks and validation was made for 48 prime number equation types in Table 2.

Principal area literature was on the related properties of electromagnetic fields, vectors, and related Doppler properties were selected due to the 90-degree and 180-degree vector properties of the model. Principal area literature also covered harmonic properties and horizontal expansion represented by the model's wave and dimension growth.

Literature areas reviewed for system model validation in Table 3 are included as a summary of potential expansiveness of the component model characteristics. The model's vector behaviors led to the review of literature on tensors, quantum fields, flux fields, force, fluid flow, gravity, radiated energy, and image projection for possible partial derivative distribution over a grid or polar coordinate system. Literature on seismic properties was also reviewed due to the 180-degree Doppler behavior of the model. With the potential propagation of topics, the current findings only address the summary of the principal areas and the topics discussed in the historical overview.

Table 2*Summary of references by date and principal areas*

Journal / Publication	Number of References by Publication Date										Principal Literature References			
	2021	2020	2019	2018	2017	2016	2015	2014	Core Concept	Historical	Gap, Sequence & Residue	Electro-Magnetic	Doppler	Harmonic & Horizontal
Advances in Pure Mathematics						1				1				
American Mathematical Society									1999					1
An Invitation to Mathematics									2011				1	
Applied Science	1													
Applied Mathematics					2		1			2	1			
Applied Physics B: Lasers & Optics		1												
Astrophysics & Space Science			1											
Asymptotic Analysis		1												
Beilstein journal of nanotechnology						1							1	
Canadian Journal of Physics					1	2						1		
Clay Mathematics Institute									2000	1				
CSEE Journal of Power and Energy Systems		1												
Dissertation (Ph.D.), California Institute of Technology	1	1		1	1				1993	1		1	2	1
Electronics Letters						1								
Elemente Der Mathematik							1			1				
European Biophysics Journal			1											
European Physical Journal C: Particles and Fields		2		1										
Fractional Dynamics						1							1	
General Mathematics									2008		1			
High Energy Physics									2011					1
IEEE Access	12	15	7	2								2	1	1
IEEE Communications Surveys & Tutorials		1	1											
IEEE Journal of Selected Topics in Quantum Electronics					1									
IEEE Journal of Solid-State Circuits				1										
IEEE Journal on Multiscale and Multiphysics Computational Techniques				1										
IEEE Photonics Journal	1	1			2	1								
IEEE Transactions on Information Theory	3				1	1								
IEEE Transactions on Instrumentation and Measurement	1													
IEEE Transactions on Neural Networks and Learning Systems						1								
IEEE Transactions on Quantum Engineering		1												
International Journal of Applied Electromagnetics & Mechanics						1	1							
Inventiones Mathematicae							1							
Inventions				1										
JETP Letters			1											
Journal of Atmospheric & Oceanic Technology		1												
Journal of Communications and Networks			1											
Journal of Nonlinear Science							1							
Journal of Systems Engineering and Electronics						1								
Mathematics	1									1				
Mathematics Magazine									2013		1			
Physical review								1				1		
Physics Essays	1	3	1		3									1
Physics Today							1							1
Proceedings of the IEEE	1			1	2									
Proceedings of the National Academy of Sciences						1					1			
Results in Physics	1											1		
Results in Physics	1				1									
Revista Brasileira de Geofísica									2001					
Sadhana	1													
Scientific Reports		2										1		
Seminario Interuniversitario de Investigación en Ciencias Matemáticas							1				1			
St. Petersburg Mathematical Journal									2012	1				1
Teaching Science: The Journal of the Australian Science Teachers Assoc.						1								1
The Journal of Engineering				1										
The On-Line Encyclopedia of Integer Sequences	48									48				
University of St Andrews	2									2				
WCECS Inter. Conf. on Computer Sci. and Appl.									2008,9					
WSEAS Applied Mathematics in Electrical and Computer Engineering									2012					
WSEAS Transactions on Mathematics									2010					
TOTALS	162	51	28	29	14	13	16	7	4					

Table 3

Summary of comprehensive validation references

Historical Overview

Prime numbers have been essential to understanding the structure and roots for all the natural numbers for as long as mathematicians and philosophers have contemplated the meaning of numbers. As early as 500 BC, Pythagoras's school studied prime numbers for "their mystical and numerological properties" and by 300 BC Euclid presented his "Fundamental Theorem of Arithmetic: Every integer can be written as a product of primes in an essentially unique way." (MT1, 2021). Gauss claims his estimated "density of primes behaves like the function $1/(\log(n))$ " was originated in 1793 (MT2, 2021). Over 2300 years after Euclid's theorem, mathematicians and engineers are using the unique property of prime numbers in algorithms to provide information confidentiality and integrity.

The search for ways to generate larger prime numbers continues with the promise of greater information protection. The search also continues for more unique characteristics that describe their nature to find what is really happening inside the prime numbers and what (if anything) they represent. Understanding them starts with understanding other benefits to their unique identity.

What is a prime number?

A prime number is a natural number (integer) that can only be factored by "1" and itself. With the ability to express all other non-prime (composite) numbers as the product of two or more prime numbers, prime numbers are commonly called the "building blocks" of numbers. This property is the basic factoring of a natural number taught early in any mathematical education. As a number not easily divided evenly, each prime number stands as a potential structural solution for stability in several systems.

How have prime numbers been used?

Prime numbers provide a method of preventing easy decomposition of a system, force, or distance into smaller equivalent forces. Dangers to both human life and material abound when an object, or structure, is vibrated at its resonant frequency that will cause a rhythmic force on its joints literally shaking it to pieces. The resonant frequency is determined by the length and dimension of an object, which affects the time it takes for a vibration to travel through an object. The famous example of the effect from resonant frequency is shown in Figure 8 with the collapse of the Tacoma Narrows Bridge, where the speed of the wind matched the resonant frequency of the structure and it vibrated like guitar string and increased in magnitude until its collapse (Olson et al., 2015). Using prime numbers in varying material lengths and structure mathematically reduces that type of risk.

Figure 8

Resonant frequency destroying Tacoma Narrows Bridge



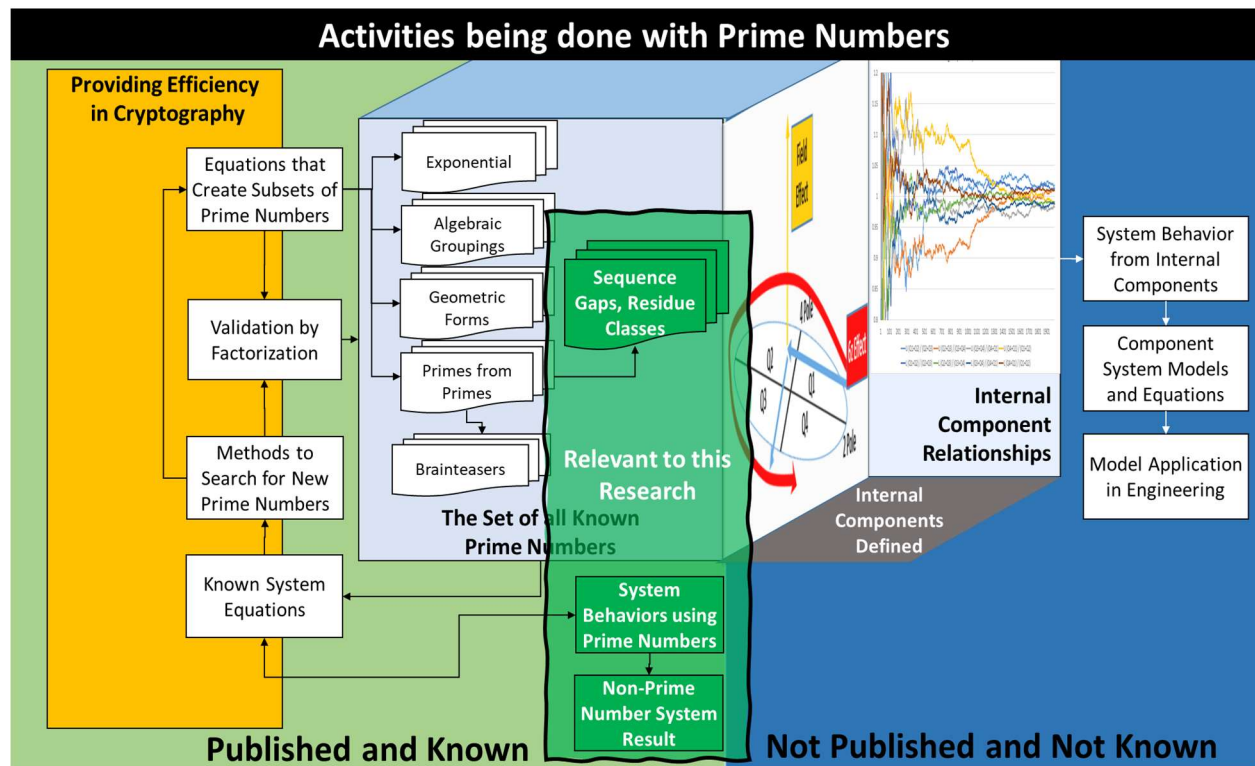
Along with their contribution to controlling harmonic behavior, the difficulty in finding an exact decomposition has also made the prime numbers a perfect candidate in cryptology for coding and decoding messages. Figure 9 contains a high-level diagram of the relationships these groups have to other prime number research and publications.

What is being done with Prime Numbers?

In this age of information warfare and information security, it is no surprise that providing more efficient cryptographic methods would claim the top priority of the current knowledge and use of prime numbers. While Figure 9 shows the associations between efforts involving prime numbers, the intention of current efforts is obviously creating a more rapid cryptographic factoring scheme.

Figure 9

Activities being done with prime numbers



Different secure processing methods, such as the Diffie-Hellman algorithm, focus on the manipulation of public and private key merges, modulo, and hash functions performing RSA-type constraints and requirements. In that case, the cry of the community is for a bigger prime number that will provide more decryption time and the security that time provides. Figure 9 separates the efforts into the categories of “Published and Known” and “Not Published and Not Known”. Although much of the known activity on the left side of Figure 9 is not relevant to this research, it still deserves a summary to differentiate it from the published works that do apply.

Published and not relevant to this research

The search for better cryptographic security does not apply to the goals of this research for two reasons. First, the core premise of cryptographic is that prime numbers are atomic unfactorable elements. Second, most searches are for individual prime numbers, not the entire set of all prime numbers operating, as if defining a system. Table 4 contains examples of equations being used to generate prime numbers. The categories are summarized as prime numbers that are generated from exponential functions, generated using other prime numbers, generated in algebraic and geometric forms, and generated from other primes to what could be considered cognitive brain teasers. The next section will discuss the published items relevant to this research: prime numbers generated in gap patterns and sequences; and prime numbers generated in modulo and residue functions.

Prime numbers generated from exponential functions

Besides the academic search for a set of comprehensive functions, the clear intent for using these exponential functions is to create large even numbers and then take a small delta (± 1) to look for an existing prime number. If generating the number first, it requires validation by factoring. The validated prime can then expedite decryption functions. These functions are not

relevant to this research because the exponential value (such as 2^n) creates results too sparse for the analysis of consistent growth gaps.

Prime numbers generated by other prime numbers

These prime numbers have a breadth of characteristics; using prime numbers in a sum, product, period, exponent, or even as indexes to generate another prime number. The attempt here is clearly to increase the possible uniqueness by starting with a prime number source. These subsets are insufficient for defining prime number behavior in this research.

Prime numbers generated in algebraic and geometric forms

These prime numbers are cases of single integer results that happen to be prime. There are not the complete set that satisfied the equation(s). From a modeling perspective, they only provide limited instances of a single geometric object. While they, like many types, provide another opportunity for unique identification in cryptological functions, these suboptimized sets are not relevant to this research.

Prime numbers generated as cognitive brain teasers

These functions use prime numbers in forms of palindromes, ambigrams, concatenation, and changing a single digit to create a limited unique set from unique sets. Their extreme uniqueness could also be a negative characteristic as telltale indicators in a cryptographic algorithm. Even though they may be perfect for checksum development in information integrity, they are not relevant for the purpose of this research.

Prime numbers used in known system equations

Traditional studies consider each prime number as a singular part of a harmonic function that threatens the stability of a structure, as with Euler and partial sums (Pollack, 2015; Jara-Vera & Sánchez-Ávila, 2020). The Prime Number Theorem also counts the individual occurrences

over a gap on the number line (MT2, 2021). These types of methods evaluate the unique results of standard equations using primes, with the common issue of placing primes in a different reference system.

Table 4

Examples of prime number types by group

Primes Generated	Examples	
Exponentially	Carol: $(2^n - 1)^2 - 2$; A091516	Pierpont: $2^u * 3^v + 1$; A005109
	Fermat: $2^{(2^n)}+1$; A019434	Proth: $K * 2^n + 1$; A080076
	Kynea: $(2^n + 1)^2 - 2$; A091514	Solinas: $2^a + 2^{n-a} + 1$; A165255
	Mersenne: $2^n - 1$; A000668	Thabit: $3 * 2^n - 1$; (A007505)
	Mills: (Mills Constant) 3n ; A051254	(Related) Thabit: $3 * 2^n + 1$; A039687
Using Primes	Double Mersenne: $2^{(2^P-1)} - 1$; A077586	Sophie Germain: $(p, 2p+1)$; A005384
	Mersenne exponents: $2^P - 1$; A000043	Super Primes: (P^{th} primes) $\{P_1, P_3, P_5, \dots\}$; A006450
	Perrin: $P_n = P_{n-2} + P_{n-3}$; A074788	Unique period primes at $1/p$; A040017
	Primorial: [Product of first n primes]+1; A018239	Wagstaff: $(2^P+1)/3$; A000979
	Ramanujan: Smallest prime with n count in $[x/2, x]$; A104272	
In Algebraic Groupings & Geometric Forms	Form of $n^4 + 1$: A037896	Quartran: $x^4 + y^4$; A002645
	Leyland: $x^y + y^x$; A094133	Regular: Where “numerators of the Bernoulli numbers are not divisible by p”; A007703
	Minimal: No shorter prime sequence of the digits; A071062	Stern: P_n with no existing $P_m + 2b^2$, $m < n$; A042978
	Partition and Primeval: Related to sets permutations; A049575; A119535	Super Singular: Related to monster groups and super singular elliptic curves; A002267
In Gap Patterns & Sequences	Balanced: $2 * P_n = P_{n-1} + P_{n+1}$; A006562	Sexy: $(p, p+6)$; A046117
	Cousin: $(p, p+4)$; A023200	Triplets: $(p, p+2, p+6)$; A007529
	Isolated: No other prime in $[p-2, p+2]$; A007510	Triplets: $(p, p+4, p+6)$; A007529
	Quadruplets: $(p, p+2, p+6, p+8)$; A007530	Twin: $(p, p+2)$; A001359, A006512
Residue (Dirichlet)	Eisenstein Integers: $3n-1$; A003627	Modulo (a) with residue (d); an+d
	Integer Gaussian: $4n + 3$; A002145	Pythagorean: $4n + 1$; A002144
Using Primes in Cognitive Brain Teasers	Circular primes: Remain prime under cyclic shifts of digits; A016114	Smarandache-Wellin: (Concatenated sequence): $\{2,3,5,7\} = 2357$; A069151
	Palindromic: Form of abcba; A002385	Strobogrammatic (Ambigram rotated 180° upside down): (181, 619, 16091, 18181, 19861); A007597
	Palindromic Wing: 1117111, same except middle; A077798	Truncate-able [sic]: Right truncated 593 to 59; Left or Two-sided truncation; A024785
	Repunit: $(10^n - 1)/9$, with only the digit “1”; A004022	Weakly: (Changing one digit) = composite number; A050249
	Self-primes [sic] in base 10: not sum of integer and its decimal digits; A006378	
Examples verified at The On-Line Encyclopedia of Integer Sequences <a data-bbox="448 1848 1183 1890" href="https://oeis.org/A##### (Alphanumeric Code) Extracted 02-13-2021 1600.">https://oeis.org/A##### (Alphanumeric Code) Extracted 02-13-2021 1600.		

A related issue exists with the most significant work on the exact nature of the prime numbers, the Riemann Hypothesis. The perspective of complex roots has been used to define how harmonic activity and asymptotic growth is taking place (van Putten, 2014). It could also be considered as a method to find a unique dimension that defines primes, and it uses a harmonic zeta function (Bombieri, 2000), which involves real and imaginary roots of each prime number.

Although some models address the perspective of a prime number elliptical structure (Socrates, 1993), primes are still treated atomic and incompressible (Andrianov, 2012). These manipulations of external (atomic) prime number characteristics force the use of a complex plane approach that does not compensate for the lack of an internally self-referential model.

In summary, these items are not relevant because the atomic and system characteristics do not align with movement into the component model. The many prime number exponential equations merely produce reduced subsets that could “coincidentally” be prime numbers. Single and sparse results from limited criteria do not represent the total systemic behavioral characteristics relevant to this research.

Published and Directly Related

The green boxes in the center of Figure 9 depict the limited amount of material with relevant information going forward in this research. There are two published groups of prime number types relevant to this research: prime numbers generated in gap patterns and sequences; and prime numbers generated in modulo and residue functions. Gap and residue functions align with the types of increments in the component model.

As far as activities using prime numbers, the behavior and characteristics of systems that implement prime numbers are of some interest due to the realization that whatever structure is derived from the component model research will have some traditional form of system behavior.

These systems are depicted in the two lower green boxes in Figure 9. Real number vector values will be the results from of the use of prime numbers in describing the component relationships.

What is not being done with Prime Numbers?

There is no integrated model for the prime numbers as a tightly coupled system. A totally self-referential framework is not defined. As depicted in Figure 9, this effort would require a new approach both to defining the internal component from the aspect of a self-referential framework and to gathering the internal component relationships. Even the most robust approaches using modulo functions with multiple bases (Andrianov, 2012) operate on the prime number itself, not considering the starting structure (after number 5) and not considering the existence of separate components or poles.

System behavior cannot be defined until a new coordinate and component approach is developed. Any attempt to derive or define system behavior from internal components without a new approach to defining internal components only results in continued dependency on a complex plane and imaginary roots. There are also philosophical disagreements on the exact purpose, scope, and definition of prime numbers.

Conflicting Views

The first debate topic relevant to this research would probably be the purpose of the prime numbers. Are they only supportive in nature and limited to the fundamental theorem of mathematics as the lowest level of factors? Those searching for primes that can create exponential or geometric forms would see primes valuable in those areas also. What is the total scope of prime numbers, does it involve the almost primes, near primes, negative primes, or another significant characteristic that prioritizes one prime above the other? The answers will

depend on a community's modeling goals. On some topics, debate is necessary to be maintained just for a historical record of knowledge regarding proven or disproven philosophies.

One such debate that will always surface is the official set definition for prime numbers. Is the number "one" a member of the primes? Why do we allow the number "two" to be a member of the primes? These will continue to be debated by purists with legitimate reasons on both sides. This new component model will also add a new conflict; it is not concerned about primes below 5 because they are outside the "system" model of pole repetition.

Philosophically, if this new internal component approach is taken, another conflict arises by questioning the value of the prime number counting function. The traditional approach is to know how many primes occur over a certain gap on the number line. Packaging becomes the new conflict. The component model packages by quadrants. Traditional counting packages the pole values with the magnitude of $6z$ multiples as a single instance. The new conflict would be based on the considering the physical location of the significant multiples of $6z$ with the constant incremental pole values (of 2 and 4) essentially having no weight except as coordinate markers for the movement of $6z$. It also considers the complete distinction and analysis of two separate systems with clear harmonic behavior, without the use of imaginary roots. With every new model new conflict can be expected.

Considering the traditionally utilitarian function of prime numbers to a scientist's or mathematician's goal, the worst question to ask would be: "Which view is the correct view?" Correctness is rather a matter of shoe size and type that fits the worker and the work. These internal conflicts will always exist between experts requiring different conceptual set definitions for executing the different tasks in algebraic, geometric, and scientific models. Insisting on perfect agreement may be the most unproductive task in prime numbers.

Current Findings

The findings for information in the published and known realm are clearly a continuation of current popular historical themes in cryptological efficiency in information security. Documentation exists for searches of specific equations and systems that produce prime numbers. Literature shows that the prime numbers were manipulated due to their unique characteristic of providing a level of obfuscation and difficulty in factoring that will continue to assist in cryptographic efforts. This research investigates a totally different concept of prime numbers, the concept of prime numbers as a comprehensive system with vector relationships between its components within its internal self-referential coordinate system.

With that research focus, there are only two aspects of the known areas relevant to this research: gap sequences and modulo residue. However, they also are of little benefit due to their reference points, structures, and treatment of even the prime number properties as a non-decomposable occurrence. This section of current literature findings will provide a summary of those issues prior discussing literature findings for the use of prime numbers in known systems.

The last part of these current literature findings will cover the “Not Published and Not Known” literature, which is a summary of how properties of the new component concepts will be validated. In the case of the last section, it is the “relationship” to the textbooks and reference literature that is “Not Published and Not Known” because any relationship to the unknown component properties has never been published.

Findings Using Gap, Sequence and Residue

As close as literature on the sequences and gaps (Twin, Cousin, Triplets, etc.) come to describing some specific structure, even the gaps addressed in that literature are still considered as individual elements. The best example is that the gap of “8” is considered as just that, “8”, not

as the gap of “6” overlaid on the thread value of “2”. Research in the concepts of prime number gaps (Treviño, 2014), patterns (Ferreira, 2017), and detailed logic sequences (Hahn, 2008) also offer potentially multiple options of overlapping sequences. Yet, they lack an internal reference axis.

Publications and equations on the modulo residue approach (or Dirichlet Theorem) suffer a similar curse. First, the modulo is performed on the odd prime number instead of its increment, or gap. Second, the modulo residue is a single value, not considering the continually alternating axis of “2” or “4” as is found in the done in prime number increments. Third, modulo research has provided the option of concurrent multiple modulo forms (Oliver & Soundararajan, 2016). Flexibility in modulo approaches sounds attractive, but it hinders the commitment to an internally self-referential axis as with the component approach. While this literature provides detailed decomposition of sequences, the system’s overall harmonic behavior still needs a specific direction or purpose. The shortfall of a definitive structure still exists in that literature.

Findings Using Known Systems

Literature with descriptions of using prime numbers in known system behavior (Euler series, Taylor series) only provide a prime number variant of the known system. The most known example with prime numbers is the series equation to determine of the convergence or divergence of harmonic. These types of system equations could be considered customers of prime numbers and it was normal to have non-prime number results (composite, real, or complex). Integer results were only due to specific constraints on the outcome of the equations and thus become subsets of those types of equations discussed in Table 2. The literature about those systems documents that something different is happening with prime numbers, yet with no specific comprehensive prime number system approach noted. While one publication describes

the complex architecture of prime numbers raising the question if there exists a method to tame them (García-Pérez et al, 2014) and another is considering the potential underdamping control systems behavior (Marshall & Smith, 2013), these still addressed prime numbers in the traditional definition as atomic indivisible elements almost as if reaching a sacred glass ceiling imposed by previous approaches.

The results of these findings are both discouraging and exhilarating; discouraging because there is a lack of framework previously completed, exhilarating because this appears to be untouched territory. Where does that leave the literature review? Reference literature will be necessary to validate the relationships and the model behaviors of this new component approach. Literature will guide the selection of engineering properties.

Finding Literature that Validates New Models in Similar Systems:

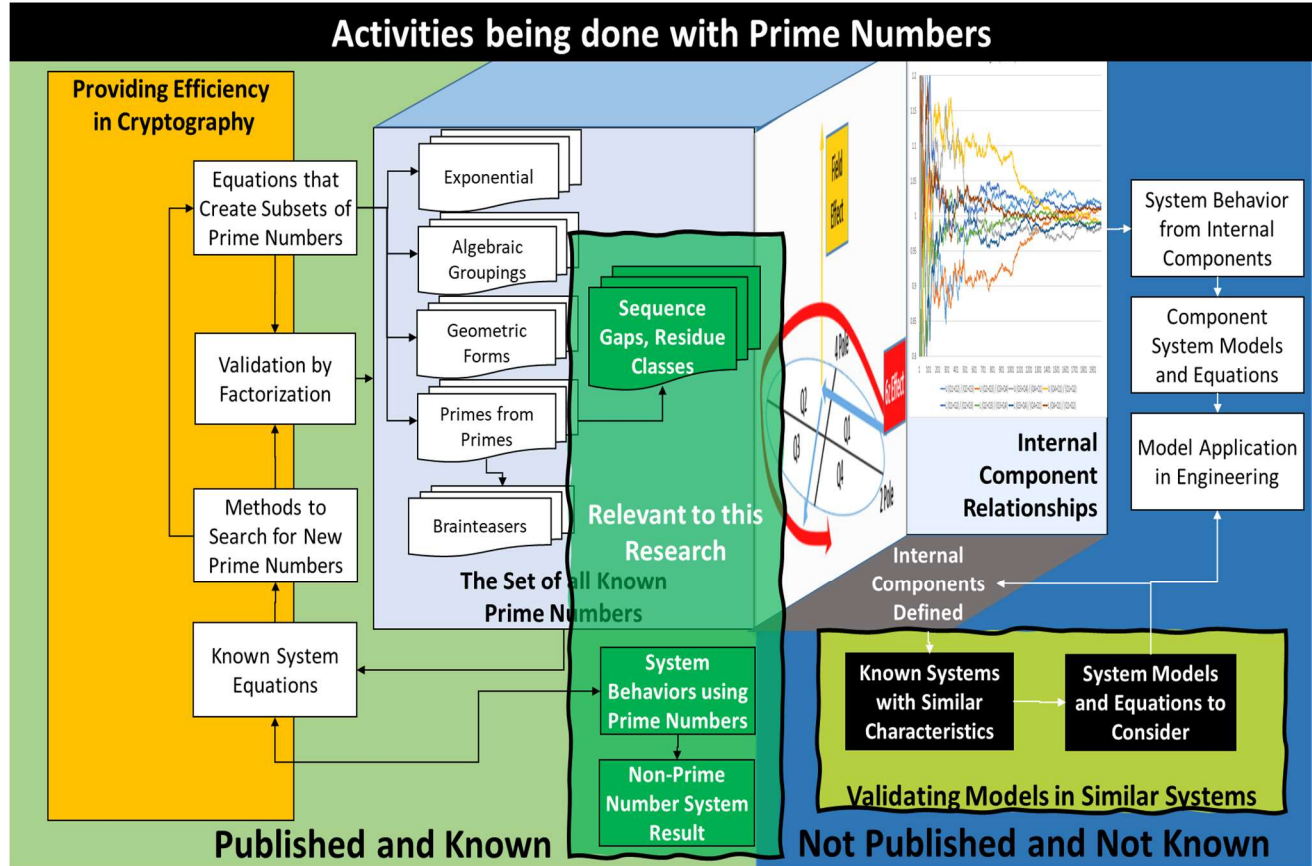
Until this point in the literature view, material has been discussed about three approaches: producing a limited set of prime numbers, using a limited set of prime numbers, or using all prime numbers in a limited set of equations. What should be done with these newly discovered prime number internal system equations and component behaviors? With the component and coordinate approach as apparently new territory, this makes considering the validity of these new models and relationships mandatory.

A clear distinction must be made on exactly when, how, and what reference literature will be used. The reference literature used for validation will only be for properties generated from the new component concepts. It is placed in the category of “not published and not known” due to the “similarities” of the new component system itself being unknown. Figure 10 modifies Figure 9 by adding the search for references that validate behavior on similar systems. This is totally different than examining current systems that are using prime numbers as their input. The effort is also on the right side of Figure 10 because it could easily become open-ended, as new

properties and models are discovered. A goal in any future research with the component model should probably consider expanding that validation.

Figure 10

When model reference literature for similar systems is gathered



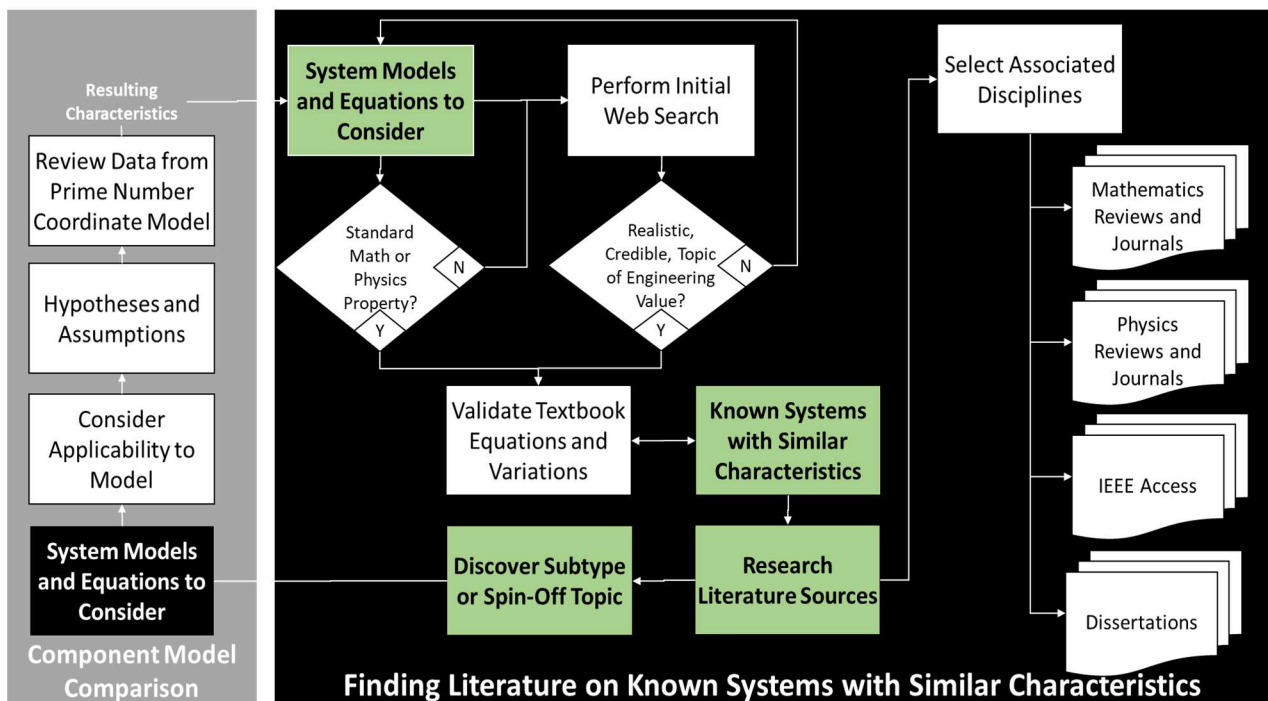
At first it may not seem significant, but a transition in the role of prime numbers using the component model takes place here. Prime numbers transition from being numbers following an existing system's behavior to numbers leading system behavior. They become a framework and structure that will drive new topical literature research. Inside the effort described as “Validating Models in Similar Systems” in Figure 10, there will be specific steps taken to validate defined internal components using reference literature containing “Known Systems with Similar

Characteristics". As a result of literature and model comparison, new concepts and potential properties revealed through the reference literature will generate secondary "System Models and Equations to Consider". Figure 11 provides a zoom-in of the black process box and the specific steps taken to examine reference literature containing "Known Systems with Similar Characteristics".

Figure 11

How model reference literature for similar systems is gathered

Process of Selecting Reference Literature for System Models



The iterative process for finding literature on known systems with similar characteristics starts in the upper left corner of Figure 11 with the 'resulting characteristics' from the prime number component coordinate model. Next, it will be determined what system-like models and equations are occurring. From that model's system behavior or equation, a decision is made

whether the topic is a standard physics property or if the topic requires some initial investigative research. From validation with textbooks, a determination will be made how much research and correlation with specific literature is required. The iterative nature of the literature review makes it mandatory to consider a subtopic that generates a new system model, property, or equation to consider regarding its applicability to the component model. The information gathered during the process steps of the green boxes in Figure 11 will lead to documenting what reference information will be found for similar systems. Table 5 is an example of literature and topics based on the predominant characteristics in the initial component model; characteristics of electromagnetic, Doppler, and the combined harmonic horizontal growth properties.

Table 5

What reference literature was found for similar systems

Principal Aspects of Math and Science Literature for Prime Numbers as a System Model				
Characteristic	System Models and Equations to Consider	Known Systems with Similar Characteristics	Research Literature Source	Subtypes and Spin-offs
Electromagnetic Properties	<ul style="list-style-type: none"> •Force and power distribution •$1/(n^2)$ wave amplitude reduction 	<ul style="list-style-type: none"> •Electromagnetic Waves •Wave power intensity over area •Motor/generator rotor activity 	<ul style="list-style-type: none"> •IEEE Access •Dissertations •Physics Textbooks •Differential Equations Textbook 	<ul style="list-style-type: none"> •90-degree Poynting, normal, E-M vectors •Quadrant partial derivatives of $6z$
Doppler	<ul style="list-style-type: none"> •Vector ratios •Comparison of Incremental Frequency / Rates 	<ul style="list-style-type: none"> •Construction beams shock distribution •Antenna dipole performance 	<ul style="list-style-type: none"> •Physics Textbooks •Differential Equations Textbook •Dissertations •Open Science Journals 	<ul style="list-style-type: none"> •Doppler ratios •Seismic N/S, E/W directional vectors •Trigonometric vectors
Harmonic and Horizontal Growth	<ul style="list-style-type: none"> •Sum of $(6z)/(t^2)$ •Dynamically balancing •Second Derivative of cubic function $(6z of z^3)$ 	<ul style="list-style-type: none"> •Radiation •Wave power intensity over area •Image Projection •Helical angular acceleration •Planetary elliptical gravity 	<ul style="list-style-type: none"> •Physics Textbooks •Mathematics Journals •Open Science Journals •NASA.gov 	<ul style="list-style-type: none"> •Horizontally expanding geometric forms •Vertical Gravity •Force and power distribution •Zeta and Lorentz forms

The systems behavior and expected systems equations from this reference information will be used in the definition of models and methods in Chapter 3. After the review of over 110 publications using the process defined in Figure 11, the initial similar system references list only the principal publications with new or additional depth beyond textbooks for the respective system characteristic.

Chapter Conclusion

Information in the published and known realm of prime numbers is clearly a continuation of current popular historical themes in cryptological efficiency in information security. With the traditional focus on the “building block” function of prime numbers, an abundance of documentation exists to fulfill the continual search of specific equations and systems that produce prime numbers. The types of prime numbers fall into the categories of primes in exponential equations, primes generated from prime numbers, primes in algebraic and geometric form, modulo residue primes and unique cognitive brain teasers. Only two aspects of the known areas were slightly relevant to this research: gap sequences and modulo residue. However, they also are of little benefit due to their treatment of even the prime number properties as a non-decomposable occurrence.

With the focus of this research introducing a new component model built from a totally self-referential coordinate system, related literature on prime numbers was limited in both quantity and relevance. The most beneficial information for this research will probably be from properties of system that do not necessarily involve prime numbers, properties of a comprehensive system with vector relationships between its components. Some reference material discovered was related to the model’s principal areas of science and mathematics with properties of electromagnetics, Doppler, and the combined harmonic horizontal growth. Bounding the research to the principal areas was necessary due to the almost unlimited list of system topics for future research and model correlation.

Chapter Summary

This chapter discussed the process for determining if there was any literature with the characteristics of this new component model. This required research of literature in three areas: prime number sets and properties, prime number use in systems, and existing systems with behavior related to the new component model.

Literature artifacts were discussed in three main sections: historical overview, conflicting views, and current findings. The historical overview grouped the literature into several categories that determined its relevancy. The relevancy of each publication category was discussed in the current findings section. Findings from literature for models of known systems was addressed and organized with principal areas of science and mathematics selected from a more comprehensive list using a defined process. The properties of the principal areas of science and mathematics will assist in defining the models, methods, and measurements in Chapter 3 in preparation for examining the research data in Chapter 4.

CHAPTER 3: METHOD

With this new prime number model, preparing the approach for gathering and analyzing data would be the most beneficial if it is aligned with the four main system characteristics: growth, trigonometric, normal vectors, and Doppler vectors. A method for capturing the events and behaviors of these characteristics is proposed to be accomplished by documenting them in an event trace table. Trends and unique control events will be noted and compared to determine different modes and interdependent relationships of the system. Two types of models will be used to compare system-wide behavior, due to the potential wave, power emission, radiation, and electromagnetic properties revealed in the initial data sample models for 2,000 primes. One model that will be used is a magnitude model that deals with the raw data vector values by noting events, as just discussed. The other model will be an inverse-squared approach to the amount of growth occurring per coil by dividing each new increment by its radius squared, in this case their coil number squared. A brief review of the coordinate system and the core components that will create the characteristics is necessary to understand the appropriateness of this modeling and analysis approach.

Research Method and Design Appropriateness

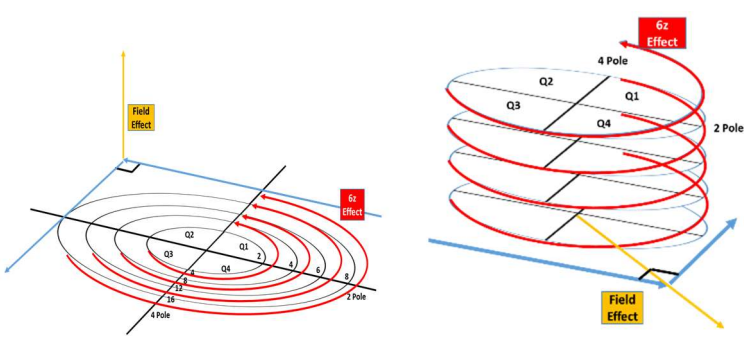
The new coordinate system, driven by cardinal heading changes when shifting between the 2-thread and the 4-thread, provides the framework for allocating multiples of $6z$ into their appropriate quadrant. Figure 12 provides overall logical progression for the concept of allocating multiples of $6z$ into components that align with the coordinate system (Hibbs & McAndrew, 2021). Figure 12.a displays the multiples of $6z$ as they occur on and between the 2-thread and the 4-thread. The values of “2” and “4” are intentionally temporarily removed from

their thread locations in the columns of Figure 12.a only to magnify the placement of $6z$ in the quadrant components. Quadrant activity and interaction will be the core to all analysis in both models, magnitude and inverse squared. Quadrants will provide a common self-referential framework that is most easily understood for mathematicians, engineers, and scientists. Quadrants will also provide a more rapid structure for further analysis and research.

Figure 12

Allocating multiples of $6z$ into the coordinate system

#	Northside				Southside			
	Quadrant 1	Quadrant 2	Quadrant 3	Quadrant 4	Quadrant 1	Quadrant 2	Quadrant 3	Quadrant 4
1	2	2 to 4	4	4 to 2	0	0	0	0
3	0	0	6	0	0	6	0	0
5	0	0	6	6	0	6	0	0
7	0	6	0	6	6	0	0	0
9	0	0	0	0	0	0	0	0
11	12	0	6	0	0	6	0	0
13	0	6	6	0	6	6	0	0
15	0	0	0	0	12	12	0	0



12.a. Multiples of 6 as components

12.b. Horizontal growth only

12.c. Vertical growth only

The quadrant approach for organizing data will also accommodate any correlation to a horizontally expanding system (Figure 12.b) or a vertically expanding system (Figure 12.c). This coil-based quadrant structure will be used to determine the four main characteristics of growth, trigonometric, normal vectors, and Doppler vectors. While the growth values and the trigonometric values of sine and cosine will be relatively easy to extract from the quadrant values, some preparation with data grouping and will need to be done for defining normal vectors and Doppler vectors.

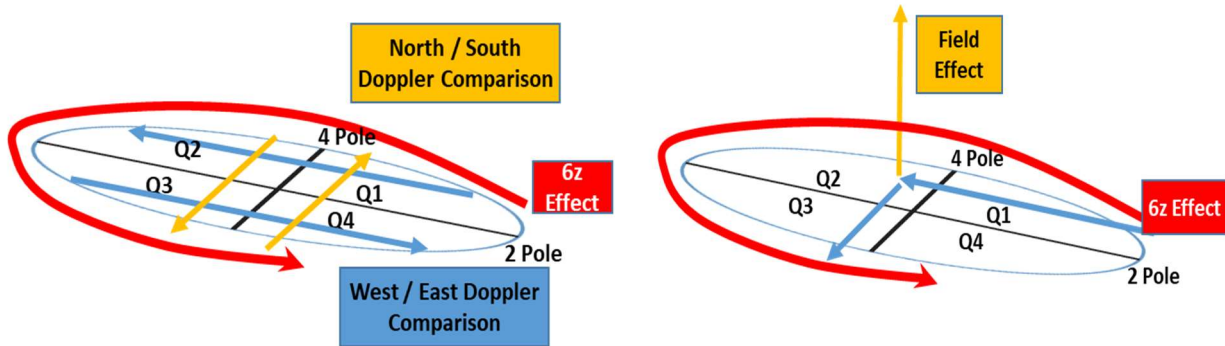
Population, Sampling, and Data Collection Procedures and Rationale

For the first 100,000 prime number increments, data will be placed into the quadrant format for both the lower plane (values on poles) and the upper plane (transition between poles). The total sums of $6z$ values on these quadrant components will be gathered, and growth rate comparisons will provide derivative forms of relational growth. Preparing sets of data for vector comparisons will be done. The coordinate system will provide the framework so that the “coordinate mapping is used to fully develop the model’s vector forms for component comparison in the system” (Hibbs & McAndrew, 2021).

Figure 13 shows those pairing relationships between the quadrants that will be necessary to create data for the normal vectors and the Doppler vectors (Hibbs & McAndrew, 2021). The yellow lines in Figure 13.a show how grouping of quadrants Q4+Q1 will be used in comparing the grouping of quadrants Q2+Q3 to develop the North/South relativistic Doppler. In Figure 13.b, the structure shows how a normal vector with a field effect will be created for all values in a 90-degree relationship between Q1+Q2 and Q2+Q3.

Figure 13

Quadrant data to build vectors



13.a. Relativistic Doppler vectors

13.b. 90-degree normal field vectors

Validity: Internal and External

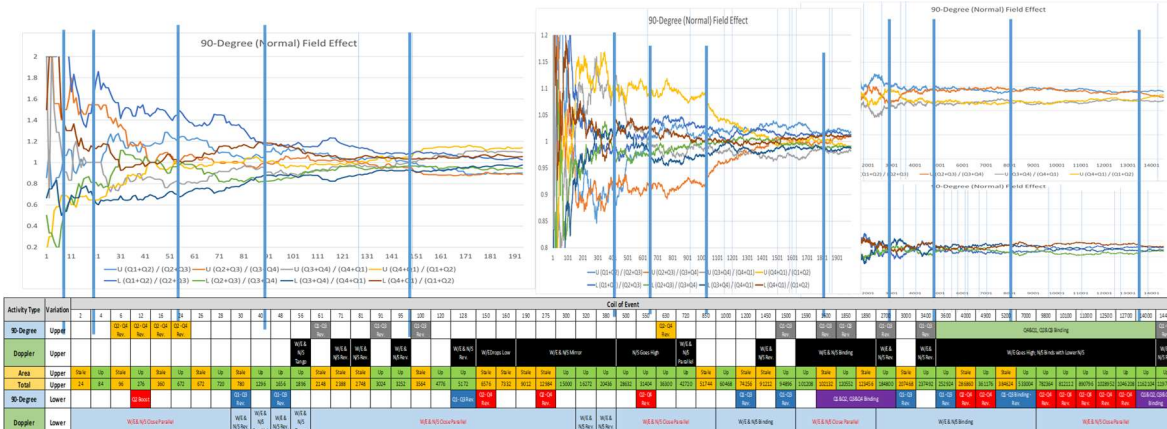
As vector and growth data is gathered, random sampling of row and column cell

projection formulas will be performed prior to extracting a graph for inclusion of data into the event trace table. As information gets inserted into the event trace table, validation of the overall growth values of the lower and upper planes will be reviewed so relationships can be explained or flagged for possible synchronization with other components. Figure 14 has a sample of normal vector data points and methods used to annotate behavior and activity. As data is entered (in Figure 14), vertical event lines will be compared between upper and lower plane activity. Creating a compass of activity will provide a visual means for defining synchronized upper and lower vectors of $6z$ that might represent a transfer of energy or other natural system behavior. This type of event data format is not expected to be relevant to the inverse-squares model unless the resulting values continue to change after the first few hundred coils.

Figure 14

Validating and entering data

Sample of Data Points, Preparing for Analysis

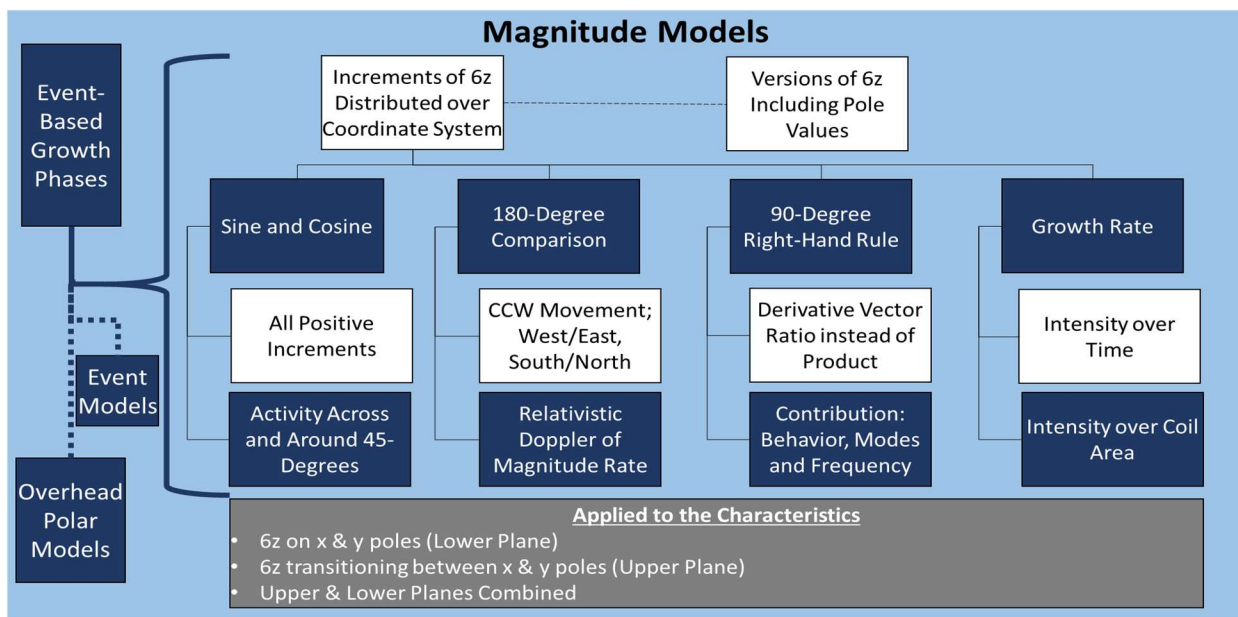


Data Analysis

Probably the largest concern with reviewing and describing systematic events across different component interactions will be potential research distraction from the extensive details and possibilities. This new component and coordinate system approach might open too many paths to investigate. The plan for keeping the analysis structured and disciplined is to describe the four component system characteristics within the bounds of the two models (magnitude and inverse-squared). Figure 15 is a summary of the disciplined workplan for associating the expected discoveries and benefits from each of the four types of characteristics.

Figure 15

Plans for analysis with magnitude models.

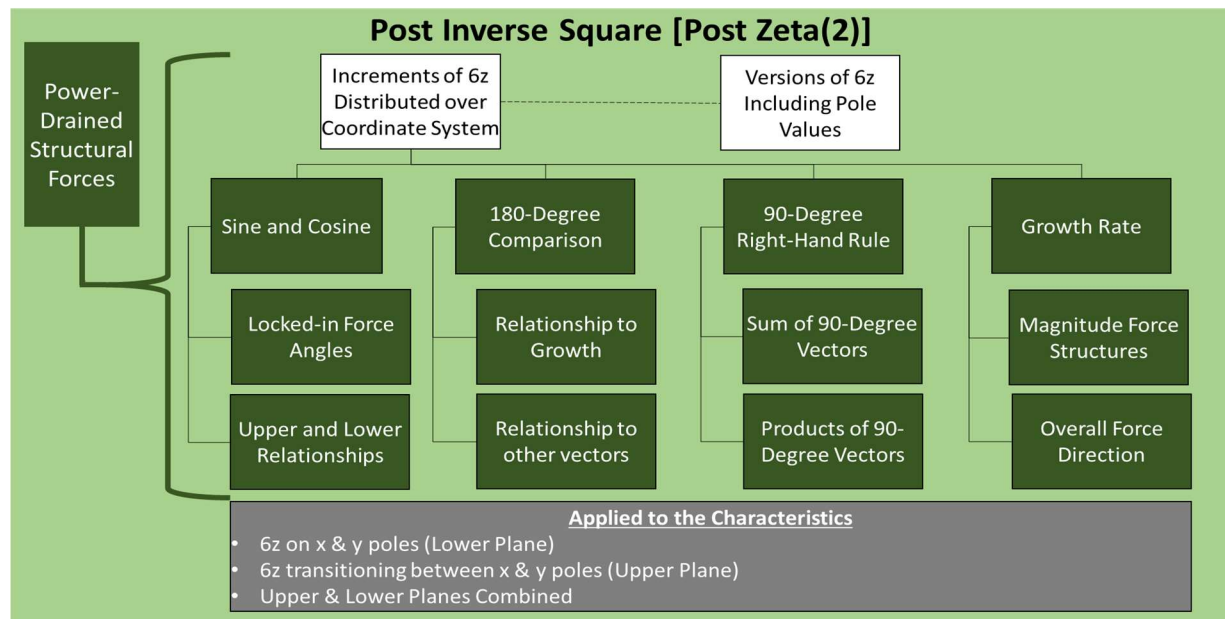


The white boxes at the top of Figure 15 are the common sets of data to be used for both the magnitude model analysis and the inverse squared analysis. Integrated sets of data are on the left with the event-based growth phases that will provide data to integrated event models and

polar coordinate models. With the unknown level of detail this may produce, consistent goals for all magnitude analysis are described in the grey box at the bottom of Figure 15. The standard framework variations need to be reviewed. Those variations are from interaction on the lower plane, the upper plane, and the combined effect from both planes. Under each of the four characteristics is a white box that describes an overall theme that needs to be remembered. Each characteristic also has under it a darkened box for the type of expected results from the analysis, whether the results reveal any integrated properties is yet to be determined. Figure 16 presents a different type of expected analysis using the results of the inverse square model.

Figure 16

Plans for analysis with inverse-squared models.



Relatively flattened values are expected to result from this post-zeta(2) area operation, due to the increments divided by the growth of the radius (or coil-time) squared ($\Sigma_1^t \frac{6z}{t^2}$). The

inverse square model is equivalent to applying a zeta(2) function ($\Sigma_1^n \frac{1}{n^2}$). To facilitate analyzing the function's impact over coil area, a modified version that could be called the zeta(2) area, where $\Sigma_1^t \frac{6z}{\pi t^2}$. The value π can be easily removed at any point during the analysis to determine if any significant volume, area, or circumference variations exist.

This means that the analysis will mostly consist of constant vector values and the analysis will need to include products, sums, and sums of products. Figure 16 presents the planned approach for the inverse-squared (post-zeta(2) area) model analysis. These discrete vector values will probably present a quagmire of relationships and ratios to be sorted. With no clear indications from the initial data samples exactly where the actual values will become essentially “locked-in” place, the data might reveal a purely stable state or catch the system in the middle of a mode transition.

Organization and Clarity

The analysis will summarize the findings in terms of each research model (magnitude and inverse-squared). Part of the organizing the findings will combine component concepts into the overall magnitude growth model to intentionally describe the system with some form of an integrated behavioral model. Findings from both models will be placed in a comprehensive summary table that describes their relationship to the three hypotheses: self-referential; harmonic, dynamical behavior; and descriptive system engineering models.

Chapter Summary

This new prime number model will require two types of models to compare system-wide behavior, a magnitude model that deals with the raw data vector values and an inverse-squared

model that deals with potential wave and power emission. The magnitude model will use raw data to build an event trace table. The inverse-squared model will provide a general direction of growth by dividing each new increment by its radius squared. The coordinate system and the core components will create the quadrant-based characteristics of growth, sine and cosine, normal vectors, and Doppler vectors. The summary of findings will include a table for each model type and a comparison of how the system-related finding provides details that support the three hypotheses of this dissertation.

CHAPTER 4: RESULTS

This initial study on the behavior and synchronization of the prime numbers used the core components from the self-referential coordinate system to determine the extent that the defined model meets the three hypotheses of this research. Those three hypotheses progressively built on each other by examining the harmonic vector and quadrant growth relationships from the self-referential framework and defining consistent reproducible system models. Reliability and consistency of the data built on itself as the models grew in complexity. As more data was analyzed and found congruent with the hypothesized expectations from the component and coordinate model, the near factorial permutations reinforced confidence in the data and the model. The initial basic model had 17,480 “nines” of reliability, due to 14,512 elliptical coils with 4 possible pole occurrences of “2” or “4”, the probability having the incorrect model was $1 - (1/2)^{58,048} = 1.0 \times 10^{-17,480}$.

Pilot Study

Two logical models were used for examining the properties of the integrated data sets from the components: a magnitude model and an inverse squared model. The magnitude model compares the total growth with respect to another vector or quadrant growth internal to the component model that was relational to the system’s coil time instead of relational to the number line. The inverse squared model took the same vectors and relationships from the magnitude model and divided each increment of $6z$ by the square of the coil number $\frac{6z}{t^2}$, the sum of which was referred to as a zeta(2) function where $\text{zeta}(2) = \sum_1^n \frac{1}{n^2}$. To accommodate an examination of relationships in area growth, our zeta function included π , with the $\sum_1^n \frac{1}{\pi n^2}$. The results of those two models (magnitude and inverse squared) drove the analysis.

The analysis with both models examined three sets of coil-based information: coils 1-200, coils 102,000, and coils 1-14,512. Any set of information or diagram for the coils 1 to 14,512 encapsulated all the increments for the first 100,000 prime numbers. Examining the system and vector properties involved the data for the four sets of system characteristics: trigonometric (sine and cosine, hypotenuse, tangent), 90-degree normal (field) vectors, and 180-degree Doppler vectors. The behavior analysis of the magnitude models was synchronized through the notable activities in an event trace table for each of the vector types for both the lower plane (axis values) and the upper plane (transition values). Validation of the combined lower and upper plane effects contributed to defining common system modes and themes throughout the analysis.

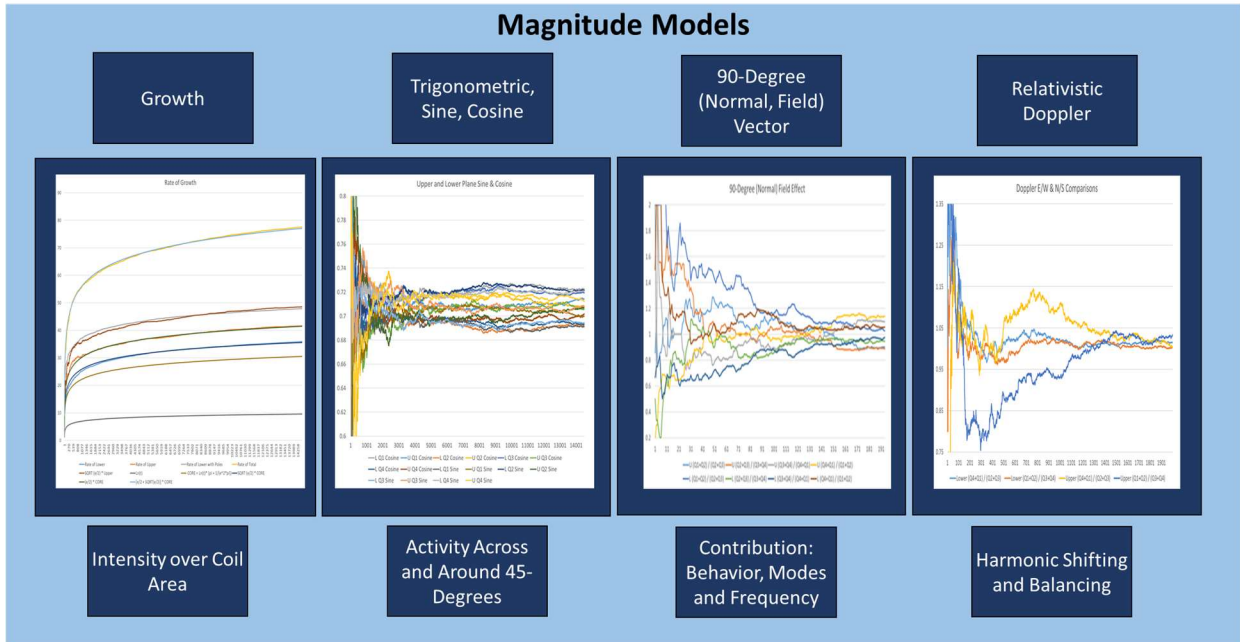
Magnitude Model Results

A baseline model was necessary to progressively build the system definition. This also required a specific sequence of concepts to be executed as the analysis progressed. The first concept selected to be described and bounded with this new component examination was the overall growth of the multiples of 6 ($6z$) over coil time. After the upper and lower plane growth was baselined, the next step was capturing all major movements on a standard timescale (coil time) and periods (1-200, 1-2,000, 1-14,512) and placing them in an integrated set data in the event trace table. As more systemic characteristics were discovered, those characteristics were used to update the common growth model(s) involved. Figure 17 provides examples of the four different types of magnitude growth characteristics provided by each model. The different plane intensity, or density, over the coil-time is revealed from the sine and cosine graphs. The 90-degree field across and around 45-degrees is revealed from the sine and cosine graphs. The 90-degree field

effect reveals frequency of changes in behavior modes. Periodic and harmonic changes in directional growth are revealed through a relativistic Doppler model.

Figure 17

Magnitude models and their contribution



Baseline of Growth Functions

Examining and comparing different aspects of overall growth in the component model guided the selection of a baseline model. Addressing the component growth characteristic would not be complete without explaining the parallel to current growth models in the common prime number distribution theorem. The traditional theorem of prime number distribution has a different twist in defining growth...where the question is “how many primes are on the number line within the value of x?” There is an underlying assumption that supposes the best way is to

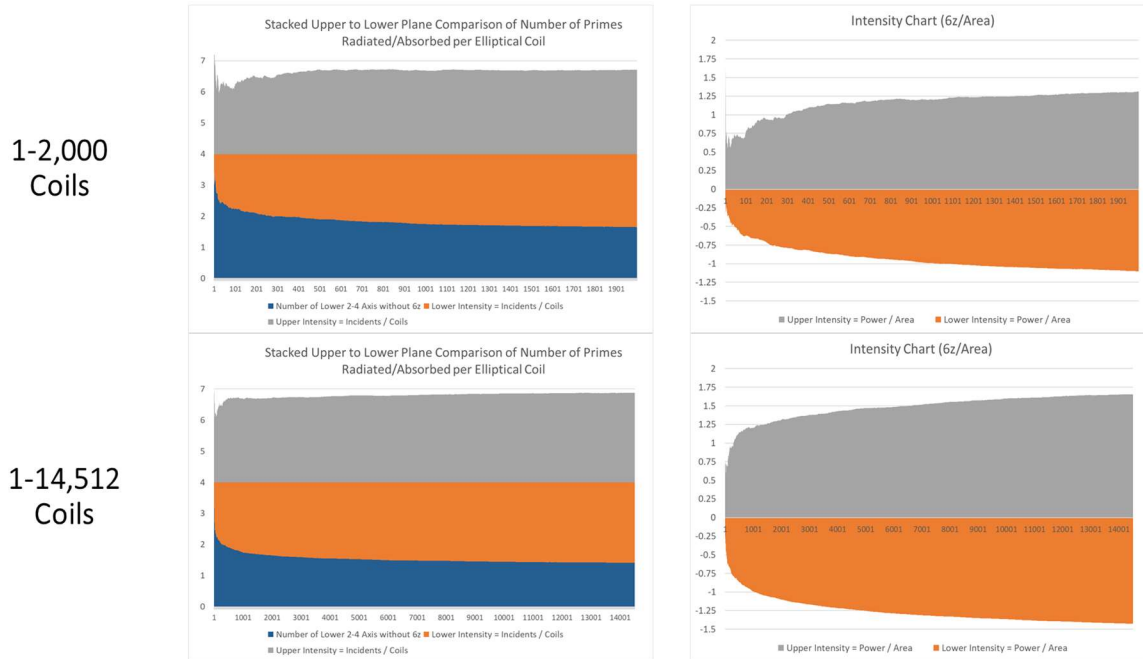
treat a prime number as an incompressible atomic single value. The component model in this research is much different than the traditional prime distribution approach on the number line.

The difference is best thought as a packaging of components. The component model has every prime number after 5 as an additive accumulation of the component multiples of 6 ($6z$) along with the additive accumulation of axis values (2-4-2-4-2-4, etc.). A prime number is a “package” of those component values; hence, a component approach allows for more than one function to influence the prime number growth over a coil or time slice. System-like smoothness with natural logarithmic related growth characteristics were both desired and delivered with the component model. The same could not be said using the traditional prime number distribution packaging in the coil distribution model. Figure 18 shows the comparison.

Figure 18

Traditional distribution package versus component 6z growth

Occurrences of Prime Numbers vs. Growth of 6z System



18.a. Distribution of incidents over components

18.b. Magnitude of 6z component growth

The traditional approach to prime number distribution is one of binary occurrence of a prime number, without regard for the components discussed in this research. The leftmost graphs (Figure 18.a) placed the occurrences of prime number traditional packaging as incidents of into the component model to examine systemic behavior. The result was that their frequency of occurrence flattened relatively early. The straight line at the value of four in Figure 18.a, separating grey from orange, is the constant total of four prime number “incidents” at each of the four axis intersections. For the purpose for comparison in this research, the incidents of prime numbers that included an increment of $6z$ is noted as a parameter. They grey represents the upper plane incidents (that would naturally only be $6z$) and the lower plane incidents of $6z$ in orange. In both upper and lower planes, the average incidents of $6z$ are relatively flat. This implies that the real systematic growth is found in the magnitude of the $6z$ increments, not in the number of incidents.

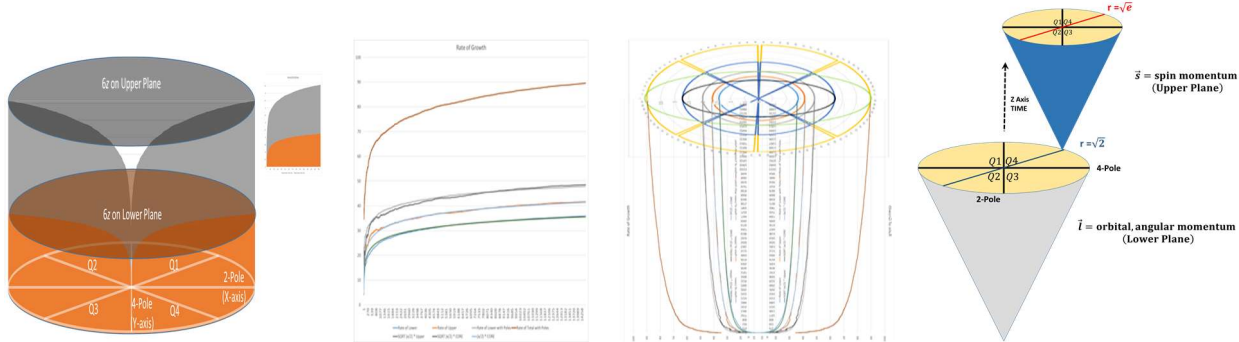
The magnitude of $6z$ growth in Figure 18.b shows that logarithmic and systemic behavior for both the upper and lower multiples of 6 ($6z$). A forced negative value on the pole magnitudes of $6z$ (in orange) was used in Figure 18.b mainly for visual comparison of $6z$ magnitude to incidents in Figure 18.a. The exact ratio between the lower and upper plane magnitude growth provides the baseline for the next stages of modeling and analysis.

The examination of the ratios between overall component growth (upper and lower) are reflected in Figure 19. Figure 19.b displays a graph of these logarithmic values compared to the estimates of the ratios. Those ratios were depicted on a polar coordinate graph with the circular values of 4 (outer), e (blue), 2 (grey), \sqrt{e} (red), and $\sqrt{2}$ (light blue) in Figure 19.c. The persistent

ratio of $\frac{\sqrt{e}}{\sqrt{2}}$ in different relationships also led to consider to \sqrt{e} and $\sqrt{2}$ as radius values. A more detailed diagram of the polar view is provided in Appendix A.

Figure 19

Systematic logarithmic magnitude 6z growth



19.a. Horizontal growth 19.b. Comparison of planes 19.c. Vertical polar growth 19.d. Notional natural system

The overall relationships relying on a common ratio of $\frac{\sqrt{e}}{\sqrt{2}}$ helped reveal a core function of $(\pi + \frac{1}{e^2\pi}) t \ln(t)$ since the lower plane growth is $\frac{\sqrt{e}}{\sqrt{2}} (\pi + \frac{1}{e^2\pi}) t \ln(t)$. The upper plane growth was approximately $\frac{\sqrt{e}}{\sqrt{2}}$ times the lower growth. The lower plane “after” pole values were added was $\frac{\sqrt{e}}{\sqrt{2}}$ times the upper plane. This was a definite structural relationship for the magnitude growth that provided an alert for potential relationships in reviewing the system’s behavior with the event trace table.

Two earlier general properties led to the possible quantum behavior associated with electron acceleration and electron spin. Those two properties were the field vector relationships that resembled an electromagnetic field and the physical model’s distribution of 6z that fit well with the expectations for a current flow behavior. For possible quantum behavior, Figure 19.d is

a notional model for a natural physical system based on the upper and lower plane growth relationships of $\frac{\sqrt{e}}{\sqrt{2}}$.

While Figure 19 provides a vertical and conical model of growth, Figure 19.a provides the horizontal growth model over 2π . The upper right sub-diagram shows the stacked quantities of the $6z$ logarithmic on the lower plane (orange) and the upper plane (grey). These generic models provided a baseline of concepts for analysis in the vent trace table.

Event Trace Table Analysis

Building a table of events that trace the upper and lower vector behaviors over coil time required marking and annotating the events for each of the four component characteristics. Events included not just spikes but also events of stability, transitions, pairing, flipping, and increased growth rates. The sample in Table 6 covers the initial stages of data from 90-degree, Doppler, area, total magnitude, and the activity compass.

Table 6

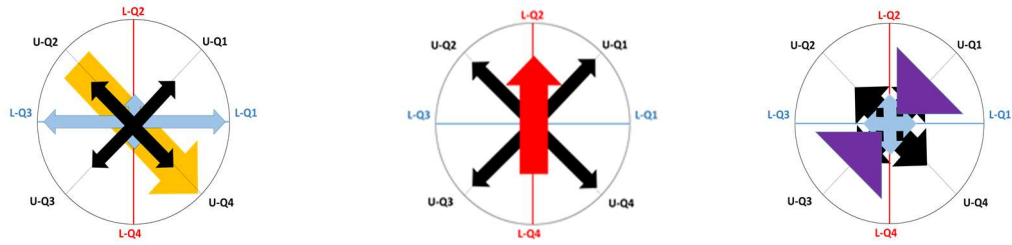
Sample of capturing data points and activity compass

Method for Capturing Data Points, Preparing for Analysis													
Variation	Activity Type	Coil of Event											
		2	4	6	12	16	24	26	28	30	40	48	56
Upper	$\ln(t+6), e^x$	2.08	2.30	2.48	2.89	3.09	3.40	3.47	3.53	3.58	3.83	3.99	4.13
	Upper Growth Estimate	9.00	9.97	10.76	12.51	13.38	14.72	15.00	15.26	15.51	16.57	17.27	17.86
	90-Degree			Q2 - Q4 Rev.									
	Doppler												
	Area	Stale	Up	Stale	Up	Stale	Up	Stale	Up	Stale	Up	Up	Up
Upper and Lower	Total	24	84	96	276	360	672	672	720	780	1296	1656	1896
	Activity Compass												
	Lower Growth Estimate	7.72	8.55	9.23	10.73	11.48	12.63	12.87	13.09	13.30	14.21	14.81	15.32
	90-Degree				Q2 Boost					Q1 - Q3 Rev.		Q1 - Q3 Rev.	
	Doppler	W/E & N/S Close Parallel								W/E & N/S Rev.	W/E & N/S Parallel	W/E & N/S Rev.	W/E & N/S Tango
Lower	Area	Up	Stale	Up	Stale	Up	Stale	Up	Stale	Up	Stale	Stale	Stale
	Total	0	12	48	144	228	420	468	564	612	876	1140	1368
Ratio	Upper/ Lower Area	--	7.000	2.000	1.917	1.579	1.600	1.436	1.277	1.275	1.479	1.453	1.386

For vector values and their potential relationships, an activity compass was placed in the table to annotate directional W-E Doppler reversals in the same circle with 90-degree Doppler reversals and paring. What is an “activity compass”? An activity compass documents, in picture form, the movement or shift in amplitude between vectors. It was done to capture the Doppler movement and compare it with the 90-degree field vector movement in the same combined diagram. Figure 20 gives the most prevalent activity compass examples of amplitude movement (or flipping) between the upper plane (diagonal) quadrants and the lower plane (cardinal axis) quadrants. In Figure 20.a, the light blue (lower plane) and black (upper plane) arrows display a proportional expression of the Doppler vectors, while the yellow shows a large shift from upper Q2 to upper Q4.

Figure 20

Sample of color-coded 90-vector activity compass



20.a U-Q2Q4 Quadrant flipping

20.b L-Q4Q2 Quadrant flipping

20.c U-Q1Q3 Pairing

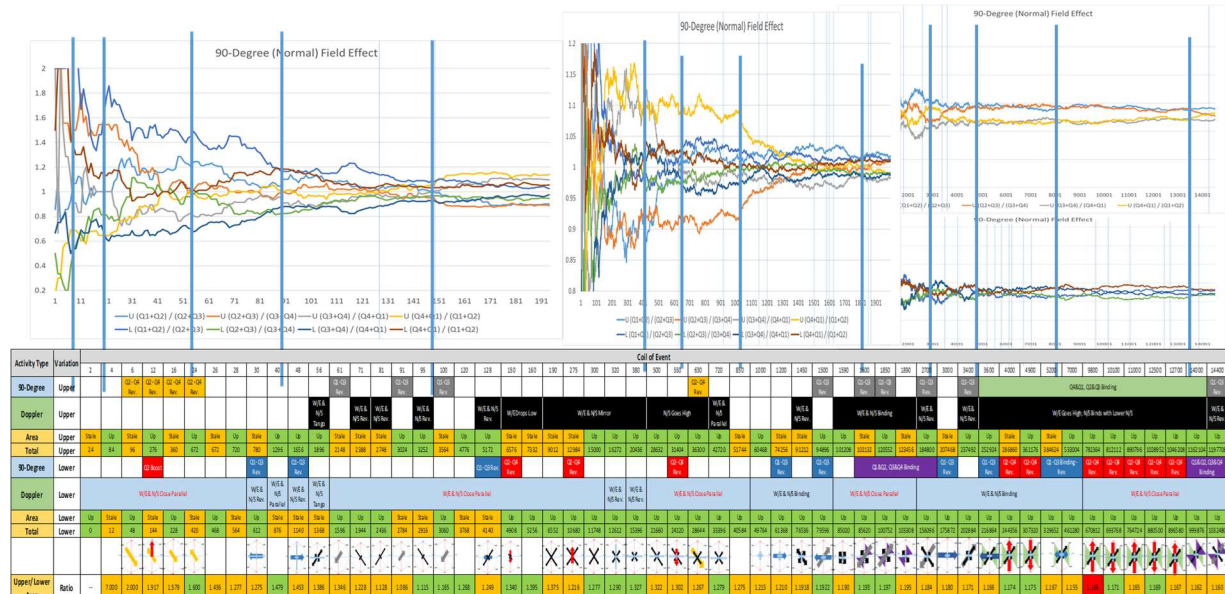
Figure 20.b shows an evenly dispersed upper plane Doppler (black arrows) and a large lower plane shift making the lower Q2 greater than the lower Q4. When the values of the upper

plane 90-degree vectors form a pairing or parallel relationship, inner-facing triangles (purple) were used to annotate this behavior, as seen in Figure 20.c.

Figure 21 is a high-level summary of the annotated data points for flipping and magnitude shifts. Activity flips were the lines performing a functional cross over the balancing growth ratio value of “1”. In the rightmost graphs, valuable data was also gathered at external crossovers on the extreme outside borders. These values portrayed how a relationship between different quadrants may form “heavy” or “light” pairing of values on adjacent quadrants, not just the reciprocal behavior on diagonal quadrant values. This would help identify periods of flywheel effects from increased off-balance magnitudes. If the values only presented perfectly symmetrical reciprocal relationships, there would be no expression of balancing bursts of acceleration. It would be much like a magnetic field without a changing flux of a current. In that manner, the paring variations aligned with the expected behavior of an electromagnetic field.

Figure 21

Sample of event analysis performed with vector graphs, activity compasses



The extent of cross examination required during and after this data was captured cannot be trivialized. It was an integrated review of the sine, cosine, hypotenuse, tangent, Doppler, and field vectors. All data sets were aligned with the key sets of coil activity in mind. Activity on the first 200 coils, the first 2000 coils, and then the first 14,512 coils were compared. A grouping of all diagrams and vectors marked for the event trace analysis is in Figure 22. Separate pages are provided in Appendix A for each of the diagrams for closer examination. The grey box inside Figure 22 notes that fact that the upper plane sine and cosine had no change when the 2-4 poles/axis were added, due to all 2-4 pole/axis values only residing on the lower plane.

Figure 22

Grouping of all diagrams for event trace

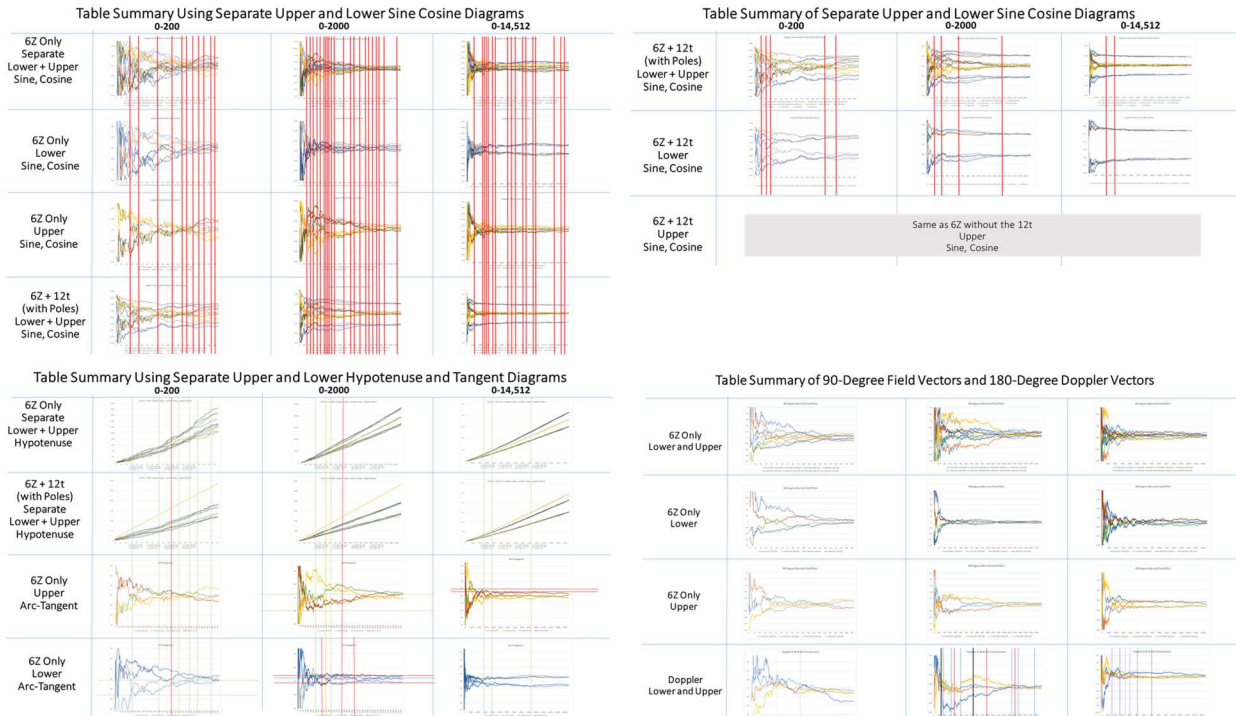


Figure 23 shows the final event trace table. The analysis revealed specific trends and themes. Large flipping and reversing vector activities are annotated by either red or yellow cells inside the appropriate system characteristic rows. In general, long periods of vibration around 45-degrees on one plane were occurring at the same time the systematic flipping or inverting of roles were occurring on the other plane. There were also long periods of vector pairing for the upper plane vectors, while lower plane vectors indicated a mode almost like a fuel and air mixture in an engine as it reached its next mode of torque level and fuel demand. The clear trade-offs between the upper and lower plane sines showed something like the synchronization of seismic force and vibrations between the West/East (upper plane) vectors and the North/South (lower plane) vectors. Two expanded landscape pages are provided in Appendix A for closer review of details.

Figure 23

Even trace of all vector properties

		(Yellow Rows) Tradeoff between Upper and Lower Sine vibration at 45-Degrees		System-Wide Activity and Flipping		(Yellow Rows) Multiple Lower Sine vibration Flipping while Upper is mainly Pairing		System-Wide Mode Shift to Pairing		(Orange Rows) Upper Tangent Q1&Q3 Controlling 45-degree vibrations	
Vector	Activity	1	2	3	4	5	6	7	8	9	10
	1	2	3	4	5	6	7	8	9	10	11
Lower	1	2	3	4	5	6	7	8	9	10	11
	1	2	3	4	5	6	7	8	9	10	11
Upper	1	2	3	4	5	6	7	8	9	10	11
	1	2	3	4	5	6	7	8	9	10	11
Role	1	2	3	4	5	6	7	8	9	10	11
	1	2	3	4	5	6	7	8	9	10	11
Upper Lower	1	2	3	4	5	6	7	8	9	10	11
	1	2	3	4	5	6	7	8	9	10	11
Role Color	1	2	3	4	5	6	7	8	9	10	11
	1	2	3	4	5	6	7	8	9	10	11

Summary of Magnitude Analysis

This summary differentiates the types of results and behaviors in the event trace from the functional categories reviewed. The analysis of the sine and cosine revealed quantitative angular velocity characteristics that added a better correlation to a behavioral model of electron or quantum spins. Analysis of the 90-degree field vectors revealed total systemic behavior and stabilization, from an initial stabilization like a rotor and stator behavior mode stabilization to balancing all 100,000 prime number increments over the 14,512 coils. Doppler data provided an insight into the relativistic transfer of increments that produced a flywheel effect exchanged between directions and planes.

The most productive analysis was the result of examining the differences between the planes instead of the sums of upper and lower plane values. There were two reasons for this higher return on investment from separated data. One reason was that the analysis proceeded from an external total value model to an inward dissection of properties. The larger characteristics of combined behavior are the ones that led to these segmented investigations. Another detail layer of internal aspects considered from the partial derivative relationships revealed an even more defined internal dynamical balancing and discrete behaviors. After the Event Table was completed, related shift and flips in behavior between different types of vectors were compared with a resulting update to the magnitude growth model.

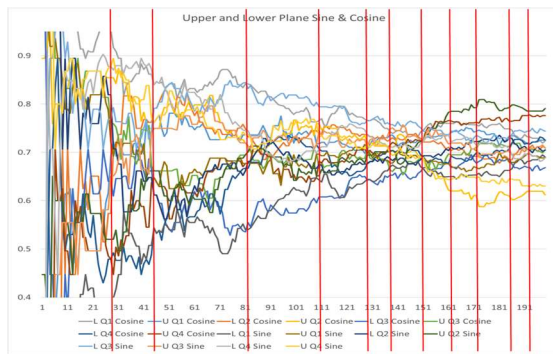
Sine and Cosine Analysis

The sine and cosine graphs provided the most meaningful data for modifying the common growth model. It should first be noted that the analysis of the hypotenuse functions

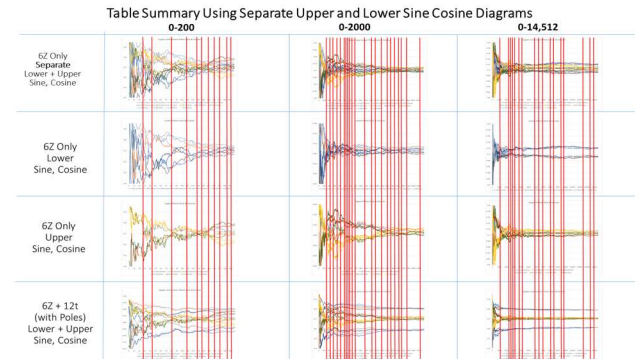
were part of the sine and cosine analysis, as an essential element. Figure 24 is a sample of event-annotated graph for the different sine and cosine behaviors over time. Another variation was reviewed that combined the sine or cosine values with sums produced excessive white space between the amplitudes, which was only good for general behavior instead of the separation between upper and lower plane. The leftmost graph in Figure 24.a provides a zoom-in of coils 1-200 as an example of the annotating the major flipping behavior between sine and cosine relationships across or around 0.707, or 45-degrees. The balancing and trading of places seemed to be the predominant theme in all models. Large convergence and flipping around coil 144 were a common theme of in all magnitude vector analysis (90-degree field vectors and Doppler vectors). Another significant behavioral indicator was revealed in the two thumbnail graphs in the middle of rightmost column of diagrams in Figure 24.b. These two graphs represent the sine and cosine behaviors on the lower and upper planes. The lower plane graphs show a white-space gap looking almost like tongs or a bug with long antennae. The upper plane provided a complement of that gap with concentrated activity over the exact timeframe.

Figure 24

Sample of sine and cosine events marked



24.a. Zoom-in of coils 1-200



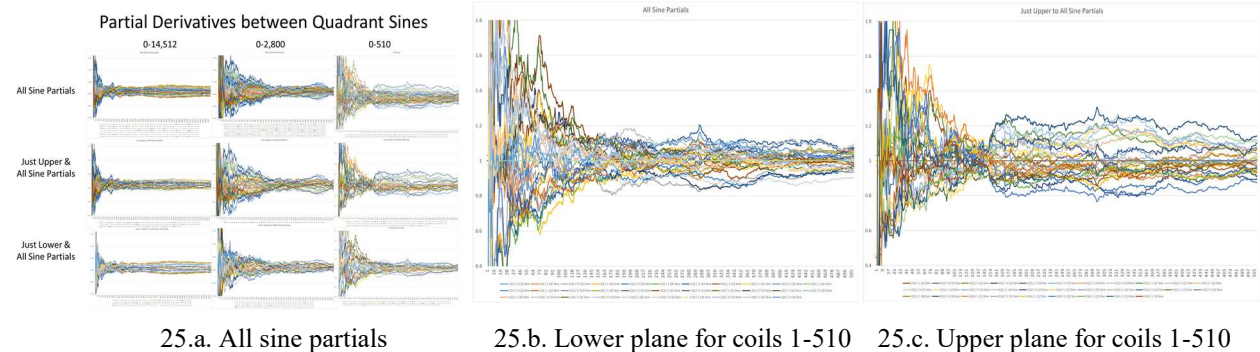
24.b. Comparison of upper and lower behavior

In the event trace summary, this behavior was one of the most significant demonstrations of the system trading, flipping, and claiming ownership of a 45-degree stability between the upper and lower planes. It appeared to drive overall synchronization. With nothing specifically declaring that the prime number increments must balance sine and cosine activity between the two planes, this was groundbreaking information. It should be mentioned here that reinserting the pole values into the sine and cosine relationship only created a large graphic gap and steady state difference seen in the lower right corner of Figure 24.b. The upper plane was not affected due to the pole values of “2” and “4” only occurring on the lower plane. Otherwise, the main contribution of the pole values was to provide placements for cardinal coordinates.

After looking even deeper into the interrelationships between the sine activity, each quadrant’s sine was compared to the sine of all other quadrants, both upper and lower. This investigation provided a partial derivative comparison between the quadrants, with the sine values representing a growth rate of the quadrant’s sine over time. Due to some unique properties for the partial relationships of the sines, a different capture of the coil periods was performed with coils 1-510, 1-2800, and 1-14,512. Thumbnail diagrams of the cumulative quadrant sine partial derivatives are shown in Figure 25.a.

Figure 25

Sine partials reveal two systems



The discovery, or contribution, of this view in Figure 25 was its depiction of two distinct separate systems between the lower plane and the upper plane. The clearest presentation of those properties was produced when comparing Figure 25.b and Figure 25.c for coils 1-510. Two distinct systemic differences exist. Figure 25.b shows the lower plane's screw-like rotary action of the relational amplitudes, with the relationships from the two mid-graph top spikes twisting at angles of 45-degrees and 30-degrees respectively to the lower base sine values over time. The upper plane is very different, it displayed very evenly radiating relationships. The upper plane sine partials in Figure 25.c were more like a consistent magnetic field. If an orthogonal time slice was done on any of the coils, the upper plane (Figure 25.c) would produce a flower-like diagram due to its balance. The same could not be said for the lower plane. Their combined relationship could be correlated to the operation of a rotor and a stator. Larger landscape version of the graphs in Figure 25 are provided in Appendix A for a closer review of details.

90-degree Field Vector Analysis

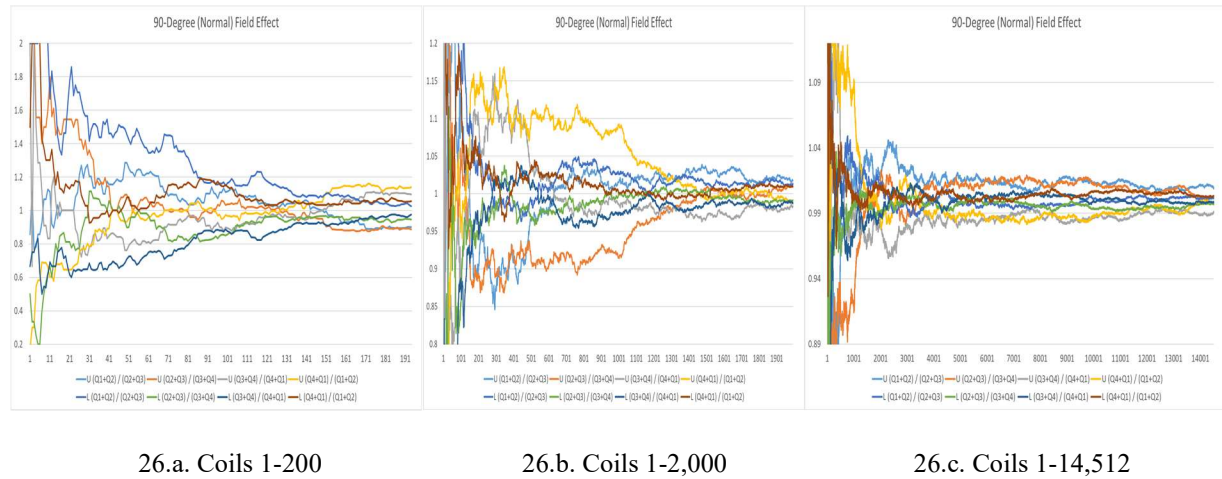
What type of systemic behavior do the 90-degree vectors produce? These vectors were also called field vectors in this research due to their form based on a right-hand-rule property expected from an electromagnetic field. Figure 26 captures all three coils period 1-200, 1-2,000, and 1-14,512 that show tightening convergence of all vectors over time. Each graph in Figure 26 is a closer zoom-in of the amplification scale around the value of one.

As expected, system reversals and mode shifts abounded, so some lower and upper plane tradeoffs should be discussed. With coils 1-200, the extreme values from the two blue lines were from the lower plane and with coils 1-2,000 the extreme values from the yellow and orange lines were from the upper plane.

From the previously discussed upper and lower plane rotor and stator behavior of the sine, some form of correlation with this larger integrated balancing of electromagnetic fields was expected. This occurred after a large system stabilization at coil 144, the same point that the sine partials distinctly moved into a clear rotary rate. It is called a stabilization mainly due to the expected lower plane reciprocal relationship between quadrant 2 and quadrant 4. A landscape page is provided in Appendix A for closer review of details.

Figure 26

Upper and lower plane 90-degree field vectors



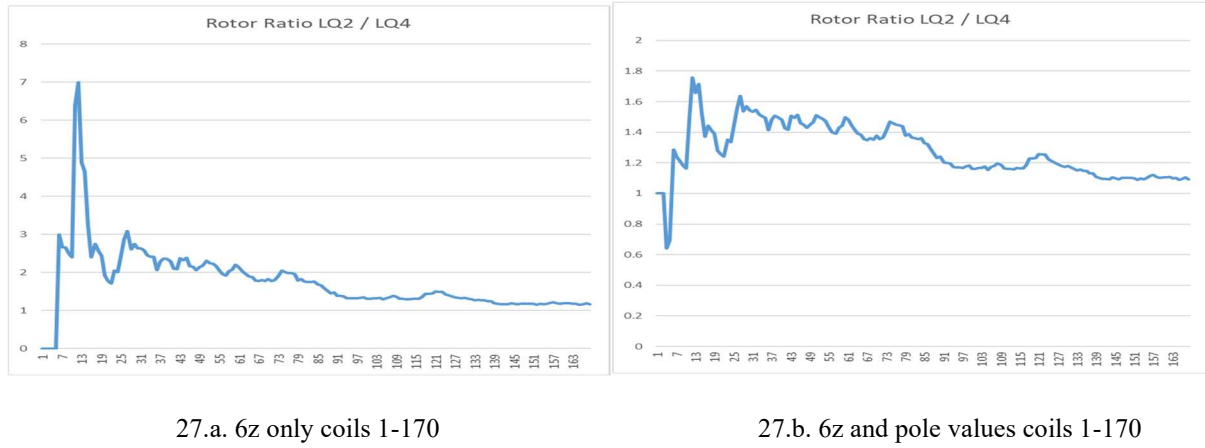
A relatively clean reciprocal relationship existed between all other vectors and their diagonal counterpart (Lower Q1&Q3, Upper Q1&Q3, Upper Q2&Q4). Not so with lower Q2&Q4, lower Q2 had either continually higher or jumped at increments more than lower Q4. A coil-by-coil comparison between lower Q2 and Q4 revealed the true behavior. Figure 27.a provided that from a magnitude perspective, a large boost occurs in Q2 at coil 12.

The strange, or troublesome part was that one large spike in what so far appears to be a non-random system. This coil 12 spike of lower Q2 in Figure 27.a was almost like a rotor's

starting offset bias, either angular or power based. Figure 27.b shows the forced stabilization that happened when the pole values of 2 and 4 are reinserted into the growth relationships of the 90-degree vectors. After it reached coil 144 the running speed overtook the initial start-up bias offset and it moved into a different mode.

Figure 27

Lower Q2 and Q4 comparison



This forced stabilization from the added poles (Figure 27.b) happened due to the total added value of “6” to both vectors in the 90-degree relationships. That added a value of “6” to both the numerator and denominator. The sum of two adjacent quadrants (with a 2 and a 4-pole added) were divided by the sum of the other two adjacent quadrants (with a 4 and a 2-pole added respectively). As a note, the forced stabilization was only on the lower plane. That extra smoothing benefit only be applied to the upper plane when a combined system view of the lower and upper plane values was used. Therefore, there were two distinct contributions of the pole values when reviewing the 90-degree field vector relationships: as coordinate placements for values of 6z and for rapid stabilization of the lower plane.

Although this stabilization at coil 144 was in the early stages of the 14,512-coil analysis of the 100,000 primes, it should be noted that it is around the 1,000th prime number. The significance is that this type of stabilization behavior was it would not have been indicated in smaller studies (under 1,000 primes), especially without the self-referential framework and component coordinate system. It occurred at what easily could have been a geometrically driven action, at the point where volume from one perspective intersected with area from another perspective. From a quantitative perspective, at coil 144, the total value of all $6z$ components was within the range of $5,428 \pm 12$, depending on the quadrant selected between coils 144-145. At coil 144, the quantity of 5,428 had two meanings in the component model. From a volume perspective, $5,428 = (12^3)\pi$, which is the number of coils (144) times the total pole value per coil (12) times π .

The logarithmic growth then splits clearly into two forms at coil 144. The total $6z$ amount at coil 144 of 5,428 aligned with the number of prime number incidents ($1,000 \pm 4$) * 2^*e . For the remaining 99,000 incidents, the total lower plane value of 521,088 ($95,848^*2^*e$) also provided less than a 4% margin of error. The larger significance to the model was that the previous rate of “total” acceleration or force ($6z$) became the rate for only the lower plane after coil 144. The upper plane generated its own value of $\frac{\sqrt{e}}{\sqrt{2}}$ times the lower plane total of $6z$. The overall system growth rate changed by some dynamic, but the lower plane appeared to have assumed the previous rate of the entire system. This aligned with the expected new role of the lower plane as a rotor that reached a stable operating speed. A more introspective look at the internal tensors and relationships of partial derivatives revealed another characteristic of reciprocals that supported the dynamically balancing system.

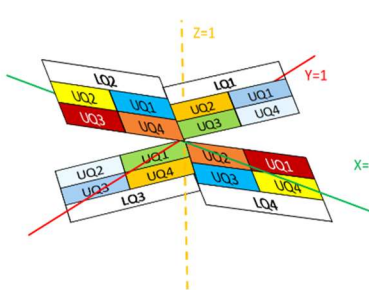
What would the relationships between these field vectors be like when they were treated as a system vibration or tensor? Did they reveal an off-balance characteristic or a reinforcement of the existence of a dynamical system? Figure 28 provides the framework and the results of that analysis. Figure 28.a displays the lower quadrants in outlying white boxes, with color-coded upper quadrant product relationships with each lower quadrant in the middle section. The cells with the same color are reciprocals of each other (e.g., $LQ1^*UQ2 = 1/(LQ4^*UQ4)$). A product matrix showing its determinate value of zero is provided in Appendix A. These 16 tensor-like properties indicated a possible system of equilibrium and a possible hyperbolic relationship of planes, depicted in Figure 28.b in concept form. Overall, the tensor products reinforced the existence of a dynamical system, along with another potential characteristic it revealed from the graphing of these values in Figure 28.c for the 100,000 primes.

Figure 28

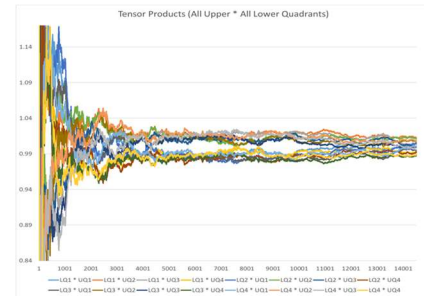
Lower to upper tensor products

LQ2		LQ1	
UQ2	UQ1	UQ2	UQ1
UQ3	UQ4	UQ3	UQ4
UQ2	UQ1	UQ2	UQ1
UQ3	UQ4	UQ3	UQ4
LQ3		LQ4	

28.a. Color-coded reciprocals



28.b. Graphic of table relationships



28.c. Tensor products of 100,000 primes

A harmonically balanced characteristic was revealed from the white or null space

between these vector product values. It also revealed an evenly distributed diffusion in the far-right side of Figure 28.c after coil 11,000. Alternating periods of inward vibration and periods of

external shell vibrations occurred at what appears to be a changing frequency. The significance of this behavior was that it balanced all growth provided by the prime number increments of $6z$. It was as if the structure built on itself and continued to absorb energy as it converged and balanced these forces. This was exactly the type of behavior that could be expected from a living system over a span of its lifecycle, assuming no defects or flaws in the structure produce a degrading offset, similar to the effect of a cancer. With the concept of the directional balancing of force, this is an appropriate point to transition into a discussion on the results from the analysis of Doppler properties.

Doppler Vector Analysis

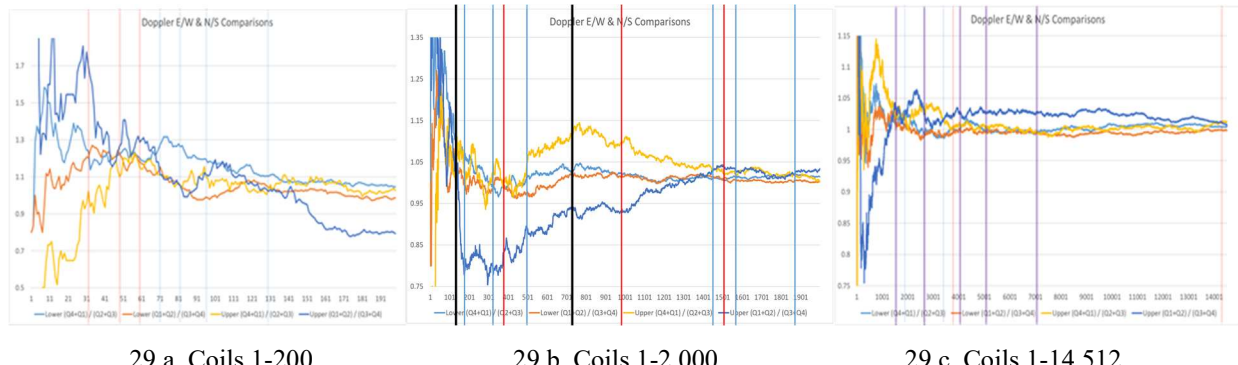
As with the sine, cosine, hypotenuse, and 90-degree field vectors, the upper and lower plane Doppler vectors were best analyzed separately with considerations later made for any combined effects. When reviewing the Doppler behavior, it helped to consider a known system that typifies the expectations from Doppler, the transmission of sound waves. While the analysis in previous sections (sine and normal vectors) correlated closely to electromagnetic properties with coil 144 stabilization of the rotor or screw-like relationship to a stator or magnetic field relationships, considering sound wave Doppler introduced a different property. Sound waves have known velocity ratios between mode transitions, such as from sonic to hypersonic.

Figure 29 provides the Doppler graphs for the three coil sections of analysis commonly used throughout this research: coils 1-200; coils 1-2,000; and coils 1-14,512. Building from the previous point of system stabilization and transition, the activity around coil 144 was the best focal point for discussing Doppler behavior. In Figure 29.a there was a large drop in the dark blue line that represents the upper plane Doppler ratio of West/East, also expressed in quadrant

relationships as $(UQ1+UQ2)/(UQ3+UQ4)$. The other three Doppler values (Lower W/E, Lower N/S, Upper N/S) all continued within a relatively close margin of balance. Comparison between a Doppler's points of mode transitions revealed key ratios. The next major activity in coils 1-2,000 exemplified and validated the importance of focusing on those ratios and relationships. Figure 29.b shows how the below-margin Doppler of the upper W/E along with the other three Dopplers were continually in close relationship until approximately coil 500. At coil 500, the upper N/S yellow line moved exactly parallel with the upper W/E (blue line) until coil 720 when both the upper N/S and W/E were straddling the equilibrium balance value of “1”. With a ratio of 5 to 1 ($720 = 5 \times 144$), it resembled a sonic and hypersonic relationship.

Figure 29

Upper and lower plane Doppler vectors



Reflecting on the earlier set of data and the large parallel movement at coil 500, it should be noted that the “joining” or pairing of the upper N/S with the two lower plane Dopplers was at approximately coil 100. That defines two different actions of joining and separating at a ratio of 1 to 5, with both occurring slightly out of phase (coil 100 versus coil 144). That ratio repeated as a theme.

Reviewing the next major intersection point at coil 1,440, it occurred at 10 times the large separation at coil 144, and 2 times the balancing activity at coil 720 for the upper W/E Doppler. Also considering the doubling factor with the ratios of 1 to 5, in Figure 29.c there was another flipping of Doppler values between upper W/E and N/S near coil 2,880, at twice the distance of coil 1,440. Yet another flipping between the upper W/E And N/S Dopplers occur around coil 3,600, or 5 times the balancing that happened at coil 720. Just within the bounds of the 100,000 primes in this research, a final concluding intersection of vector values fittingly happens near coil 14,400, which was 100 times the separation at coil 144. The conclusion was that ratios of 2, 5, and 10 have a definitive role in the Doppler behavior much like their role in the speed of sound waves. This finding added an extra dimension of validation to the component model operating as a system.

Applying Findings to Common Growth Model

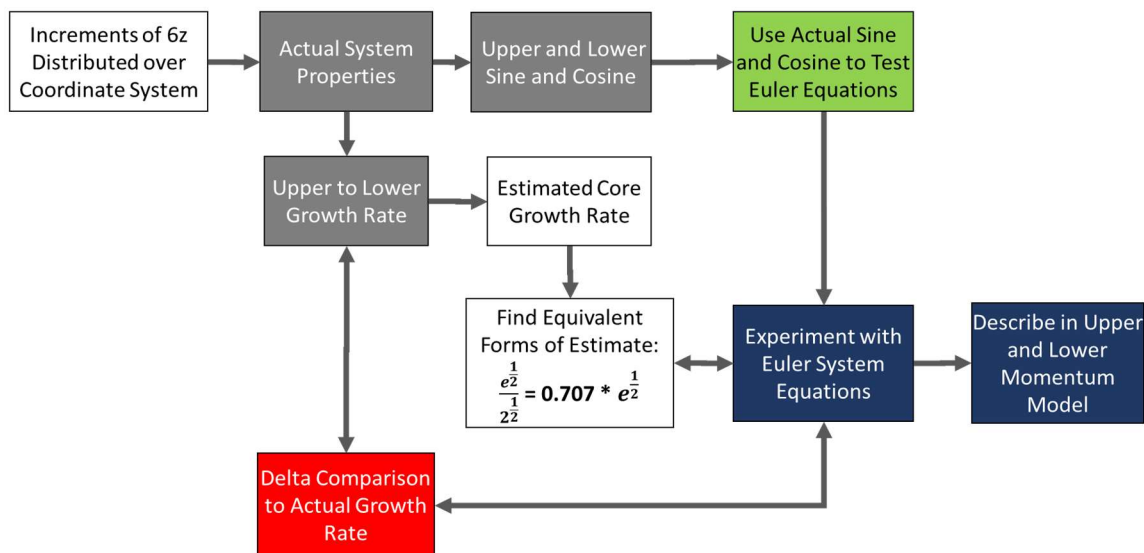
Enough additional characteristics were discovered with the internal relationships of sine and cosine, 90-degree field vectors, and Doppler vectors to consider how any refinements could have been made to the original magnitude growth model. The most important value from the earlier model was the ratio of growth relationship between the upper plan and the lower plane for the multiples of $6z$. That ratio of $\frac{\sqrt{e}}{\sqrt{2}}$ represented a total growth rate for upper/lower, yet the sine and cosine analysis, along with the vector comparisons, reveal a balanced exchange of what could have been considered vibrational energy. With some jitter in the early upper to lower coil, the ratio of $\frac{\sqrt{e}}{\sqrt{2}}$ was translated into a form that allowed the properties of sine and cosine to duplicate the jitter and find a more exact equation. This was accomplished by applying an Euler form to the growth ratio of $\frac{\sqrt{e}}{\sqrt{2}}$. With a focus on the sine and cosine values around 45-degrees,

the ratio was translated by making $\frac{\sqrt{e}}{\sqrt{2}} = (0.707)e^{\frac{1}{2}} = (0.707)e^{(0.707^2)}$. Figure 30 describes the process used to find an exact solution using the actual upper and lower plane sine and cosine values over time as the test data that drove every derived Euler translation of the growth rate. Those jitters in the actual upper to lower plane growth ratio (or what could have been mistaken as chaos) provided the fine-tuning comparison for making changes to the Euler translation.

Figure 30

Process used to find an exact solution

Approach to Finding an Exact Growth Equation



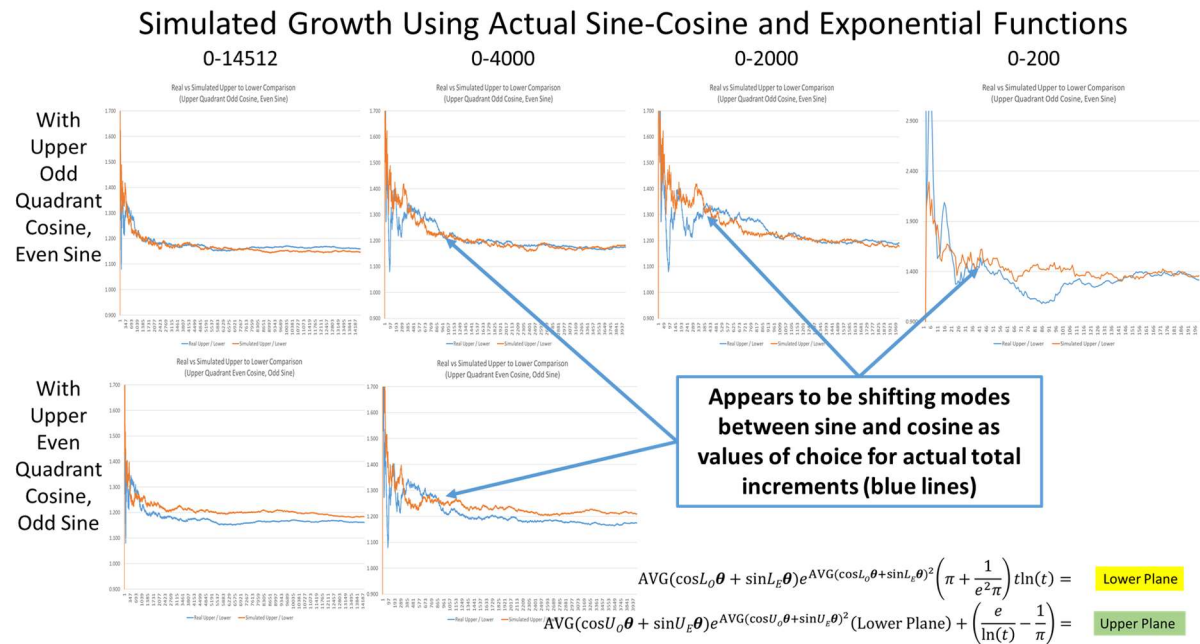
The process of discovery consisted of using the upper to lower plane growth ratio that generated possible equations and then the actual sine and cosine data from each of the 8 quadrants were used to test and stimulate system growth equations. Figure 30 describes the overall process used to generate and examine over 100 iterations of equations variations.

Initially just a cosine function was used so the $e^{(\cos \theta)^2}$ would approximately produce the $(e^{\frac{1}{2}})$, but that was too flat and lacked the desired variations.

Other attempts using all averaged sine and cosine values for each plane still produced an overly flattened line. The solution was discovered by leveraging the fact that the sine and cosine values are already derivatives, actual growth over time. Returning to the physical properties of the coordinate system also provided the best approach, due to the multiples of $6z$ on the lower plane intersecting with an axis. This guided an axis-focused selection of sines and cosine sources. The conclusion was that lower plane intersections in the odd quadrants (LQ1, LQ3) should use the cosine (x-axis), while the lower plane intersections in even quadrants (LQ2, LQ4) should use the sine (y-axis). Tradeoff and variations were done to ensure that the closest estimate of the function was being made, as shown in Figure 31.

Figure 31

Adjustments and accuracy of estimated function



For a clearer translation from the earlier growth ratio of $\frac{\sqrt{e}}{\sqrt{2}}$ and the observed relationships, Figure 32 provides a color-coded mapping of those equations. The key relationships were the upper plane to lower plane, the lower plane to the core, and the complete system equation. Many variations on the Eulerian angles and frequencies were done before settling on the equations proposed in Figure 32. Due to the needed balance around a value of 0.707, the average values of those axis intersection points from the odd quadrant cosine and the even quadrant sine were used. Further research may result in a means of exactly correlating to the minor mode shifts in Figure 31 by possibly considering the activity from the Doppler and 90-degree field vectors mode shifts, some property revealed by the inverse-squared vector values, or the insertion of another dimension using a radius with the imaginary value “ i ” in “ $i\sin LE\theta$ ”.

Figure 32

Resulting translation of growth rate into Euler form

Consider tailoring Euler

$$\left(\frac{e}{2}\right)^{\frac{1}{2}} = \text{AVG}(\cos L_0 \theta + \sin L_E \theta) e^{\text{AVG}(\cos L_0 \theta + \sin L_E \theta)^2}$$

L_E, L_O =Lower Even, Lower Odd Quadrant
 U_E, U_O =Upper Even, Upper Odd Quadrant
 Axis Crossing = Lower Movement = $\text{AVG}(\cos L_0 \theta + \sin L_E \theta)$
 $V_{LO} e^{(V_{LO})^2}$

$$\text{AVG}(\cos L_0 \theta + \sin L_E \theta) e^{\text{AVG}(\cos L_0 \theta + \sin L_E \theta)^2} \left(\pi + \frac{1}{e^2 \pi} \right) t \ln(t) = \quad \text{Lower Plane}$$

$$\text{AVG}(\cos U_O \theta + \sin U_E \theta) e^{\text{AVG}(\cos U_O \theta + \sin U_E \theta)^2} (\text{Lower Plane}) + \left(\frac{e}{\ln(t)} - \frac{1}{\pi} \right) = \quad \text{Upper Plane}$$

Many unsuccessful attempts were also made to place the Euler equation in a form of a compound derivative to form a simpler equation. The rude awaking was that the discovered Euler was already in derivative form, due to the sine and cosine already in derivative form.

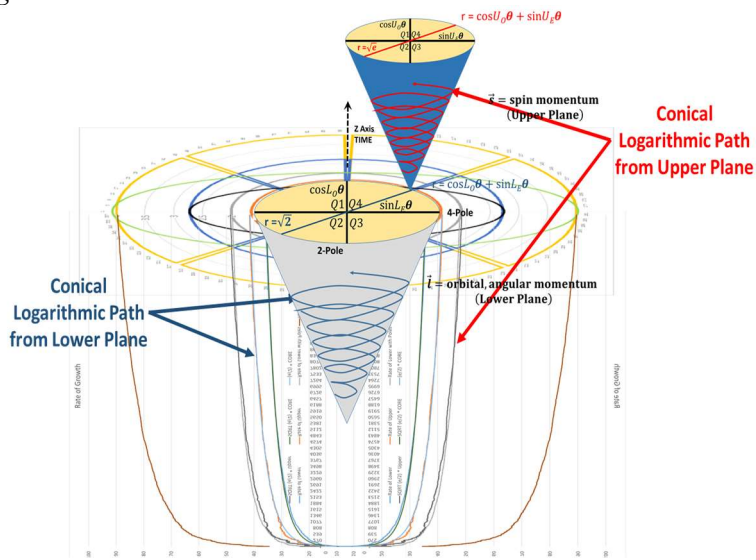
Therefore, with starting equation already a derivative, it was defined as an angular velocity, with

$(\cos LO\theta + \sin LE\theta) = \left(\frac{d}{dt} \sin LO\theta + \frac{d}{dt} \cos LO\theta \right)$. As movement was all upward and positive, no negative value rates existed, so a phase shift of $\frac{\pi}{2}$ was the characteristic that described a resulting negative derivative of cosine into the (Quadrant + $\frac{\pi}{2}$), where the negative derivative would have resided. The phase offset required to align the estimated function with the phase-jitter of the upper to lower ratio was related to the first derivative, or velocity.

Where did this leave us with information to update the magnitude growth model? With the earlier growth model, some form of spin property would have been expected. The new Eulerian approach with “velocity times $e^{(\text{acceleration})}$ ” provided those expected spin properties and has become the definitive coordinate behavior of Figure 33. Figure 33 could be considered a culmination of applying logarithmic growth to a conical model supporting electron behavior or a system that grows and stabilizes natural forces over time.

Figure 33

Updated magnitude growth model



Post-Zeta Model Results

When a $\zeta(2)\pi$ function was applied to the increments of $6z$ at their specific coil (or radius) the results were equivalent to draining the power from an emitted wave. The $\zeta(2)$ function, also known as the inverse square function, divides magnitude by the square of the radius. This inverse-squared approach was the same as evaluating typical wave functions and their dispersion over a lake's surface. For normal wave propagations, the limited kinetic energy atrophies as the wave disperses over the surface of the water. This was not the case with the prime number waves...the waves were growing as the prime numbers grow. This was much more of a power generation system, which required analysis of relationships between sets of data. A summary of the quadrant totals used in the analysis are provided in Table 7. The resulting post-zeta(2) area values for the 14,512 coils were separated by quadrant (thread) and by quadrant transition in the top section of the table, with the total in the orange middle section and comparison of the estimated equation in the section just below the total.

Table 7

Post zeta(2)area values by quadrant

Total of all Quadrants / ($\pi * t^2$)							
Q1 6-Sum, 2-thread	Q1 6-Sum, 2-4 transition	Q3 6-Sum, 2-thread	Q3 6-Sum, 2-4 transition	Q2 6-Sum, 4-thread	Q2 6-Sum, 4-2 transition	Q4 6-Sum, 4-thread	Q4 6-Sum, 4-2 transition
0.281008	0.369119	0.206801	0.915025	0.095751	1.314102	0.217343	0.183058
3.582							
Total / ($\pi * t^2$)	Minus e	Squared	$[Total/(\pi * t^2)] = e + \sqrt{3}/2$				
3.582	0.863924	0.746365	$[Total/(\pi * t^2)] = e + \sqrt{3}/2$				
3.584	0.866025	0.75	$[Total/(\pi * t^2)] = e + \sqrt{3}/2$				

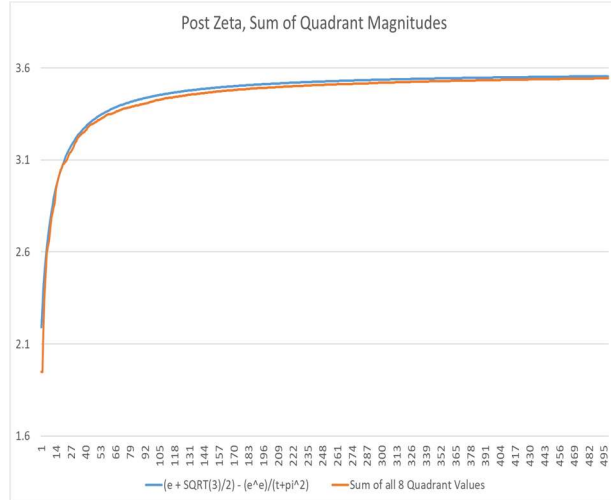
The results showed that although the prime numbers kept incrementing the magnitude of those increments quickly diminishes in impact when compared to (divided by) the value of the coil (radius) squared. Where did that leave the assessment, and what was the real value of performing this zeta function? It provided a snapshot in time of change, which had great value. If all action was totally repetitive as with a normal wave, a certain amount of power or frequency of diminishing power could be calculated. With the prime numbers, the zeta snapshot capture of a mode shift revealed some integrated and dependent behavior.

Summary of Post-Zeta Magnitude Analysis

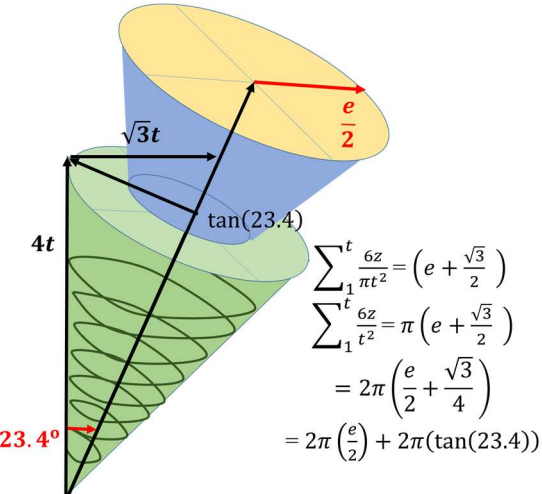
With the application of the zeta(2) area function, the magnitude growth rapidly stabilized within 500 coils to the vector that as the driving force behind the overall growth of the prime number increments. The lesson learned from the previous magnitude analysis was that the quadrant values and the dynamics between those quadrants define the actual behavior of the system. As these same magnitude values were reduced with a zeta(2) area operation they revealed different quadrant-focused relationships that would be missed if the analysis had ceased at the upper and lower plane level of detail. Figure 34.a depicts the plateauing sum of all 8 quadrants values by coil 500 at 3.584, where $\sum_1^t \frac{6z}{\pi t^2} = \left(e + \frac{\sqrt{3}}{2}\right) - \frac{e^e}{t+\pi^2}$ reduces very rapidly in time to $e + \frac{\sqrt{3}}{2}$. In Figure 34.b, when the constant π is redistributed, the resulting inverse square function aligned very well with the circumference of an electron's quantum spin dynamics. While transforming the equation into a form accommodating a 2π structure, another aspect of the conical tilt was discovered, specifically that $\sum_1^t \frac{6z}{\pi t^2} = \left(e + \frac{\sqrt{3}}{2}\right)$, so $\sum_1^t \frac{6z}{t^2} = \pi \left(e + \frac{\sqrt{3}}{2}\right) = 2\pi \left(\frac{e}{2} + \frac{\sqrt{3}}{4}\right)$. This had an interesting equivalent trigonometric form of " $2\pi \left(\frac{e}{2}\right) + 2\pi(\tan(23.4^\circ))$ ", where the angular offset of 23.4° was also the exact axial tilt of the Earth.

Figure 34

Resulting magnitude vector model



34.a. Sum of quadrant values



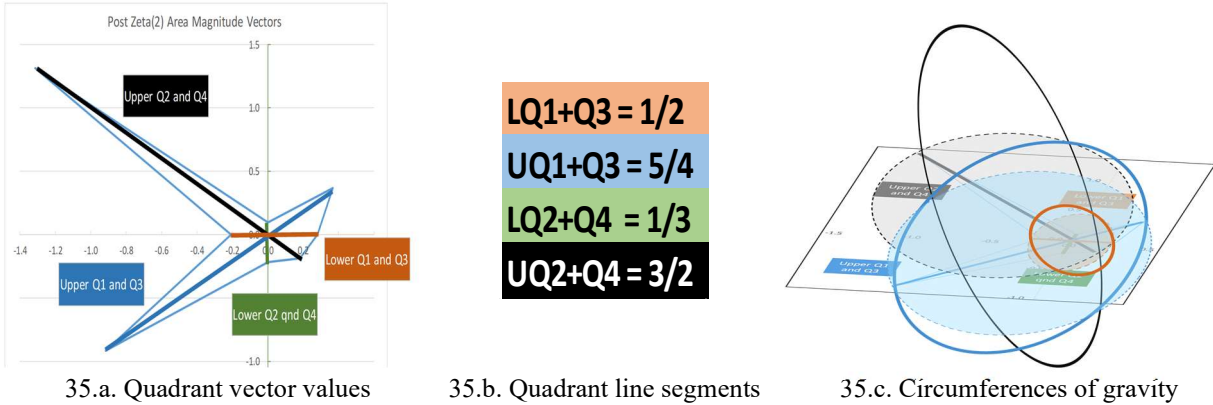
34.b. Circumference quantum model

Analysis of the individual quadrant behavior and the combined line-segment behavior

from the quadrant sets of data told a different story of interaction and balancing dynamics. As discussed in the paragraph above, all growth values plateaued by coil 500. However, the quadrant values appeared to be locked in time at a value without any perceivable significance until they were considered as combined segments, or intersections between a circumference plane and the base plane that represents that slice of time for all quadrant values. Figure 35 is presented as a visual coordination of those facts. Figure 35.a introduces the color-coded line segments formed from combining the quadrant values, with Figure 35.b containing the table of their single line segment sums. With the initial zeta(2) area function containing the constant π , the constant π was re-inserted into the results and the form of behavior became clearer in Figure 35.c as a circumference. The line segments from the combined opposing quadrant values were diameters, with each diameter times π also equal to $2\pi r$, in this case as its equivalent $\pi 2r = \pi d$. It was not a normal way of considering the same function, but it helped tie the concepts together.

Figure 35

Quadrant balancing and off-center gravity



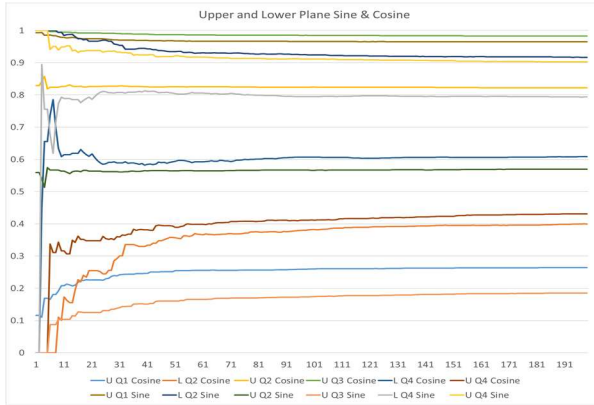
The line segments and quadrant values could then be seen in an entirely different perspective of balancing the center of each plane's circle, much like balancing different centers of gravity. The properties revealed from this balancing effect are discussed at the end of this post-zeta analysis and used to update the magnitude growth model. When this property was translated into the magnitude model for all coils, the captured coil line segments and their center of gravity movements correlated to activity much like a tornado.

Post-Zeta Sine and Cosine Analysis

In contrast to the immediate and straightforward application of the sine and cosine and their contribution to the magnitude growth model and Eulerian function, the meaning of sine and cosine in a post-zeta analysis was a little more elusive. The arcsine and arccosine results in Figure 36.b provided no clear connection to complementary angles either on the same plane or between planes.

Figure 36

Post-zeta sines and cosines



36.a. Upper and lower plane results

U Q1 Angle	U Q2 Angle	U Q3 Angle	U Q4 Angle
74.3	34.8	11.3	63.6
L Q1 Angle	L Q2 Angle	L Q3 Angle	L Q4 Angle
18.8	65.2	46.4	52.3

$$\begin{aligned} LQ1+Q3 &= 1/2 \\ UQ1+Q3 &= 5/4 \\ LQ2+Q4 &= 1/3 \\ UQ2+Q4 &= 3/2 \end{aligned}$$

36.b. Arcsine angles and line segment values

Further analysis in connection to the meaning of the concatenated quadrant-related line segment values led to an explanation. From that center of gravity perspective, the total segment values in Figure 36.b were best considered as the traditional x axis and y axis values in sine and cosine functions, each representing a total axis movement for that coil. At first it seemed to violate all definition of placement in the coordinate system until the movement (directional increments) of the line segments were considered as their expression of their moving center of gravity. The entire diameter was considered as one moving center of gravity.

The 90-degree offsets of those diameters (line segments) could be used to provide a tangent value from those sine and cosine relationships. The 90-degree relationships were based on the color-coded total segment values in Figure 36.b (lower odd plane $\frac{1}{2}$ and lower even plane $\frac{1}{3}$, upper odd plane $\frac{5}{4}$ and upper even plane $\frac{3}{2}$). As a result, the tangent relationships revealed potential reciprocal and 90-degree relationships between the upper and lower plane. Those relationships are seen in the following equations:

$$\frac{Lower\ Odd}{Lower\ Even} = \frac{\frac{1}{2}}{\frac{1}{3}} = \frac{3}{2} = Upper\ Even; \frac{Upper\ Odd}{Upper\ Even} = \frac{\frac{5}{4}}{\frac{3}{2}} = \frac{10}{12} = \frac{5}{6} = 1 - \frac{1}{6}$$

$$= 1 - (Lower\ Odd) * (Lower\ Even) = 1 - \left(\frac{1}{2}\right)\left(\frac{1}{3}\right)$$

In this case, the significance was not the traditional the “x” to “y” value relationship within the quadrant, but the total segment value and the tangent 90-degree relationships between those segments on the same plane. This reciprocal relationship was also intriguing. The products of the 90-degree relationships (lower odd and lower even) produced a complement ratio from upper odd to upper even. Another 90-degree relationship between the planes occurred when the lower tangent (odd/even) relationships also produced the upper plane even line segment of $\frac{3}{2}$.

Post-Zeta 90-degree Field Vector Analysis

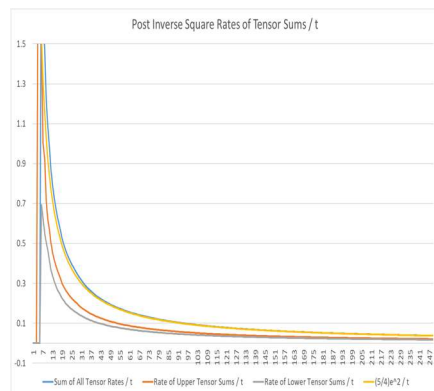
After discovering that the 90-degree balancing between post-zeta quadrant magnitudes line segments were also driving the coil-based sine and cosine definitions, reviewing the known 90-degree field vector relationships required considering different combinations of results to determine any coordinate related characteristics. Analysis of the post-zeta(2) 90-degree field vectors led to discovering two different systemic relationships: the sums of the field vectors and the products of the field vectors. An analysis of the sums revealed total areas in the form of e^2 , while an analysis of the products revealed reciprocal products and reciprocal angular acceleration.

Sums of the Field Vectors

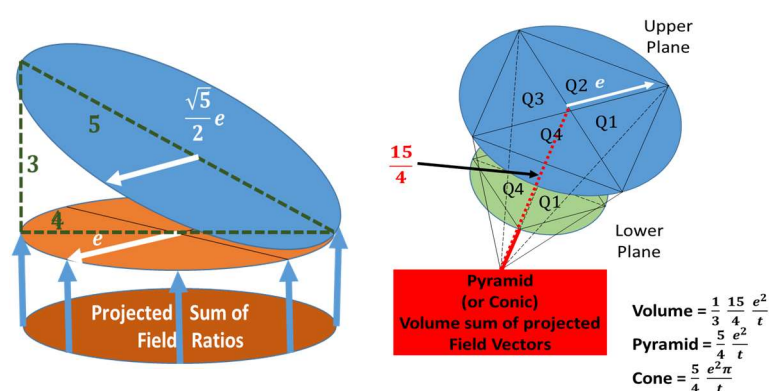
Figure 37 introduces the resulting sum of the 8 field vectors represented in the growth rate function of $\frac{5}{4}e^2\pi$ over coil time (t), in Figure 37.a. This created two possible models for expressing this overall field vector property. One approach was to define the total vector sum as an area grouping of projected fields, or radiated fields. In Figure 37.b the projection of the area created from all quadrant vectors was the concept. In Figure 37.c, the concept of volume was presented. The volume consisted of the additive area slices a circle with radius of e and a growth rate vector with the ratio of $\frac{15}{4}$. The volume model represented the vectors maintaining two separate forms of growth in each plane, upper and lower plane.

Figure 37

Post-zeta field vector sums



37.a. Rate of change



37.b. Conical or helical plate

37.c. Two plane surface expansion

The sum of the eight quadrants' 90-degree (\top) vector relationship ratios rapidly reached its range of $9.236 = \left(\frac{5}{4}\right)e^2 = e^2\sec(36.85)$. The zeta function initially included the constant π to capture the change over a circular area, so π was easily removed from πt^2 just through the rate comparison of the 90-degree vectors. This provided a sum of vectors derived from pure zeta(2)

modeling, with $\sum_1^t -QL \frac{6z}{t^2} + -QU \frac{6z}{t^2} = \left(\frac{5}{4}\right) e^2$, which may be more beneficial to the mathematical community. The value of π is still used for conceptualizing its physical coil model growth.

Various forms of interpretation could result. With the vector sum resulting in an association with e^2 , how should the scalar value of $\frac{5}{4}$ have influenced the model? Was it just an expansion of the radius squared to $\left(\frac{\sqrt{5}}{2}e\right)$ or was it a value providing another dimension of growth in volume? Figure 37 introduces those two concepts with another interesting fact that the radius expansion model aligned perfectly with a 3-4-5 (y-x-hypotenuse) triangle. Figure 37.a also provides a solid model from both a conical growth and a helical growth, with the upward angular movement of $\frac{5}{4}e^2 = \sec(36.85^\circ)e^2$. The two volume interpretations, conical or pyramid, were possible forms in Figure 37.b and Figure 37.c with $\left(\frac{1}{3}\right)\left(\frac{15}{4}\right)e^2 = \left(\frac{5}{4}\right)e^2$. Yet, one more aspect was considered as significant if it was placed in terms of the following sequence of trigonometric equations:

- Let $a = 4$, then $\frac{a^2-1}{a} = \frac{15}{4}$.
- In trigonometric terms: Let $a = \sin\theta$, then $(a^2 - 1) = \cos^2\theta$.
- Produces the form of $\frac{\cos^2\theta}{\sin\theta} = \left(\cos\theta\left(\frac{1}{\sin}\right)\right)\cos\theta = \left(\frac{d}{d\theta}\ln(\sin\theta)\right)\cos\theta$.
- Or, also in the form of $\cos\theta\cot\theta$.

Products of the Field Vectors

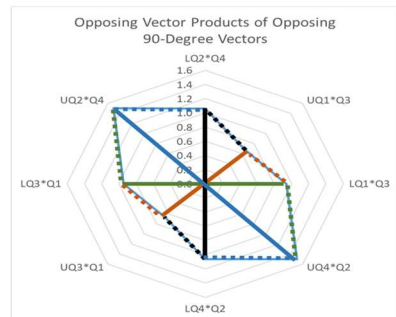
A different approach was required for vector products in this prime number component model and coordinate system, with each vector representing a growth derivative. Normally, vector products are acquired through the multiplication of the magnitude of the two vectors and their angular offset. In the prime number coordinate system, there were two types of angles: one

type was a cardinal heading angle from the $6z$ intersection with the poles and other type was the vector angle from the abstract “grouping” of the multiples of $6z$ that occur in the pole transition area (like an “xy” or “yx” plane).

With that perspective, it appeared to be cleaner to multiply the vector magnitudes and then determine any relationships between vector products from their location in the coordinate system. The model diagram in Figure 38 resulted. Figure 38.a was the result of vector products from the post zeta(2)-area 90-degree normal vectors. The four pairs of vectors that were 180-degrees opposite on the coordinate plane were multiplied to investigate internal dynamics unique to the lower plane versus the upper plane.

Figure 38

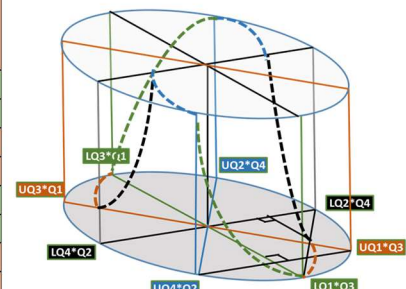
Applying angular velocity to previous vector products



38.a. Previous 90-degree products

Vector Products	Value	Location	Next Value from present (p)	Alternating (p, 1/p) every 45	Alternating (0.707, 1/0.707) every 90
LQ1*Q3	0.944	0 DEG	p*(0.707)	p	0.707
UQ1*Q3	0.666	45 DEG	(0.707)/p	1/p	0.707
LQ2*Q4	1.060	90 DEG	p/(0.707)	p	1 / 0.707
UQ2*Q4	1.502	135 DEG	1/(0.707 p)	1/p	1 / 0.707
LQ3*Q1	0.944	180 DEG	p*(0.707)	p	0.707
UQ3*Q1	0.666	225 DEG	(0.707)/p	1/p	0.707
LQ4*Q2	1.060	270 DEG	p/(0.707)	p	1 / 0.707
UQ4*Q2	1.502	315 DEG	1/(0.707 p)	1/p	1 / 0.707

38.b. Considering velocity and reciprocals



38.c. Applying angular velocity

Figure 38.b was the result of evaluating the relational values between the vector products as they proceeded sequentially around a coil (2π). These values revealed two variables that shifted between their value and their reciprocal value at different frequencies. A “p” denotes the present product value, with “0.707” representing the angular velocity offset value. The values of $(p, \frac{1}{p})$ alternated every $\frac{\pi}{4}$, while the velocity values of $(0.707, \frac{1}{0.707})$ shifted every $\frac{\pi}{2}$.

The result was a saddle function with an angular twist in Figure 38.c, the significance of which could not have been noticed in Figure 38.a as only a two-dimensional diagram. Table 8 contains the review of the post-zeta(2) area 90-degree vector products relationships. Those initial values pointed to a reciprocal behavior between the odd and even quadrant vector products. A closer landscape view of the details of Figure 38 is provided in Appendix B. The next section will also show how these product relationships are related to Doppler vectors.

Table 8

Review 90-degree vector product relationships

Coils	Upper Q1	Upper Q2	Upper Q3	Upper Q4	Lower Q1	Lower Q2	Lower Q3	Lower Q4
	U (Q4+Q1) / (Q1+Q2)	U (Q1+Q2) / (Q2+Q3)	U (Q2+Q3) / (Q3+Q4)	U (Q3+Q4) / (Q4+Q1)	L (Q4+Q1) / (Q1+Q2)	L (Q1+Q2) / (Q2+Q3)	L (Q2+Q3) / (Q3+Q4)	L (Q3+Q4) / (Q4+Q1)
14,515	0.3280	0.7551	2.0300	1.9886	1.3227	1.2453	0.7133	0.8511
	2/3 Factor	3/2 Factor	2/3 Factor	3/2 Factor	50/53 Factor	53/50 Factor	50/53 Factor	53/50 Factor
	Q1*Q3	Q2*Q4	Q3*Q1	Q4*Q2	Q1*Q3	Q2*Q4	Q3*Q1	Q4*Q2
14.515	0.6659	1.5016	0.6659	1.50163	0.9435	1.0598	0.9435	1.0598

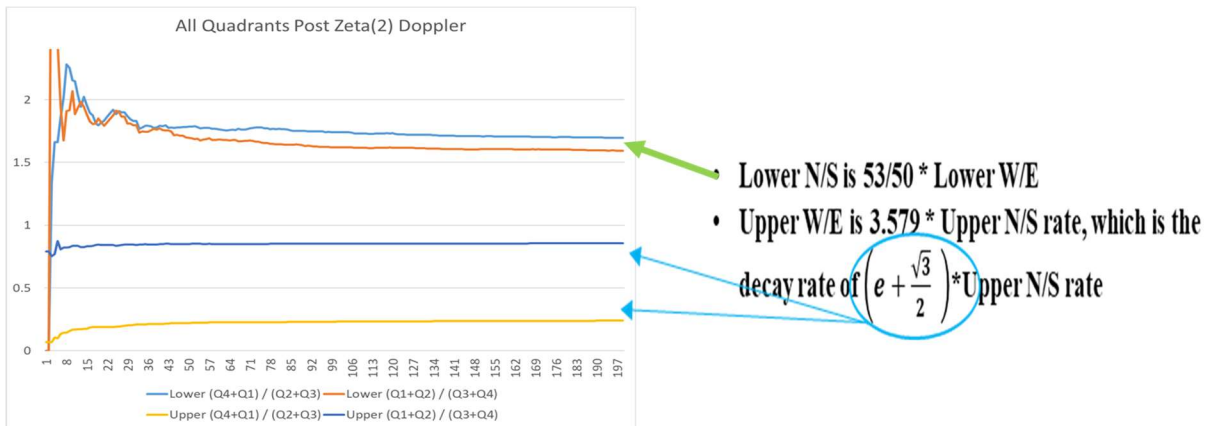
Post-Zeta Doppler Vector Analysis

Analysis of the post-zeta 180-degree Doppler vector ratios revealed tightly coupled relationships within their own plane, either the lower or the upper plane. When the ratios of those relationships were reviewed, the rates were closely associated with the post-zeta growth rate and the post-zeta 90-degree vector ratios. For the upper plane Dopplers, the West/East Doppler equaled 3.579 times the value of the North/South Doppler. This aligned directly with the behavior of the overall $6z$ magnitude growth, where $\left(e + \frac{\sqrt{3}}{2}\right) = 3.583$. Contrary to the growth rate relationship, a different relationship existed for the ratio between the two lower plane Dopplers.

The ratios for the lower plane Dopplers had an interesting and unsuspected correlation to the lower plane's post-zeta 90-degree field vector values. The lower plane North/South Doppler was $\frac{53}{50}$ times the lower West/East Doppler, and correspondingly the West/East Doppler was $\frac{50}{53}$ times the lower North/South Doppler. Figure 39 provides a summary of these two relationships with annotated lines connecting to these two bulleted points of interest.

Figure 39

Post-zeta Doppler relationships



Both values of $\frac{50}{53}$ and $\frac{53}{50}$ were also the 90-degree field vector product values, also displayed in Table 8. The $\frac{50}{53}$ ratio had driven a significant relationship between the 90-degree vectors and the overall magnitude model, due to the UQ1/LQ1 ratio of post-zeta 90-degree field vector products of $\binom{2}{3} \div \binom{50}{53} = \binom{2}{3} \frac{53}{50} \binom{2}{3} \cong 0.707$. That not only represented one of the periodically oscillating reciprocal variables, but also 0.707 was the main modeling value used to generate the Eulerian formulas of angular velocity and spin acceleration.

All the models clearly had interdependent relationships. The lower plane (which had angular velocity) had the triggering Doppler ratio $\left(\frac{53}{50}\right)$ that was multiplied by the upper plane 90-degree field vector $\left(\frac{2}{3}\right)$ in an electron spin related to the value that drove the sine and cosine value used in their respective Eulerian formulas:

$$\frac{\sqrt{e}}{\sqrt{2}} = (0.707)e^{(0.707^2)} = \text{AVG}(\cos LO\theta + \sin LE\theta)e^{\text{AVG}(\cos LO\theta + \sin LE\theta)^2} = \mathbf{VLO}e^{(VLO)^2}.$$

Applying Post-Zeta Findings to Common Growth Model

With results from each of the post-zeta models of growth, sine and cosine, 90-degree field vectors, and Doppler vectors revealing related properties, this section discusses how those models contributed to the overall growth model from the magnitude analysis section. By integrating the sets of magnitude behavior and power drained post-zeta structure, possible research topics were revealed, and specific characteristics were provided for focused research.

Contribution from Post-zeta magnitudes

The post-zeta magnitude analysis produced two concepts that directly correlate to the growth magnitude model's conical logarithmic growth angular velocity (lower plane) and spin field dynamics (upper plane). The first concept was the moving centers of gravity that came from the balancing quadrant line segments sums. This required a little expansion from the post-zeta individual quadrant values to the magnitude model's quadrant values over time. The second concept was the angular tilting discovered from sum of all eight quadrants (upper and lower) post-zeta values.

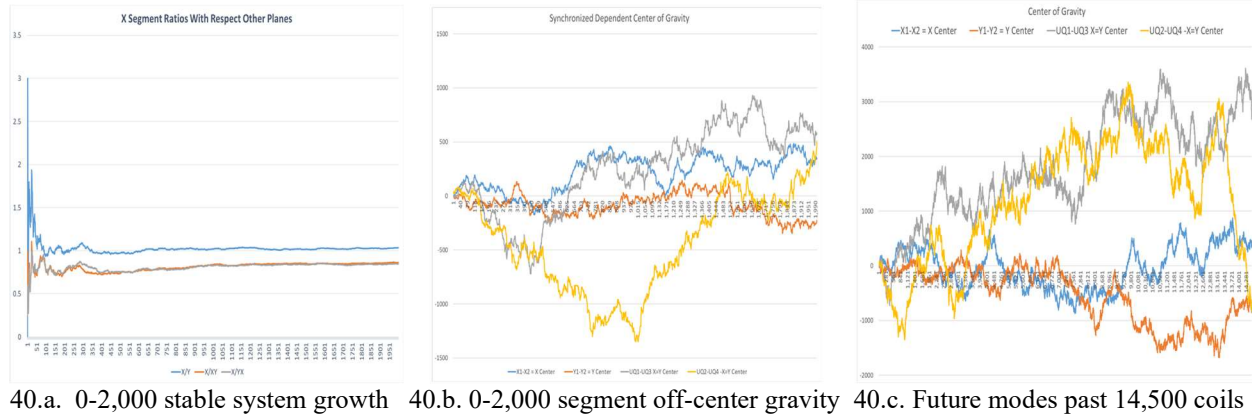
Expanding the investigation of the quadrant segment centers produced a totally integrated and balanced approach to growth, which was growing concurrently with the shifting centers of gravity in Figure 40. The system showed growth stability ratios with respect to the 2-pole (x-

axis equivalent) while it synchronized the changing off-center gravity of a multi-plane model.

Figure 40 shows the two dynamics over the same period. The significance of this cannot be trivialized...a flatten overall control of one aspect of force while an off-centered balancing gravitational aspect of the force seems out of control like a tornado. Figure 40.a displays those relative growth ratios of the segment total on the 2-pole (x axis) with respect to the other three sources: the 4-pole (y axis), the 2-4 transitions ($x = y$ plane), and the 4-2 transitions ($-x = y$ plane).

Figure 40

Balancing growth and centers of gravity



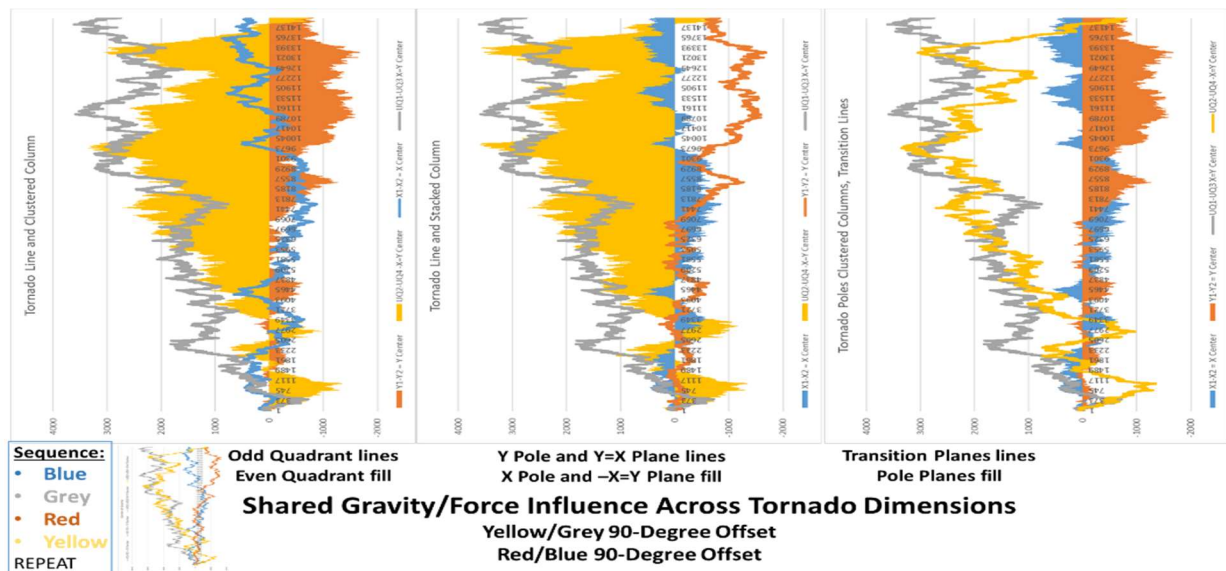
While Figure 40.a has the relative growth ratios with respect and “x axis” equivalent, Figure 40.b shows the line segment dynamics over the same period (0-2000 coils). Figure 40.b shows the how each of the four segments are growing with respect to the coordinate system’s center. Figures 40.a and 40.b display two totally different, but vital dynamically balancing, aspects of their growth. Figure 40.c shows a promise of more system modes past 14,512 coils, which would be a perfect starting point for future research. The blue line in Figure 40.c clearly

shows all multidirectional growth was related to growth on the 2-pole (equivalent x-axis), and as a result the growth was also interdependent.

Even with that synchronization, broad variations in centers of gravity existed and a method for translating this to the magnitude growth model were necessary. This translation is presented in Figure 41, where the variation and balance of the centers of gravity and growth resemble the velocity and spin behavior of a tornado. Figure 41 displays different variations on a conical model over time that were used to align this tornado-like behavior with the conical components of the magnitude growth model. Each sub diagram was labeled for the different color-coded combination that paired poles and pole transitions when the best options for aligning with the magnitude growth model were reviewed. Each horizontal set of values represented a set of activities in one coil (or slice of time), with rotational sequence color-coded always in the order of blue-grey-red-yellow.

Figure 41

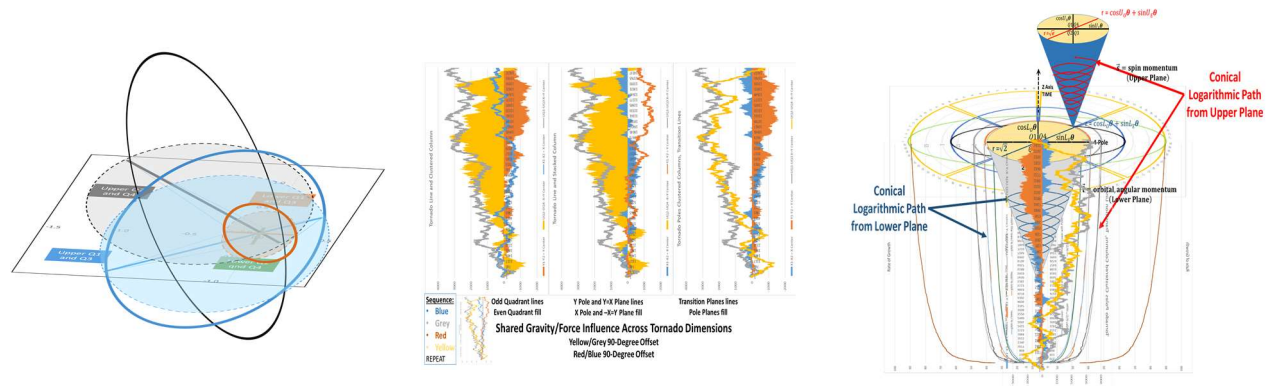
Aligning tornado-like, gravity balancing behavior



Due to the clear distinction of the red and blue pole values, the rightmost diagram was selected as the diagram that most aligned this tornado and balanced acceleration model with the previously presented magnitude conical growth and acceleration model. Figure 42 provides the logical progression of thought used when the segment behavior was re-evaluated as the center of a gravitational force (Figure 42.a) reduced to a single time slice by the zeta function. The comparison of segment values was then expanded to all 14,512 coils and the color-coded variations were inserted for the lower and upper gravitational forces (Figure 42.b), which was aligned and inserted into the magnitude growth model (Figure 42.c). Figure 42.c also aligned the upper plane gravitational force lines with the conical representation of spin on the upper plane, under the blue cone in the diagram.

Figure 42

Centers of gravity balancing in magnitude growth model



42.a. Quadrant gravity segments 42.b. Magnitude off-center quadrant gravity 42.c. Upper and lower gravity model

With the balancing gravitational forces placed into the conical magnitude growth model, integrating the second concept was much more straightforward. The second concept discovered from sum of all (upper and lower) quadrant post-zeta values was the concept of conical angular

offset. More specifically and maybe more significant was that the discovered tangential angular correction was at the same as the Earth's axial tilting of 23.4° . In the diagrams of Figure 43 that parallel a 23.4° tilting of the magnitude conical growth model, some other obvious correlations existed visually.

Figure 43 provides more than just a parallel alignment; it shows how the upper plane activity of both models both were tied to Eulerian behavior. The post-zeta Earth-tilted model provided a circumferential aspect of applied force $2\pi \left(\frac{e}{2}\right) = \pi e$. The magnitude model also produced an upper plane cone area (that varied from the Eulerian sine and cosine) around the value of $\pi \left(e^{\frac{1}{2}}\right)^2 = \pi e$. It was a noteworthy discovery about the fundamental properties that correlated the two system descriptions. The circumference of a post inverse squared value of force represented as a radiated field was also the same as the magnitude model's area of growth multiplier, πe .

Figure 43

Adjusting the earth-tilt of the conical growth model

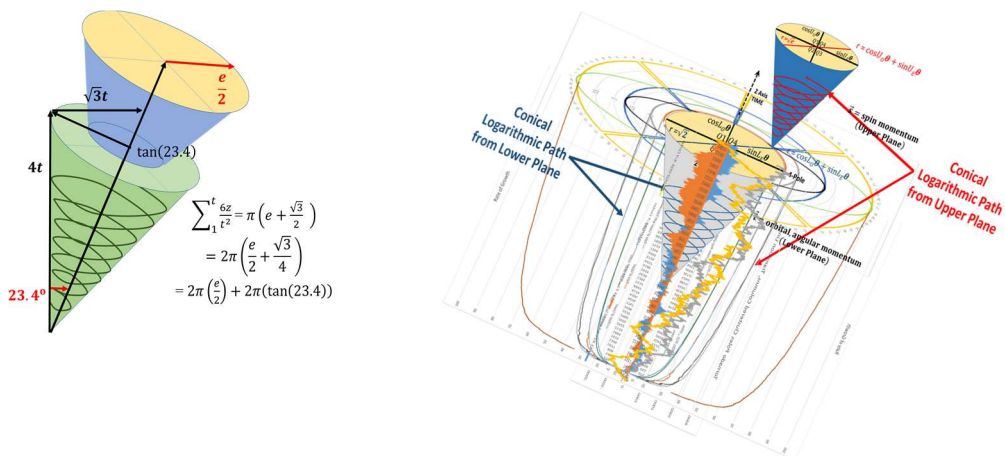


Figure 43 also provides the summary of several growth properties. It has the ratio of logarithmic growth between the lower plane, upper plane, and the total (with poles). It shows that logarithmic growth in terms of increasing conical form, at the rate of coil-time cycles. It contains the effect of applying the exact sine and cosine relationships to the logarithmic growth model ratios that discovered an Euler-based angular velocity model. With final additions, it demonstrates the balancing of an off-center gravitational growth of force, tilted to the Earth's axial offset.

Findings

The overall findings from this research data analysis provided a very tightly integrated the framework of system definitions and engineering models for research using the prime number component model and coordinate system. The final diagrams integrating all major concepts into the coil-based conical magnitude growth model that integrated Eulerian sine and cosine functions, logarithmic growth ratios, angular velocity, balancing off-center gravitational growth of forces, all tilted to the Earth's axial offset.

Two logical models were used for examining the properties of the integrated data sets from the components: a magnitude model and an inverse square model. The magnitude model compared the total growth with respect to another vector or quadrant growth internal to the component model, that is relational to the system's coil time instead of relational to the number line. The inverse square model took the same vectors and relationships from the magnitude model and divides each increment of $6z$ by the square of the coil number $\frac{6z}{t^2}$, the sum of which is referred to as a zeta(2) function where $\text{zeta}(2) = \sum_1^n \frac{1}{n^2}$.

Examining the system and vector properties involved the data for the four sets of sine and cosine, hypotenuse, tangent, 90-degree field vectors, and 180-degree Doppler vectors. Four different types of magnitude growth characteristics provided by each model. The different plane intensity or density over the coil-time is revealed from the magnitude growth. The activity across and around 45-degrees is revealed from the sine and cosine graphs. The 90-degree field effect reveals frequency of changes in behavior modes. Magnitude changes in directional growth were revealed through a relativistic Doppler model.

Some of the less mentioned (but just as tightly integrated) characteristics were discovered from the impact of key ratios $\frac{50}{53}$ and 0.707 between components. The post-zeta ratios relationship for the lower plane Doppers was $\frac{53}{50}$, which was also related to all lower plane 90-degree field vector values. The value $\frac{53}{50}$ also connected the products of post-zeta 90-degree field vector products to produce the value of $\frac{53}{50} \left(\frac{2}{3}\right) \approx 0.707$, which also was the main modeling value used to generate the Eulerian formulas of angular velocity and spins acceleration through the following equation:

$$\frac{\sqrt{e}}{\sqrt{2}} = (0.707)e^{(0.707^2)} = \text{AVG}(\cos LO\theta + \sin LE\theta)e^{\text{AVG}(\cos LO\theta + \sin LE\theta)^2} = VL\theta e^{(VL\theta)^2}.$$

With all properties pointing to an integrated system, a one-page storyboard is provided in Figure 44 as a summary of the coordinated results and the relationships between the magnitude models and the post-zeta models.

Summary

Conclusions can be clearly drawn from the overall findings from this research data analysis that led to declaring the first 100,000 prime number increments to be strictly adhering to a self-referential framework. Figure 44 provides a summary and a correlation between the resulting model behaviors in both the magnitude analysis and the post-zeta(2) area analysis.

Figure 44

Storyboard summary of findings

Type of Model	Storyboard Summary of Findings		
	Graph	Diagram(s)	Concepts
6z Growth			$\vec{i} = \text{angular momentum (Lower Plane)}$ $\vec{s} = \text{spin momentum (Upper Plane)}$
Rapid Growth Stabilization			Decay to constant spin $\sum_{t=1}^{\infty} \frac{6z}{\pi t^2} = \left(e + \frac{\sqrt{3}}{2} \right) - \frac{e^{\pi}}{t + \pi^2}$
Plane / Diameter Segments			Stable relative growth, moving center of gravity (diameter segment)
Sums of Diameter Segments			$LQ1+Q3 = 1/2$ $UQ1+Q3 = 5/4$ $LQ2+Q4 = 1/3$ $UQ2+Q4 = 3/2$
Sine, Cosine			Sine and Cosine involved in Angular Velocity and Growth (Magnitude) $V_{10} e^{(V_{10})^2} = \text{AVG}(\cos L_0 \theta + \sin L_0 \theta) e^{\text{AVG}(\cos L_0 \theta + \sin L_0 \theta)^2}$
Sine & Cosine From Diameter Segments			$LQ1+Q3 = 1/2$ $UQ1+Q3 = 5/4$ $LQ2+Q4 = 1/3$ $UQ2+Q4 = 3/2$
90-Degree (Normal/Field) Vectors			Can be Horizontal, Vertical, or Conical
Sums of 90-Degree Vectors			Rate of Area or Volume over time Pyramid = $\frac{5}{4} e^{\frac{2}{3}\pi}$ or Cone = $\frac{5}{4} e^{\frac{2}{3}\pi}$
Products of 90-Degree Vectors			Angular velocity changes every $\frac{\pi}{2}$; Reciprocal growth multiplier changes every $\frac{\pi}{4}$
180-Degree (Doppler) Vectors			Angular offset needs to be considered if not used in a Horizontal Model
180-Degree Vectors			<ul style="list-style-type: none"> Lower N/S is $53/50 * \text{Lower W/E}$ Upper W/E is $3.579 * \text{Upper N/S rate}$, which is the decay rate of $\left(e + \frac{\sqrt{3}}{2} \right) \text{Upper N/S rate}$

Examining the interactions between quadrant components of 6z revealed dynamically balancing harmonic growth characteristics. The coordinated mode shift performed by the stabilization at coil 144 provides an overwhelming agreement with the expected behavior of an integrated system. Those growth characteristics described a system that contains mode shifts

controlled by the relativistic Doppler and 90-degree field effect vectors. The angular velocity and electron spin characteristics generated the potential for further investigation and possible implementation of the framework in technology.

These integrated models and system definitions are the exact type of results that would have been expected from an actual system (such as a motor or generator), with measurable and distinct behaviors and interactions. Chapter 5 provides a detailed summary of the related system equations, models, adaptation required for different approaches and foundational models, and possible principles for future research.

CHAPTER 5: FINDINGS AND RECOMMENDATIONS

The recommendations and detailed findings in this chapter are summarized in five tables showing the correlated equations and associations to the three hypotheses of this dissertation. After a summary table of the common structures and definitions is discussed, tables with the results from the two different model analyses are presented, the magnitude analysis and the post-zeta analysis. The results from those two models were used to consider recommended translations to other existing systems. In each summary (common structure, magnitude analysis, post-zeta analysis, system translation) separate columns are provided to document the related system engineering model, the self-referential perspective, and the harmonic and dynamic properties. The taxonomy describes how the two models used the characteristics of both the coordinate system and the generic component relationships used to perform the analysis and gather results for Chapters 3, 4, and 5.

In the recommendations section, a separate table describes contributions the component model could possibly provide to the Millennium Prize Problem efforts. Recommendations are also made in a table for translating the component model properties to other physical systems, along with potential research topics. As a result of the integrated properties, several recommendations for further theoretical research are documented. Prior to introducing the summary of findings using those five tables, this chapter starts with a brief discussion on the scope and limitation of the study.

Limitations

There were two reasons the selected sample set was limited to 100,000 primes. One reason was that an initial set of data (2,000 primes) indicated that 100,000 primes would produce

between 10,000 and 20,000 coils of the component structure. This would be sufficient to annotate characteristics of compound or exponential growth, along with variations and shifting modes over time. The other reason for limiting the selection to 100,000 primes was the expected demand on processing power for the integrated component relationships from sample sets near and over 1,000,000.

As expected, there were some performance issues when relationships like tensors, second order tensors, or partial derivative relationships would produce 56 data points per coil from the sets of 8 quadrant values. The 56 data points per coil for the 14,512-coil graph of sine partial relationships produced 812,672 data points. A different approach is recommended for future model research with larger data samples. Data separation, indexing, or segmentation should be a part of the future research engineering plans. With just 100,000 primes the examination of model component interactivity resulted over 1GB of workbook spreadsheets for the variations of the component functions with $6z$ only, with poles, with inverse square zeta, and with tensor products. The set of slides used for system analysis was over 550 slides and took 100MB of storage. Proceeding to 1,000,000 with the same level of analysis will require more of a formal software development configuration and baseline data management approach.

For processing, spreadsheets and workbooks exceeding 200MB had to be segmented for further detailed analysis. Even with the 2020 Intel Core i7 processor with 117GB RAM, every save of the spreadsheet would lock Microsoft Excel capabilities for over a minute.

With this as the first study of its type using this model, the largest limitation was the lack of comparative parallel studies. Except for the assumed system behaviors related to natural systems and the assurance of the framework reliability, this was all new research territory that required initial models.

Findings and Interpretations

A seemingly endless potential amount of correlated behavior was revealed from the analysis of the two models (magnitude and post-zeta). Tables 9-12 in this summary of findings describes how each model provides justification and alignment with the three hypotheses of this research. Columns are provided under the headings of “System Engineering Models”, “Self-Referential”, and “Harmonic/Dynamical”. Those types of concepts also helped make recommendations for future research. The most essential part of the analysis was discovering the significance of standardizing the common concepts and coordinate definitions used to both build the components and use them as system engineering models and structures. Table 9 is a summary of the core engineering definitions in terms of the quadrant components that should be understood before proceeding in any analysis of the framework.

Table 9 introduces some new concepts in that the sine value is really the rate of the sine over coil time, therefore it is really the derivative of sine activity and should be treated as such. The same concept applies to all vector and growth rates over time. Another new concept is considering the multiples of $6z$ as the result of a second derivative of a cubic function as a variation z^3 . This considers the growth of $6z$ as the possible result of acceleration, heat transfer, force, or some radiated form of energy.

The 90-degree vectors that can be considered as normal or field effect vectors, required the association between sets of two quadrants physically located at a right angle and assuming some form of right-hand-rule relationship. The Doppler vectors also required sets of two quadrant groupings in opposing (180-degree) relationships. These Doppler vectors are labeled as relativistic Dopplers due to the point of original and reference being at the edge of the coil

structure instead of the center which would also involve negative values. With those basic core concepts understood, proceeding to the findings for the models used in the analysis is in order.

Table 9*Concepts and Common Formal Equations*

Summary of Overall Common Structure Equations				
System Engineering Models	Equations	Adapted to System	Self- Referential	Harmonic / Dynamical
Coordinate and Quadrant Axis Translation	Lower plane x and y axis values: Lx[+], Lx[-], Ly[+], and Ly[-] Upper plane x and y axis values: Ux[+], Ux[-], Uy[+], and Uy[-] E.g.: Ux[+] is after Lx[+] and before Ly[+]	Lx[+] = LQ1, Lx[-] = LQ3, Ly[+] = LQ2, and Ly[-] = LQ4	As coordinates and components	N/A
Magnitude Growth (Total)	Total = $\sum_1^t 6z = \sum_1^t (LQ1 + LQ2 + LQ3 + LQ4 + UQ1 + UQ2 + UQ3 + UQ4)$	Total force or acceleration, velocity, pressure, temperature.	Total Prime Growth, without poles	Balanced distribution of second derivative
Sine (LQ1), Cosine (LQ1), Hypotenuse (LQ1)	Sine (LQ1) = $\frac{\sum_1^t Ly[+]}{\sum_1^t Hyp \cdot LQ1}$, Cosine (LQ1) = $\frac{\sum_1^t Lx[+]}{\sum_1^t Hyp \cdot LQ1}$, Hypotenuse (LQ1) = $\sqrt{Ly[+]^2 + Lx[+]^2}$	Sine (LQ1) is delta over time $\frac{\Delta Ly[+]}{\Delta Hyp \cdot LQ1}$, Best described as "sin LQ1 dt".	As coordinates and components	Show Upper and lower sine-cosine tradeoffs at 45-degrees
Tangent	Tangent (LQ1) = $\frac{\sum_1^t Ly[+]}{\sum_1^t Lx[+]}$	Tangent (LQ1) is delta over time $\frac{\Delta Ly[+]}{\Delta Lx[+]}$, Best described as "tan LQ1 dt".	As coordinates and components	Direction of conical acceleration
Acceleration	$\frac{d^2}{dz^2}(z^3 + c_1z + c_2) = 6z$ $\int \int 6z dz^2 = (z^3 + c_1z + c_2)$	Force or acceleration, rate of increase in velocity	Quadrant 6z values; Integral showing original force	Balancing and changing Coriolis effect of a cubic function
Rate	$\frac{dz}{dt}(6z) = 6 dt$	Rate of growth or acceleration, rate of assigned value 6z	Rate over coil time	
Angular Distribution of 6z	$\frac{\sum_1^t 6z}{2\pi t}$; Per Quadrant: $\frac{\sum_1^t 6z}{(\frac{1}{2})nt} = \frac{2\sum_1^t 6z}{\pi t}$	Angular force or acceleration, velocity, pressure, temperature.	Circumference over coil-time	Balanced angular distribution of second derivative
90-degree Field Effect Vectors	$\tau LQ1 = \left[\frac{\partial 6z}{\partial LQ4} + \frac{\partial 6z}{\partial LQ1} \right] / \left[\frac{\partial 6z}{\partial LQ1} + \frac{\partial 6z}{\partial LQ2} \right]$ $\tau LQ2 = \left[\frac{\partial 6z}{\partial UQ1} + \frac{\partial 6z}{\partial UQ2} \right] / \left[\frac{\partial 6z}{\partial UQ2} + \frac{\partial 6z}{\partial UQ3} \right]$ $\tau LQ3 = \left[\frac{\partial 6z}{\partial LQ2} + \frac{\partial 6z}{\partial LQ3} \right] / \left[\frac{\partial 6z}{\partial LQ3} + \frac{\partial 6z}{\partial LQ4} \right]$ $\tau LQ4 = \left[\frac{\partial 6z}{\partial UQ3} + \frac{\partial 6z}{\partial UQ4} \right] / \left[\frac{\partial 6z}{\partial UQ4} + \frac{\partial 6z}{\partial LQ1} \right]$	Rate-Translated Right-Hand-Rule and Normal 90-vector, Field vector. Upper plane has same form as Lower plane equations.	As coordinates and components	From quadrant coordinates and components
Relativistic Doppler	$\frac{\partial LN}{\partial LS} = \left[\frac{\partial 6z}{\partial LQ1} + \frac{\partial 6z}{\partial LQ2} \right] / \left[\frac{\partial 6z}{\partial LQ2} + \frac{\partial 6z}{\partial LQ3} \right]$ $\frac{\partial LW}{\partial LE} = \left[\frac{\partial 6z}{\partial UQ1} + \frac{\partial 6z}{\partial UQ2} \right] / \left[\frac{\partial 6z}{\partial UQ3} + \frac{\partial 6z}{\partial LQ4} \right]$	Relativistic Doppler	Single-point orientation (from East or North)	Flywheel effect

Tables 10 and 11 present the results of analysis for the quadrant-based components' four characteristics of growth, sine and cosine, field vectors, and Doppler vectors.

Table 10*Findings from Magnitude Analysis*

Summary of Magnitude Analysis Equations				
System Engineering Models	Equations	Thumbnail Diagrams	Self- Referential	Harmonic / Dynamical
Growth Rate	Upper/Lower 6z rate: $\frac{\sqrt{e}}{\sqrt{2}}$, Upper/Lower 6z rate over area: $\pi \left(\frac{\sqrt{e}}{\sqrt{2}} \right)^2 = \frac{1}{2} \pi e$ $\left(\frac{\sqrt{e}}{\sqrt{2}} \right) t \ln(t)$, starting lower plane		Ratio between Upper and Lower planes	Balance of 6z partials applied force from all quadrants
Segment Growth (with respect to x-axis)	$\frac{dx}{dy} = \frac{d(LQ1 + LQ3)}{d(LQ2 + LQ4)}, \frac{dx}{d(y-x)} = \frac{d(UQ1 + UQ3)}{d(UQ2 + UQ4)}$		Relational segment growth	Balancing growth with off-center gravity
Segment Growth Balance of Gravitational Center	Amount Segment Vectors Off-center $\frac{(\sum LQ1 - \sum LQ3)}{2}, \frac{(\sum LQ2 - \sum LQ4)}{2},$ $\frac{(\sum UQ1 - \sum UQ3)}{2}, \frac{(\sum UQ2 - \sum UQ4)}{2}$		Relational segment growth	Balancing growth with off-center gravity
Sine and Cosine Relationships	$VLoe^{(VLo)^2} = AVG(\cos L_O \theta + \sin L_E \theta) e^{AVG(\cos L_O \theta + \sin L_E \theta)^2}$ 45-degree stability Vibration and Oscillation		From quadrant coordinates and components	Spin and acceleration vectors Changing Coriolis effect
Sine Partial Derivative Relationships, Snell's Law Ratios	$\frac{\partial \sin [LQ1] dt}{\partial \sin [Qn] dt} =$ $\frac{(\sin [LQ1] dt \cdot \sin [LQ1] dt)}{(\sin [LQ2] dt \cdot \sin [LQ3] dt \cdot \sin [LQ4] dt \cdot \sin [UQ1] dt \cdot \sin [UQ2] dt \cdot \sin [UQ3] dt \cdot \sin [UQ4] dt)}$		From quadrant coordinates and components	Lower plane (poles/axis) Rotor and screw-like action, Upper Plane (transition) magnetic field.
Sine and Cosine Concept of Quantum Spin	$\vec{j} =$ $\left[\frac{\partial 6z}{\partial LQ1} + \frac{\partial 6z}{\partial LQ2} + \frac{\partial 6z}{\partial LQ3} + \frac{\partial 6z}{\partial LQ4} \right] + \left[\frac{\partial 6z}{\partial UQ1} + \frac{\partial 6z}{\partial UQ2} + \frac{\partial 6z}{\partial UQ3} + \frac{\partial 6z}{\partial UQ4} \right]$		From quadrant coordinates and components	$\vec{j} = \vec{l} + \vec{s}$ \vec{l} = angular momentum (Lower Plane) \vec{s} = spin momentum (Upper Plane)
Sine Velocity and Derivative Translation	Upper Plane: $AVG(\cos L_O \theta + \sin L_E \theta) e^{AVG(\cos L_O \theta + \sin L_E \theta)^2} (\text{Lower Plane}) + \left(\frac{e}{\ln(t)} - \frac{1}{\pi} \right)$ Lower Plane: $AVG(\cos L_O \theta + \sin L_E \theta) e^{AVG(\cos L_O \theta + \sin L_E \theta)^2} \left(\pi + \frac{1}{e^2 \pi} \right) t \ln(t)$ Lower Plane: $VLoe^{(VLo)^2} \left(\pi + \frac{1}{e^2 \pi} \right) t \ln(t)$		From quadrant coordinates and components	The equation $[V^* e^{(\text{acceleration})}]$ aligns with spin properties
90-degree Field Effect Vectors	$LQ1^\perp = \left[\frac{\partial 6z}{\partial LQ4} + \frac{\partial 6z}{\partial LQ1} \right] / \left[\frac{\partial 6z}{\partial LQ1} + \frac{\partial 6z}{\partial LQ2} \right]$ $LQ2^\perp = \left[\frac{\partial 6z}{\partial LQ1} + \frac{\partial 6z}{\partial LQ2} \right] / \left[\frac{\partial 6z}{\partial LQ2} + \frac{\partial 6z}{\partial LQ3} \right]$ $LQ3^\perp = \left[\frac{\partial 6z}{\partial LQ2} + \frac{\partial 6z}{\partial LQ3} \right] / \left[\frac{\partial 6z}{\partial LQ3} + \frac{\partial 6z}{\partial LQ4} \right]$ $LQ4^\perp = \left[\frac{\partial 6z}{\partial LQ3} + \frac{\partial 6z}{\partial LQ4} \right] / \left[\frac{\partial 6z}{\partial LQ4} + \frac{\partial 6z}{\partial LQ1} \right]$		From quadrant coordinates and components	Upper plane has same form as Lower plane equations. TYPICAL 90-vector diagram and findings At Coil 144 Rotor-Stator
Field Vectors Product Tensor Reciprocal inverse transposed matrices	$LQ1 * UQ1 = \frac{1}{(LQ3 * UQ3)} ; LQ1 * UQ2 = \frac{1}{(LQ3 * UQ4)} ;$ $LQ1 * UQ3 = \frac{1}{(LQ3 * UQ1)} ; LQ1 * UQ4 = \frac{1}{(LQ3 * UQ2)} ;$ $LQ2 * UQ1 = \frac{1}{(LQ4 * UQ3)} ; LQ2 * UQ2 = \frac{1}{(LQ4 * UQ4)} ;$ $LQ2 * UQ3 = \frac{1}{(LQ4 * UQ1)} ; LQ2 * UQ4 = \frac{1}{(LQ4 * UQ2)} .$		From quadrant coordinates and components	Balanced intense reciprocal perturbation and vibration with focused areas of null, non-activity.
Field Vectors After adding 2-4 poles, axis	$LQ1^\perp = \left[\frac{\partial 6z}{\partial LQ4} + 4t + \frac{\partial 6z}{\partial LQ1} + 2t \right] / \left[\frac{\partial 6z}{\partial LQ1} + 2t + \frac{\partial 6z}{\partial LQ2} + 4t \right]$ $LQ2^\perp = \left[\frac{\partial 6z}{\partial UQ1} + 2t + \frac{\partial 6z}{\partial UQ2} + 4t \right] / \left[\frac{\partial 6z}{\partial UQ2} + 4t + \frac{\partial 6z}{\partial UQ3} + 2t \right]$ $LQ3^\perp = \left[\frac{\partial 6z}{\partial LQ2} + 4t + \frac{\partial 6z}{\partial LQ3} + 2t \right] / \left[\frac{\partial 6z}{\partial LQ3} + 2t + \frac{\partial 6z}{\partial LQ4} + 4t \right]$ $LQ4^\perp = \left[\frac{\partial 6z}{\partial UQ3} + 2t + \frac{\partial 6z}{\partial UQ4} + 4t \right] / \left[\frac{\partial 6z}{\partial UQ4} + 4t + \frac{\partial 6z}{\partial LQ1} + 2t \right]$		From quadrant coordinates and components	Applying Poles (2t, 4t) back into Lower Plane, comparing stabilizing effect of axis-pole values
Dopplers	$\frac{\partial LN}{\partial LS} = \left[\frac{\partial 6z}{\partial LQ4} + \frac{\partial 6z}{\partial LQ1} \right] / \left[\frac{\partial 6z}{\partial LQ2} + \frac{\partial 6z}{\partial LQ3} \right]$ $\frac{\partial LW}{\partial LE} = \left[\frac{\partial 6z}{\partial UQ1} + \frac{\partial 6z}{\partial UQ2} \right] / \left[\frac{\partial 6z}{\partial UQ3} + \frac{\partial 6z}{\partial UQ4} \right]$		From quadrant coordinates and components	Upper plane has same form as Lower plane equations. Ratios of 2, 5, and 10 repeating

Table 10 is limited to the findings using the magnitude model, while Table 11 contains the inverse-squared (post-zeta) findings. The order of the four main characteristics were documented with underlined text and a different shade of color-coding that helps annotate them as the core concepts. Supportive subsets were not bolded or underlined.

Table 11

Findings from Post-Zeta Analysis

Summary of Post-Zeta Analysis Equations				
System Engineering Models	Equations	Thumbnail Diagrams	Self- Referential	Harmonic / Dynamical
<u>Growth Force</u>	$\text{Over Area} = \sum_{n=0}^t \left[\frac{6z}{(n^2\pi)} \right];$ $\sum_1^t \frac{6z}{r^2} = \left(e + \frac{\sqrt{3}}{2} \right) - \frac{e^e}{t+\pi^2} = \left(e + \frac{\sqrt{3}}{2} \right)$ $\sum_1^t \frac{6z}{r^2} = \pi \left(e + \frac{\sqrt{3}}{2} \right) = 2\pi \left(\frac{e}{2} + \frac{\sqrt{3}}{4} \right)$ $= 2\pi \left(\frac{e}{2} + \tan(23.4^\circ) \right)$	$\sum_1^t \frac{6z}{r^2} = (e + \frac{\sqrt{3}}{2}) - \frac{e^e}{(\frac{\pi}{2} + \frac{23.4^\circ}{2})} = 2\pi \left(\frac{e}{2} + \frac{\sqrt{3}}{4} \right) = 2\pi \left(\frac{e}{2} + \tan(23.4^\circ) \right)$	Gravity as a force Inverse square	Electron movement circumference at the tilt of Earth (23.4°)
<u>Sums</u> of inter-quadrant products	$(LQ1UQ1+LQ2UQ2) = (LQ3UQ3+LQ4UQ4).$ $LQ1Q3 = LQ1 + LQ3 = 0.488 = \frac{1}{2} \left(\frac{1}{3} \right) \left(\frac{3}{2} \right) = LQ2Q4 * UQ2Q4$ $UQ1Q3 = UQ1 + UQ3 = 1.284 = \frac{5}{4} = \left(\frac{3}{2} \right)^2 - 1 = (UQ2Q4)^2 - 1$ $LQ2Q4 = LQ2 + LQ4 = 0.313 = \frac{1}{\pi} \text{ or } \frac{1}{3}$ $UQ2Q4 = UQ2 + UQ4 = 1.497 = \frac{3}{2} = \left(\frac{5}{4} + 1 \right)^{\frac{1}{2}} = (UQ1Q3 + 1)^{\frac{1}{2}}$ $\frac{5}{4} = \left(\frac{3}{2} \right)^2 - 1 = \sec^2 \theta - 1 = \tan^2 \theta; \tan^2(48.19^\circ) = \frac{5}{4}$		From quadrant coordinates and components	Balancing plane circumference ratios
<u>Sine and Cosine</u> from Quadrant Plane Line Segments	$COT(\text{Lower}) = \frac{\text{Lower Odd}}{\text{Lower Even}} = \frac{\frac{1}{2}}{\frac{3}{2}} = \frac{3}{2} = \text{Upper Even};$ $COT(\text{Upper}) = \frac{\text{Upper Odd}}{\text{Upper Even}} = \frac{\frac{5}{4}}{\frac{3}{2}} = \frac{10}{12} = \frac{5}{6} = 1 - \frac{1}{6}$ $= 1 - (\text{Lower Odd}) * (\text{Lower Even}) = 1 - \left(\frac{1}{2} \right) \left(\frac{1}{3} \right)$		From quadrant coordinates and components	Balancing plane circumference ratios
<u>90-degree Field Effect Vectors</u> Sums	$\text{Rate of Area or Volume over time Pyramid} = \frac{5}{4} \frac{e^2}{t}$ $\text{or Cone} = \frac{5}{4} \frac{e^2 \pi}{t}$ $\sum_1^t -QL \frac{6z}{t^2} + -QU \frac{6z}{t^2} = \left(\frac{5}{4} \right) e^2 = e^2 \sec(36.85^\circ) = 9.236$		From quadrant coordinates and components	Balanced projection of force, emitting power
<u>90-degree Field Effect Vectors</u> Products	$\text{Angular velocity changes every } \frac{\pi}{2} :$ $\text{Reciprocal growth multiplier changes every } \frac{\pi}{4}$		From quadrant coordinates and components	Reciprocal in rotational angle and magnitude multiplier
<u>Doppler</u>	<ul style="list-style-type: none"> Lower N/S = $53/50 * \text{Lower W/E}$ Upper W/E = $3.579 * \text{Upper N/S rate}$, <ul style="list-style-type: none"> Which is the decay rate of $(e + \frac{\sqrt{3}}{2})$ * Upper N/S rate Post-zeta 90-degree field vector products of $\frac{53}{50} \left(\frac{2}{3} \right) \cong 0.707$ 	<ul style="list-style-type: none"> Lower N/S = $53/50 * \text{Lower W/E}$ Upper W/E = $3.579 * \text{Upper N/S rate}$, which is the decay rate of $(e + \frac{\sqrt{3}}{2})$ * Upper N/S rate 	From quadrant coordinates and components	Lower N/S and W/E reciprocals associated with Upper and Lower Field Vector Rates

Content for Table 11 differed slightly in that there were no overarching generic diagrams for sine and cosine, 90-degree normal (field effect) vectors, or Doppler vectors. This was due to the post-zeta models compiled from either products, sums, or sums of products of discrete vector

values. Besides the suspicious growth force tilting at a tangent equivalent to the tilt of the Earth, another oddity was the tangent relationships of the line segments having a reciprocal and complementary relationship between the upper and lower planes.

Conclusions regarding Hypotheses

The initial hypotheses of this dissertation were the existence of a self-referring, harmonic, dynamical, and systematic behavior of the prime numbers. A significant quantity of evidence has been uncovered that proves uniquely synchronized systematic properties exist in the prime number component structure. The results from the separate analyses of the magnitude models and the post inverse-squared models align with the hypothesis that the prime number behavior can be described using system engineering models. Both models have produced more data than was expected to reinforce and validate those hypotheses from the relationships and interactions between the components of the prime number coordinate system. More application of the models will be discussed in the recommendations of this chapter. In completing the validation of the hypotheses, the specific fulfillment of each is summarized.

Validating the Self-Referential System Hypothesis

The first research hypothesis (H_A1) was that the prime number components will reveal the self-referential systemic behavior of the prime numbers. This would have been demonstrated by the consistent system behavior of the vector relationships for the hypotenuse, tangent, sine, cosine, Doppler, and normal vector field effects. Research results showed the effect of sine and cosine in driving the angular velocity vector and the electron-like spin relationships that are also part of the systematic mode shifts of the Doppler and normal field vectors. Therefore, H_A1 is

true and H_01 is false, due to the requirement that H_01 would be demonstrated by the inconsistent and systematically inexplicable behavior of the vector relationships.

Validating the Harmonic and Dynamical Behavior Hypothesis

The second research hypothesis (H_A2) is that the specific components of this prime number growth model consistently maintain a harmonic and dynamically balanced behavior throughout the first 100,000 prime number increments. This would have been demonstrated by continuously self-balancing reciprocal values between interdependent diagonal quadrant components, related to a zeta function dynamic. Research results showed the product of post inverse-squared normal (90-degree) vectors to be reciprocally balanced with their angular rate of rotation and their product rate of previous vector values. A reciprocal tensor product balancing was also discovered between diagonal sets of quadrant plane tensors. The overall system balanced and converged its growth through what appeared to be different modes. Therefore, H_A2 is true and H_02 is false, due to the requirement that H_02 would have been demonstrated by uncontrolled drifting of the derivative relationships, thereby showing either a gradual or a reactive unbalanced behavior between interdependent diagonal quadrant components.

Validating the Reproducible System Model Hypothesis

The third research hypothesis (H_A3) was that the prime number growth can be defined in a system model with this component coordinate system and vector relationships that align with natural or manufactured system behaviors. This would have been demonstrated by the ability to define the system's specific phases and relationships that mirror behaviors of currently known systems, such as electromagnetic fields, force, or acceleration. Research results showed several

relationships that mirror behaviors of currently known systems in Table 10 for the magnitude model and in Table 11 for the post inverse-squared model. The updated magnitude model is the epitome of a well-defined and reproducible system model. Therefore, H_A3 is true and H_03 is false, due to the requirement of H_03 that the prime number growth cannot be defined in a system model with this component coordinate system, and this would have been demonstrated by the inability to define the system's specific phases and relationships that mirror behaviors of currently known systems.

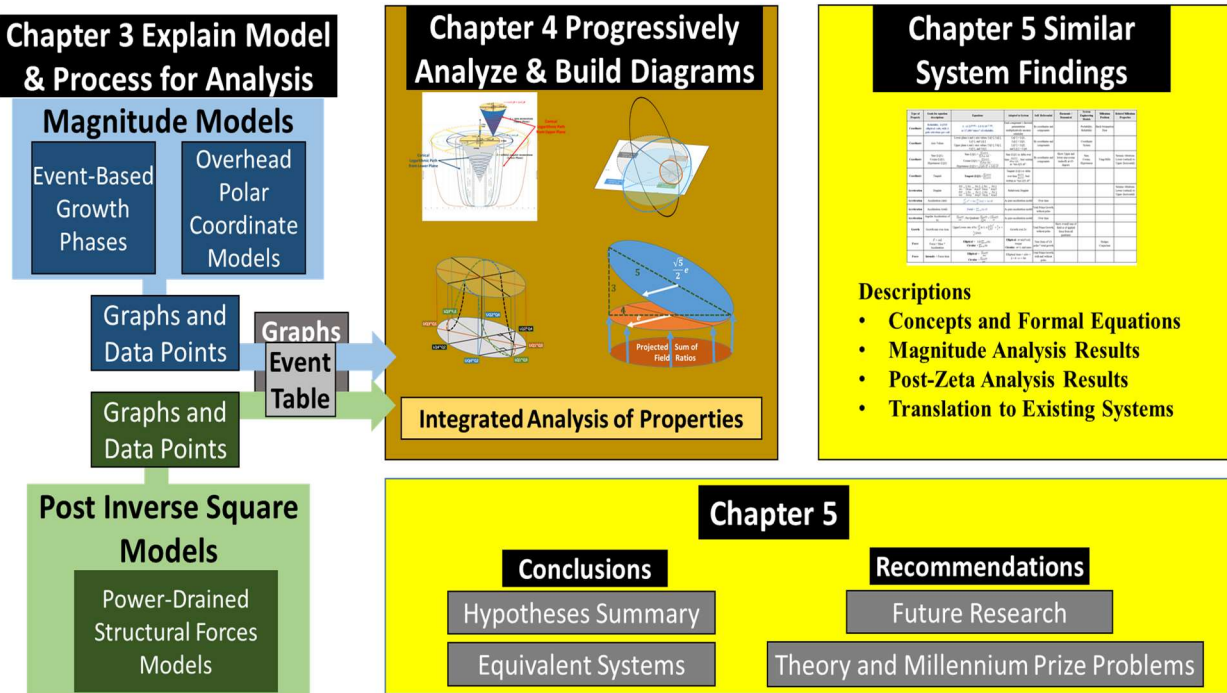
Study Taxonomy

The framework and taxonomy of the study strictly followed the model-driven analysis of magnitude and post inverse-squared data of the first 100,000 prime numbers placed in the quadrant-based component and coordinate system. Figure 45 captures the associated flow of data and the progressive analysis performed in this research.

The two models (magnitude and post inverse-squared) provided the desired different aspects to the components' four main characteristics. The benefit of the magnitude model was that it provided data to define dimension and mode shifts of the system over time. The benefit of the post inverse squared model was that it provided a clear analysis of an equivalent horizontally expanding system in a specific direction or method. System properties discovered from the post inverse squared model were aligned with the properties of the magnitude model. This produced a holistic view of all models working synchronously, which was used to consider how its overall properties would translate to existing systems and their properties.

Figure 45

Taxonomy of progressive data analysis



Due to the focus of the hypotheses on correlating behavior and finding contributions to existing systems, any correlation contributed a practical validation of all three hypotheses. The tightly coupled associations between the harmonic and the self-referential properties formed the concepts to derive the logical and physical engineering models. Applying this system engineering and modeling approach under the control of its own coordinate system resulted in multiple recommendations for future research along with possible contributions to rethinking the Millennium Prize Problems.

Recommendations

The recommendations for applying these findings depend mainly on each individual researcher's area of expertise and goals. Noncommittal as that may sound, that may be the best way to introduce the potential flexibility of the models in different disciplines. The overall recommendation is to use this component and coordinate structure of the prime numbers as a logical and a physical model for reevaluating some of our most complex problems. The immediate recommendation is a little more practical: Use this model as an architecture for the optimization, efficiency, and control of systems. Table 12 describes some parallels and the suggested means to translate this model into related physical models and known system characteristics.

Table 12

Translating findings to known systems

Translation into Other Known Systems				
System Engineering Models	Equations	Adapted to System	Self- Referential	Harmonic / Dynamical
Force	$\vec{F} = m\vec{a}$ Force = Mass * Acceleration Elliptical = $12t \sum_1^t 6z$; Circular = $\sum_1^t 6z$	Elliptical: mass related to torque from 12t axis expansion; $m=axis*coil$. Circular: $m=1$, unit mass	Coordinate values of 6z and 12t poles	Total flow or force in an elliptical structure
Intensity = Force/Area or Pressure = Force/Area	Elliptical = $\frac{\sum_1^t 6z}{8\pi t}$ Circular = $\frac{\sum_1^t 6z}{2\pi t}$	$\frac{\sum_1^t 6z}{Area}$ Elliptical Area = $ab\pi = 2 * 4 * \pi = 8\pi$	Total Prime Growth, with and without poles	Balanced distribution
Force Screw Theory	Sum of all partial of forces. Sum of torque (force) on all planes $\frac{\partial 6z}{\partial x} + \frac{\partial 6z}{\partial xy} + \frac{\partial 6z}{\partial y} + \frac{\partial 6z}{\partial yx}$; x and y = lower plane xy and yx = upper (transition) plane	$\frac{\partial 6z}{\partial x} = \left[\frac{\partial 6z}{\partial LQ1} + \frac{\partial 6z}{\partial LQ3} \right]$ $\frac{\partial 6z}{\partial xy} = \left[\frac{\partial 6z}{\partial UQ1} + \frac{\partial 6z}{\partial UQ3} \right]$ $\frac{\partial 6z}{\partial y} = \left[\frac{\partial 6z}{\partial LQ2} + \frac{\partial 6z}{\partial LQ4} \right]$ $\frac{\partial 6z}{\partial yx} = \left[\frac{\partial 6z}{\partial UQ2} + \frac{\partial 6z}{\partial UQ4} \right]$	As coordinates and components	Show overall sum of field or of applied force from all quadrants
Force Electromotive	$V_{Q1} = \frac{\sum_{n=0}^t (\partial 6z dQ4)}{\sum_{n=0}^t (\partial 6z dQ1)} + \frac{\sum_{n=0}^t (\partial 6z dQ1)}{\sum_{n=0}^t (\partial 6z dQ2)}$; V=Electromotive Force, E=Energy, Q=Charge. The electromotive force (V) of energy (E) to move the charge (Q)	Altered Right Hand rule from S = E=M*B to S/E = M or S/M = B 90-degree Vector Relationships. V=E/Q; Normal, Poynting, Tensor, and EM Field Vectors	Total Prime Growth by coordinates and components	Show tensor product reciprocal diagonal planes and values
Power Power = Force * Area	Elliptical = $8\pi t \sum_{n=0}^t 6z$ Circular = $2\pi t \sum_{n=0}^t 6z$	Elliptical Area = $ab\pi = 2 * 4 * \pi = 8\pi$	Total Prime Growth, with and without poles	At a smoothed logarithmic rate of $t \ln(t)$
Vibrations and Equilibrium Mechanical, Molecular	$LQ1 * UQ1 = \frac{1}{(LQ3 * UQ3)}$; $LQ1 * UQ2 = \frac{1}{(LQ3 * UQ4)}$; $LQ1 * UQ3 = \frac{1}{(LQ3 * UQ1)}$; $LQ1 * UQ4 = \frac{1}{(LQ3 * UQ2)}$; $LQ2 * UQ1 = \frac{1}{(LQ4 * UQ3)}$; $LQ2 * UQ2 = \frac{1}{(LQ4 * UQ4)}$; $LQ2 * UQ3 = \frac{1}{(LQ4 * UQ1)}$; $LQ2 * UQ4 = \frac{1}{(LQ4 * UQ2)}$.	90-Tensor Products, N/S Lower and W/E Upper plane seismic sine-cosine vibration and doppler	Upper to Lower Plane	Balancing Zeta and Lorentz forms

Recommendations for Future Research

The potential for future research appears to be so vast that the scope of future research may deserve several dissertations of its own. Any one of the individual magnitude or post inverse-squared models used to describe each of the four main characteristics (growth, trigonometric, normal vectors, Doppler vectors) could be used to generate its own theoretical and practical research plan. Any future research will require a paradigm shift regarding the purpose and functional contribution of prime numbers, transitioning from the traditional factor and root-based understanding to considering prime numbers as a framework for multidimensional or abstract problems. Only after that conceptual shift can the structure of the prime numbers can provide possible practical impacts for stabilizing current systems.

Regarding Millennium Prize Problems

With the request from the Clay Mathematics Institute regarding new and fresh and innovative ways to rethink some of the Millennium Prize Problems (CMI, 2000), it might be a proper time to consider a shift in logic regarding the prime numbers. Traditionally, understanding the prime numbers and their systemic behavior has been internally focused on their contribution to finding more primes and understanding more about primes. Prime numbers have been considered a problem to understand. A new concept is considering prime numbers to be the solution to other problems, such as the Millennium Prize Problems. Considering the different system engineering models discovered through analyzing the characteristics of each model (magnitude and post-zeta), Table 13 describes their possible contribution to five of the Millennium Prize Problems.

As for the Riemann Hypothesis, the coil-based component model provides a different aspect to the prime number distribution. This distribution is based on the occurrence of coils and the cardinal heading they provide, not on the placement of real and imaginary roots from an accumulated packaged value of the cardinal headings (2 and 4) and all multiples of $6z$. Considering the prime numbers as a result of the $6z$ harmonic (or quantum) function applied to its own integrated pole values (2 and 4) suggests that a different approach to defining and finding primes is possible.

Table 13

Possible contributions to Millennium Prize Problem efforts

Suggested Possible Component Model Contributions to Millennium Prize Problem Efforts					
System Engineering Models	Riemann Hypothesis	Navier-Stokes	Yang-Mills	Birch-Swinnerton-Dyer	Hodge's Conjecture
Coordinate and Quadrant Axis Translation	As reference coordinates and components considered as complex plane, abstract dimension	As reference coordinates and components considered as complex plane, abstract dimension	As reference coordinates and components considered as complex plane, abstract dimension	As reference coordinates, Elliptical major and minor axis (4 and 2), considered as complex plane, abstract dimension	Prepare geometrically expanding coordinates, considered as complex plane, abstract dimension
Trigonometric and Angular	Lower (angular, velocity), Upper (spin and magnetic field)	Upper and lower plane sine tradeoffs at 45-degrees, Direction of conical acceleration and flow	Seismic and quantum vibrations, lower plane vertical movement, upper plane horizontal movement	Angular balance of force on an elliptical model	Angular dynamics driving expansion
Growth (Total)	Growth of nonlinear harmonic $6z$ function on two stable (2&4) poles.	Balanced distribution of second derivative regarding flow of current	Dynamical growth, radiation, spin, and acceleration vectors, 2 and 4 pole increments and mass-torque.	Logarithmic balance of force on an elliptical model	Horizontal hemispherical growth model, Vertical cylindrical growth model, Conical Growth model, 2 planes of growth
Quadrant Segment Growth	Balanced harmonic segment relational growth	Flow balancing relational segment growth with off-center gravity	Quantum translation of the circles from quadrant segments as fields (upper plane) or mass (lower plane)	Translation of lower quadrant ellipse force when poles added, centers stay the same	Total area growth by quadrant
Acceleration (Rate)	System definition as $6z$ force or acceleration, rate of increase in velocity	$6z$ as fluid viscosity, temperature, or pressure change	Spin and acceleration vectors, Balance of $6z$ partials applied force from all quadrants	Balancing and changing Coriolis effect	Increase over coil (time)
90-degree Field Effect Vectors	System definition as electromagnetic with a Rotor-Stator relationship Lower-Upper	Translated and Normal 90-vector, Field vector. Upper plane has same form as Lower plane equations. Applying $6z$ as acceleration or force.	Tensor products have intense reciprocal perturbation and vibration with focused areas of null, non-activity.	Applying elliptical poles (2t, 4t) back into Lower Plane, comparing stabilizing effect of axis-pole values	Sums of vectors in volumetric or area forms. Products of vectors as a growing saddle function.
Relativistic Doppler	Relativistic movement or relativistic center, instead Real and Imaginary coordinates	Single-point orientation (from East or North)	Seismic vibrations Lower (vertical) to Upper (horizontal)	Elliptical flywheel effects	Shifting depth and circumference from velocity of emitted field
Quantum and Spin	System definition as electromagnetic or quantum, Lower plane rotor with screw-like action, Upper Plane (transition) magnetic field.	Lower plane (poles/axis) Rotor with screw-like action, Upper Plane (transition) magnetic field.	$\vec{j} = \vec{l} + \vec{s}$ \vec{l} = angular momentum (Lower Plane) \vec{s} = spin momentum (Upper Plane)	Applied quantum spin to an elliptical structure, selecting angular offset of ellipse growth	Two separate geometric forms expanding

A common contribution of this component model could be the use of the coordinate system as an alternative approach to the complex plane to define harmonic and oscillating behavior. The angular and trigonometric contribution is varied, based on the translation of the lower and upper plane properties. With the lower plane representing vertical movement on a pole and the upper plane representing horizontal movement between poles, a correlation exists to seismic North/South and East/West vibrations. The characteristic of growth directly relates to any selected system structure, but maybe relates even more specifically to potential geometric system models in multiple dimensions that partially fulfill the expectations of systems associated with Hodge's Conjecture.

The quadrant balancing of force, much like centers of gravity, combines wave properties with possible mass properties. This provides a framework that appears to have an intrinsic ability to transpose one physical model into another physical model. Correspondingly, this may open some possible approaches to Yang-Mills and investigating radiated wave properties.

The potential representation of the multiples of $6z$ as the result of acceleration (or the second derivative of a cubic function), opens the possibility of the growth representing balanced acceleration (or heat and force dissipation) logarithmically along the lower and upper planes. With the known contiguous flow of the increments over the coil structure, this provides a framework for different aspects of flow associated with Navier Stokes. The 90-degree relationships that display normal and field vector behavior from a source of force can also be associated with current, fluid, or heat flow.

Almost as a culminating possibility, any or all these properties can be implemented in an elliptical framework with the insertion of the pole values (2 and 4) as the major and minor ellipse axis. Although the designated pole values of the primes are already determined, other pole

values could be used and the increments of $6z$ placed on the locations of the new pole values. This would apply the harmonic behavior of $6z$ to a desired elliptical geometric model, in any dimension. In that case, research efforts in both Hodge's Conjecture and Birch-Swinnerton-Dyer might benefit. Apart from the popular Millennium Prize Problems, the component model could possibly contribute to other theoretical research topics.

Regarding Theoretical Research

Where could this framework take research over the next twenty years? What contribution could it make to foundational theories in science, mathematics, and engineering? Some of these potential research and theory areas will be dependent on using the examples in Table 12 for conceptual methods translating these component properties. With this chapter recently summarizing the integrated properties, addressing these potential research areas starts with the most integrated topic, quantum behavior models and simulations. A summary of its potential for a quantum-level of cybersecurity is covered prior to the discussion of its potential mathematical models in abstract space. The potential for research in the closely related topics of mechanical engineering stress and vibration, along with equilibrium and stabilization are then discussed. The polar coordinate views provide a topic for consideration in fluid dynamics, followed by the consideration of an optical version of the sine relationships in refraction and Snell's Law. A final correlation is made to the different types of computer languages and Turing Machines.

Quantum behavior models and simulations

The model's characteristics of angular velocity in the lower plane and spin on the upper plane provide a potential connection to current quantum computing research. This connection to

computing framework would be the result of considering the quantum behavior of the prime number component structure as equivalent to the results from a mainframe instruction set. The instructions and combinations of functions are yet to be described but the starting point would naturally be the instructions from vector properties discovered in this component model.

What is the larger desired outcome from a sequence of quantum operations? Is it just to do more brute force computations with all permutations of a problem? The larger and ultimate computing challenge would be to perform multiphysics nonlinear operations. Quantum computation of quantum properties is a goal more aligned to the intrinsic computing structure. If properties of the component model were used to provide known and repeatable nonlinear quantum computing results, the model could potentially save orders of magnitude in efficiency for testing and validating computing performance.

Can the component structure, either at a point in time or with combined component relationships, produce the desired result of a quantum-based computational problems? In that manner, it might be a better starting point instead of freezing quantum behavior and reducing it down to the computational impact of a single binary bit for binary computations forced into nonlinear differential equations for solving or simulating quantum-based problems. The binary approach would appear to create a binary computing bottleneck for multiphysics problems. At a minimum, this component model could provide an instruction or translation model between desired and guaranteed results. Having known values that are tied to a quantum model of behavior also presents a different aspect to the contribution of prime numbers to cybersecurity.

Quantum-level of Cybersecurity

While discussing the topic of quantum computing, it is probably best to propose a solution to the threat to encryption. Instead of allowing some paralyzing fear to dominate these

discussions, more productive thoughts may be in the methods to apply this component model and provide a new quantum-level of improved cybersecurity. In the case of this component model, unique quantum characteristics and values are generated as the system balances itself over time. Using sets of these quantum value combinations to encrypt data immediately takes the challenge of breaking its encryption to an entirely new level of difficulty. Using the data that exists from this research, efforts could start on a practical implementation of these discovered quantum-like component properties and interactions to provide a quantum level of security. That security could only be understood within selected specific combinations of this framework (Hibbs & McAndrew, 2021). This is one of the largest benefits from the multiple abstract models the framework provides.

Mathematical models in abstract space

The model also provides mathematical combinations that are the most flexible when considered in their own abstract dimension. In some ways the component coordinate system may already provide a solid representation of a system in Hilbert abstract space. With this nonlinear system's growth independent of the standard number line framework, a new directional axis is provided. Does that mean there is no longer a need for a complex plane with this new model? Absolutely not. It can provide a complex extension to the component coordinate system, yet another dimension to a system initially defined in an abstract dimension.

In considering abstract space and dimensions, an abstract matrix approach was used in the grouping of the transition $6z$ values in the upper plane that provides rotational movement. This is related to the approach used by Einstein for summation of properties in abstract matrixes. As an intrinsic property of the component model, potential exists for correlating this model's stress and vibration into mechanical movement in abstract space.

Mechanical Engineering Stress and Vibration

From comparing the different the upper and lower planes balancing around 45-degrees with the sine and cosine values, a close relationship to seismic vibrations appears to exist. The coordinate system's physical model has unique instances of $6z$ intersecting with the lower plane axis, as with a vertical value assigned to an axis. This leads to the assignment of vertical vibration to the lower plane. The upper plane facilitating the rotational radius movement would lead to the assignment of horizontal vibration. (Graphs of these relationships are provided in Appendix B.) If a vertical or conical concept is being considered, the upper plane would contain a combination of horizontal and vertical. Translating these vibrational characteristics to seismic relationships could provide an architecture for the placement of reinforcement bars in structural beams, which could harmonically and evenly displace, absorb, or divert energy flow. The flexibility of the component structure in producing a state of equilibrium could have many applications.

Equilibrium and stabilization

The equilibrium and stabilization that the framework provides could also be seen as an implementation of efficiency. It appears to have no “wasted” energy that does not contribute to the stability of force being applied to another component. This would be extremely beneficial for the desired underdamped properties of antenna structures. While there are currently helical antennas that provide efficiencies for specific wavelengths based on their coil structure, the insertion of additional receptors at the $6z$ locations would most likely provide an optimum reception and convergence of the transmitted data. Comparing the reception of data over the quadrant components may also assist in directional tuning.

From the perspective of a sequential resistive ladder, the voltages across the quadrants could provide a physical phase difference. In that manner, it might be worth considering the harnessing and taming of forms of electricity into a phase-based windings for the storage of energy. Providing efficiency with solar energy receptors in the $6z$ structural sequence could possibly advance means for readily supplying worldwide power in the demand for electric cars.

The harmonic convergence associated with the coil timing also provides a specific sequence in a physical structure to apply course corrections, or torquing pulses, to an unmanned vehicle. On a more extreme level, it does have a specific structure that might apply to harvesting the energy in lighting, due potential phases alignments in current flow.

Fluid Dynamics

The graphs in Appendix B that display information for “Vibration and harmonic periodicity analysis” could also be considered as related to fluid flow. The polar coordinate view of the 90-degree normal vector values could be correlated to the concentrated fluid flow and vibration near a pipe’s circumference. Although the aspect of fluid dynamics was mentioned regarding the Navier-Stokes equations, a detailed correlation of the $6z$ relationships to viscosity could also be researched. Appendix B also contains examples of repeating the lower plane normal vector values at different frequencies. That is done by varying the timeline (size) of the total lower plane values to align with the upper plane’s almost shell-like behavior. This was to demonstrate the potential for internally repeated iterations of the lower plan (rotor) that cannot be seen with the external values of $6z$ on the outer shell provided by the upper plane (stator). The possible concept for exploration here is the same property within the unknown realm of the $6z$ system...that is, if it represents a system with one of the many second integral forms of $6z = \iint c_1 z^3 + c_2 z + c_3$ that could be applied to the overall flow structure.

Refraction and Snell's Law

Part of the examination and comparison of sine values between upper and lower planes also opened the potential for different forms of wave refraction. Snell's Law relationships between the upper and lower plane should be researched more. Appendix B contains the four quadrant-to-quadrant comparisons of upper to lower sines. The appearance of selective and temporary paring of refraction values seems to be occurring.

Further investigations into the sine partial derivatives and relationships (Appendix A) might be considered. In Chapter 4, the review of lower plane sine partial derivatives revealed a corkscrew behavior with elongated frequency over time. With both the quantum angular velocity of the lower plane and the sine wave properties, research in the optical refraction properties within the component framework should probably be considered.

Another concept or component of unified theories

The combined characteristics resembling systems with balanced centers of gravity, sound wave Doppler, electromagnetic rotor and stator fields, quantum electron spin, and elliptical acceleration could lead to some type of consolidated model of fundamental forces in nature. Do the growth characteristics of the prime numbers provide a solid starting point or logical ending point for multi-physics relationships? Are they the result of one system and the starting framework for another system? Are there any new integrated theories that this new component model suggests? Finding correlations between previous unified theories and the prime number component model characteristics might reveal some interdependent characteristics. A logical start would be determining a minimum set of translation functions (as in Table 12) for the future research. As an abstract example of a potentially vital case in astrophysics, the component model's $6z$ acceleration behavior to infinity could be related to the elliptical planetary

acceleration that occurs toward a black hole. Apart from the physical models of the prime number logic, the component model's connection to computational linguistics and computer languages may provide an even more abstract research topic.

Computer Languages and Turing Machines

Due to the multiple physical properties revealed in this research, one topic related to prime numbers and computability was not specifically covered. This may be best summarized with a question: "What type of computational language is expressed by the prime numbers?" A quick review of Chomsky's hierarchy of languages would always address the four types of languages; where Type 0 is the least constrained recursively enumerable language processed in a Non-Deterministic Turing Machine (NDTM). Type 1 is a context-sensitive language with a linear-bounded automaton and Type 2 is a context-free language with a push-down automaton (PDA), which is also called a stack. The most restrictive for processing with finite state automaton is a regular language, Type 3. The two languages of most interest to the component model are the Type 3 regular language and the Type 0 NTDM. The two-pole structure provides the regular language with only two syntax rules: $[a \rightarrow ab]$; $[b \rightarrow ba]$, where $\{a = 2, b = 4\}$. This means that an occurrence of "a" implies succession of one and only one "b". Likewise, this means that an occurrence of "b" implies succession of one and only one "a". The language is implemented with the characters (values) of $a = 2$ and $b = 4$. What about the multiples of $6z$? They are clearly a nonlinear system of flexibility and equilibrium, which strongly points to $6z$ being a NDTM.

Why is this significant? The prime numbers generate an intersection of two languages, both languages are on the extreme scale of the hierarchy of languages from the most constrained to the most dynamically expanding. Implications could apply to the combination of natural

languages, to the rules for the extent and balancing of natural languages, and to the related processing of combined computer languages. In a more practical form, combined computer languages can often allow holes between the language semantics, which are manipulated by cyber criminals. More plainly, the power of more than two types of commands exists without all the tight controls of data types, which can more easily allow an executable set of code to be inserted and enabled.

If the self-balancing properties of prime number incremental structure could be implemented as a supervisory higher-order metalanguage, could it be used to determine if a combined language structure is leading away from any possible chance for a “language equilibrium”? Developing a Machine Learning approach of the language structural rules could also provide the necessary framework that enables Artificial Intelligence self-healing recommendations against combined language vulnerabilities.

In conclusion, the recommendations are to use the framework to facilitate the research in areas of combined system characteristics to discover forms of potentially integrated solutions. As a framework that embodies combined system characteristics, it may show the prime numbers to be more of a solution to be implemented than a problem to be solved.

Chapter Summary

This chapter provided tables of system related findings from the analysis of the prime number component interactions in both the magnitude model and the post zeta(2) (or, inverse-squared) model. Results of the hypotheses are conclusive: The prime numbers in their own coordinate system provide a reliable self-referential framework that represents intrinsic harmonic and dynamically balanced behavior, which can be described and defined in system engineering models that correlate in function to existing systems and engineering approaches.

Two significant recommendations are the result: Use the model as an architecture for the optimization, efficiency, and control of systems; Use the logical and physical model to rethink complex problems. Recommendations for future research are in two aspects: Consider the possible contributions of the component model to different characteristics of the Millennium Prize Problems; Consider how the new concepts could contribute to other theoretical research topics. With the foundational characteristics discovered in the component model, almost open-ended possibilities for research exists. This chapter summarized the integrated system properties of the component model and the potential research areas of quantum behavior models and simulations, quantum-level of cybersecurity, mathematical models in abstract space, mechanical engineering stress and vibration, equilibrium and stabilization, fluid dynamics, refraction with Snell's Law, and different types of computer languages with Turing Machines. The starting point for all further research begins with a paradigm change that considers the prime numbers as providing a framework for system stabilization.

REFERENCES

Akhmetgaliyev E. (2016). *Fast Numerical Methods for Mixed, Singular Helmholtz Boundary Value Problems and Laplace Eigenvalue Problems - with Applications to Antenna Design, Sloshing, Electromagnetic Scattering and Spectral Geometry*. Dissertation (Ph.D.), California Institute of Technology.

doi:10.7907/Z97P8W93. <https://resolver.caltech.edu/CaltechTHESIS:08202015-162838809>

Andrianov A. (2012). Zeta functions of harmonic theta-series and prime numbers, St. Petersburg Mathematical Journal Tom 23 (2011), 2 Vol. 23, No. 2, Pages 239-255 S 1061-0022(2012)01195-7 Online: <https://www.ams.org/journals/spmj/2012-23-02/S1061-0022-2012-01195-7/S1061-0022-2012-01195-7.pdf>

Anshu A., Jain R., Mukhopadhyay P., Shayeghi A., & Yao P. (2016). "New One Shot Quantum Protocols With Application to Communication Complexity," in IEEE Transactions on Information Theory, vol. 62, no. 12, pp. 7566-7577, Dec. 2016, doi: 10.1109/TIT.2016.2616125

Aouane K., Sandre O., Ford I. J., Elson T., & Nightingale C. (2018). Thermogravitational Cycles: Theoretical Framework and Example of an Electric Thermogravitational Generator Based on Balloon Inflation/Deflation. Inventions, 3(4), 79. <https://doi.org/10.3390/inventions3040079>

Babar Z. et al. (2019). "Duality of Quantum and Classical Error Correction Codes: Design Principles and Examples," in IEEE Communications Surveys & Tutorials, vol. 21, no. 1, pp. 970-1010, Firstquarter 2019, doi: 10.1109/COMST.2018.2861361

Baibekov, S. & Durmagambetov, A. (2016). Infinite Number of Twin Primes. *Advances in Pure Mathematics*, 6, 954-971. doi: [10.4236/apm.2016.613073](https://doi.org/10.4236/apm.2016.613073).

Barbaraci, G. (2020). On the Poynting vector and the curvature of a charged particle travelling in the electro-magnetic field. *Results in Physics*, 16(102989-).

<https://doi.org/10.1016/j.rinp.2020.102989>

Betinis, E. (2016). Estimates of the superluminal graviton velocity and rest mass from Newtonian quantum gravity. *Physics Essays*, 29(4), 526–531.

<https://doi.org/10.4006/0836-1398-29.4.526>

Blanco-Pérez, C. (2016). Vacuum quanta and the nature of gravity. *Canadian Journal of Physics*, 94(12), 1265–1274. <https://doi.org/10.1139/cjp-2016-0448>

Bombieri E. (2000). Problems of the millennium: The Riemann hypothesis. Clay Mathematics Inst., Cambridge, MA.: http://www.claymath.org/millennium/Riemann_Hypothesis/riemann.pdf

Callister T. A. III (2020). *Searching for the Astrophysical Gravitational-Wave Background and Prompt Radio Emission from Compact Binaries*. Dissertation (Ph.D.), California Institute of Technology. doi:10.7907/xthf-1p70.

<https://resolver.caltech.edu/CaltechTHESIS:05262020-184547015>

Cao H., & Ma W (2018). "Verifiable Threshold Quantum State Sharing Scheme," in IEEE Access, vol. 6, pp. 10453-10457, 2018, doi: 10.1109/ACCESS.2018.2805724

Chandra D. et al. (2017). "Quantum Coding Bounds and a Closed-Form Approximation of the Minimum Distance Versus Quantum Coding Rate," in IEEE Access, vol. 5, pp. 11557-11581, 2017, doi: 10.1109/ACCESS.2017.2716367

Chang J., Yu J., Li J., Xue G., Malekian R., & Su B. (2019). "Diffusion Law of Whole-Space Transient Electromagnetic Field Generated by the Underground Magnetic Source and Its Application," in IEEE Access, vol. 7, pp. 63415-63425, 2019, doi: 10.1109/ACCESS.2019.2916767.

Cheng P., Yang F., Luo H., Guo H., Ran W., Yang Y., & Ullah I. (2016). A method to calculate the reactive power of iced transmission line based on Poynting vector and FDFD. International Journal of Applied Electromagnetics & Mechanics, 50(3), 417–433.
<https://doi.org/10.3233/JAE-150118>

Choi W., Lee J., & Li L (2020). Analysis of Three-Dimensional Circular Tracking Movements Based on Temporo-Spatial Parameters in Polar Coordinates. Appl. Sci. 2020, 10, 621.

Clark, M. (2018). Cosmic rays and galactic rotation curves. Astrophysics & Space Science, 363(10), 1–12. <https://doi.org/10.1007/s10509-018-3434-7>

Clay Mathematics Institute, CMI (2000). The Millennium Prize Problems. Clay Mathematics Inst., Cambridge, MA.: <https://www.claymath.org/millennium-problems/millennium-prize-problems>

Davies-Jones, R., Wood, V., & Rasmussen, E. (2020). Doppler Circulation as a Fairly Range-Insensitive Far-Field Tornado Detection and Precursor Parameter. *Journal of Atmospheric & Oceanic Technology*, 37(6), 1117–1133. <https://doi.org/10.1175/JTECH-D-19-0116.1>

Deligne, P. (2000). The Hodge Conjecture. Clay Mathematics Inst., Cambridge, MA.: <https://www.claymath.org/sites/default/files/hodge.pdf>

Deninger C. (1998). Some analogies between number theory and dynamical systems on foliated spaces, Proc. Int. Congress Math. Berlin, Vol. I, 163– 186.

Dhiman, D. (2020). Unification of fundamental forces under normal atmospheric conditions. *Physics Essays*, 33(3), 325–341. <https://doi.org/10.4006/0836-1398-33.3.325>

Dorroh D., Ölmez S., & Wang J. (2020). "Theory of Quantum Computation with Magnetic Clusters," in IEEE Transactions on Quantum Engineering, vol. 1, pp. 1-8, 2020, Art no. 5100508, doi: 10.1109/TQE.2020.2975765

Duan X., Dang Y., & Lu J. (2020). "A Variational Level Set Method for Topology Optimization Problems in Navier-Stokes Flow," in IEEE Access, vol. 8, pp. 48697-48706, 2020, doi: 10.1109/ACCESS.2020.2980113.

Duha, Jânia, Afonso, Germano B., & Ferreira, Luiz D. D. (2001). Relativistic thermal re-emission model. *Revista Brasileira de Geofísica*, 19(2), 177-184. <https://doi.org/10.1590/S0102-261X2001000200006>

Edwards J. (2017). Non-commutativity in polar coordinates. European Physical Journal C -- Particles & Fields, 77(5), 1–7. <https://doi.org/10.1140/epjc/s10052-017-4873-y>

Eingorn, M., Yükselci, A. E., & Zhuk, A. (2019). Effect of the spatial curvature of the Universe on the form of the gravitational potential. European Physical Journal C -- Particles & Fields, 79(8), N.PAG.

Fedorov, S., Rosanov, N., & Veretenov, N. (2018). Structure of Energy Fluxes in Topological Three-Dimensional Dissipative Solitons. JETP Letters, 107(8), 327.

Fefferman, C. (2000). Existence and smoothness of the Navier-Stokes equation. Clay Mathematics Inst., Cambridge, MA.: http://www.claymath.org/millennium/Navier-Stokes_Equations/navierstokes.pdf

Fernandez V., Gómez-García J., Ocampos-Guillén A., & Carrasco-Casado A. (2018). "Correction of Wavefront Tilt Caused by Atmospheric Turbulence Using Quadrant Detectors for Enabling Fast Free-Space Quantum Communications in Daylight," in IEEE Access, vol. 6, pp. 3336-3345, 2018, doi: 10.1109/ACCESS.2018.2791099.

Ferreira, J. (2017). The Pattern of Prime Numbers. *Applied Mathematics*, 8, 180-192.
doi: [10.4236/am.2017.82015](https://doi.org/10.4236/am.2017.82015)

Filippitzis F. (2021). *Identification of Structural Damage, Ground Motion Response, and the Benefits of Dense Seismic Instrumentation*. Dissertation (Ph.D.), California Institute of Technology. doi:10.7907/x0sf-pq18. <https://resolver.caltech.edu/CaltechTHESIS:11052020-043034327>

- Fokas A. S. (2019). Ultra-relativistic gravity has properties associated with the strong force. European Physical Journal C: Particles and Fields, 79(3), 1–11.
<https://doi.org/10.1140/epjc/s10052-019-6779-3>
- Gao J., & Wang Y. (2019). "New Non-Binary Quantum Codes Derived From a Class of Linear Codes," in IEEE Access, vol. 7, pp. 26418-26421, 2019, doi:
10.1109/ACCESS.2019.2899383
- García-Pérez, G., Serrano, M. Á., & Boguñá, M. (2014). Complex architecture of primes and natural numbers. *Physical review. E, Statistical, nonlinear, and soft matter physics*, 90(2), 022806. <https://doi.org/10.1103/PhysRevE.90.022806>
- Gonzales A., & Chitambar E. (2020). "Bounds on Instantaneous Nonlocal Quantum Computation," in IEEE Transactions on Information Theory, vol. 66, no. 5, pp. 2951-2963, May 2020, doi: 10.1109/TIT.2019.2950190
- Guardia, M., Martín, P., & Seara, T. (2016). Oscillatory motions for the restricted planar circular three body problem. *Inventiones Mathematicae*, 203(2), 417–492.
<https://doi.org/10.1007/s00222-015-0591-y>
- Guariglia, E. (2015). " Fractional Derivative of the Riemann Zeta Function". In *Fractional Dynamics*. Berlin, Boston: De Gruyter. doi: <https://doi.org/10.1515/9783110472097-022>
- Guo R., Yu H., Xia T., Shi Z., Zhong W., & Liu X. (2018). "A Simplified Subdomain Analytical Model for the Design and Analysis of a Tubular Linear Permanent Magnet Oscillation Generator," in IEEE Access, vol. 6, pp. 42355-42367, 2018, doi:
10.1109/ACCESS.2018.2859021.

Gyongyosi L., Imre S., & Nguyen H. (2018). "A Survey on Quantum Channel Capacities," in IEEE Communications Surveys & Tutorials, vol. 20, no. 2, pp. 1149-1205, Second quarter 2018, doi: 10.1109/COMST.2017.2786748

Hahn, H.K. (2008). About the logic of the prime number distribution. *arXiv: General Mathematics.* online <https://arxiv.org/pdf/0801.4049.pdf>

Heremans F., Yale C., & Awschalom D. (2016). "Control of Spin Defects in Wide-Bandgap Semiconductors for Quantum Technologies," in Proceedings of the IEEE, vol. 104, no. 10, pp. 2009-2023, Oct. 2016, doi: 10.1109/JPROC.2016.2561274.

Hibbs E. (2008). The double-helix pattern of prime number growth. WCECS *Inter. Conf. on Computer Sci. and Appl. San Francisco, CA*, IAENG, ISBN: 978-988-98671-0-2: http://www.iaeng.org/publication/WCECS2008/WCECS2008_pp278-283.pdf

Hibbs E. (2009). Electromagnetic sequence and vector behavior of the prime number growth double helix. WCECS *Inter. Conf. on Computer Sci. and Appl. San Francisco, CA*, IAENG, ISBN: 978-988-17012-6-8: http://www.iaeng.org/publication/WCECS2009/WCECS2009_pp508-513.pdf

Hibbs E. (2010). Applying the new primer on prime numbers. *WSEAS Transactions on Mathematics*, 4(9), ISSN: 1109-2769: <http://www.wseas.us/e-library/transactions/mathematics/2010/89-420.pdf>

Hibbs E. (2012). The converging under-damped harmonic growth of prime numbers. *WSEAS Applied Mathematics in Electrical and Computer Engineering*, ISBN: 978-1-61804-064-0: <http://www.wseas.us/e-library/conferences/2012/CambridgeUSA/MATHCC/MATHCC-05.pdf>

Hibbs E. & McAndrew I. (2021). The self-referential harmonic system of prime number growth. 3rd International Conference on Mechanical and Aerospace Systems.

Holm, D. (2019). Stochastic Evolution of Augmented Born-Infeld Equations. *Journal of Nonlinear Science*, 29(1), 115.

Hosny K., Darwish M., & Eltoukhy M. (2020). "Novel Multi-Channel Fractional-Order Radial Harmonic Fourier Moments for Color Image Analysis," in IEEE Access, vol. 8, pp. 40732-40743, 2020, doi: 10.1109/ACCESS.2020.2976759.

Jaffe A., & Witten E. (2000). Quantum Yang-Mills theory. Clay Mathematics Inst., Cambridge, MA.: http://www.claymath.org/millennium/Yang-Mills_Theory/yangmills.pdf

Jara-Vera V., & Sánchez-Ávila C. (2020). New Proof That the Sum of the Reciprocals of Primes Diverges. *Mathematics*, 8(9), 1414. MDPI AG. Retrieved from <http://dx.doi.org/10.3390/math8091414>

Jarzyna M., & Kołodyński J. (2020). "Geometric Approach to Quantum Statistical Inference," in IEEE Journal on Selected Areas in Information Theory, vol. 1, no. 2, pp. 367-386, Aug. 2020, doi: 10.1109/JSAIT.2020.3017469

Jayarajan R., Fernando N., & Nutkani I. U., "A Review on Variable Flux Machine Technology: Topologies, Control Strategies and Magnetic Materials," in IEEE Access, vol. 7, pp. 70141-70156, 2019, doi: 10.1109/ACCESS.2019.2918953.

Ji W., Wang A., & Qiu J. (2017). "Decentralized Fixed-Order Piecewise Affine Dynamic Output Feedback Controller Design for Discrete-Time Nonlinear Large-Scale Systems," in IEEE Access, vol. 5, pp. 1977-1989, 2017, doi: 10.1109/ACCESS.2017.2663525

Jiang Z., Jin Y., Li M. E & Q. (2018). "Distributed Dynamic Scheduling for Cyber-Physical Production Systems Based on a Multi-Agent System," in IEEE Access, vol. 6, pp. 1855-1869, 2018, doi: 10.1109/ACCESS.2017.2780321

Johansen S.E. (2012). Unveiling of geometric generation of composite numbers' exactly and completely *Applied Mathematics and Information Sciences*. Volume 6, Issue 2, May 2012, Pages 223-231

Joksimović G., Mezzarobba M., Tessarolo A., & Levi E., "Optimal Selection of Rotor Bar Number in Multiphase Cage Induction Motors," in IEEE Access, vol. 8, pp. 135558-135568, 2020, doi: 10.1109/ACCESS.2020.3004685.

Kerr R.M., & Oliver M. (2011). The Ever-Elusive Blowup in the Mathematical Description of Fluids. In: Schleicher D., Lackmann M. (eds) An Invitation to Mathematics. Springer, Berlin, Heidelberg. https://doi.org/10.1007/978-3-642-19533-4_10

Klinaku, S. (2019). Small error--Big confusion: The deep understanding of the Doppler effect. Physics Essays, 32(4), 418–421. <https://doi.org/10.4006/0836-1398-32.4.418>

Kong D., Deng M., & Li Y. (2020). "Numerical Simulation of Seismic Soil-Pile Interaction in Liquefying Ground," in IEEE Access, vol. 8, pp. 195-204, 2020, doi: 10.1109/ACCESS.2019.2925664.

Kotlyar V., Nalimov A., Stafeev S., Kovalev A., & Porfirev A. (2020). "Orbital energy and spin flows in a strong focus of laser light," in IEEE Photonics Journal, doi: 10.1109/JPHOT.2020.3028883.

Lee D., & So J. (2019). "Adaptive feedback bits and power allocation for dynamic TDD systems," in Journal of Communications and Networks, vol. 21, no. 2, pp. 113-124, April 2019, doi: 10.1109/JCN.2019.000009

Lee, H. I., & Mok, J. (2014). Spin annihilations of and spin sifters for transverse electric and transverse magnetic waves in co- and counter-rotations. *Beilstein journal of nanotechnology*, 5, 1887–1898. <https://doi.org/10.3762/bjnano.5.199>

Leugering, G., Nazarov, S. A., & Taskinen, J. (2019). Umov–Poynting–Mandelstam radiation conditions in periodic composite piezoelectric waveguides. *Asymptotic Analysis*, 111(2), 69–111. <https://doi.org/10.3233/ASY-181487>

Li H., Chen X., Xia H., Liang Y., & Zhou Z. (2018). "A Quantum Image Representation Based on Bitplanes," in IEEE Access, vol. 6, pp. 62396-62404, 2018, doi: 10.1109/ACCESS.2018.2871691

Li L., Miyachi Y., Miyoshi M., & Egawa T. (2016). "Enhanced Emission Efficiency of Deep Ultraviolet Light-Emitting AlGaN Multiple Quantum Wells Grown on an N-AlGaN Underlying Layer," in IEEE Photonics Journal, vol. 8, no. 5, pp. 1-10, Oct. 2016, Art no. 1601710, doi: 10.1109/JPHOT.2016.2601439.

- Li W., Fay P., Yu T., & Hoyt J. (2016). "Microwave detection performance of In_{0.53}Ga_{0.47}As/GaAs_{0.5}Sb_{0.5} quantum-well tunnel field-effect transistors," in Electronics Letters, vol. 52, no. 10, pp. 842-844, 12 5 2016, doi: 10.1049/el.2016.0328.
- Li Y., Tian M., Liu G., Peng C., & Jiao L. (2020). "Quantum Optimization and Quantum Learning: A Survey," in IEEE Access, vol. 8, pp. 23568-23593, 2020, doi: 10.1109/ACCESS.2020.2970105
- Li Y., Xu C., Chen C., Yin H., Yi L., & He X. (2019). "Adaptive Denoising Approach for High-Rate GNSS Seismic Waveform Preservation: Application to the 2010 El Mayor-Cucapah Earthquake and 2012 Brawley Seismic Swarm," in IEEE Access, vol. 7, pp. 173166-173184, 2019, doi: 10.1109/ACCESS.2019.2956780.
- Lo, C. (2016). The observable temperature dependence of gravitation. Physics Essays, 29(3), 337–342. <https://doi.org/10.4006/0836-1398-29.3.337>
- Loeliger H., & Vontobel P. (2017). "Factor Graphs for Quantum Probabilities," in IEEE Transactions on Information Theory, vol. 63, no. 9, pp. 5642-5665, Sept. 2017, doi: 10.1109/TIT.2017.2716422
- Loeliger H., & Vontobel P. (2020). "Quantum Measurement as Marginalization and Nested Quantum Systems," in IEEE Transactions on Information Theory, vol. 66, no. 6, pp. 3485-3499, June 2020, doi: 10.1109/TIT.2019.2961377
- Low, D., & Wilson, K. (2017). WEIGHT, THE NORMAL FORCE AND NEWTON'S THIRD LAW: Dislodging a deeply embedded misconception. Teaching Science: The Journal of the Australian Science Teachers Association, 63(2), 17.

Ma R., & He P. (2020). "Dynamic modeling gas-electricity combined system with wind power and its stability control method," in CSEE Journal of Power and Energy Systems, doi: 10.17775/CSEEPES.2020.02670

MacTutor - 1 (MT1) Prime Numbers. 2021. School of Mathematics and Statistics. University of St Andrews, Scotland. Pulled 02-15-2021 https://mathshistory.st-andrews.ac.uk/HistTopics/Prime_numbers/

MacTutor - 2 (MT2) Prime Number Theorem (2021). School of Mathematics and Statistics. University of St Andrews, Scotland. Pulled 02-13-2021. <https://mathshistory.st-andrews.ac.uk/Diagrams/PrimeNumTheorem.html>

Marshall S. H., & Smith D. R. (2013). Feedback, Control, and the Distribution of Prime Numbers. *Mathematics Magazine*, 86(3), 189-203. doi:10.4169/math.mag.86.3.189; online: [Marshall-MathMag-2014.pdf \(maa.org\)](https://www.maa.org/sites/default/files/pdf/upload_library/22/Ford/2014/03/10.4169/math.mag.86.3.189.pdf)

Messerschmitt D. (2017). "Relativistic Timekeeping, Motion, and Gravity in Distributed Systems," in Proceedings of the IEEE, vol. 105, no. 8, pp. 1511-1573, Aug. 2017, doi: 10.1109/JPROC.2017.2717980.

Minati L. et al. (2019). "Current-Starved Cross-Coupled CMOS Inverter Rings as Versatile Generators of Chaotic and Neural-Like Dynamics Over Multiple Frequency Decades," in IEEE Access, vol. 7, pp. 54638-54657, 2019, doi: 10.1109/ACCESS.2019.2912903.

Mossa M., Al-Sumaiti A., Duc Do T., & and Diab A. (2019). "Cost-Effective Predictive Flux Control for a Sensorless Doubly Fed Induction Generator," in IEEE Access, vol. 7, pp. 172606-172627, 2019, doi: 10.1109/ACCESS.2019.2951361.

Mousavi S. M., Sheng Y., Zhu W., & Beroza G. C., "STanford EArthquake Dataset (STEAD): A Global Data Set of Seismic Signals for AI," in IEEE Access, vol. 7, pp. 179464-179476, 2019, doi: 10.1109/ACCESS.2019.2947848.

Muhibbulah M., Abdel Haleem A., & Ikuma Y. (2017). Frequency dependent power and energy flux density equations of the electromagnetic wave. *Results in Physics*, 7(435–439), 435–439. <https://doi.org/10.1016/j.rinp.2017.01.006>

OEIS. The On-Line Encyclopedia of Integer Sequences. <https://oeis.org/> Pulled 02-13-2021.

Oliver R., & Soundararajan, K. (2016). Biases in consecutive primes. *Proceedings of the National Academy of Sciences*. Aug 2016, 113 (31) E4446-E4454; DOI: 10.1073/pnas.1605366113. Online: <https://www.pnas.org/content/113/31/E4446>

Olson D. W., Wolf S. F., & Hook J. M. (2015). *Physics Today* **68**, 64-65 (2015) DOI: 10.1063/PT.3.2991

Özüpak, Y., & Mamiş, M. S. (2020). Analysis of electromagnetic and loss effects of sub-harmonics on transformers by Finite Element Method. *Sadhana*, 45(1), 1–11. <https://doi.org/10.1007/s12046-020-01473-4>

Patra B. et al. (2018). "Cryo-CMOS Circuits and Systems for Quantum Computing Applications," in IEEE Journal of Solid-State Circuits, vol. 53, no. 1, pp. 309-321, Jan. 2018, doi: 10.1109/JSSC.2017.2737549

Piyadasa, C. (2019). Antigravity, a major phenomenon in nature yet to be recognized. *Physics Essays*, 32(2), 141–150. <https://doi.org/10.4006/0836-1398-32.2.141>

Pollack P. (2015). Euler and the partial sums of the prime harmonic series. *Elemente Der Mathematik*, 70, 13-20. Online: <http://pollack.uga.edu/eulerprime.pdf>

Qiu L. et al. (2020). "Electromagnetic Force Distribution and Forming Performance in Electromagnetic Forming With Discretely Driven Rings," in IEEE Access, vol. 8, pp. 16166-16173, 2020, doi: 10.1109/ACCESS.2020.2967096.

Qin X. et al. (2020). "An FPGA-Based Hardware Platform for the Control of Spin-Based Quantum Systems," in IEEE Transactions on Instrumentation and Measurement, vol. 69, no. 4, pp. 1127-1139, April 2020, doi: 10.1109/TIM.2019.2910921.

Ren Y. et al. (2018). "System Dynamic Behavior Modeling Based on Extended GO Methodology," in IEEE Access, vol. 6, pp. 22513-22523, 2018, doi: 10.1109/ACCESS.2018.2816165

Roffe J., Zohren S., Horsman D., & Chancellor N. (2020). "Quantum Codes From Classical Graphical Models," in IEEE Transactions on Information Theory, vol. 66, no. 1, pp. 130-146, Jan. 2020, doi: 10.1109/TIT.2019.2938751.

Roudas I. & Kwapisz J. (2017). "Stokes Space Representation of Modal Dispersion," in IEEE Photonics Journal, vol. 9, no. 5, pp. 1-15, Oct. 2017, Art no. 7203715, doi: 10.1109/JPHOT.2017.2735403.

Schab K. et al. (2018). "Energy Stored by Radiating Systems," in IEEE Access, vol. 6, pp. 10553-10568, 2018, doi: 10.1109/ACCESS.2018.2807922.

Schötz J. et al. (2017). "Reconstruction of Nanoscale Near Fields by Attosecond Streaking," in IEEE Journal of Selected Topics in Quantum Electronics, vol. 23, no. 3, pp. 77-87, May-June 2017, Art no. 8700111, doi: 10.1109/JSTQE.2016.2625046.

Sha W., Liu A., & Chew W. (2018). "Dissipative Quantum Electromagnetics," in IEEE Journal on Multiscale and Multiphysics Computational Techniques, vol. 3, pp. 198-213, 2018, doi: 10.1109/JMMCT.2018.2881691.

Shi R. & Lou Y. (2019). "Three-Dimensional Contouring Control: A Task Polar Coordinate Frame Approach," in IEEE Access, vol. 7, pp. 63626-63637, 2019, doi: 10.1109/ACCESS.2019.2916911.

Sideris, C. (2017). *Electromagnetic Field Manipulation: Biosensing to Antennas*. Dissertation (Ph.D.), California Institute of Technology.
doi:10.7907/Z9RN35XW. <https://resolver.caltech.edu/CaltechTHESIS:06082017-193807440>

Socrates J. T. U. (1993). *The quaternionic bridge between elliptic curves and Hilbert modular forms*. Dissertation (Ph.D.), California Institute of Technology.
<https://resolver.caltech.edu/CaltechTHESIS:01082013-084908017>

Stafeev S., Kotlyar V., Nalimov A., & Kozlova E. (2019). "The Non-Vortex Inverse Propagation of Energy in a Tightly Focused High-Order Cylindrical Vector Beam," in IEEE Photonics

Journal, vol. 11, no. 4, pp. 1-10, Aug. 2019, Art no. 4500810, doi:
10.1109/JPHOT.2019.2921669.

Su Y., Wu X., & Liu W. (2019). "Low-Rank Tensor Completion by Sum of Tensor Nuclear Norm Minimization," in IEEE Access, vol. 7, pp. 134943-134953, 2019, doi:
10.1109/ACCESS.2019.2940664.

Tong N., Jiang Z., Zhu L., & Liu Y. (2020). "Dynamic Model Reduction for Large-Scale Power Systems Using Wide-Area Measurements," in IEEE Access, vol. 8, pp. 97863-97872, 2020, doi: 10.1109/ACCESS.2020.2992624

Treviño, E. (2014). Prime gaps: a breakthrough in number theory. Seminario Interuniversitario de Investigación en Ciencias Matemáticas, March 1, 2014; online: [Prime gaps: a breakthrough in number theory \(lakeforest.edu\)](#)

Turkle Bility, M. (2019). Reconciliation of quantum theory and gravitation via redefinition of time in a nondiscrete compressible fluid model of the universe with interactions governed by the Wheeler--Feynman transactional theory in the quantum-equilibrium theory framework. Physics Essays, 32(4), 441–450. <https://doi.org/10.4006/0836-1398-32.4.441>

University of Tennessee at Martin (UTM), 2020. PrimePages, First million primes, The first fifty million primes, Mathematics and Statistics, Downloaded June 19, 2020. Online: <https://primes.utm.edu/lists/small/millions/primes1.zip>

Vadlamani S., Agarwal S., Limmer D., Louie S., Fischer F., & Yablonovitch E. (2020). "Tunnel-FET Switching Is Governed by Non-Lorentzian Spectral Line Shape," in Proceedings of

the IEEE, vol. 108, no. 8, pp. 1235-1244, Aug. 2020, doi:
10.1109/JPROC.2019.2904011.

van Putten, M. (2014). Asymptotic Harmonic Behavior in the Prime Number Distribution. *Applied Mathematics*, 5, 2547-2557. doi: [10.4236/am.2014.516244](https://doi.org/10.4236/am.2014.516244). Online: <https://arxiv.org/abs/1104.3617>

Venayagamoorthy G., Sharma R., Gautam P., & Ahmadi A. (2016). "Dynamic Energy Management System for a Smart Microgrid," in IEEE Transactions on Neural Networks and Learning Systems, vol. 27, no. 8, pp. 1643-1656, Aug. 2016, doi:
10.1109/TNNLS.2016.2514358

Verlinde E. (2011). On the origin of gravity and the laws of Newton. *J. High Energ. Phys.*, 29 (2011). [https://doi.org/10.1007/JHEP04\(2011\)029](https://doi.org/10.1007/JHEP04(2011)029)

Wang, C. (2015). Self-consistent theory for a plane wave in a moving medium and light-momentum criterion. *Canadian Journal of Physics*, 93(12), 1510.

Wang L. (2018). Unification of gravitational and electromagnetic fields. *Physics Essays*, 31(1), 81–88. <https://doi.org/10.4006/0836-1398-31.1.81>

Wang R., Gao J., Li S., Xu J., & Liu Z. (2020). "Condition-Based Dynamic Supportability Mechanism for the Performance Quality of Large-Scale Electromechanical Systems," in IEEE Access, vol. 8, pp. 117036-117050, 2020, doi: 10.1109/ACCESS.2020.3004736

Wang W., Li D., & Jiang L. (2016). "Best linear unbiased estimation algorithm with Doppler measurements in spherical coordinates," in Journal of Systems Engineering and Electronics, vol. 27, no. 1, pp. 128-139, Feb. 2016.

Wiles, A. (2000). The Birch and Swinnerton-Dyer conjecture. Clay Mathematics Inst., Cambridge, MA.: http://www.claymath.org/millennium/Birch_and_Swinnerton-Dyer_Conjecture/birchswin.pdf

Xu W., Wang T., & Wang C. (2019). "Efficient Teleportation for High-Dimensional Quantum Computing," in IEEE Access, vol. 7, pp. 115331-115338, 2019, doi: 10.1109/ACCESS.2019.2934408

Yang F., Gao B., Chen M., Wei L., Peng Q., & Zou L. (2015). Reactive power calculation of power cable under complex operation environment based on poynting vector. International Journal of Applied Electromagnetics & Mechanics, 49(3), 375–385. <https://doi.org/10.3233/JAE-150013>

Yang H.,& Pei H. (2020). "Approximate Dynamic Inversion for Nonaffine Nonlinear Systems with High-Order Mismatched Disturbances and Actuator Saturation," in IEEE Access, vol. 8, pp. 26247-26256, 2020, doi: 10.1109/ACCESS.2020.2971649

Yin Y., Zhang J., & Duan X. (2020). "Information Transfer With Respect to Relative Entropy in Multi-Dimensional Complex Dynamical Systems," in IEEE Access, vol. 8, pp. 39464-39478, 2020, doi: 10.1109/ACCESS.2020.2973330

Yue L., Yan B., Monks J., Dhama R., Jiang C., Minin O., Minin I., & Wang Z. (2019). Full three-dimensional Poynting vector flow analysis of great field-intensity enhancement in

specifically sized spherical-particles. *Scientific Reports*, 9(1), 1–8.

<https://doi.org/10.1038/s41598-019-56761-9>

Zeng, Z., Zhou, K., & Deng, D. (2019). Propagation of cosine complex variable function Airy–Gaussian beams through the gradient-index medium. *Applied Physics B: Lasers & Optics*, 125(6), N.PAG. <https://doi.org/10.1007/s00340-019-7200-5>

Zhang W., & Yi W. (2020). "Fuzzy Observer-Based Dynamic Surface Control for Input-Saturated Nonlinear Systems and its Application to Missile Guidance," in *IEEE Access*, vol. 8, pp. 121285-121298, 2020, doi: 10.1109/ACCESS.2020.3006489

Zhou H. et al. (2017). "Orbital Angular Momentum Divider of Light," in *IEEE Photonics Journal*, vol. 9, no. 1, pp. 1-8, Feb. 2017, Art no. 6500208, doi: 10.1109/JPHOT.2016.2645896.

Zhou H., Dong J., Wang J., & Zhang X. (2016). "Tunable Image Rotator of Light With Optical Geometric Transformation," in *IEEE Photonics Journal*, vol. 8, no. 5, pp. 1-7, Oct. 2016, Art no. 6901007, doi: 10.1109/JPHOT.2016.2604041.

Zhao S. (2019). "Quantum detection theory and optimum strategy in quantum radar system," in *The Journal of Engineering*, vol. 2019, no. 21, pp. 7428-7431, 11 2019, doi: 10.1049/joe.2019.0631

Žikić, D., Stojadinović, B., & Nestorović, Z. (2019). Biophysical modeling of wave propagation phenomena: experimental determination of pulse wave velocity in viscous fluid-filled elastic tubes in a gravitation field. *European Biophysics Journal : EBJ*, 48(5), 407–411.

<https://doi.org/10.1007/s00249-019-01376-1>

Zorn P., & Cipra B. (1999). “A Prime Case of Chaos”, What's Happening in the Mathematical Sciences Volume 4, pp. 2-17, American Mathematical Society, Providence, Rhode Island, ISBN: 978-0-8218-0766-8, Online: <http://www.ams.org/publicoutreach/math-history/prime-chaos.pdf>

APPENDIX A: ANALYSIS GRAPHS

This Appendix is included to provide a detailed picture of the key graphs and analysis performed during this research. These graphs are the same sets of data that produced the 0-200, 0-2,000, and the 0-14,512 coil graphs of the trigonometric characteristics, Doppler vector values, and normal vector values. Information is grouped in the following figures and tables:

Figure A1 Polar Coordinate View of Growth Parameters	143
Figure A2 Alternating Intensity in First 120 Coils	144
Figure A3 – A11 Partial Derivatives between Quadrant Sines.....	145
Table A1 Event Trace Table (Coils 1-720).....	154
Table A2 Event Trace Table (Coils 720-14,512).....	155
Figure A12 Event Trace Analysis.....	156
Figure A13 – A17 Sine, Cosine, Tangent Analysis.....	157
Figure A18 – A20 Hypotenuse Analysis	162
Figure A21 Normal and Doppler Vectors Analysis.....	165
Figure A22 – A24 Doppler Vectors Analysis.....	166
Figure A25 – A27 Normal Vectors Analysis.....	169
Figure A28 – A29 Upper Plane Normal Vectors Analysis.....	172
Figure A30 Lower Plane Normal Vectors Analysis	174
Figure A31 – A33 Sum of Upper and Lower Normal Vectors Analysis.....	175

Figure A1 Polar Coordinate View of Growth Parameters

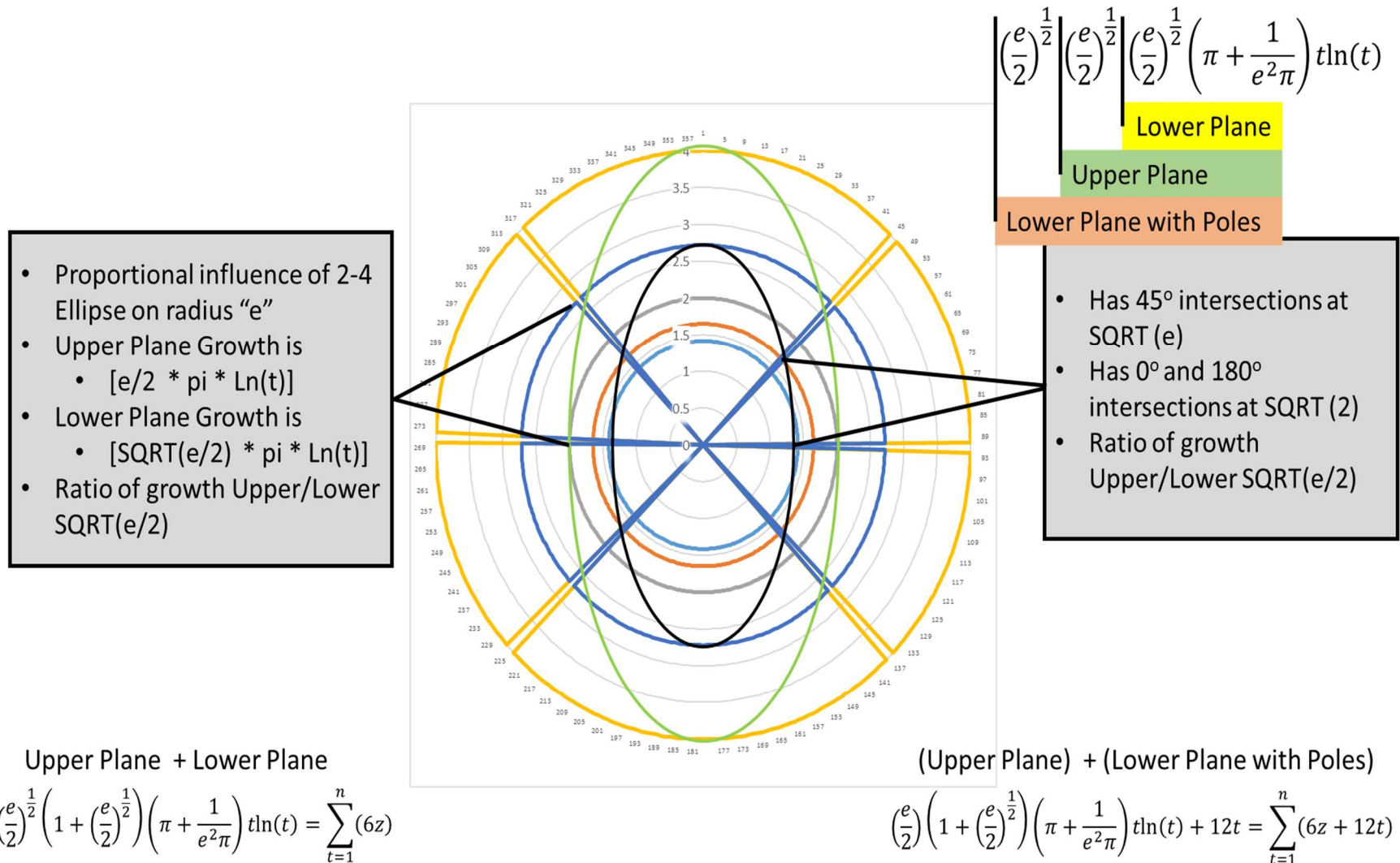


Figure A2 Alternating Intensity in First 120 Coils

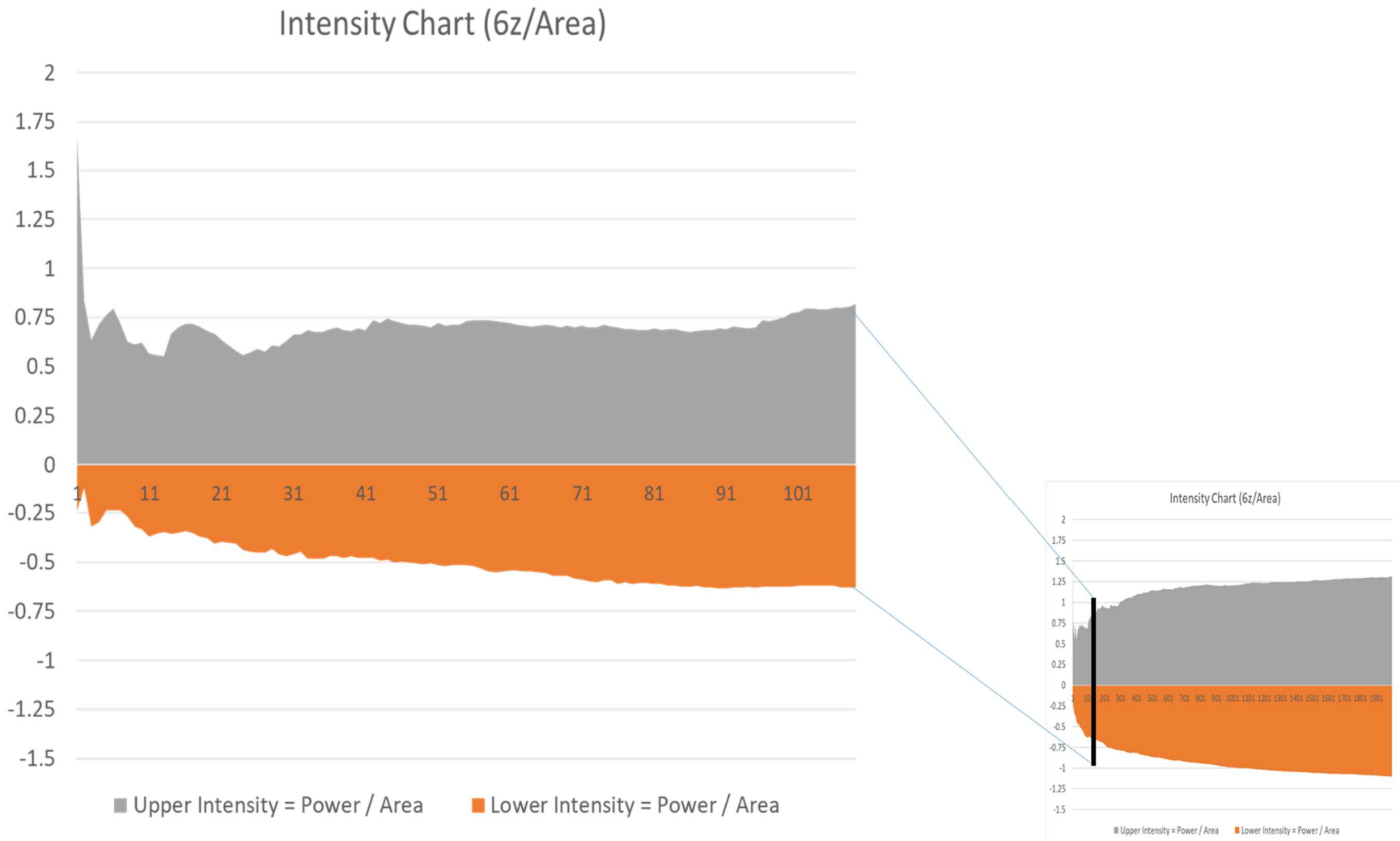


Figure A3 Partial Derivatives between Quadrant Sines

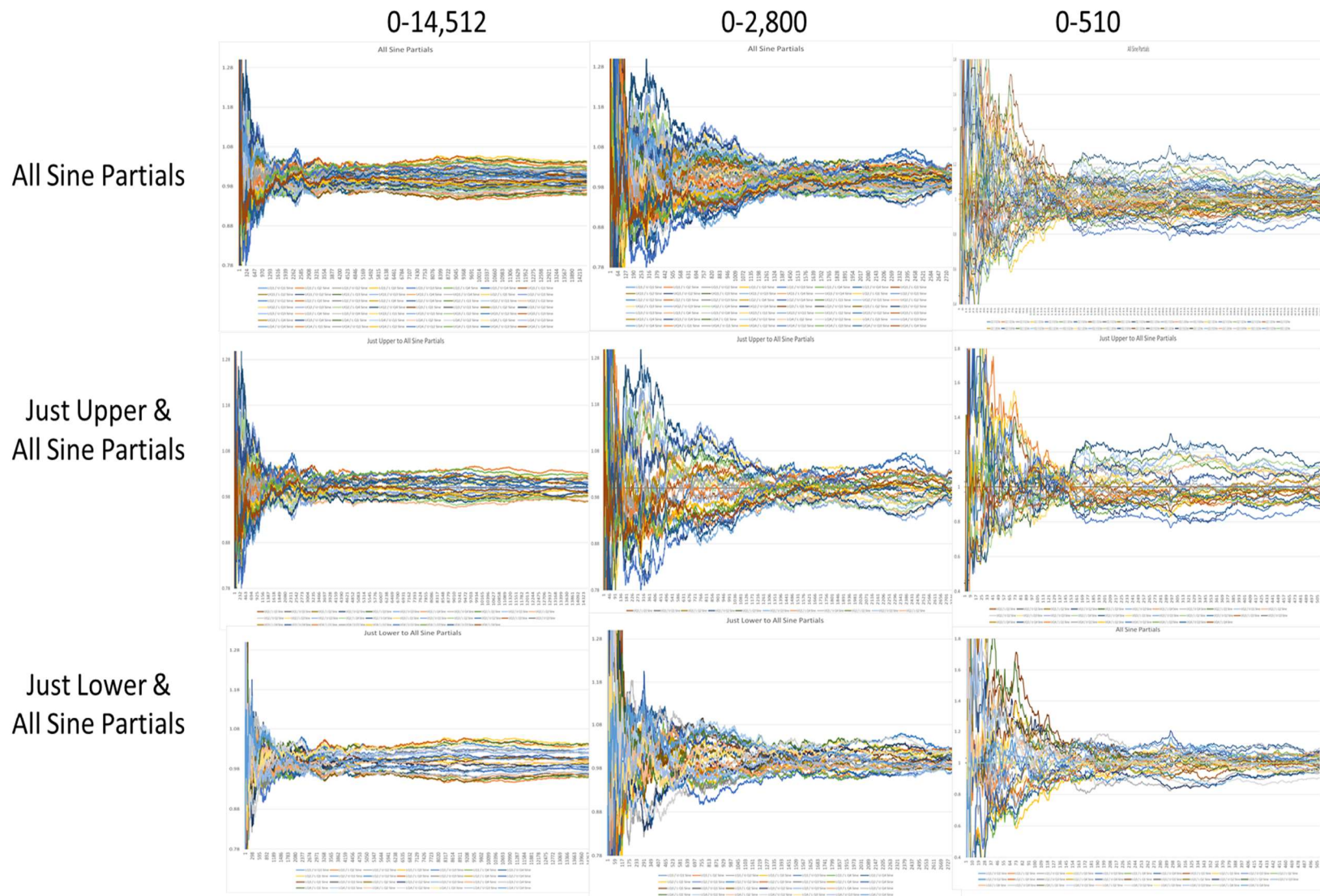


Figure A4 Partial Derivatives between Quadrant Sines

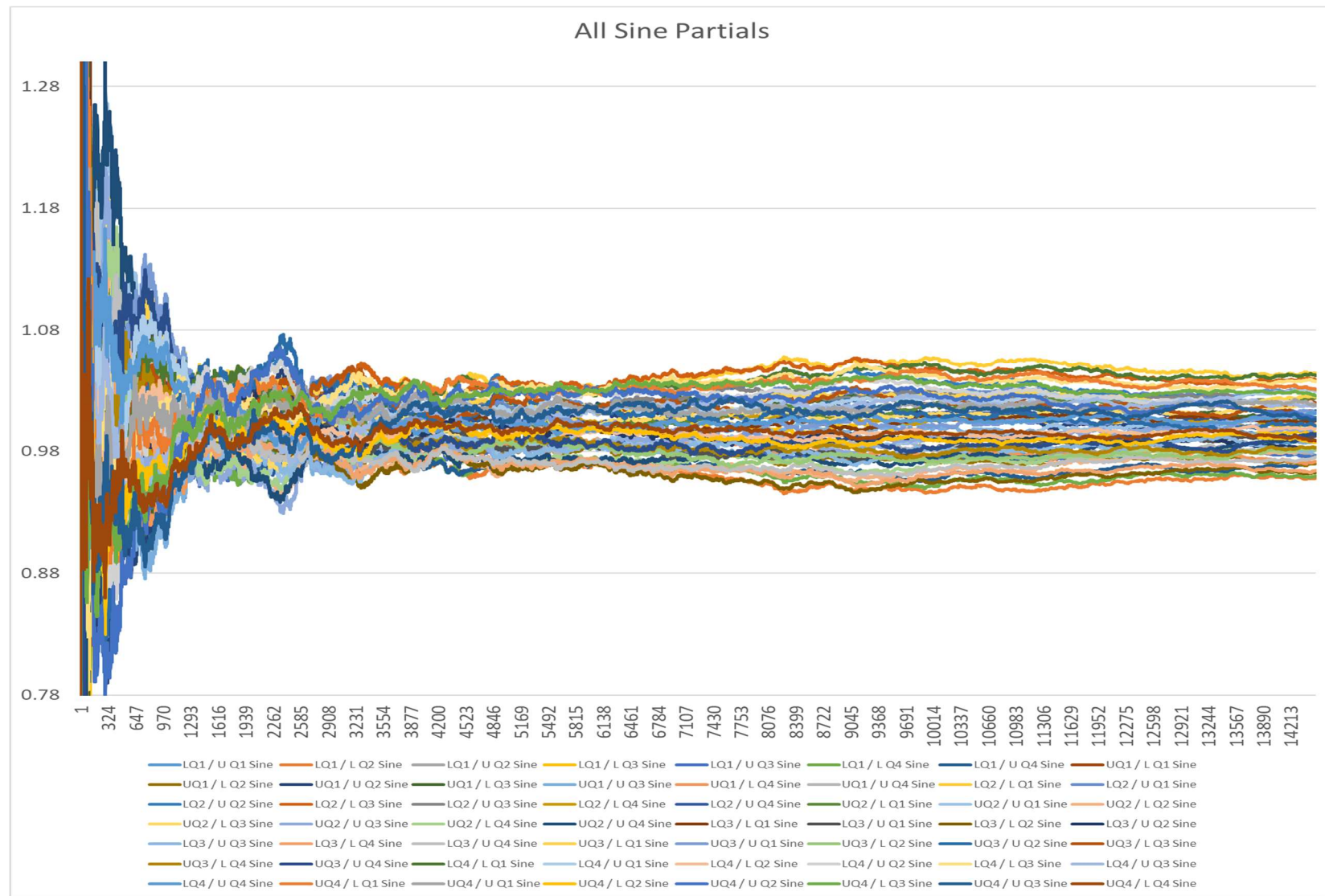


Figure A5 Partial Derivatives between Quadrant Sines

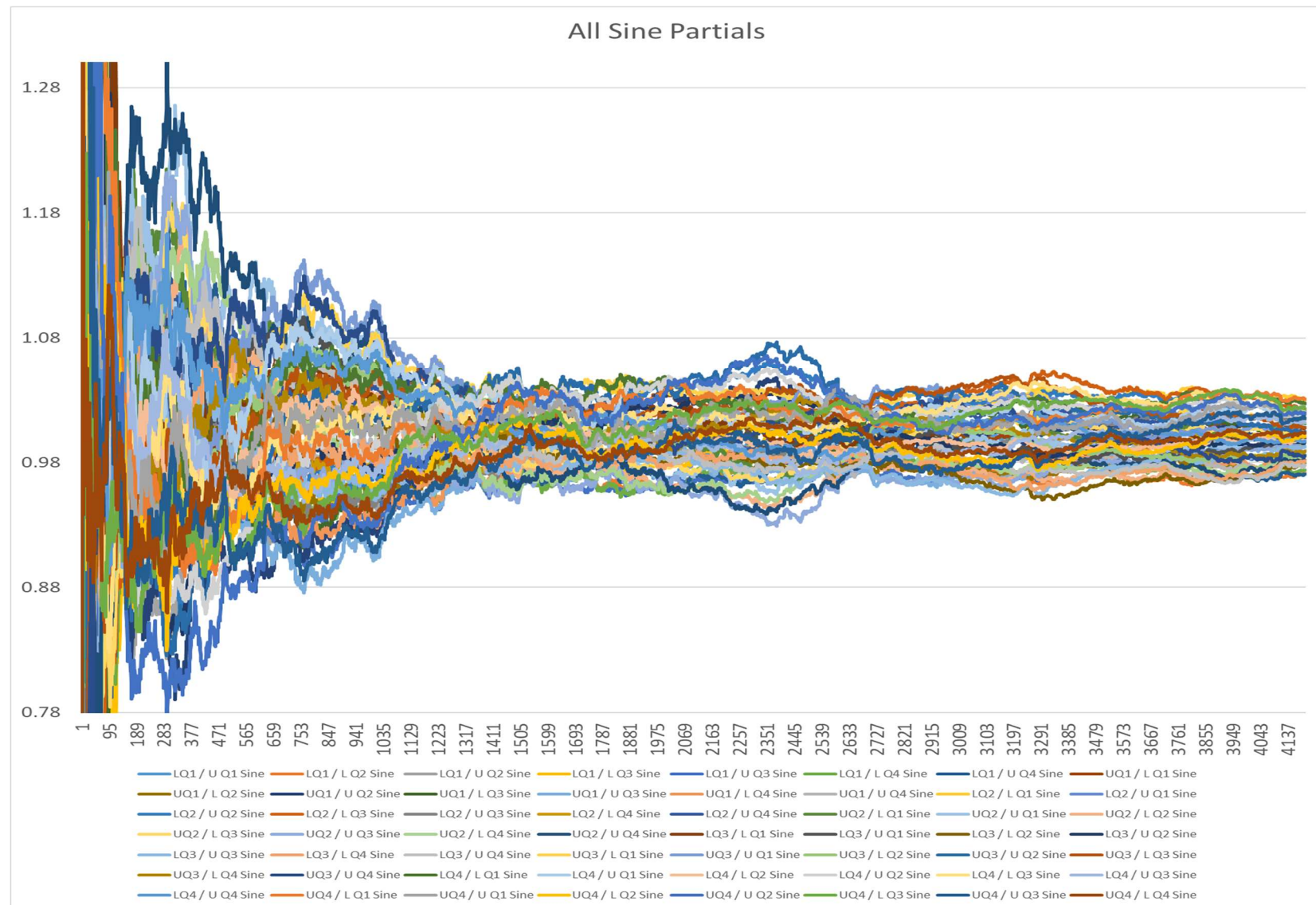


Figure A6 Partial Derivatives between Quadrant Sines

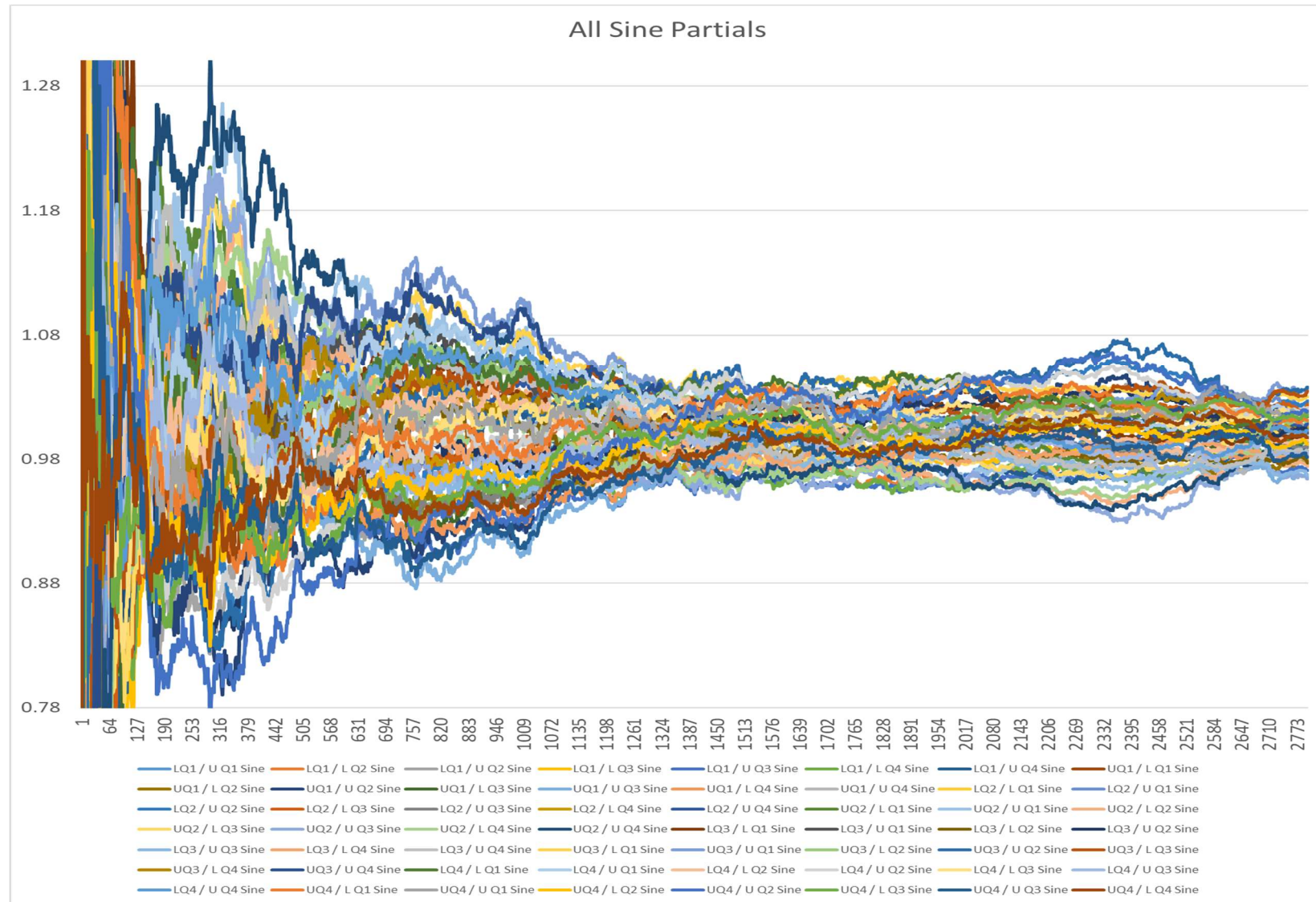


Figure A7 Partial Derivatives between Quadrant Sines

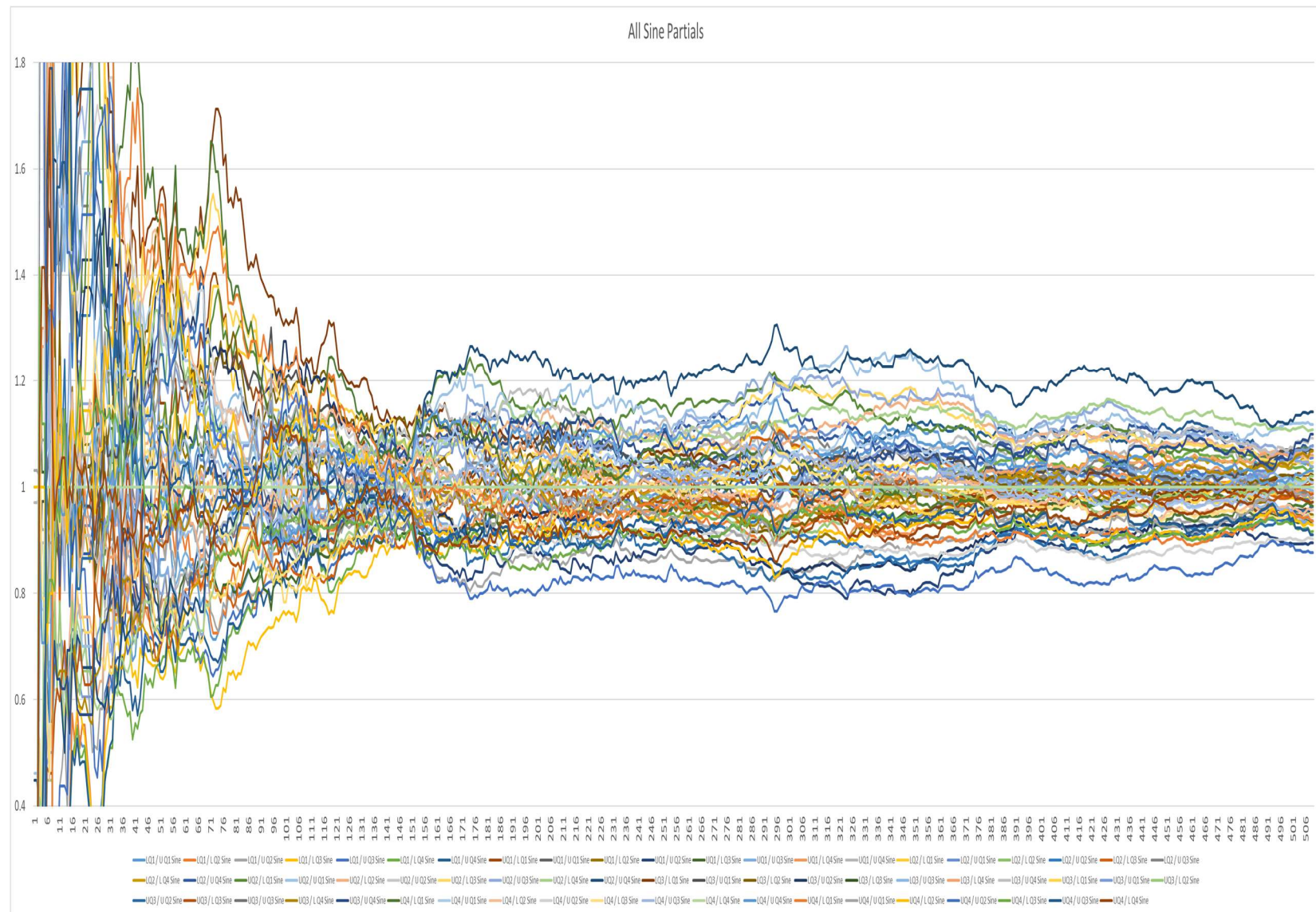


Figure A8 Upper Partial Derivatives between Quadrant Sines

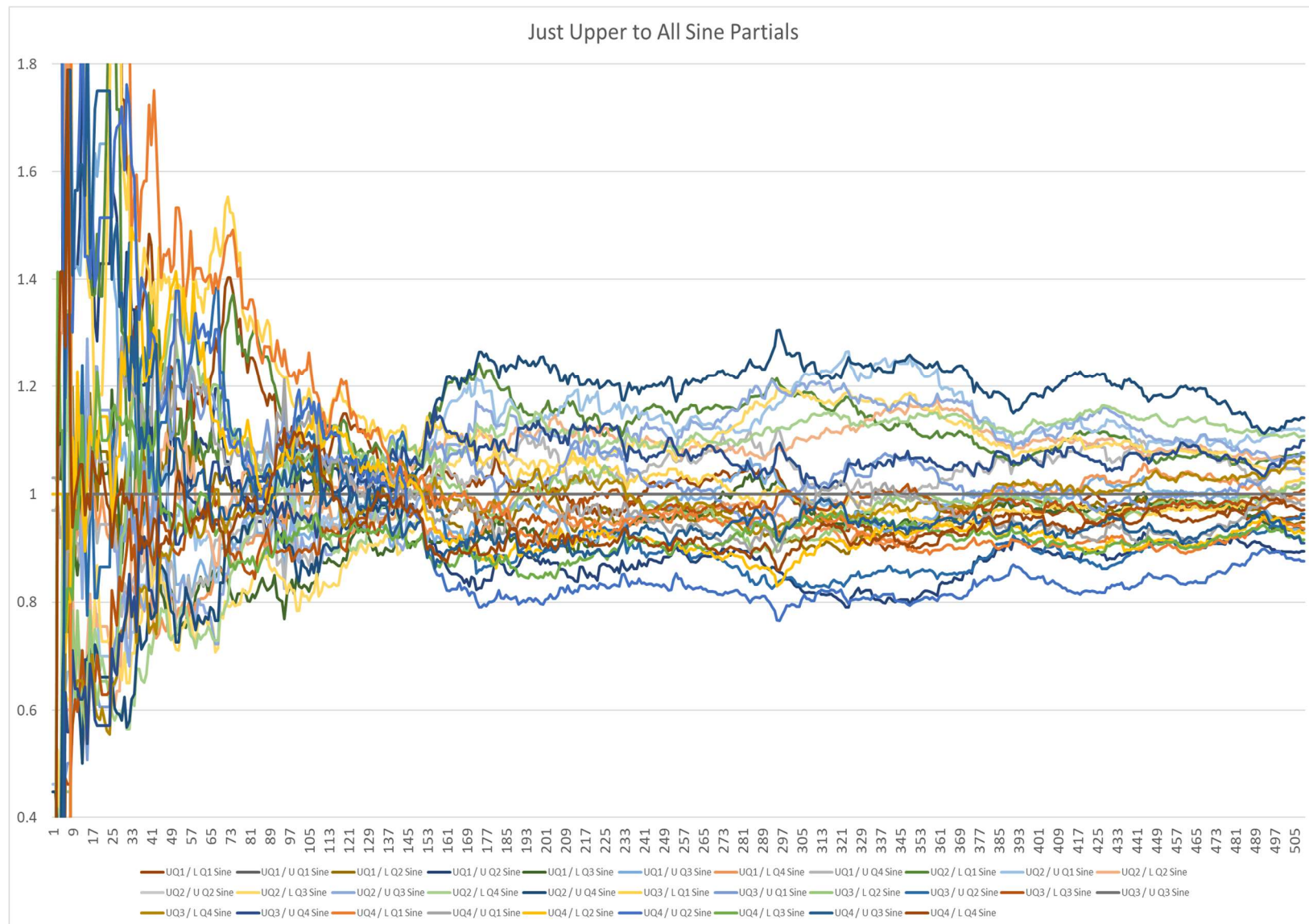


Figure A9 Lower Partial Derivatives between Quadrant Sines

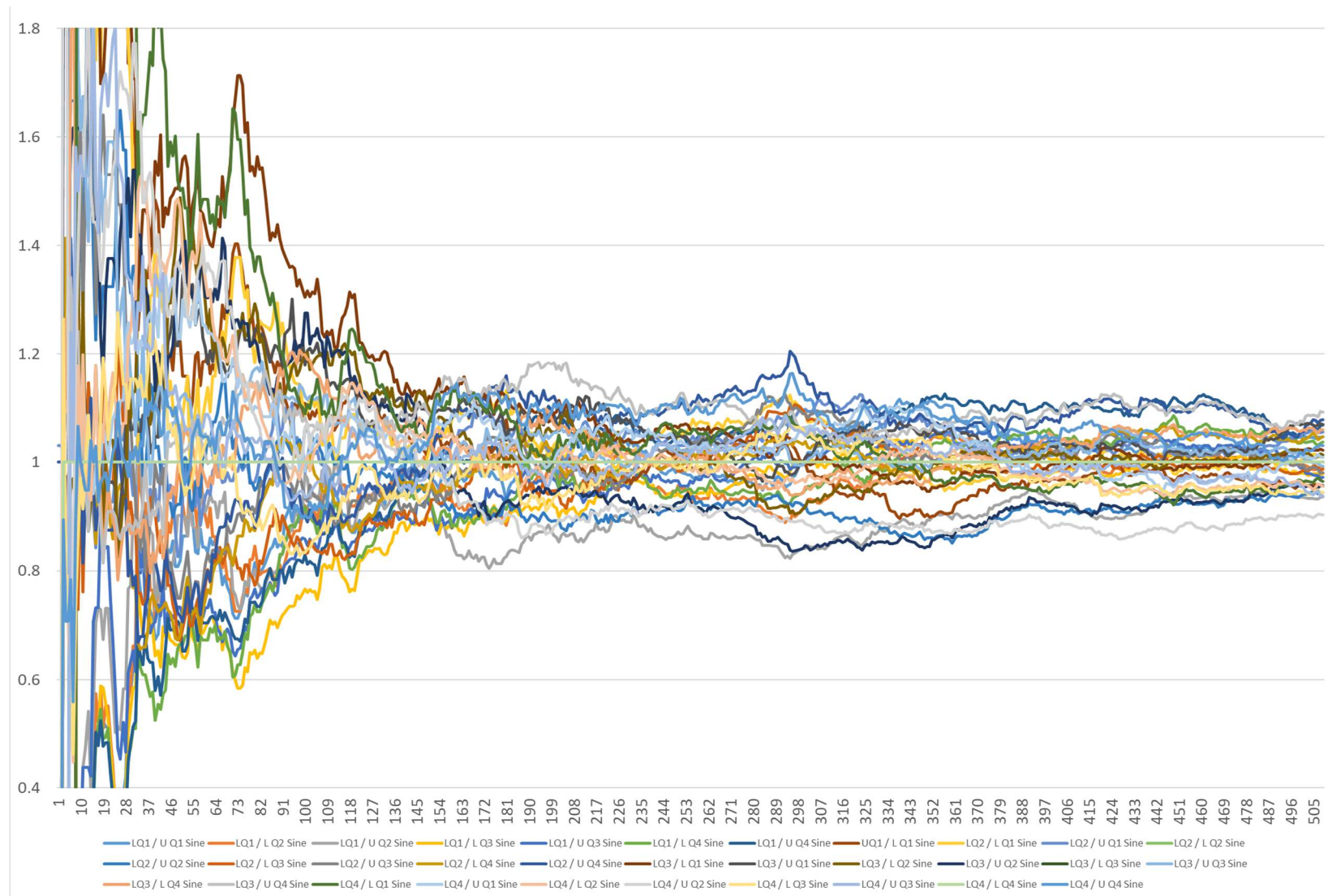


Figure A10 All Upper Partial Derivatives between Quadrant Sines

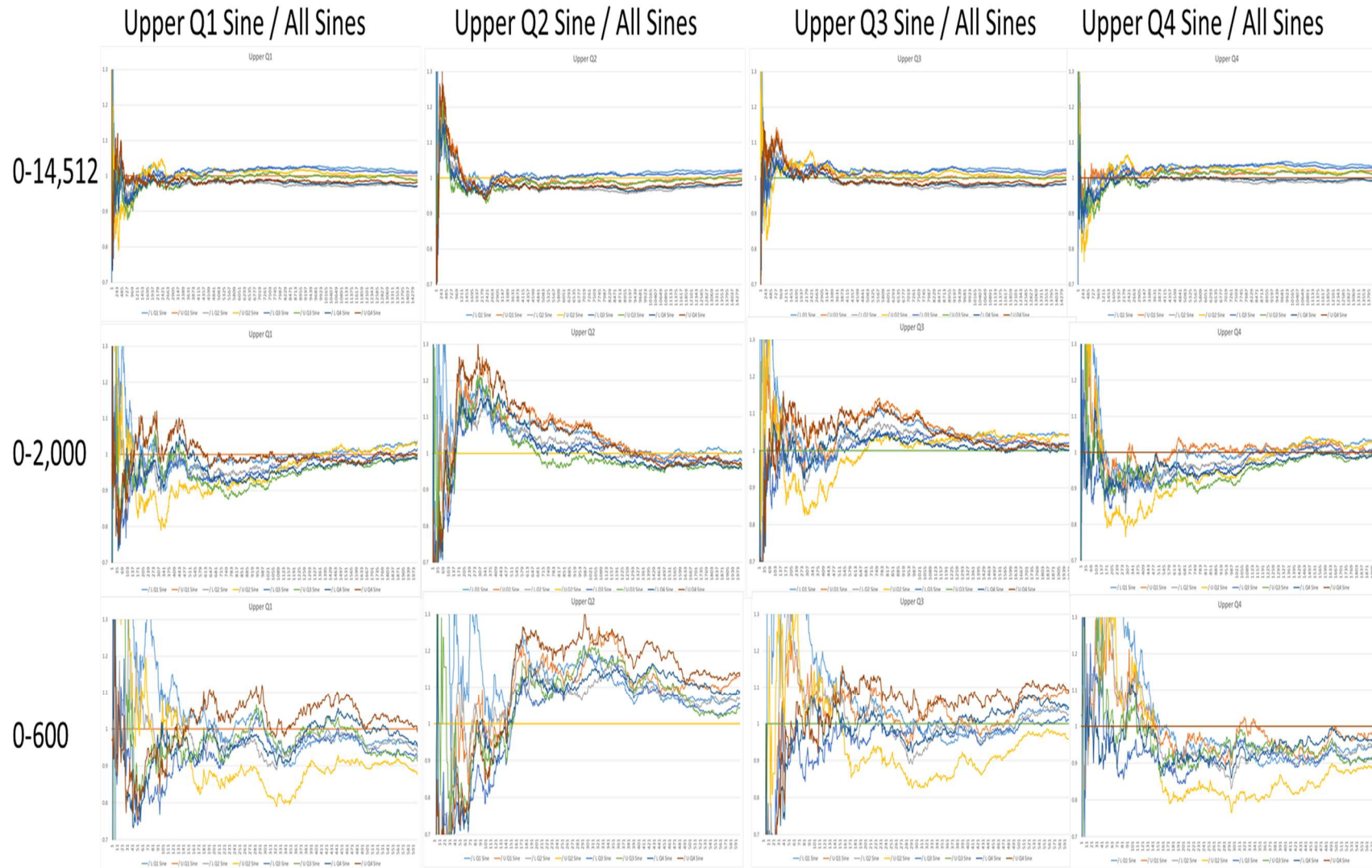


Figure A11 All Lower Partial Derivatives between Quadrant Sines

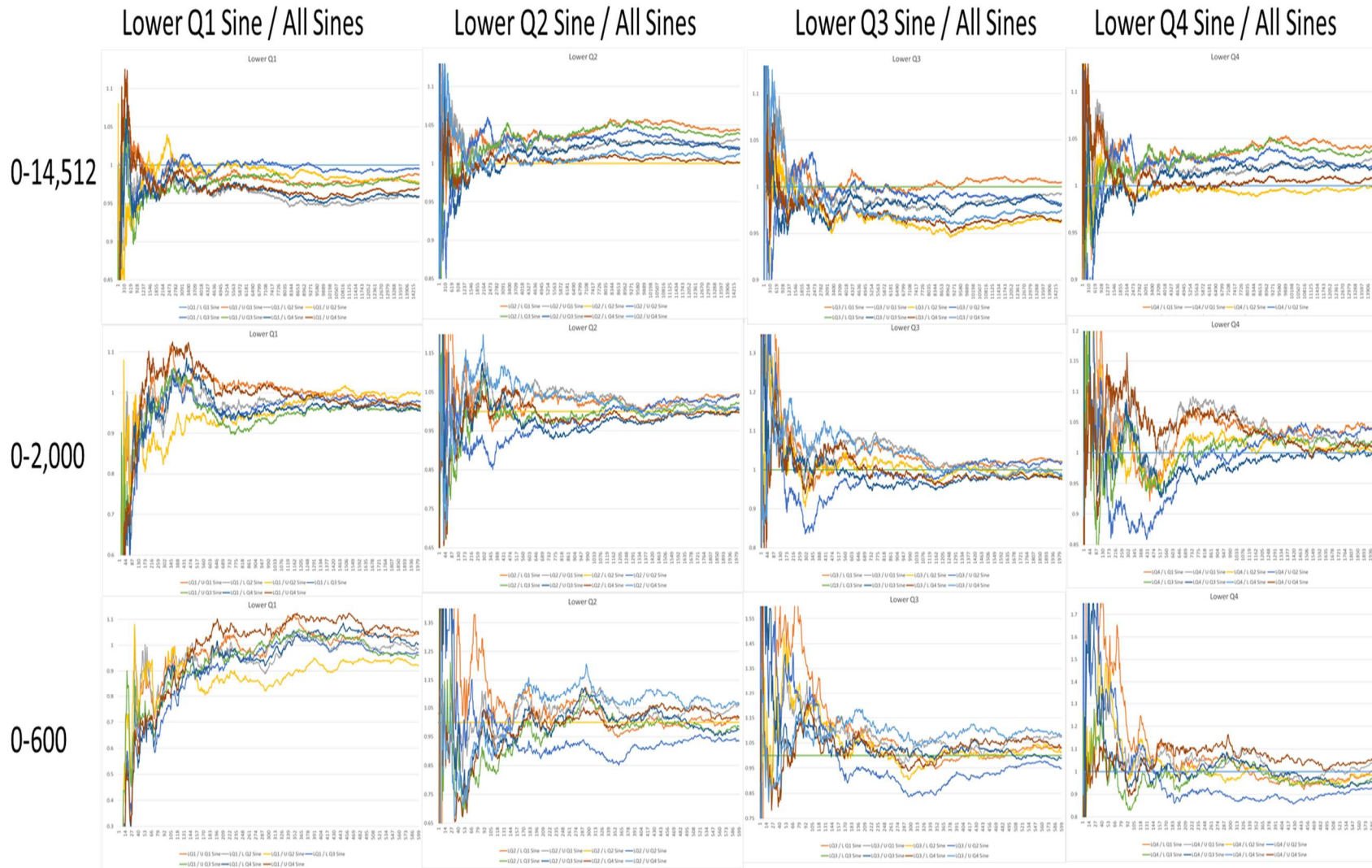


Table A1 Event Trace Table (Coils 1-720)

Table A2 Event Trace Table (Coils 720-14,512)

Figure A12 Event Trace Analysis

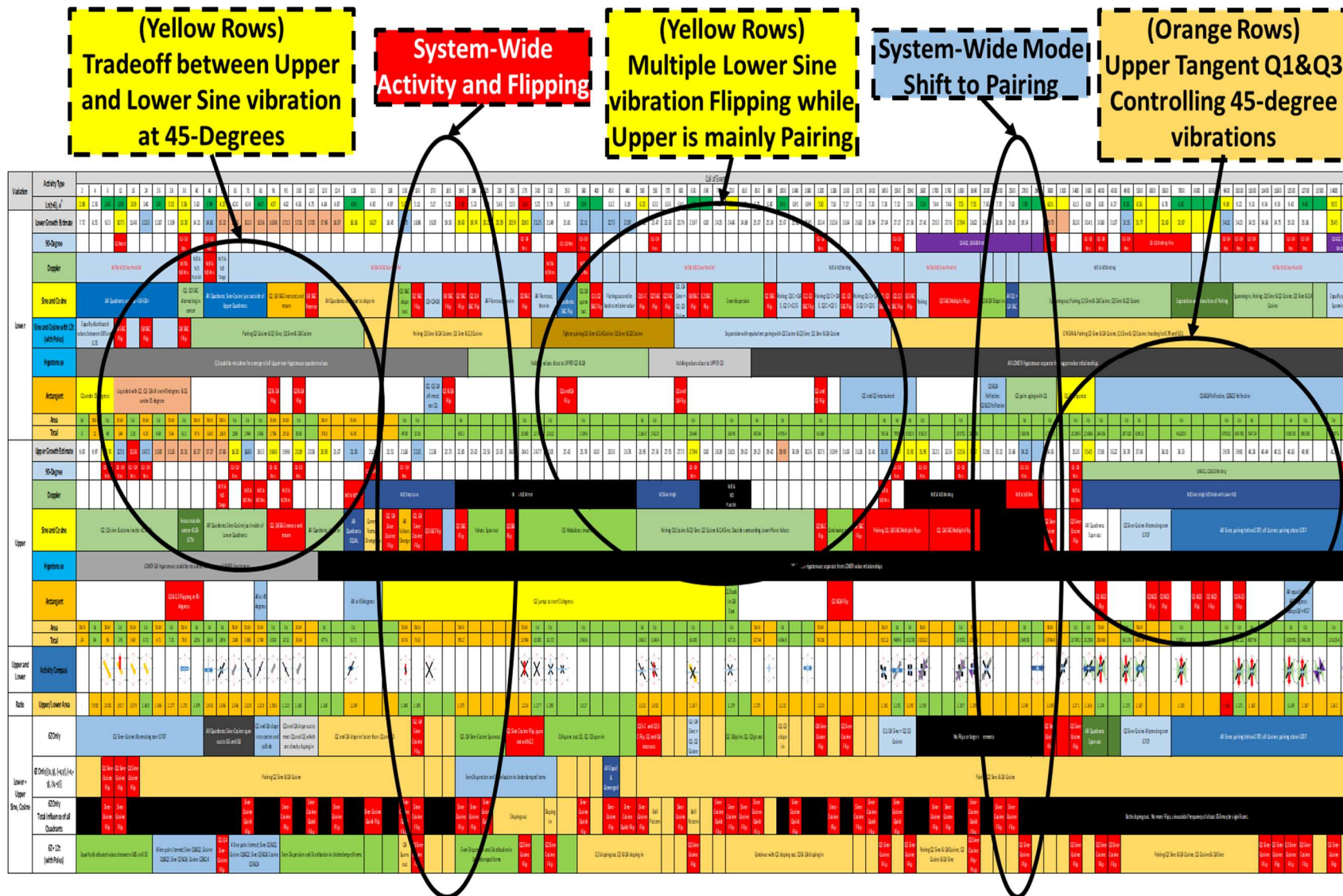


Figure A13 Sine, Cosine, Tangent Analysis

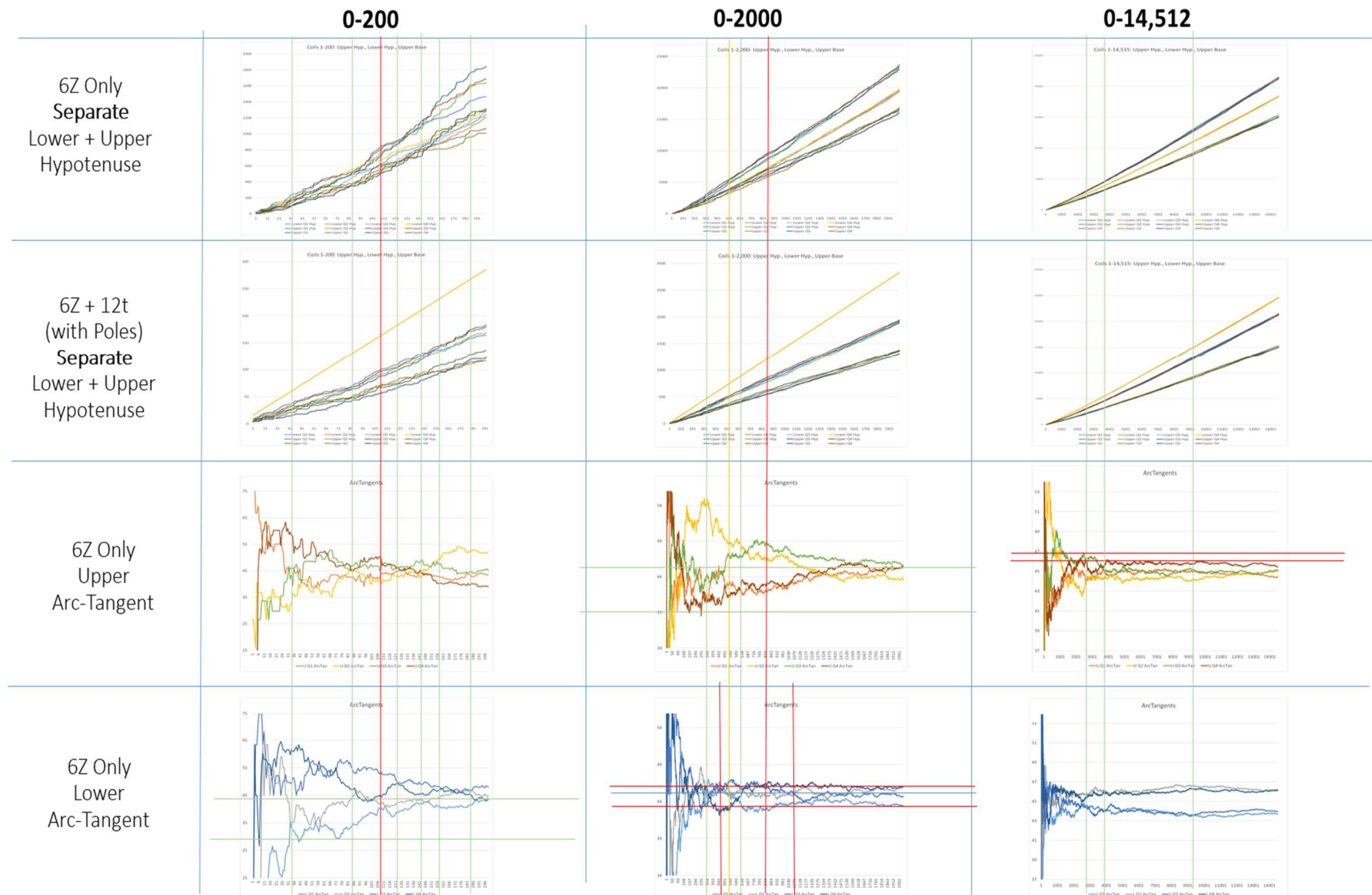


Figure A14 Sine, Cosine, Tangent Analysis

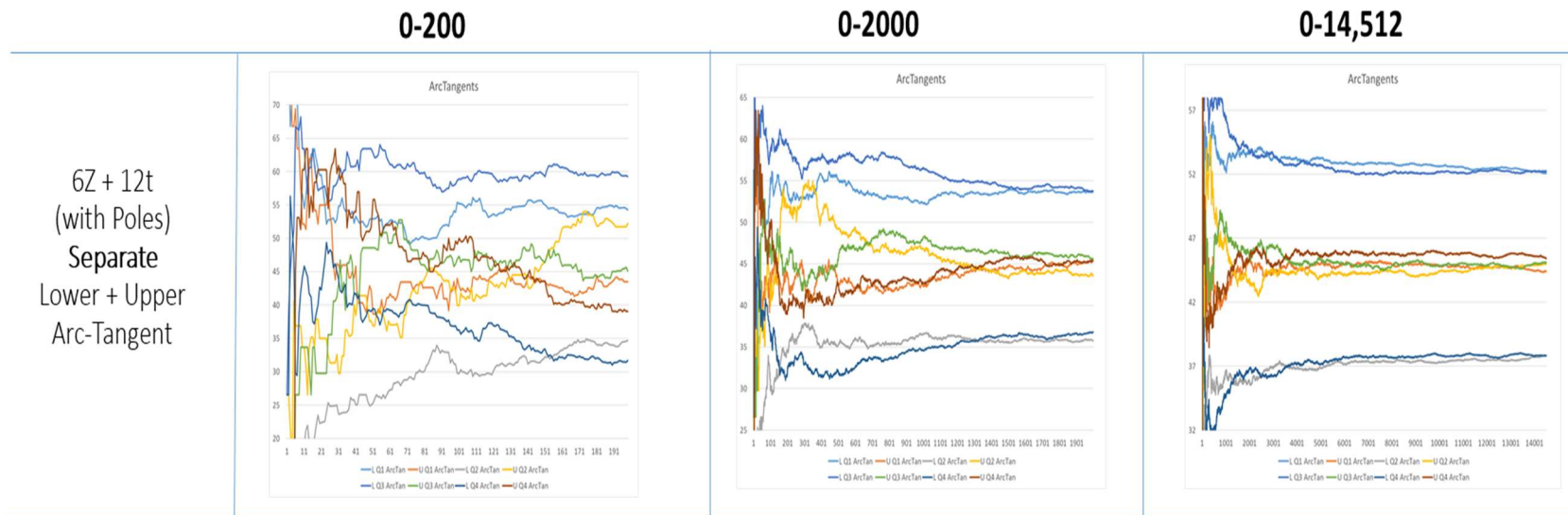


Figure A15 Sine, Cosine, Tangent Analysis

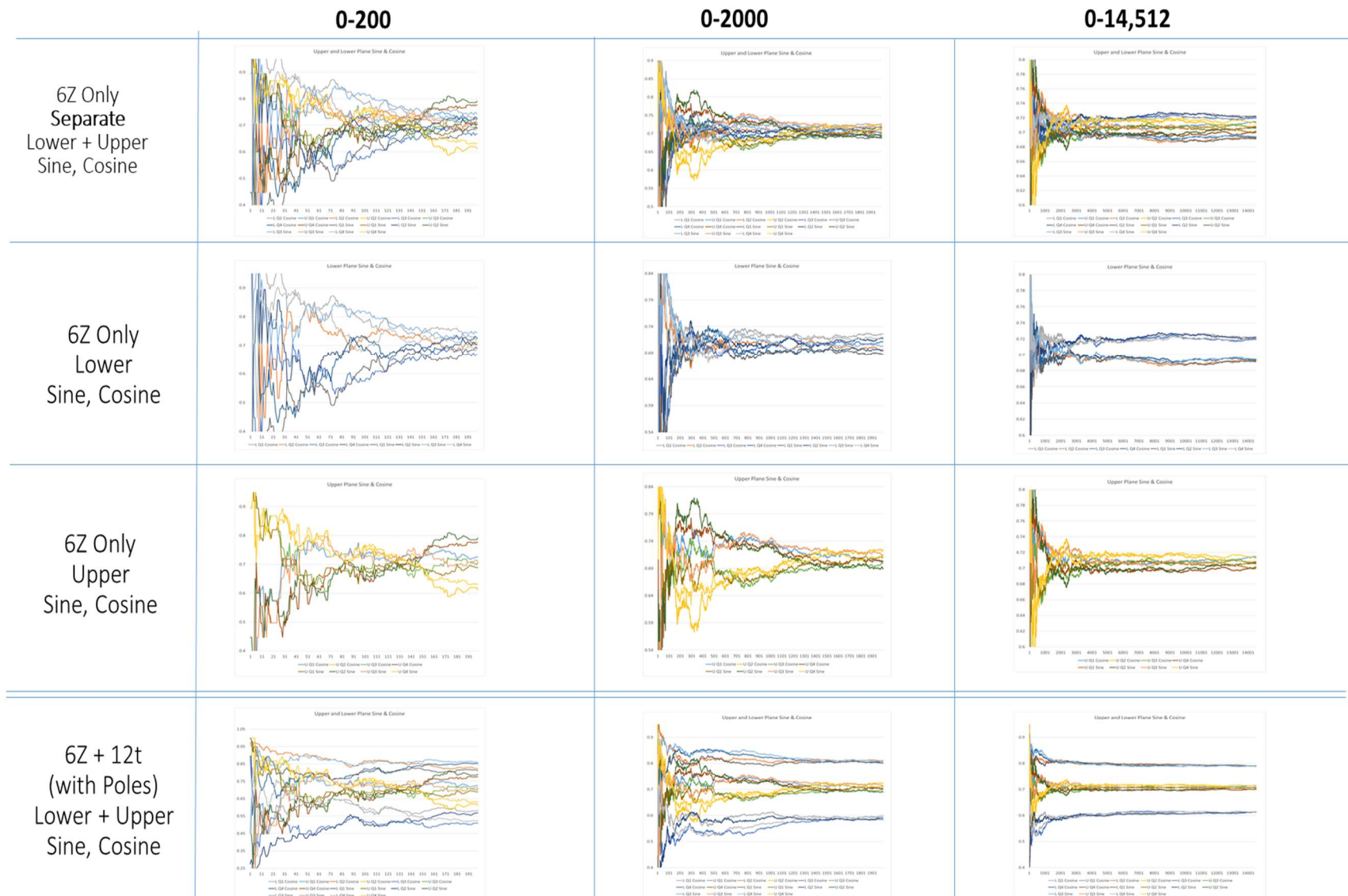


Figure A16 Sine, Cosine, Tangent Analysis

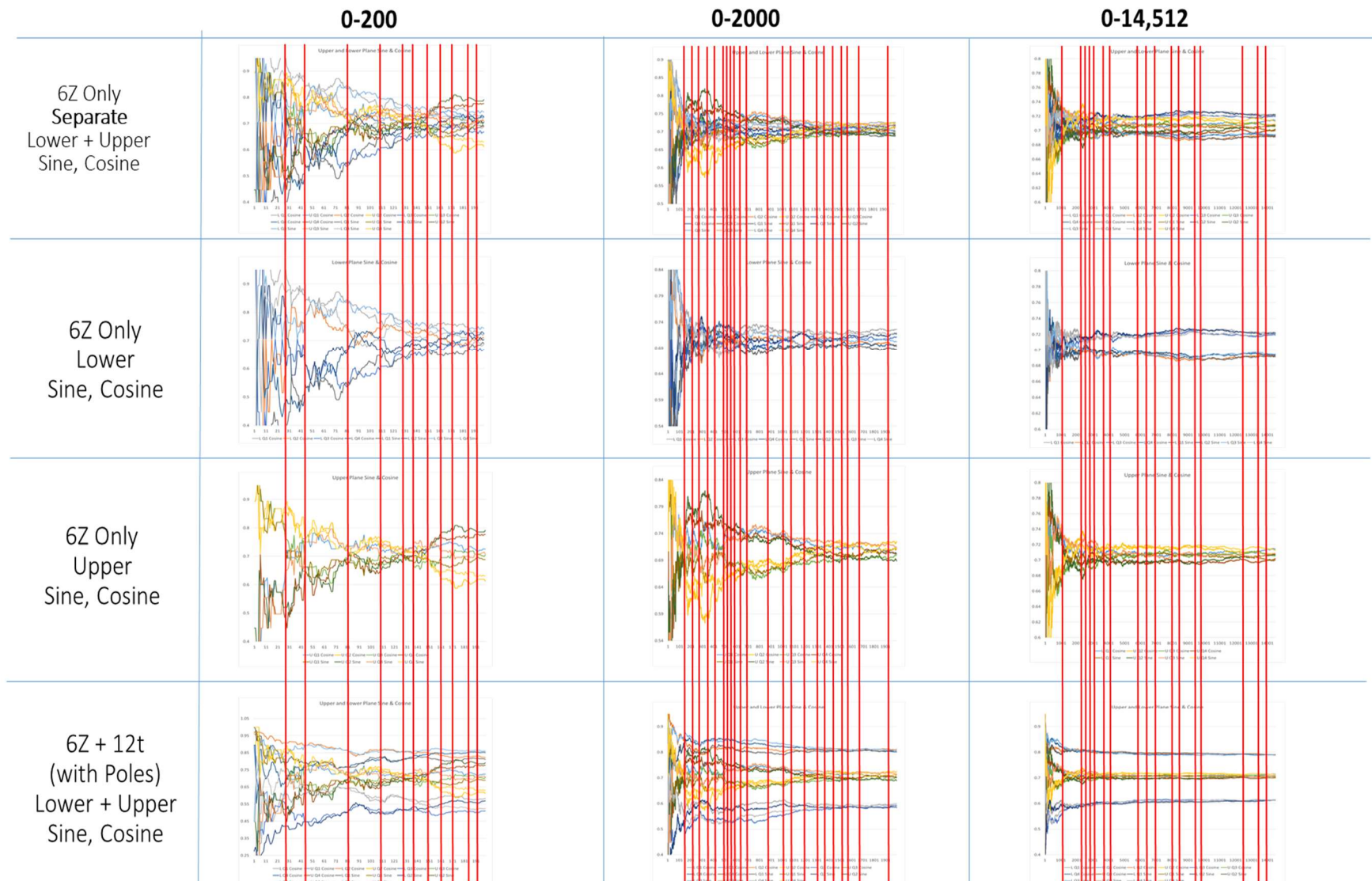


Figure A17 Sine, Cosine, Tangent Analysis

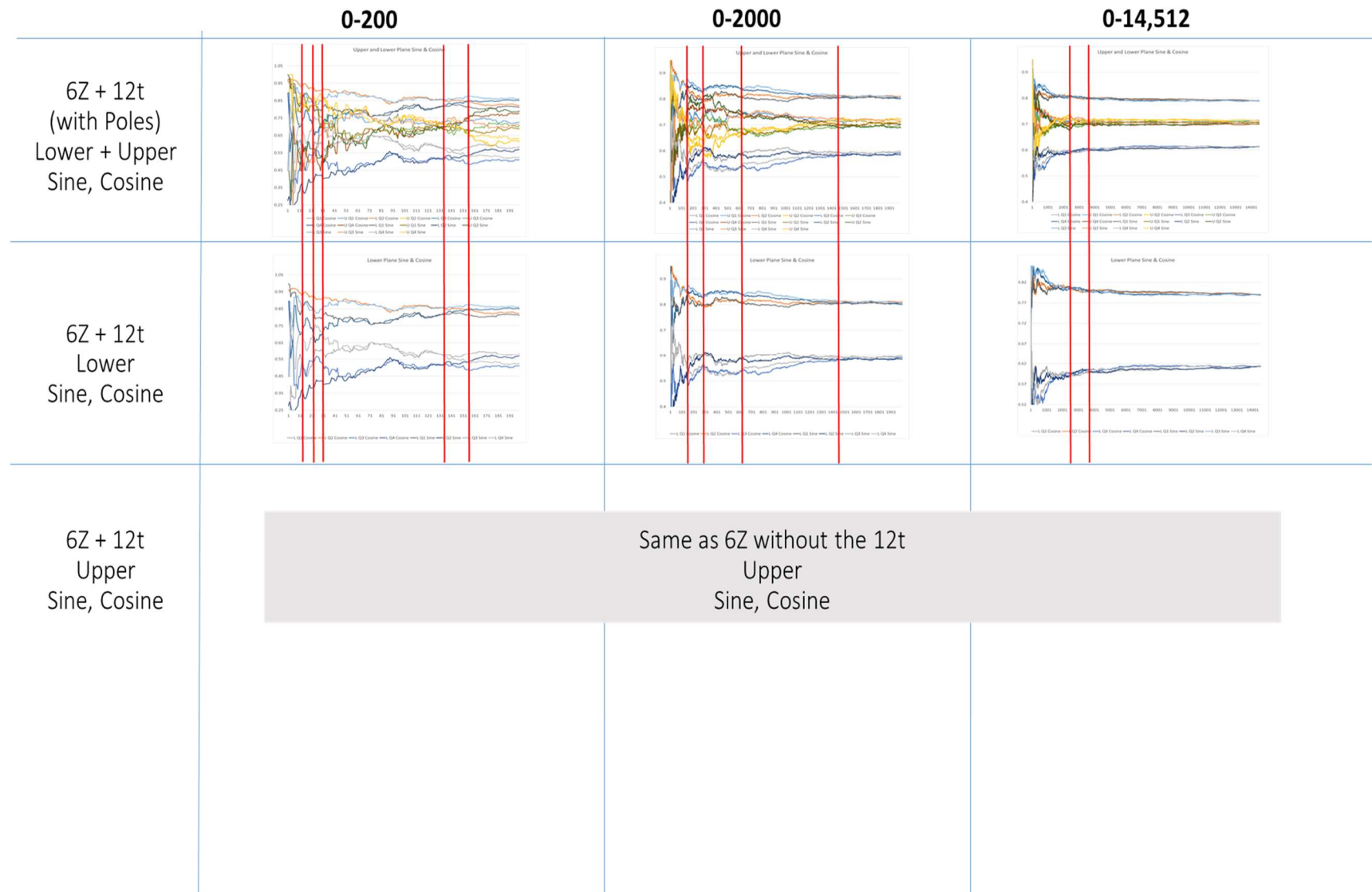


Figure A18 Hypotenuse Analysis

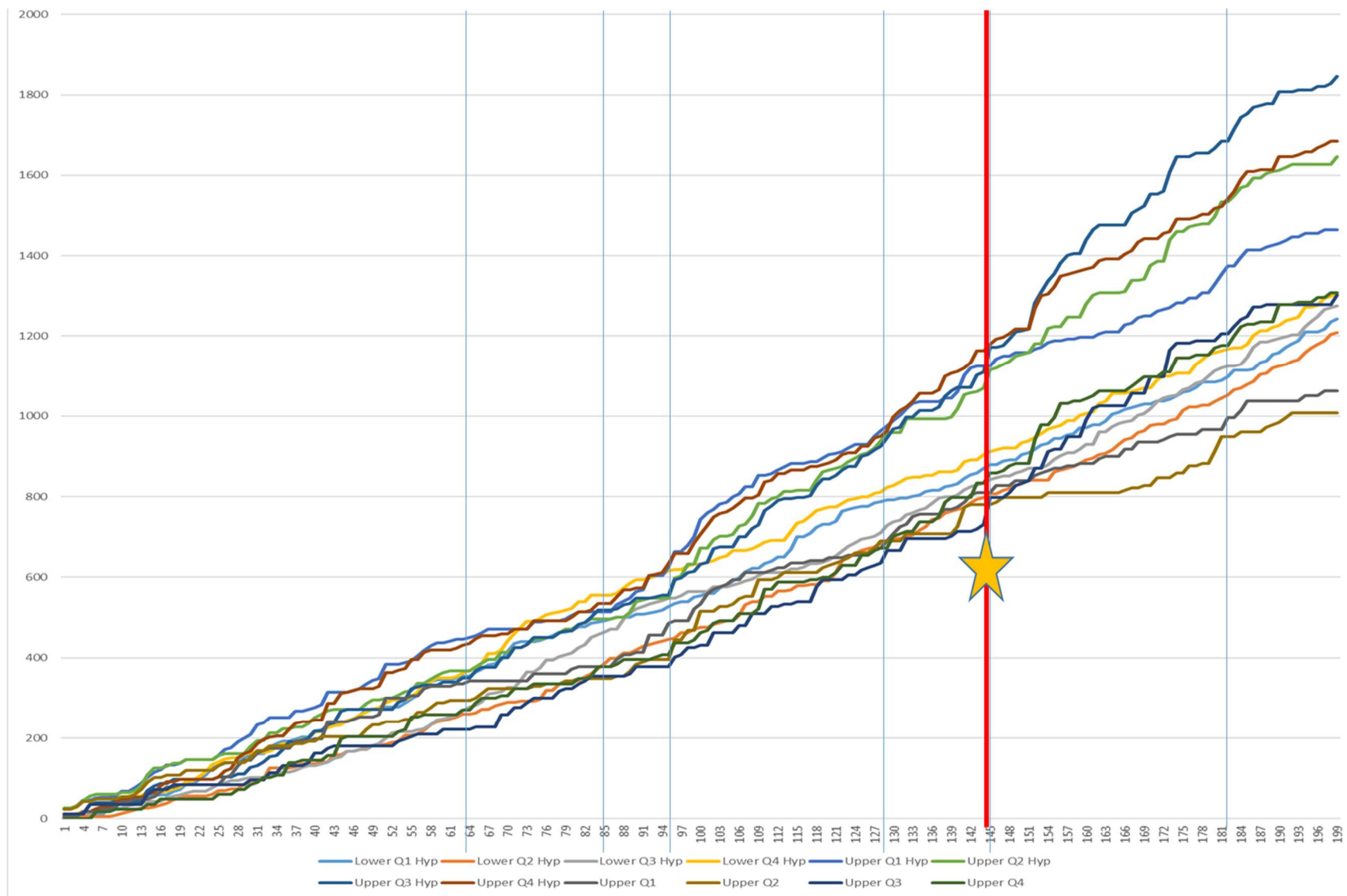


Figure A19 Hypotenuse Analysis

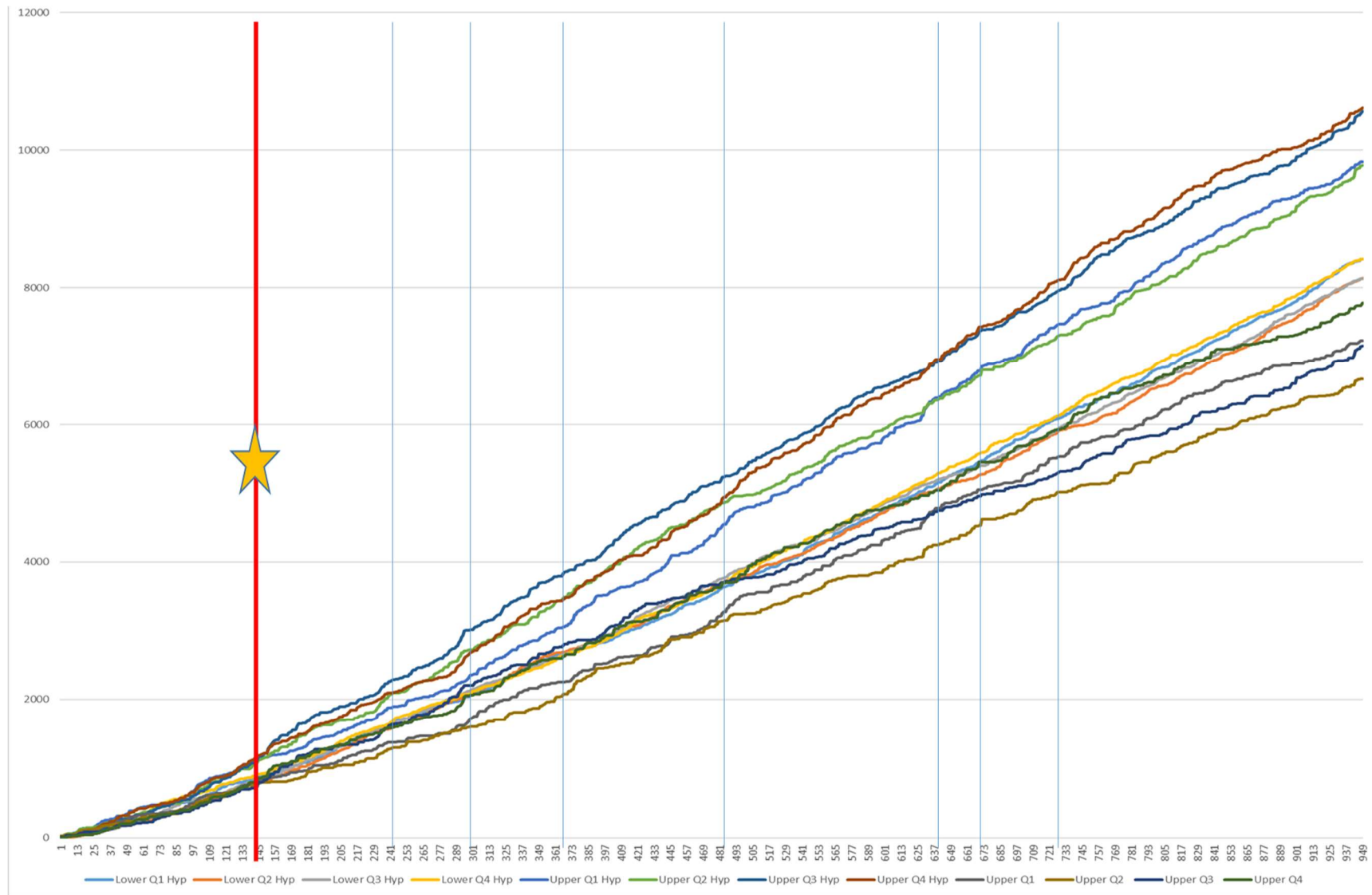


Figure A20 Hypotenuse Analysis

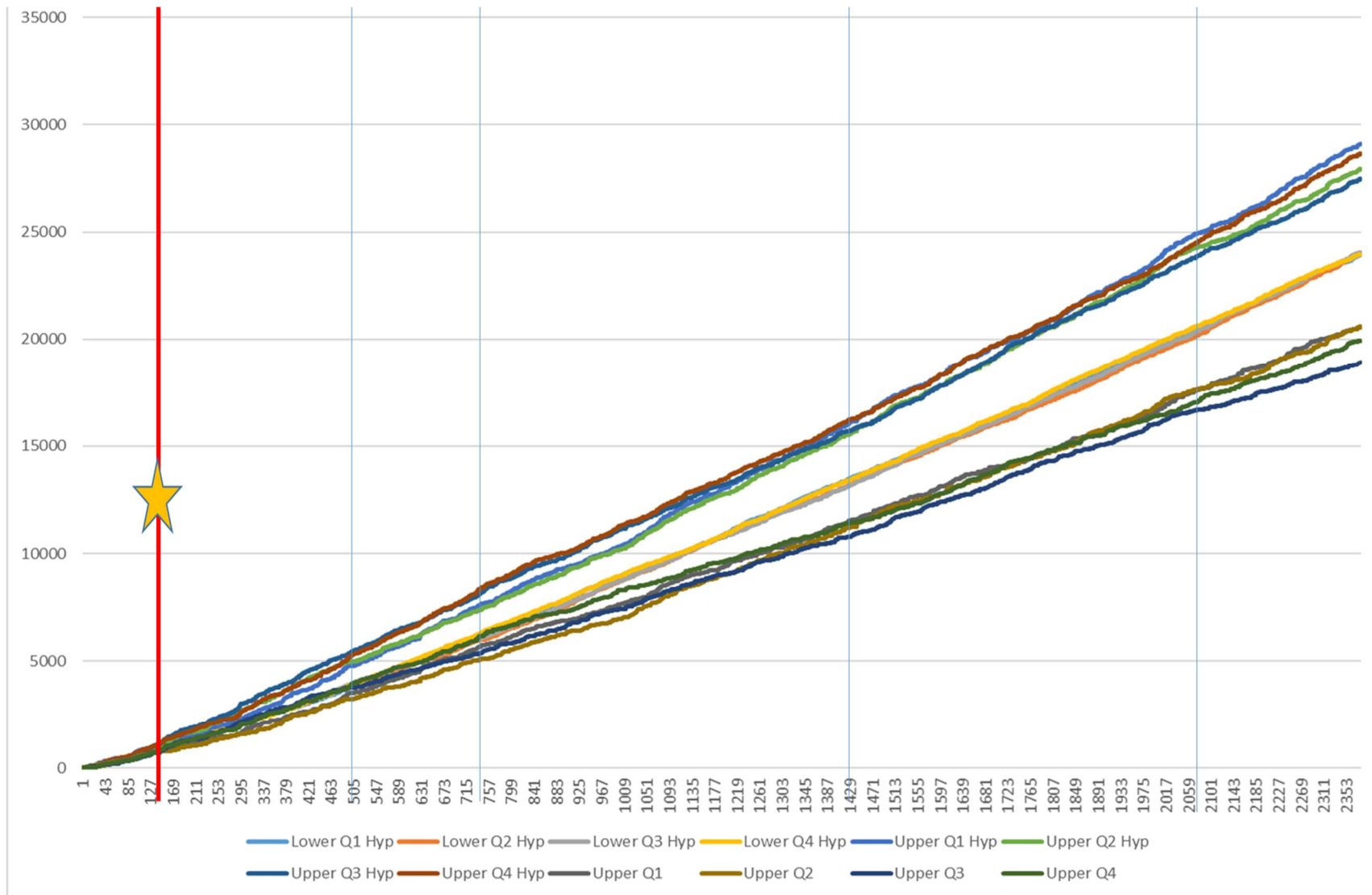


Figure A21 Normal and Doppler Vectors Analysis

Table Summary of 90-Degree Field Vectors and 180-Degree Doppler Vectors

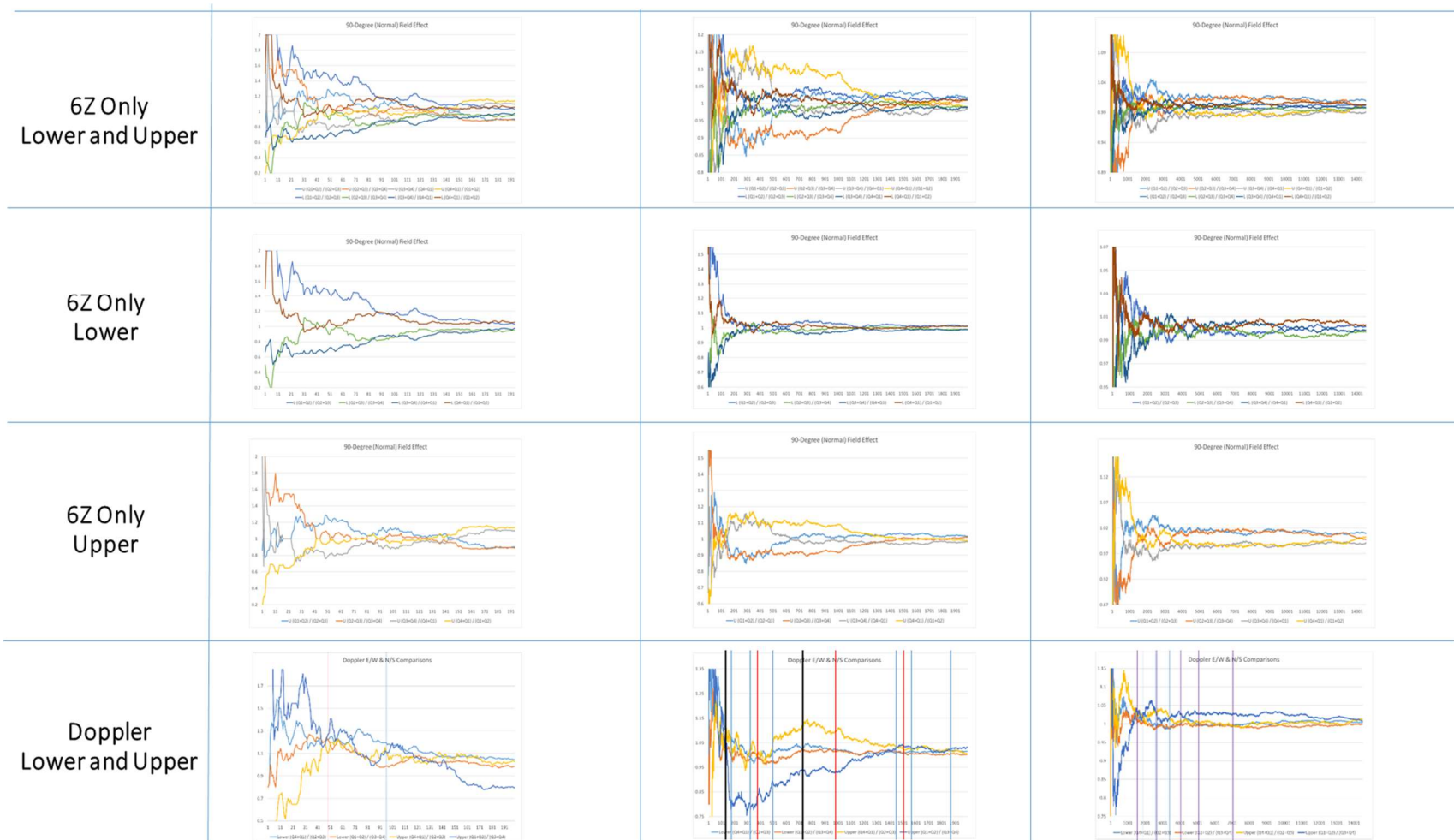


Figure A22 Doppler Vectors Analysis

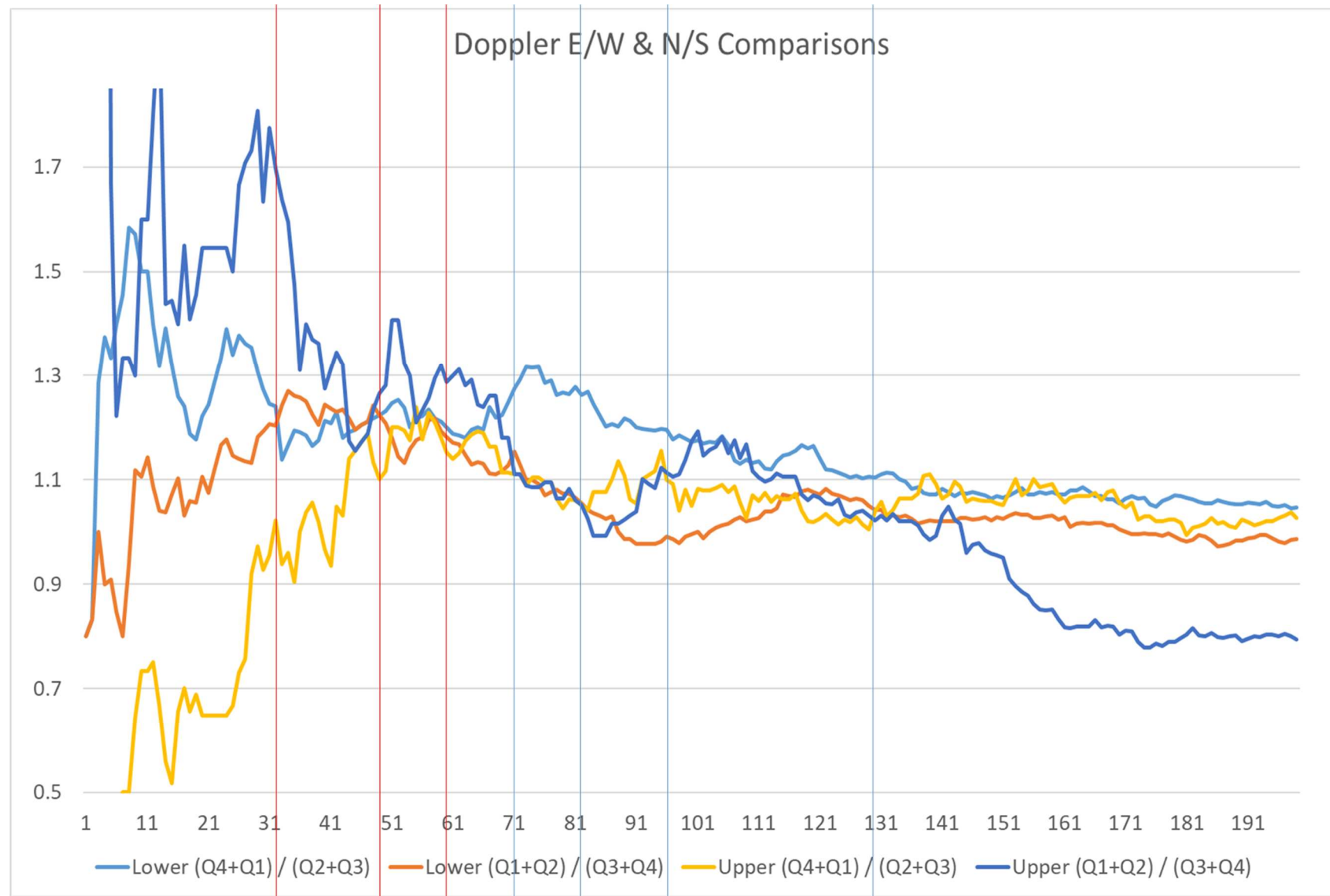


Figure A23 Doppler Vectors Analysis

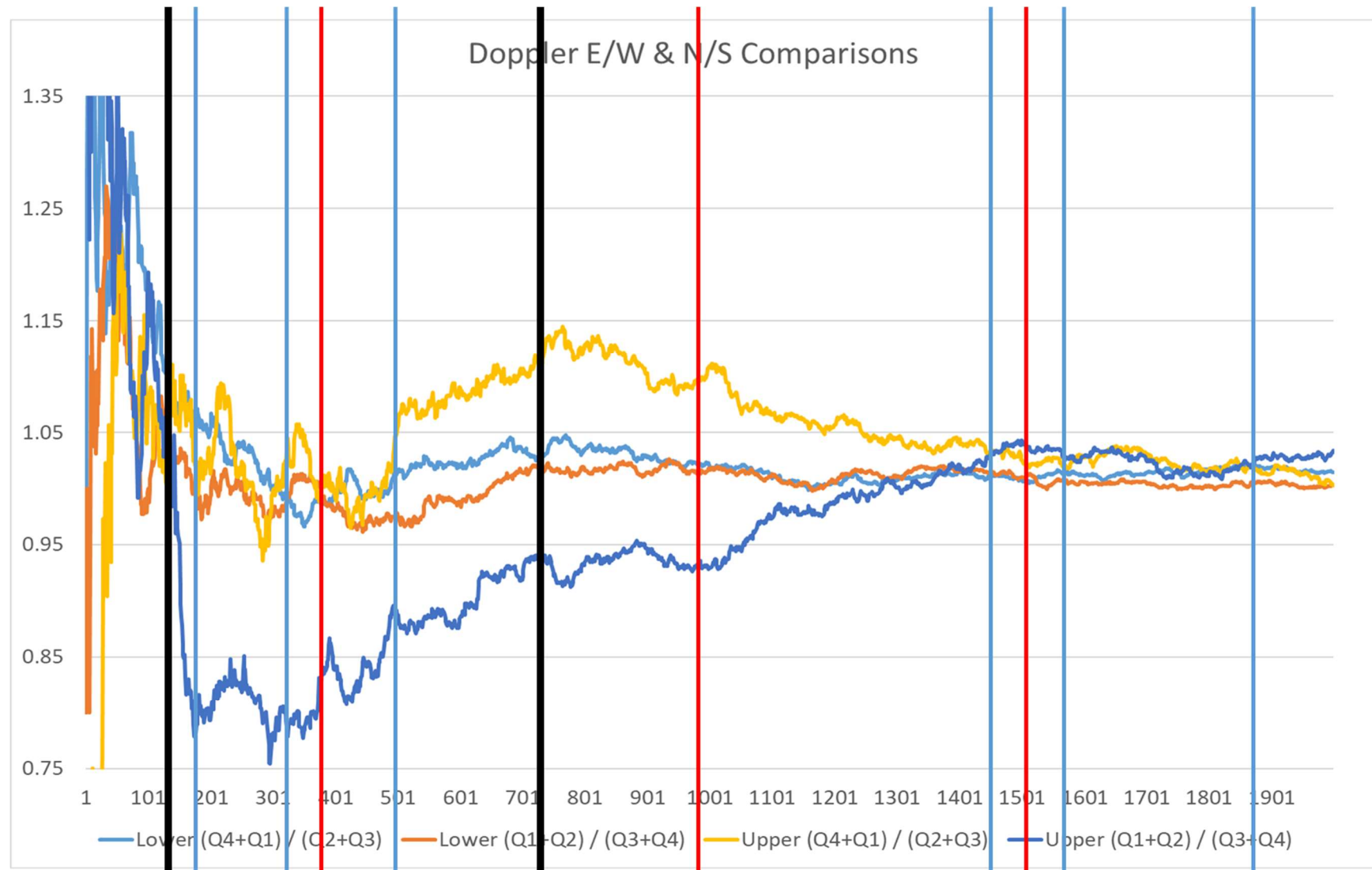


Figure A24 Doppler Vectors Analysis

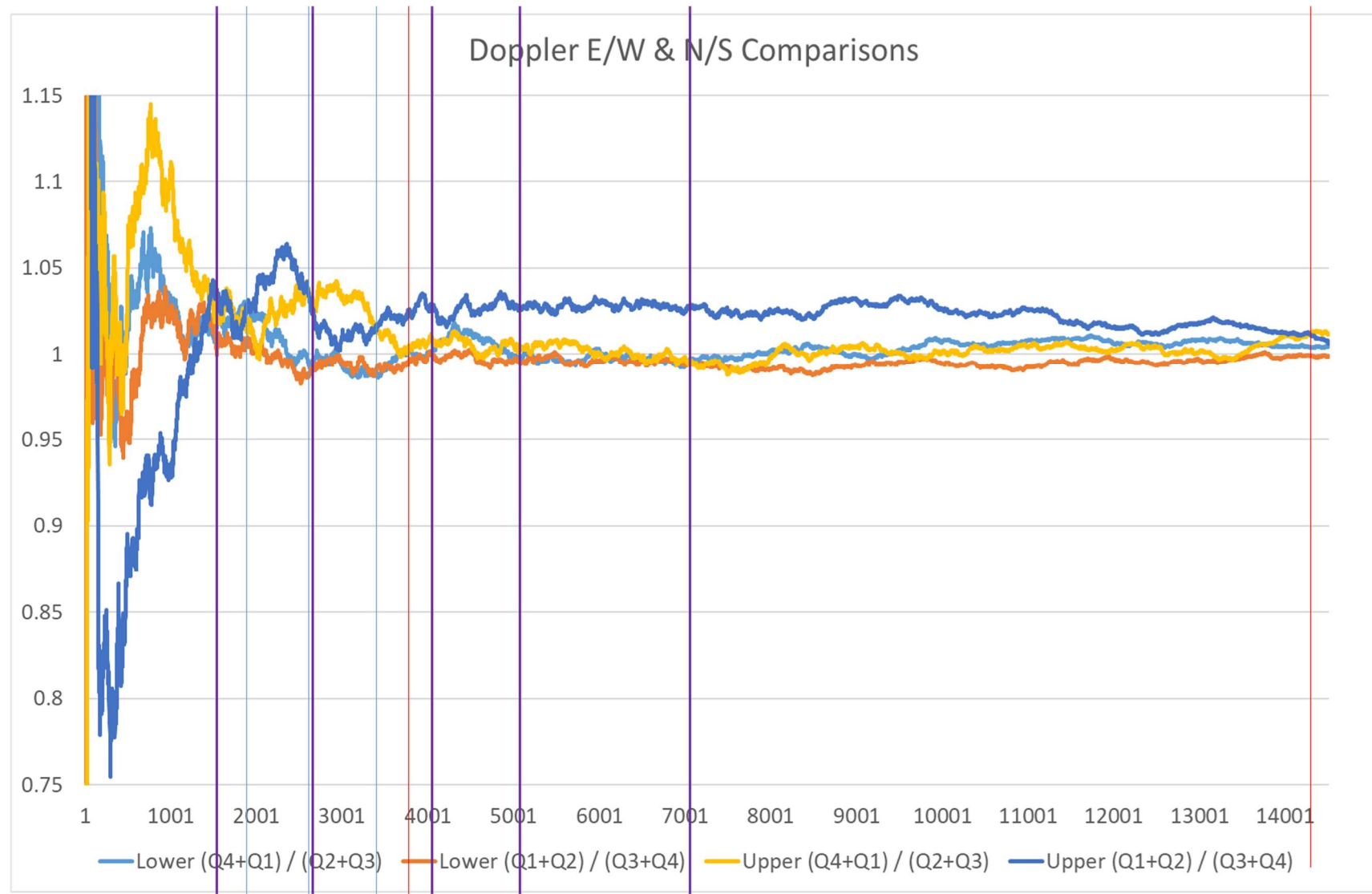


Figure A25 Normal Vectors Analysis

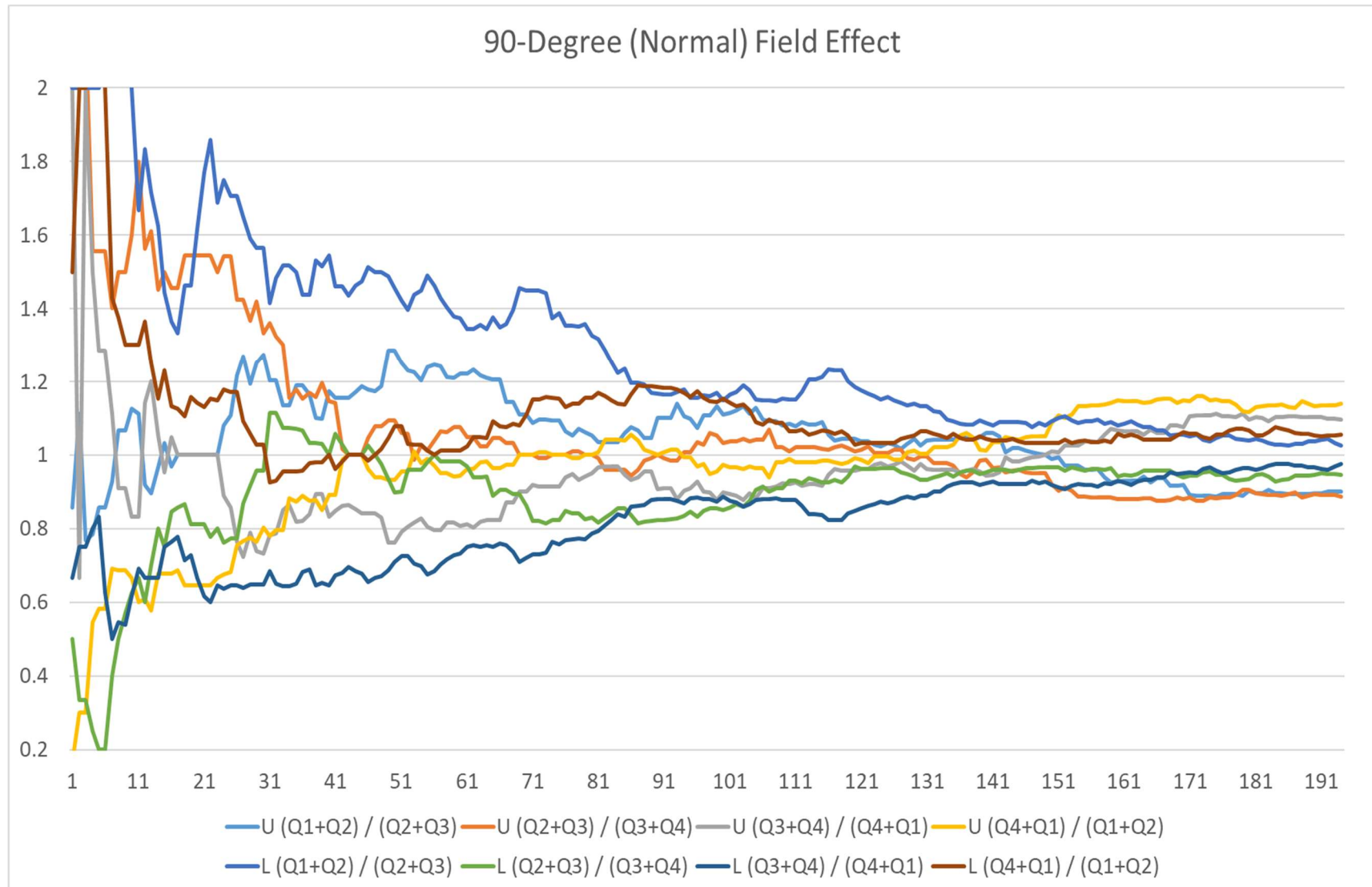


Figure A26 Normal Vectors Analysis

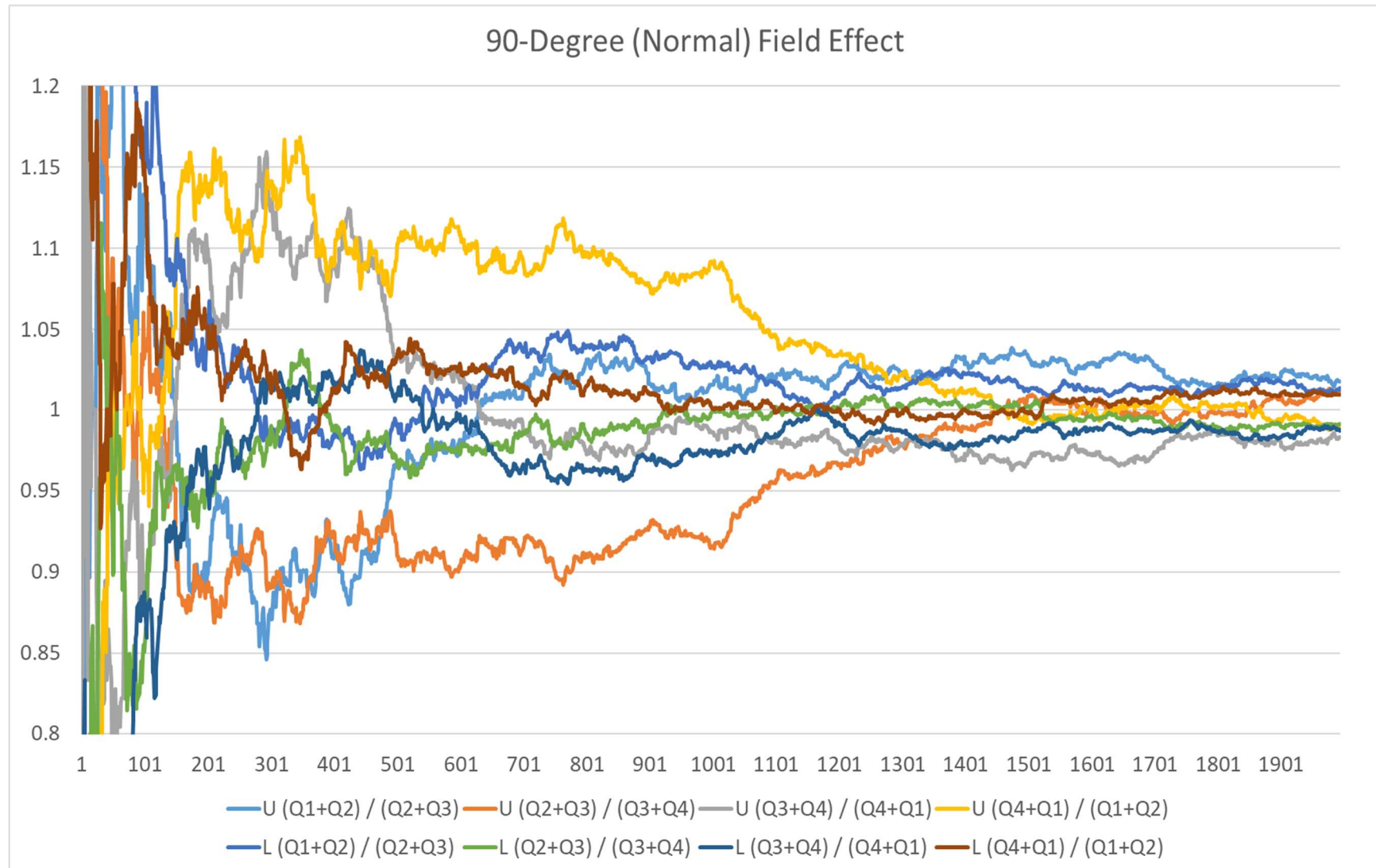


Figure A27 Normal Vectors Analysis

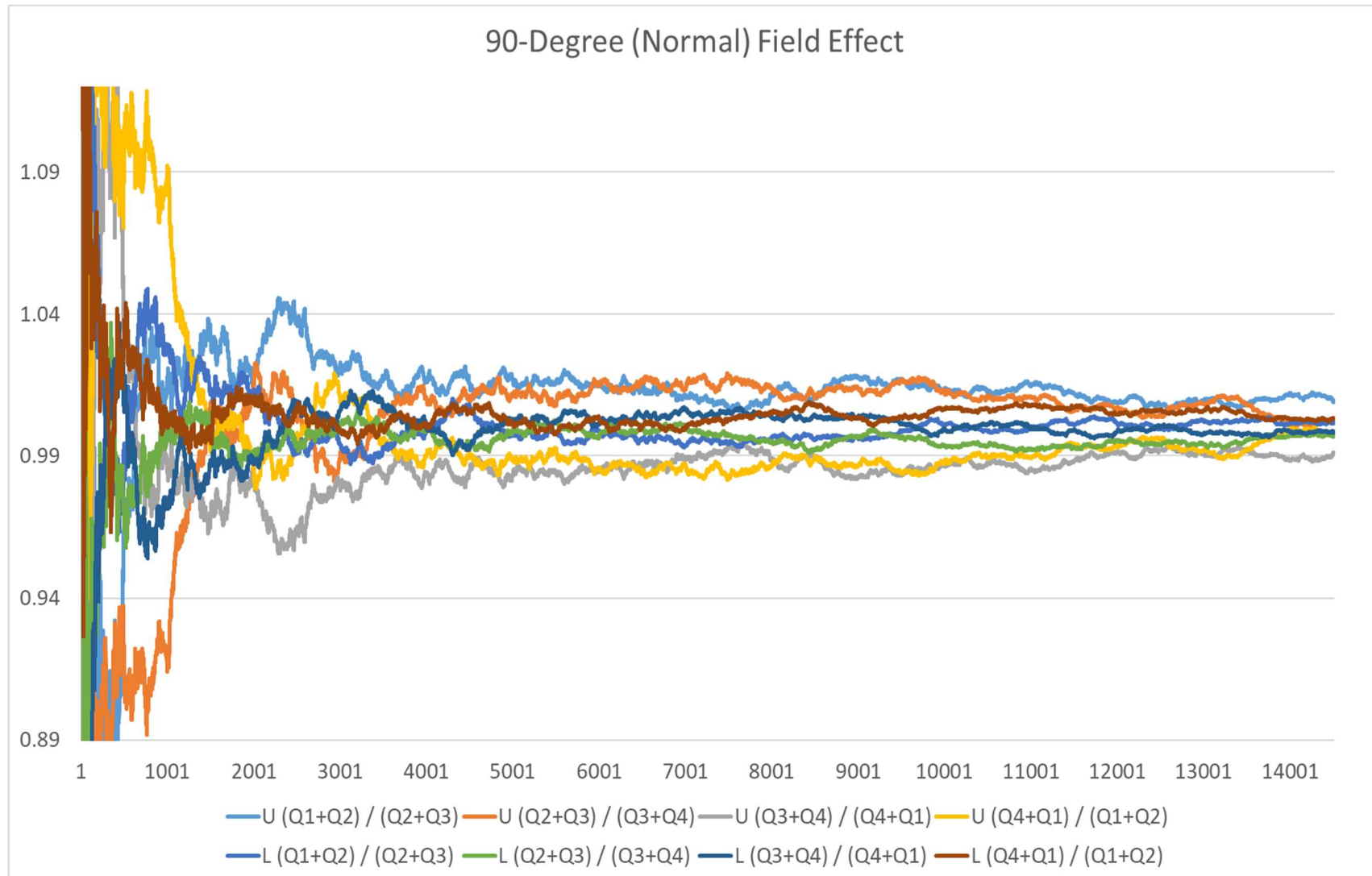


Figure A28 Upper Plane Normal Vectors Analysis

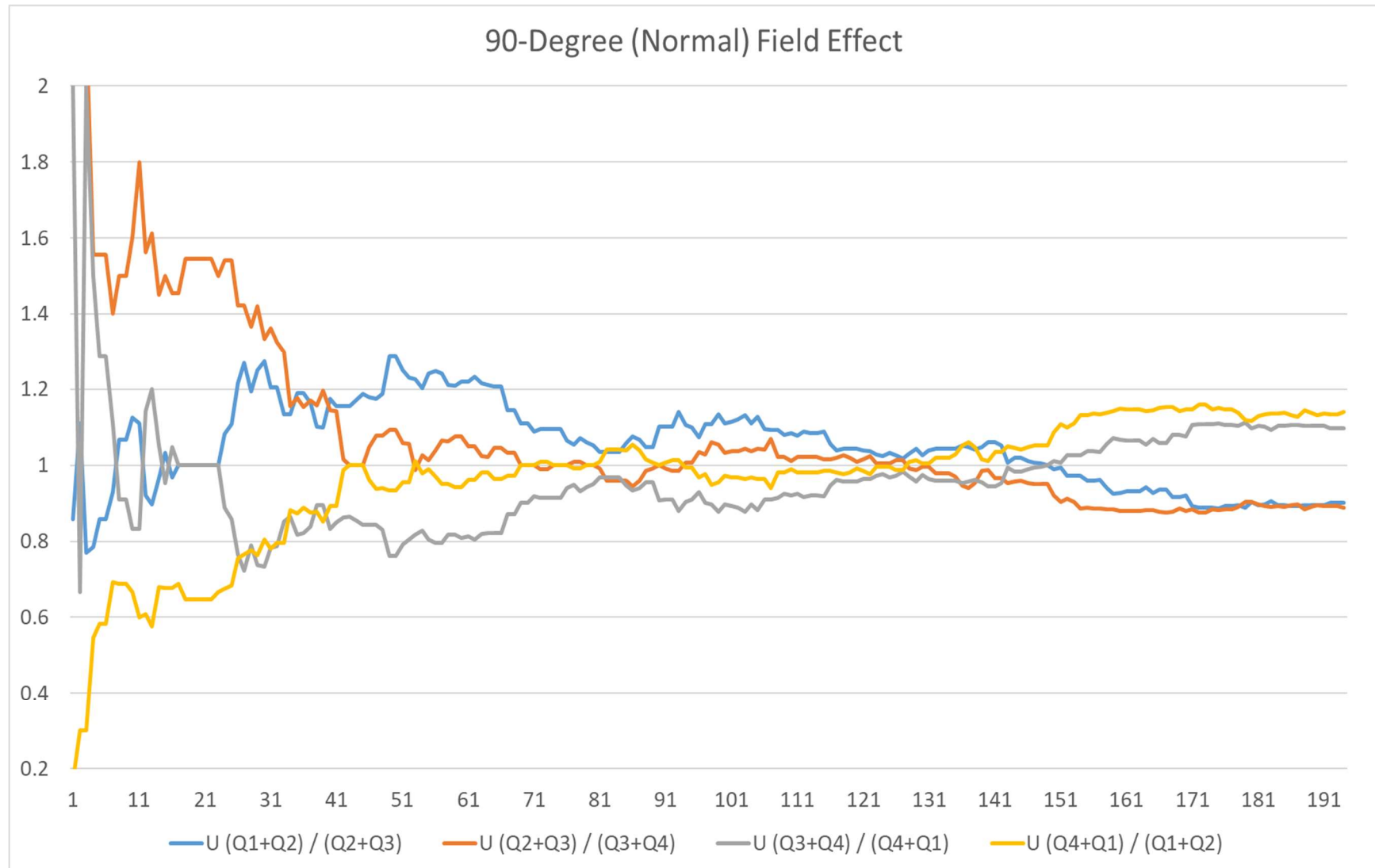


Figure A29 Upper Plane Normal Vectors Analysis

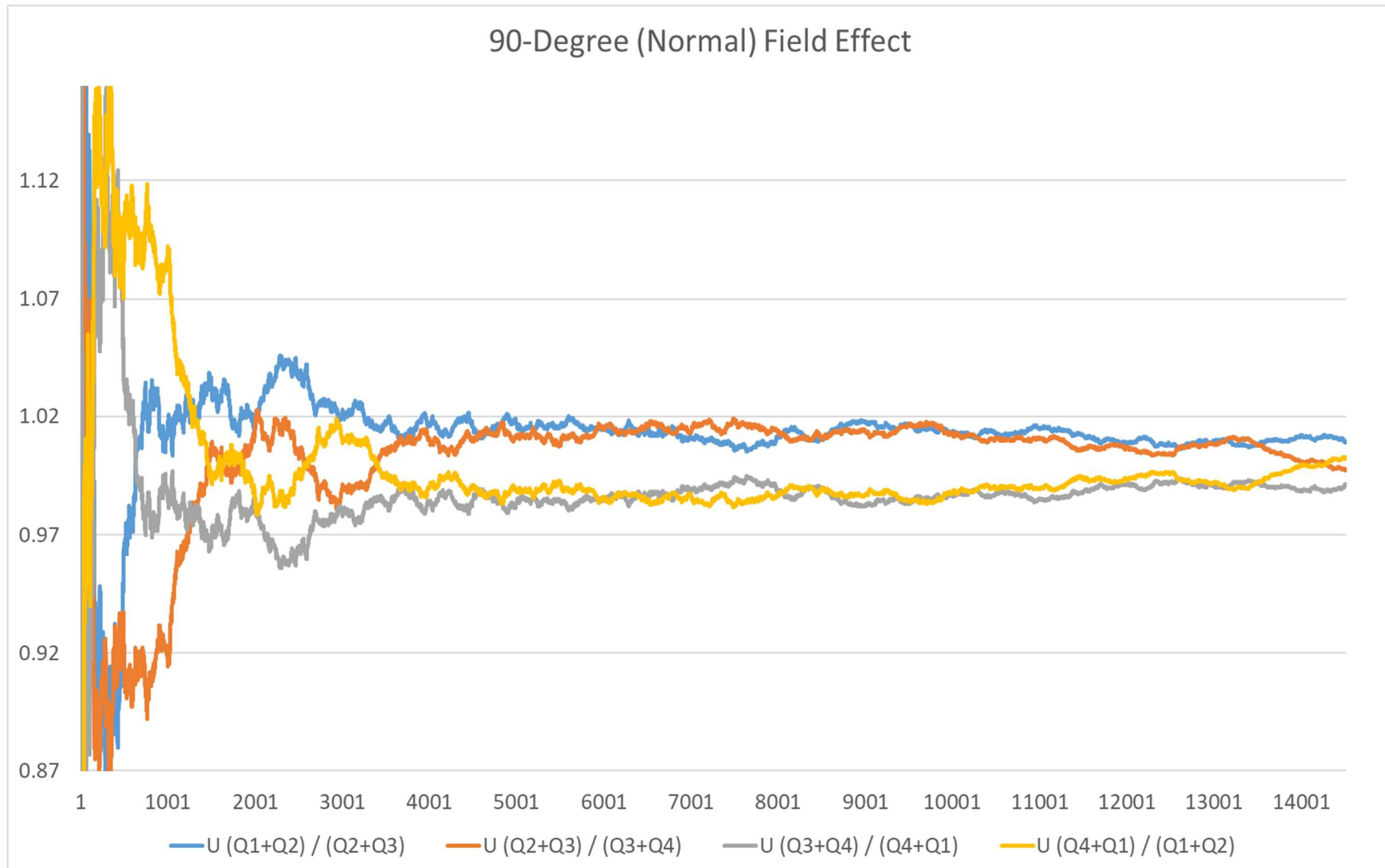


Figure A30 Lower Plane Normal Vectors Analysis

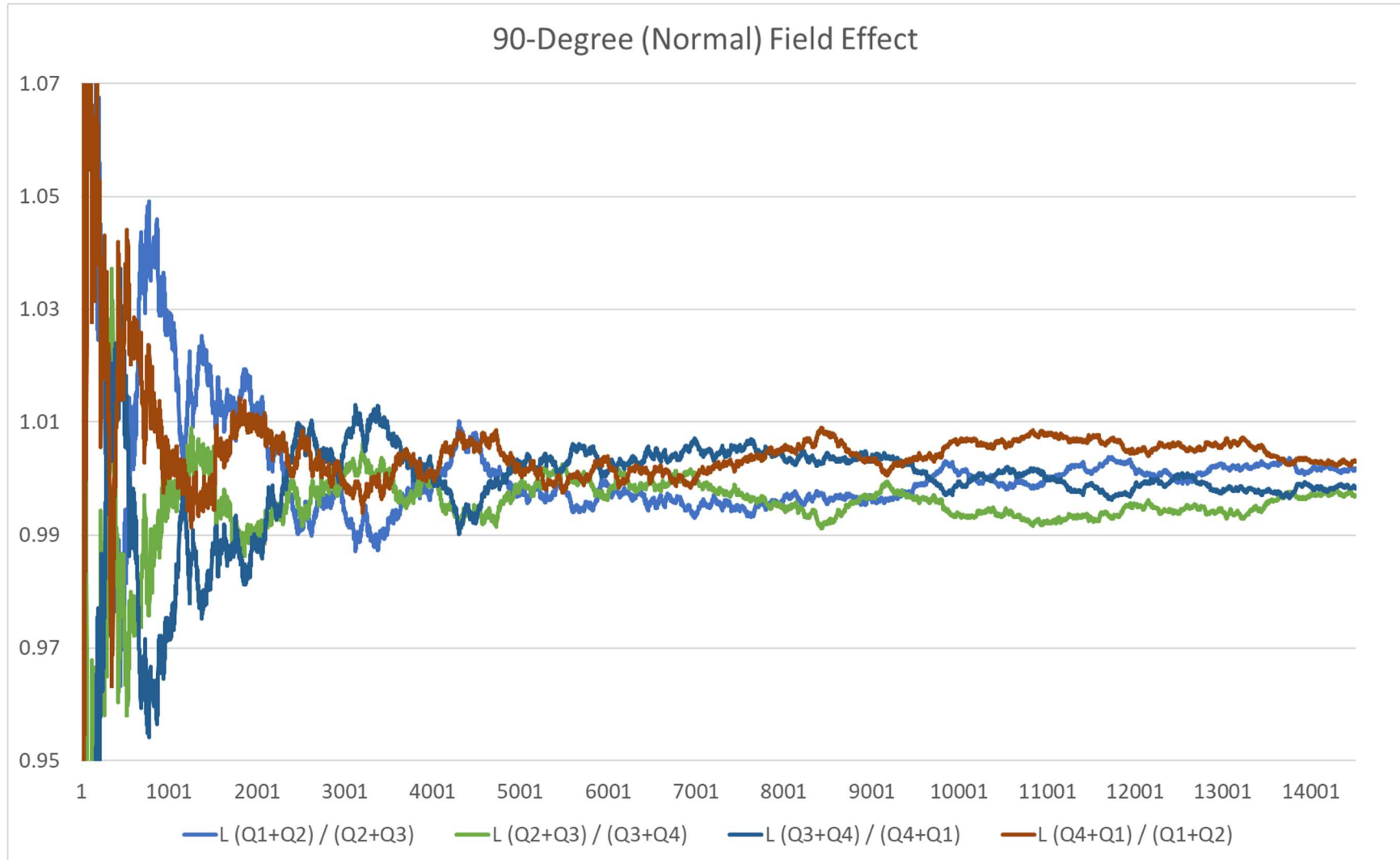


Figure A31 Sum of Upper and Lower Normal Vectors Analysis

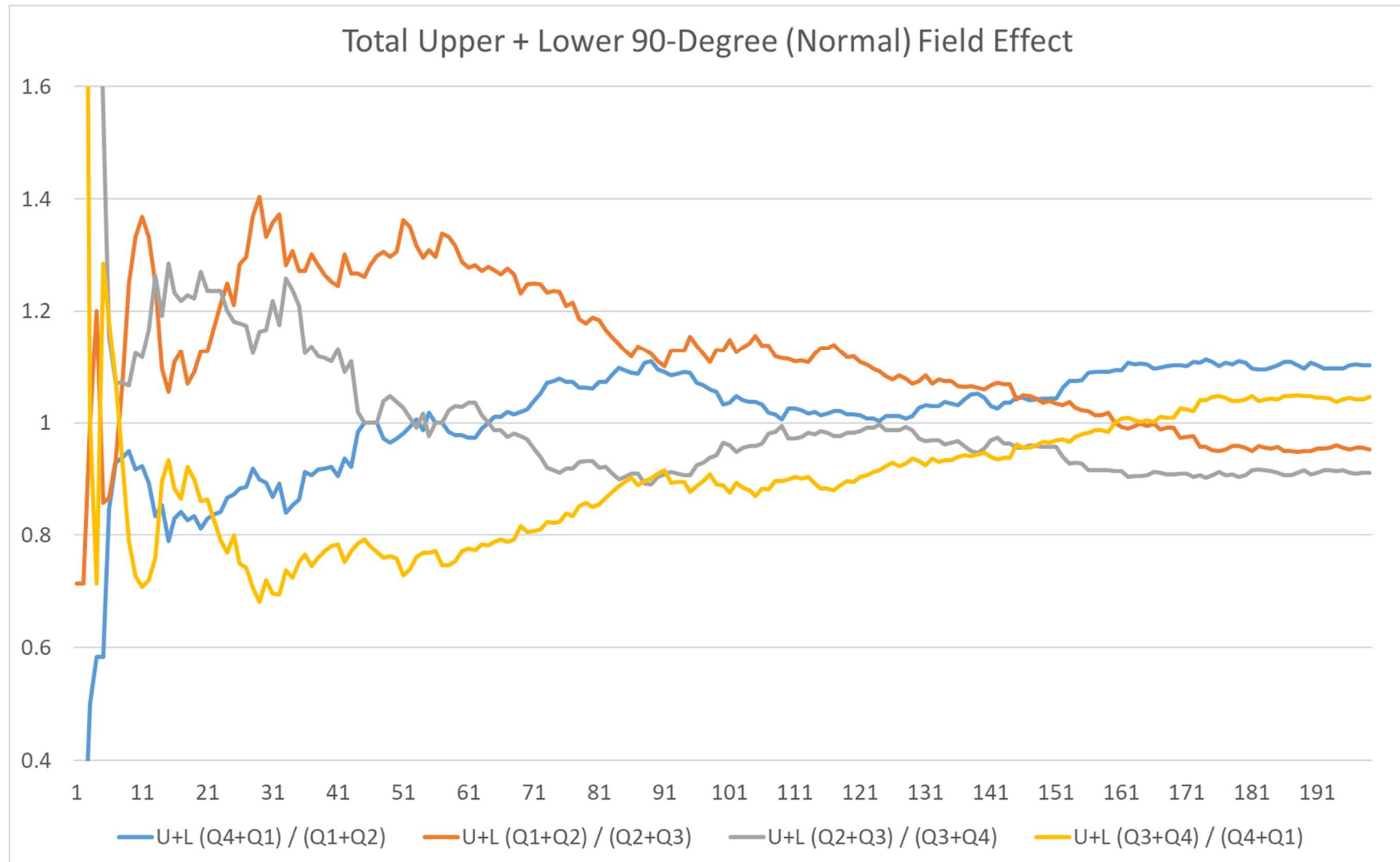


Figure A32 Sum of Upper and Lower Normal Vectors Analysis

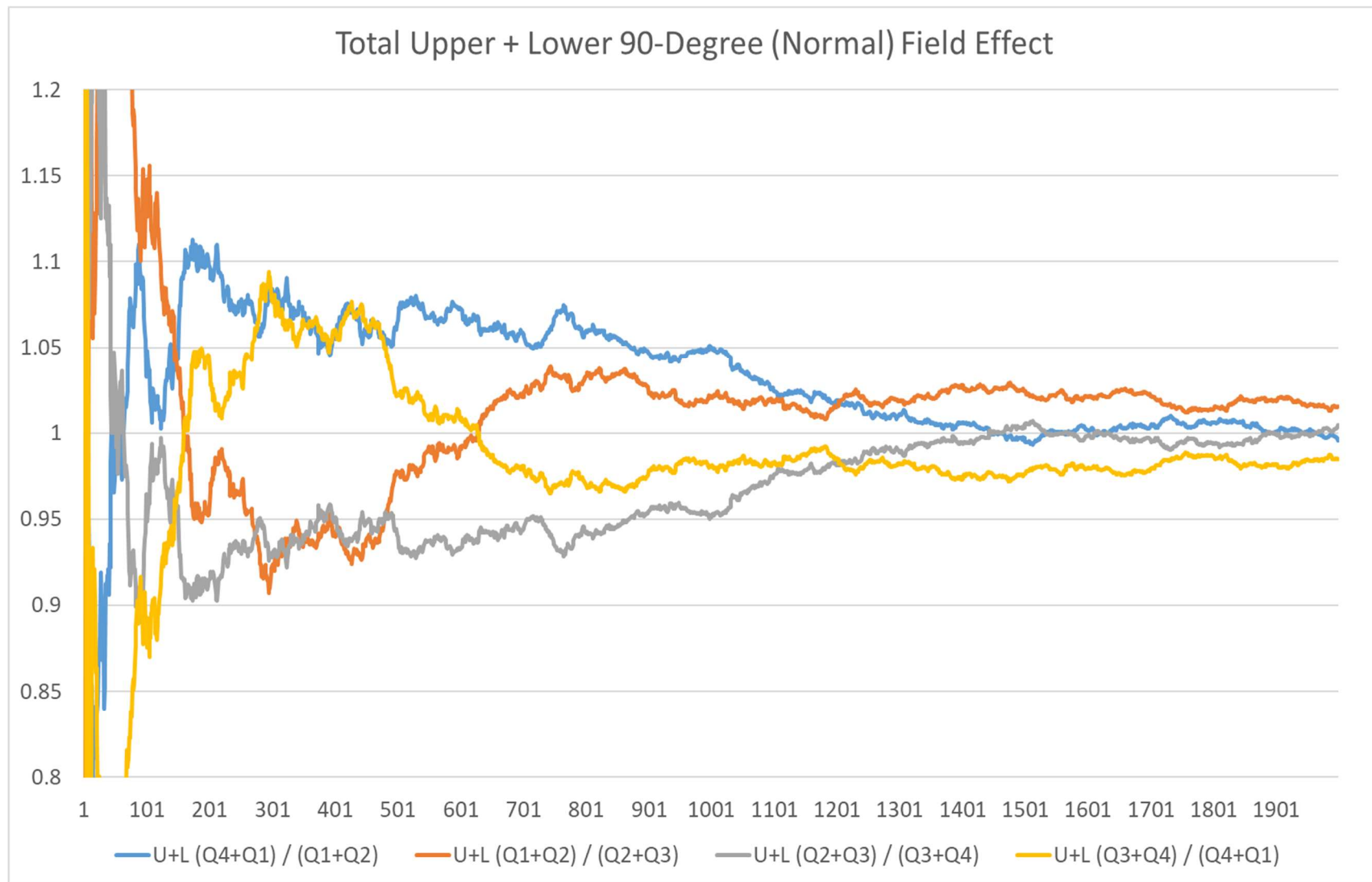
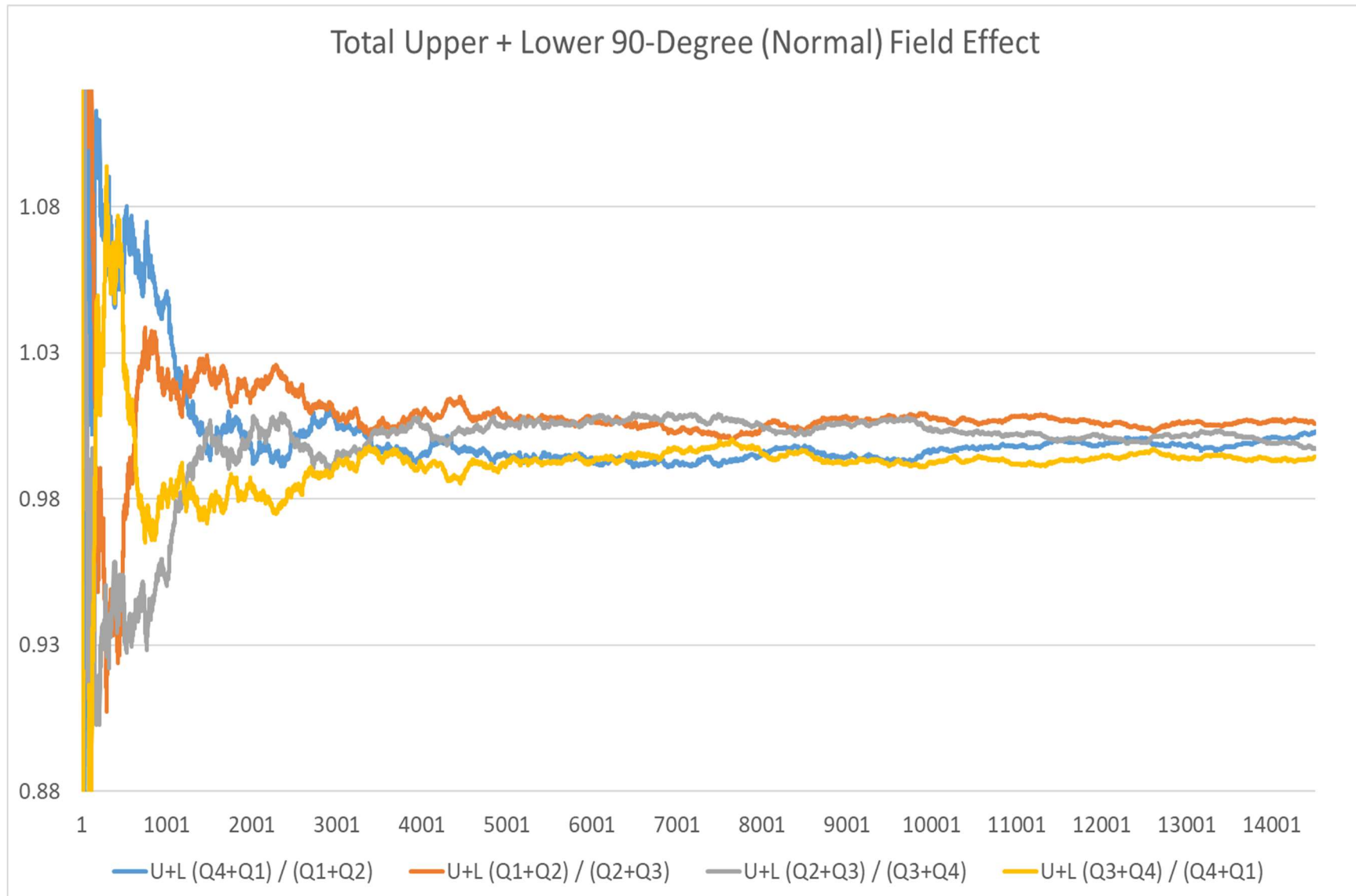


Figure A33 Sum of Upper and Lower Normal Vectors Analysis



APPENDIX B: EQUILIBRIUM AND VIBRATION GRAPHS

This Appendix is included to provide a recommended initial starting point for further harmonic and dynamical vibration analysis. The first set of graphs considers the ratio between upper and lower quadrant sines as potential offsets in a Snell's Law type of refraction relationship.

The second set of graphs are the polar views of the 90-degree (normal) vectors. These could be considered as turbulent vibrations in the flow dynamics and its ratio of error (or free space) in relation towards a pipe's circumference. The pipe size ratio is zoomed-in for the two sets of graphs (coils 251-4,000 and 3,000-9,000) to show that the direction of the vibration repeats at a tighter tolerance and frequency. Normalized flows use the changing offset ratios. Repeated lower plane vibrations are also documented to show potential lower plane alignment with the outer shell magnetic field appearance of the upper plane normal vectors.

The third set of graphs are for showing the significance of the rotating (arc)tangent, where the moving forward edges are considered equivalent to the sine and trailing edges are cosine. The moving tangent shows a long-term equilibrium of $6z$ distribution using a lower plane rotating 90-degree tangent relationship as if produced by current in an electromagnetic field. The same type of equilibrium with reciprocal values is seen in the magnitude tensor products and the post zeta normal vector products from diagonals 180-degrees out of phase. Information is grouped in the following figures:

Figure B1 – B3 Snell's Laws Ratios Upper/Lower	179
Figure B4 – B12 Vibration and harmonic periodicity analysis	182
Figure B13 – B18 Arctangent versus moving arctangent rotating equilibrium.....	191
Figure B19 – B22 Normal vector tensor products (reciprocals).....	197
Figure B23 Post zeta normal vector cross products.....	201

Figure B1 Snell's Laws Ratios Upper/Lower

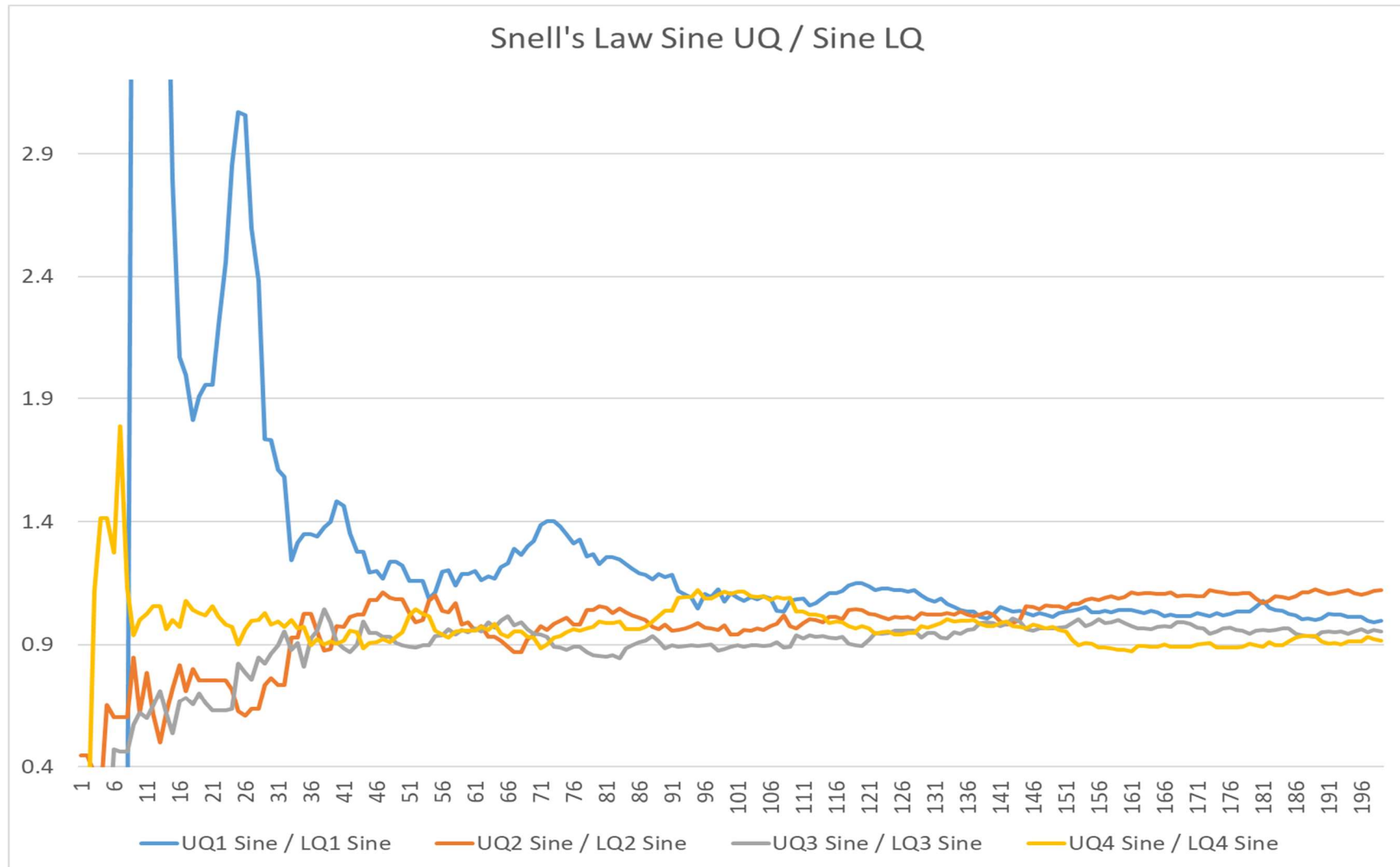


Figure B2 Snell's Laws Ratios Upper/Lower

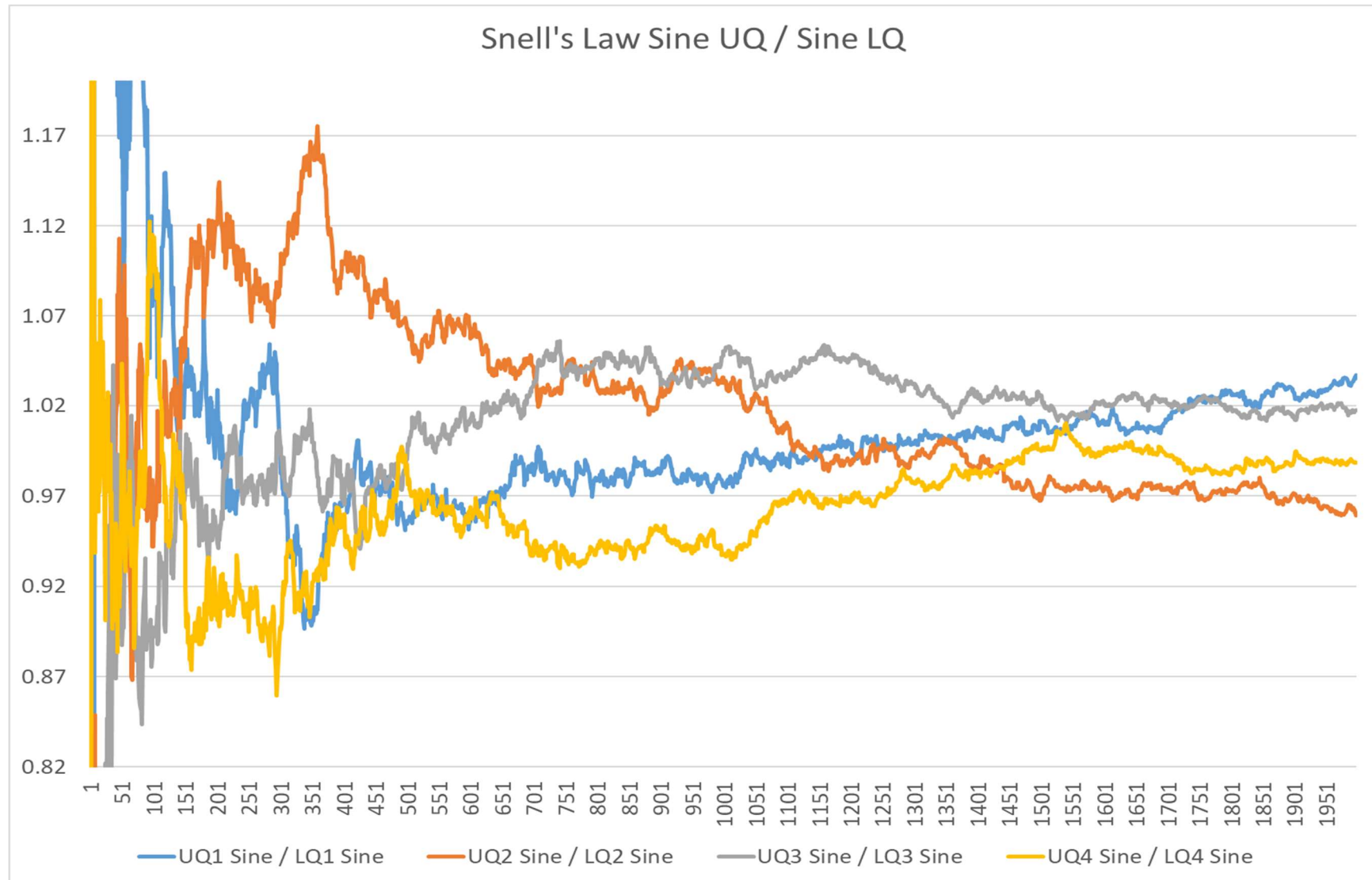


Figure B3 Snell's Laws Ratios Upper/Lower

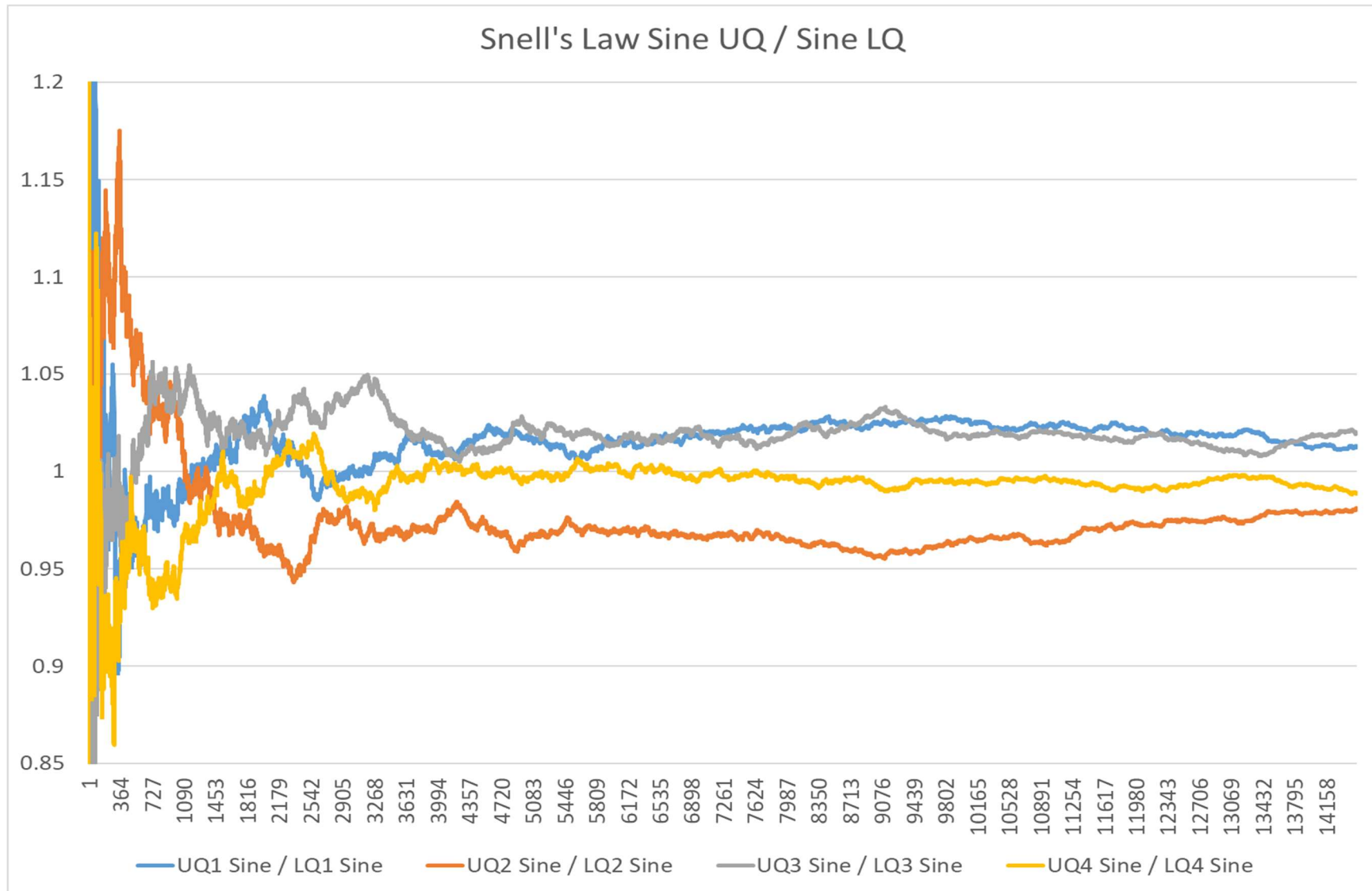


Figure B4 Vibration and harmonic periodicity analysis

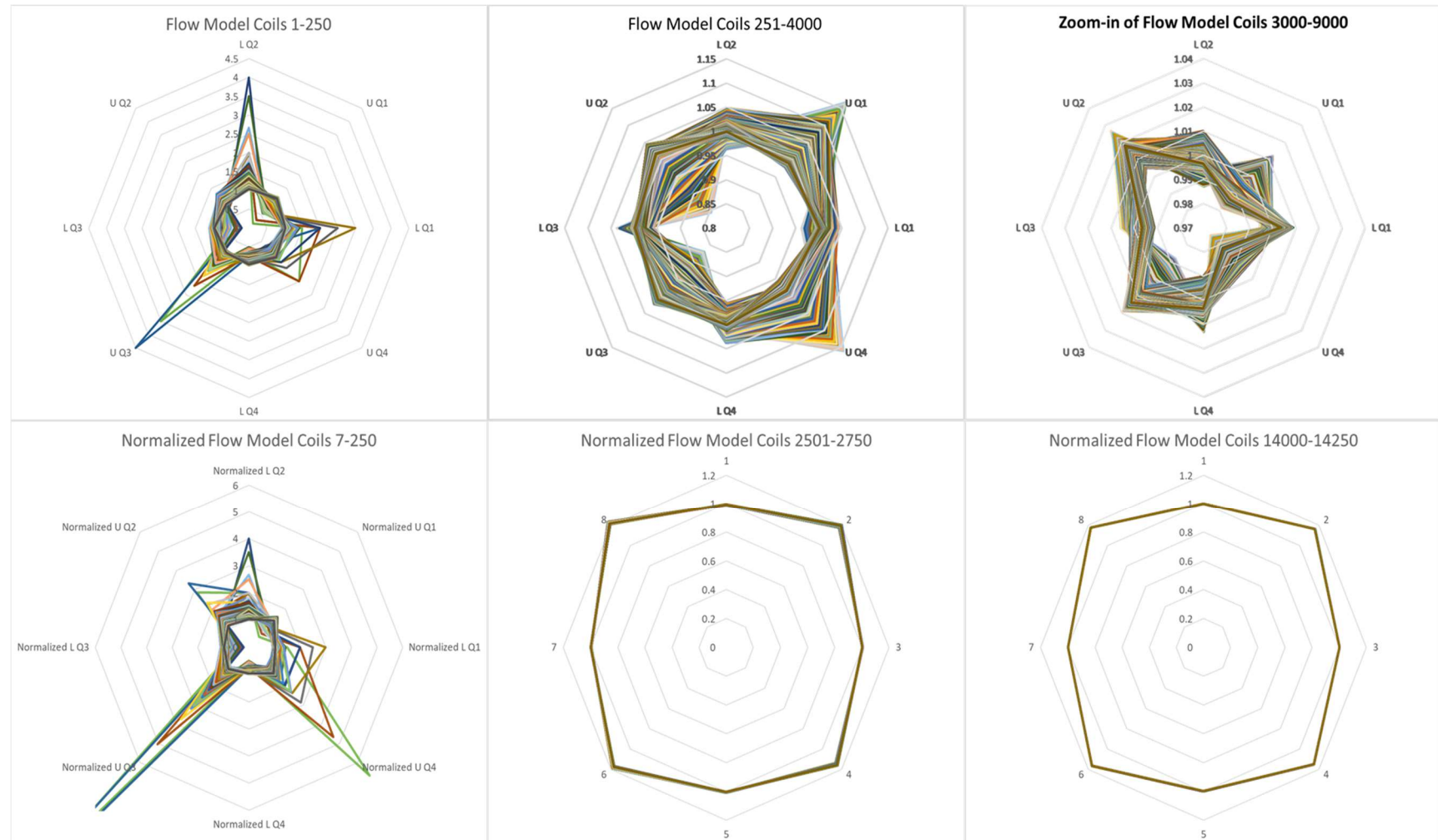


Figure B5 Vibration and harmonic periodicity analysis

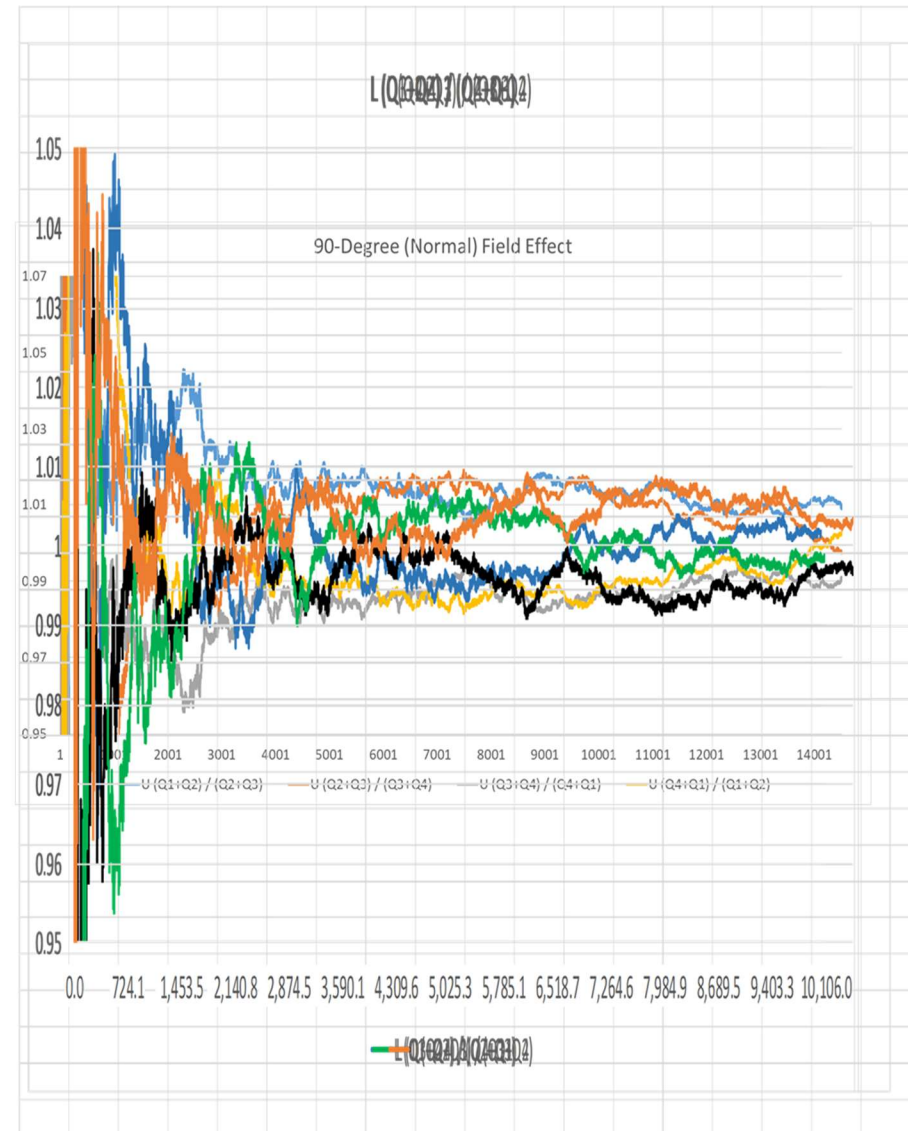
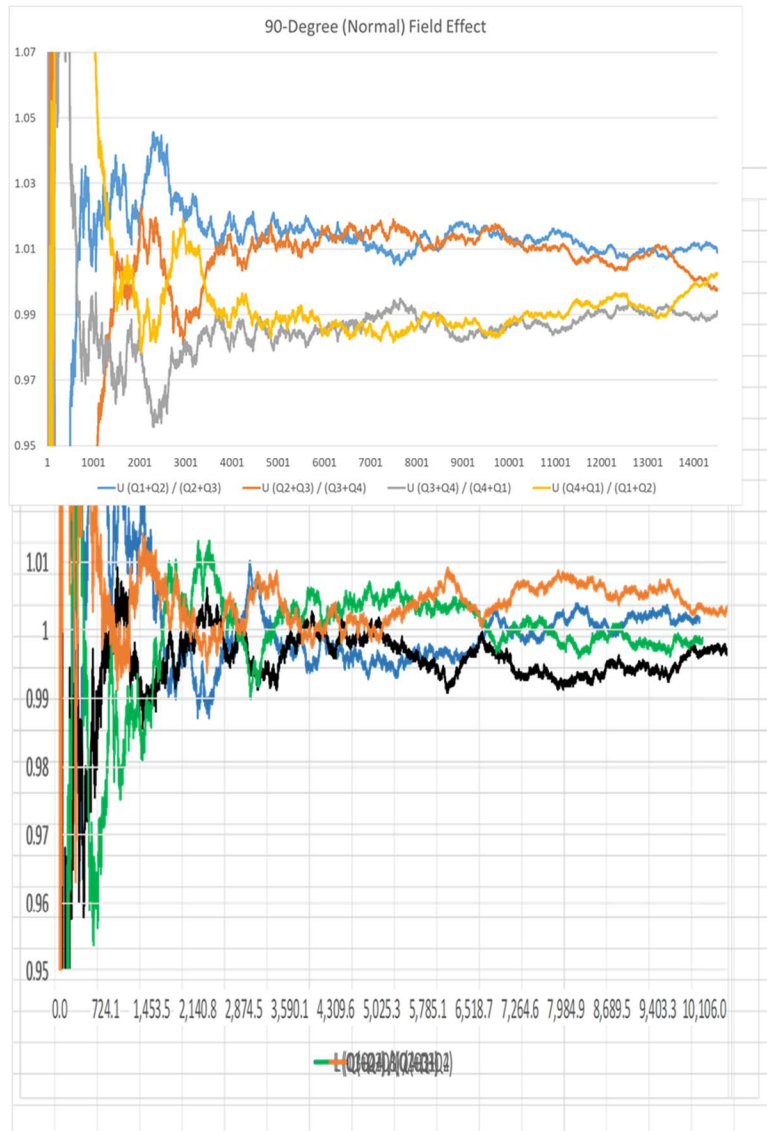


Figure B6 Vibration and harmonic periodicity analysis

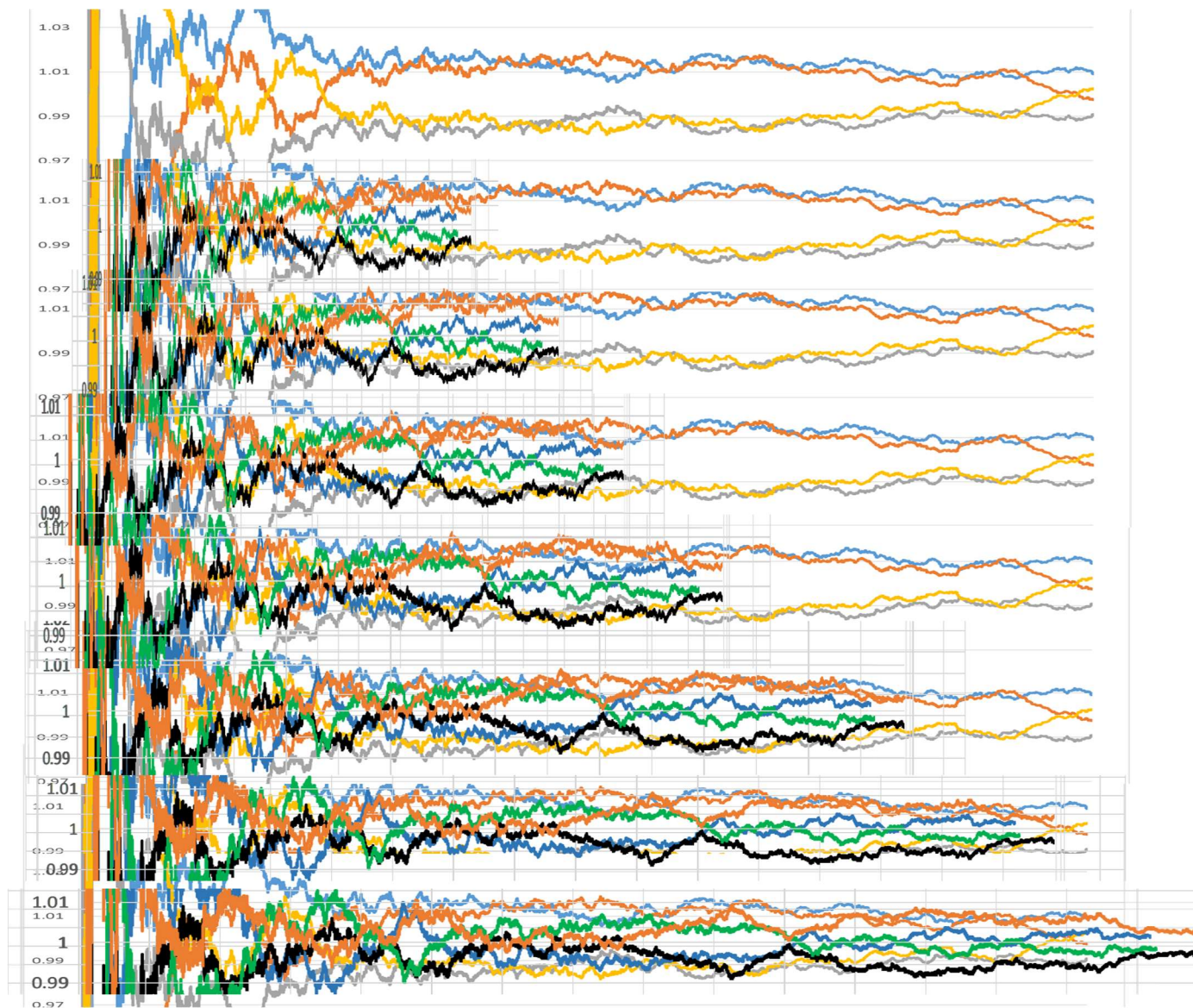


Figure B7 Vibration and harmonic periodicity analysis

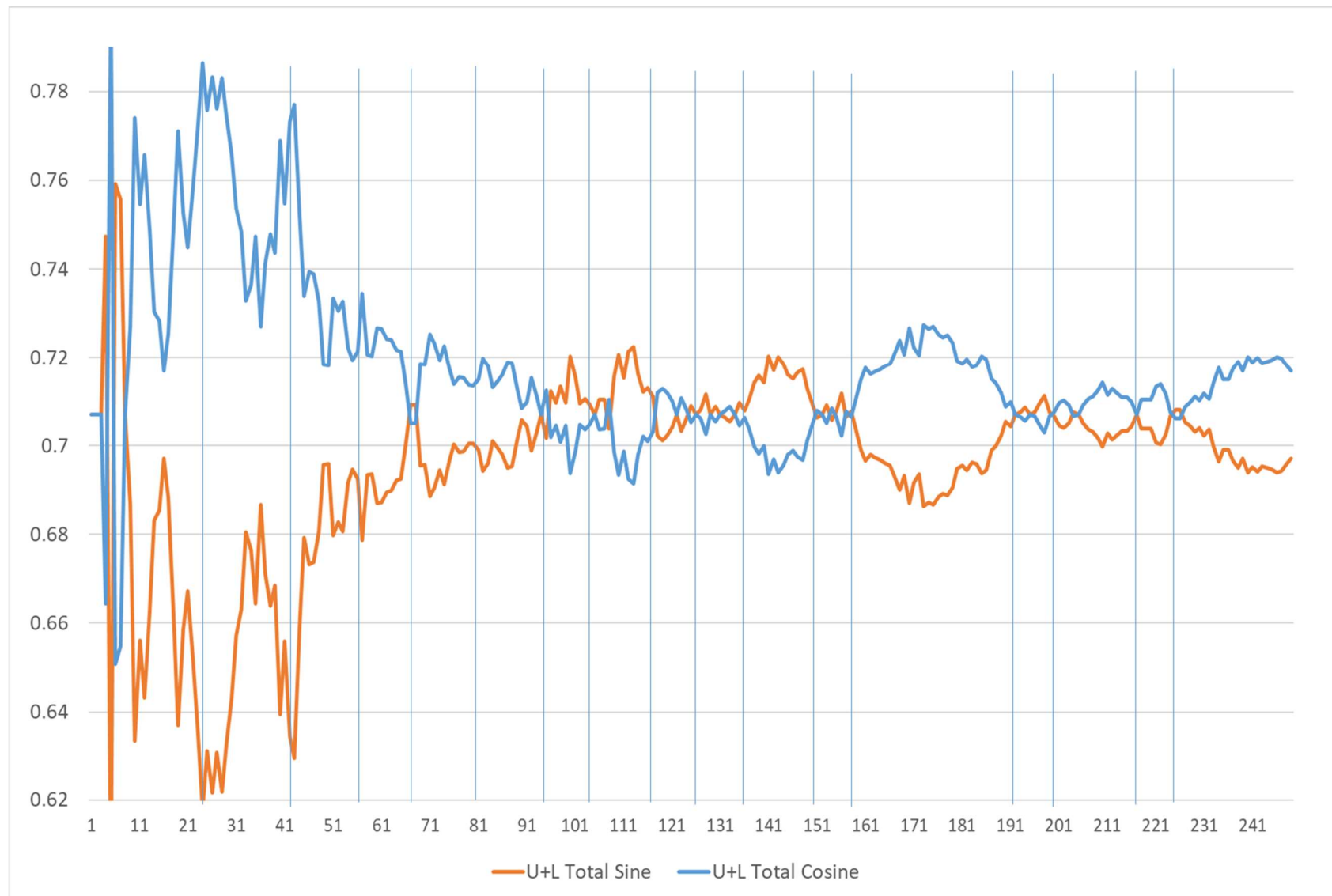


Figure B8 Vibration and harmonic periodicity analysis

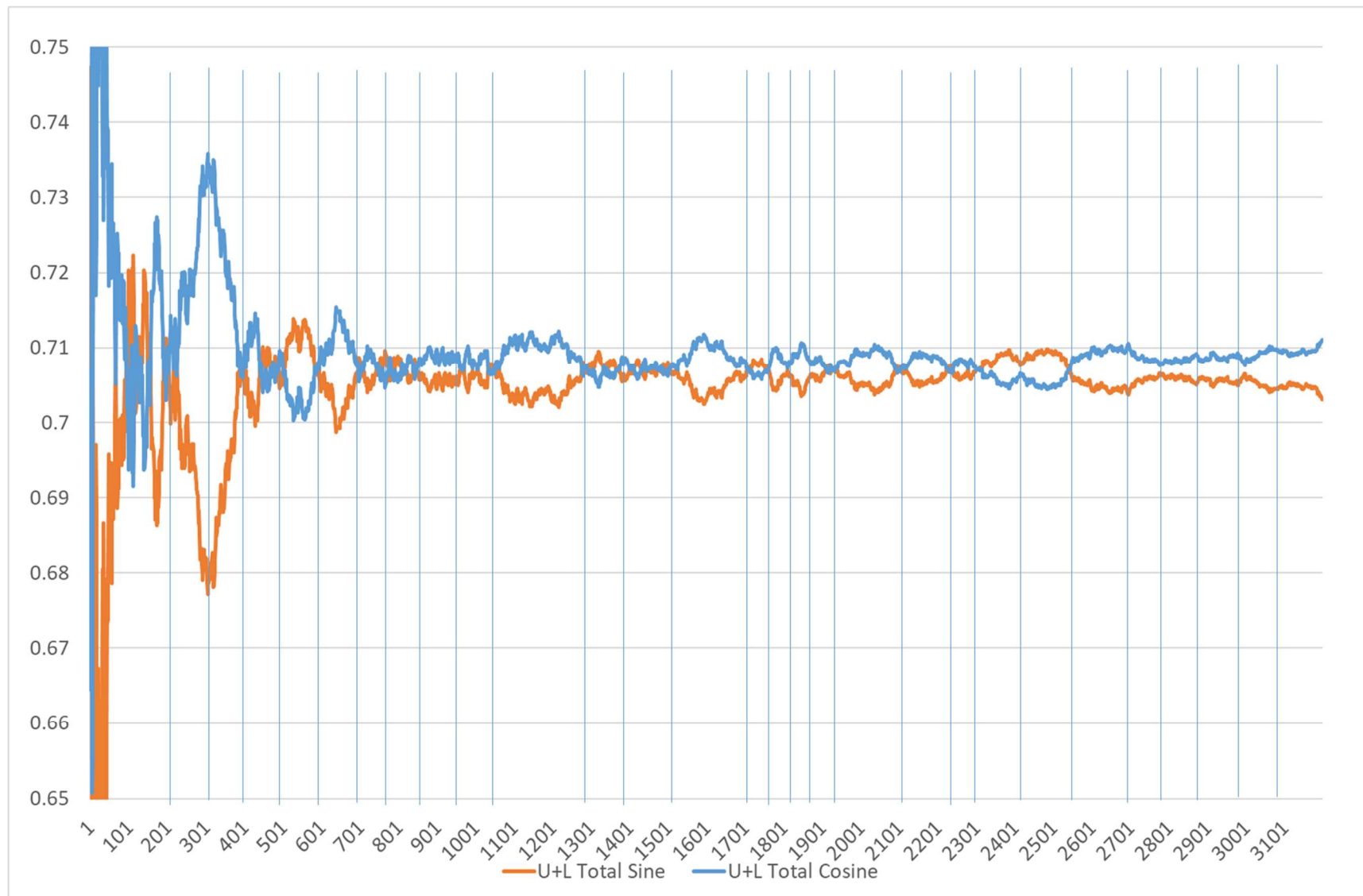


Figure B9 Vibration and harmonic periodicity analysis

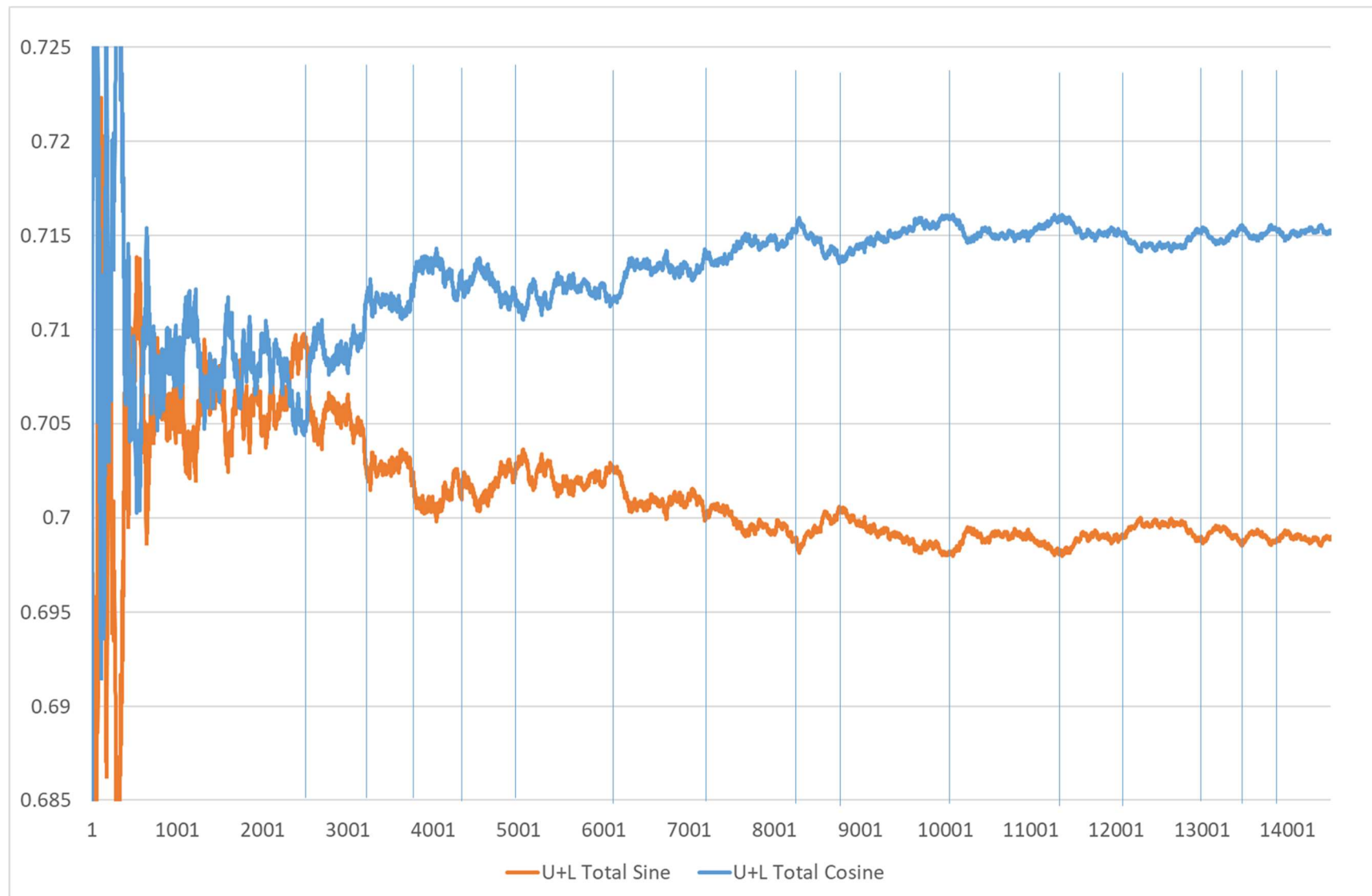


Figure B10 Vibration and harmonic periodicity analysis

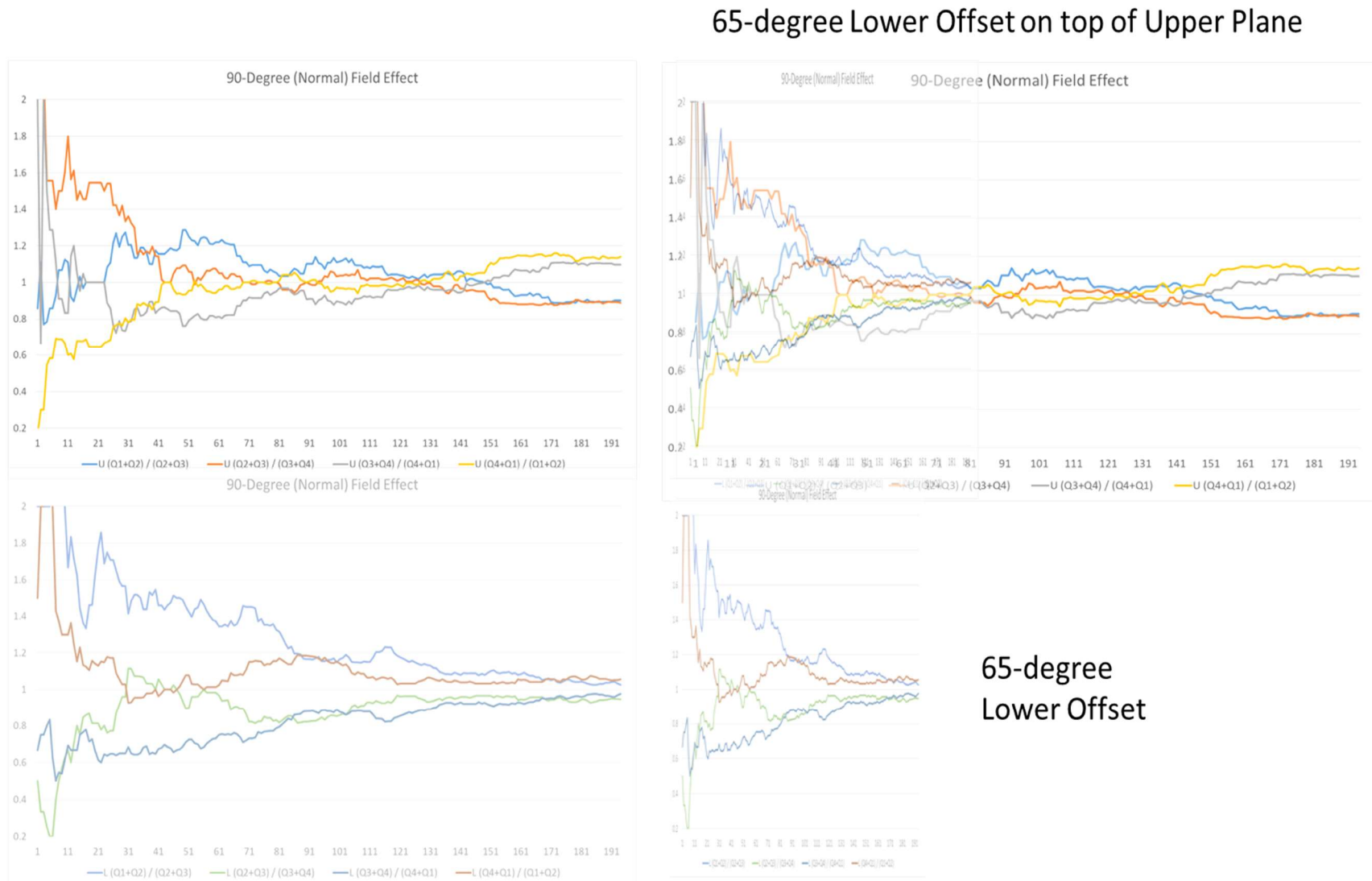
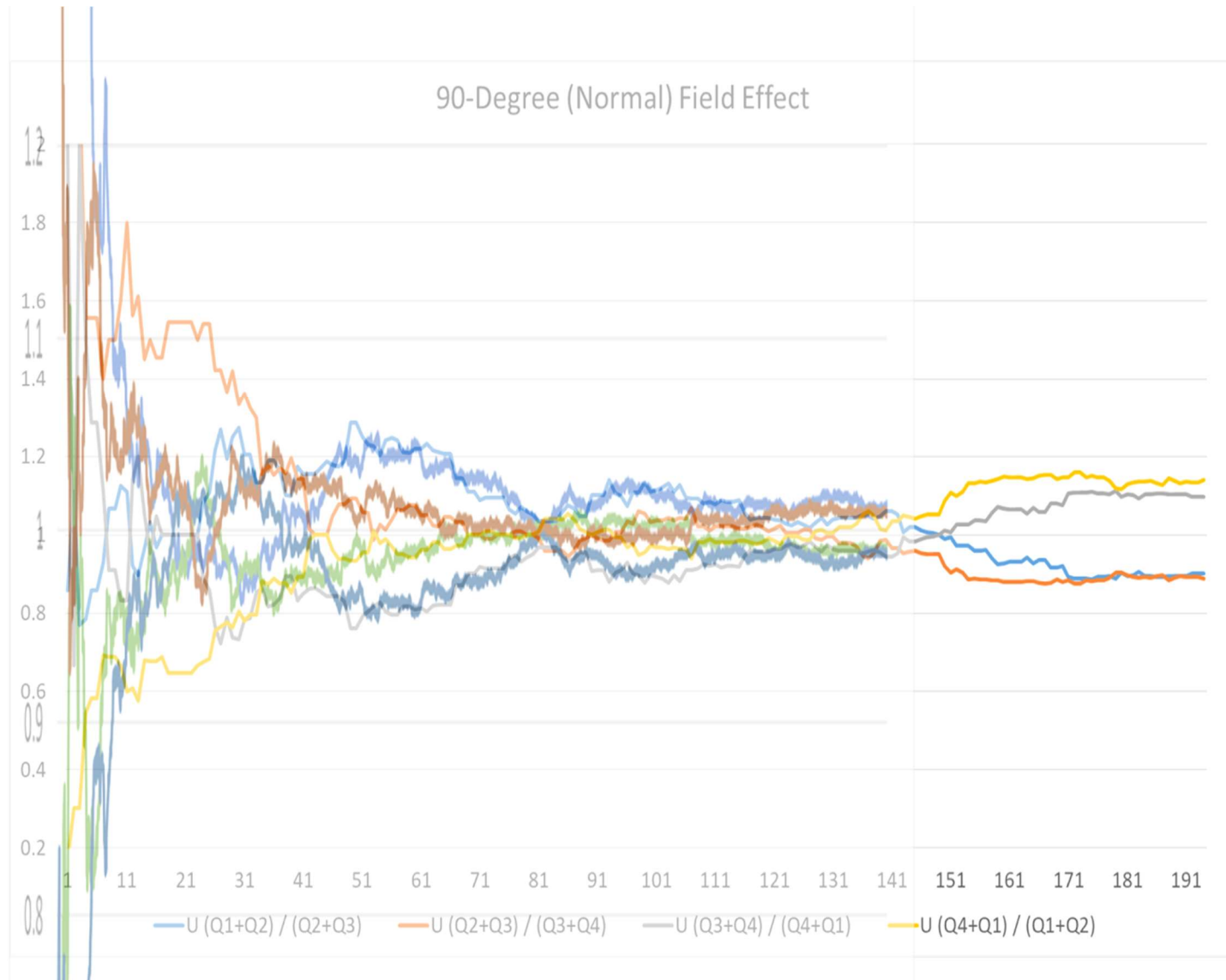


Figure B11 Vibration and harmonic periodicity analysis



45-degree
upper offset,
with $\frac{1}{2}$ width
Upper 191 at
Lower 95

Figure B12 Vibration and harmonic periodicity analysis

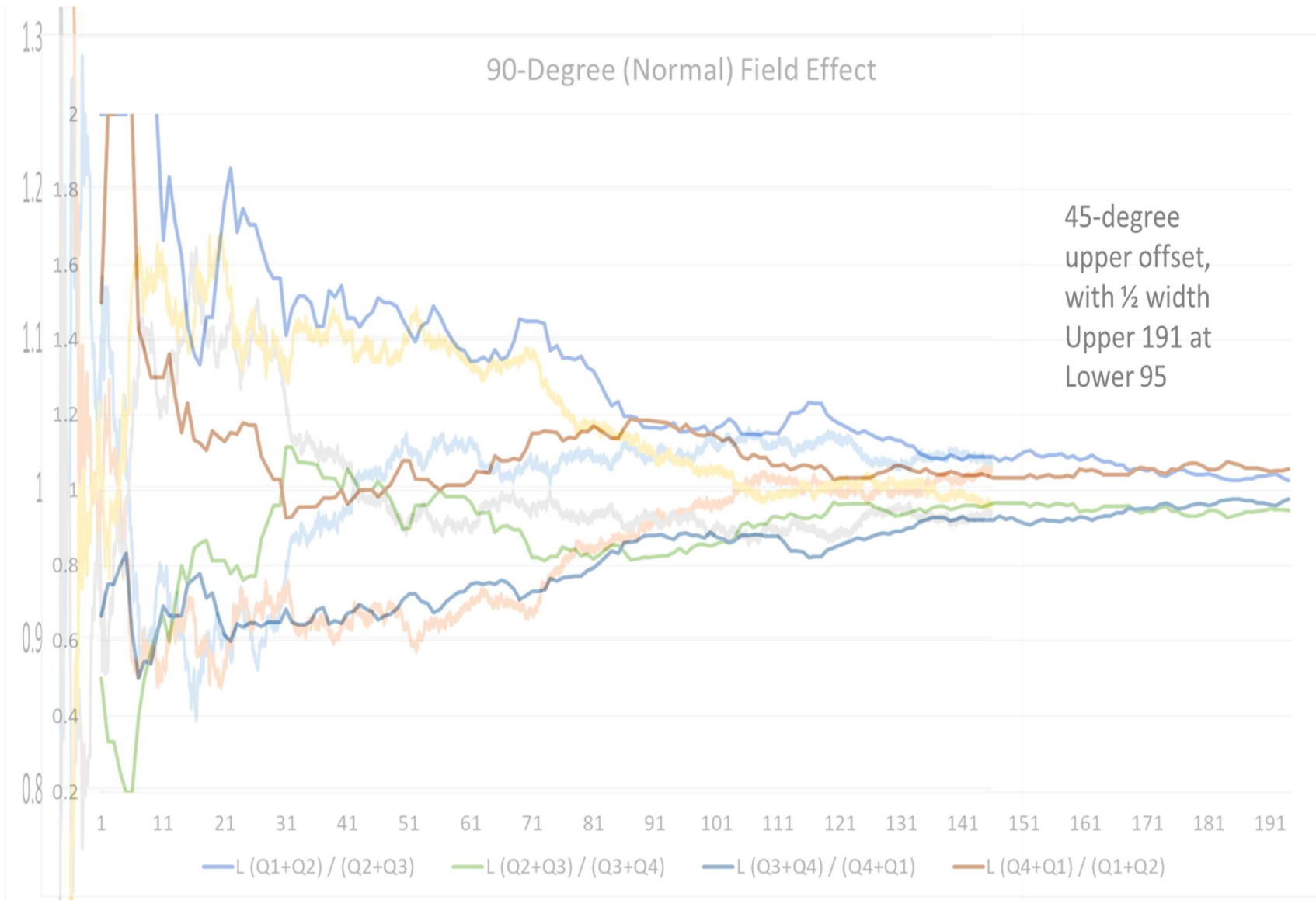


Figure B13 Arctangent versus moving arctangent rotating equilibrium

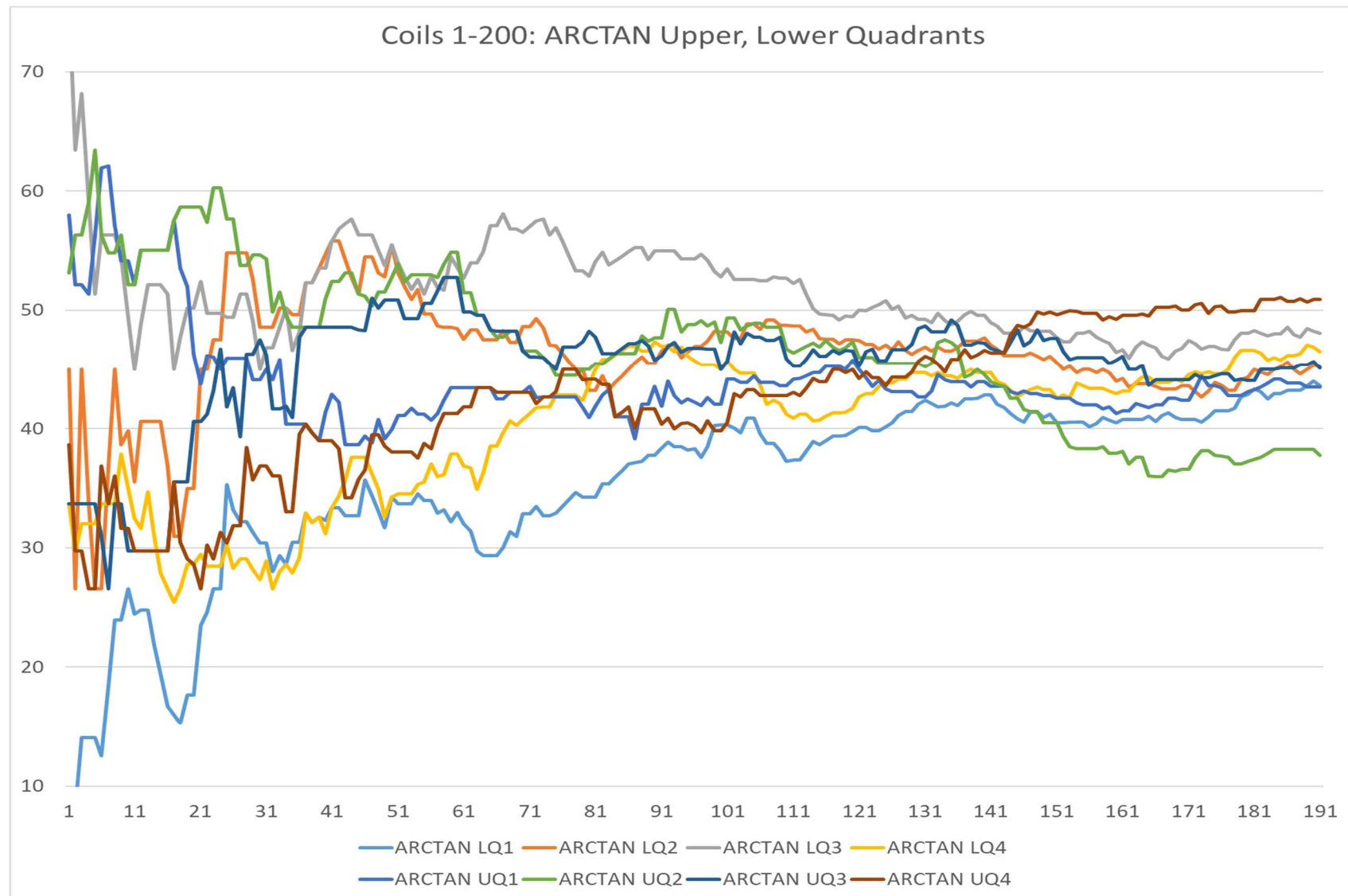


Figure B14 Arctangent versus moving arctangent rotating equilibrium

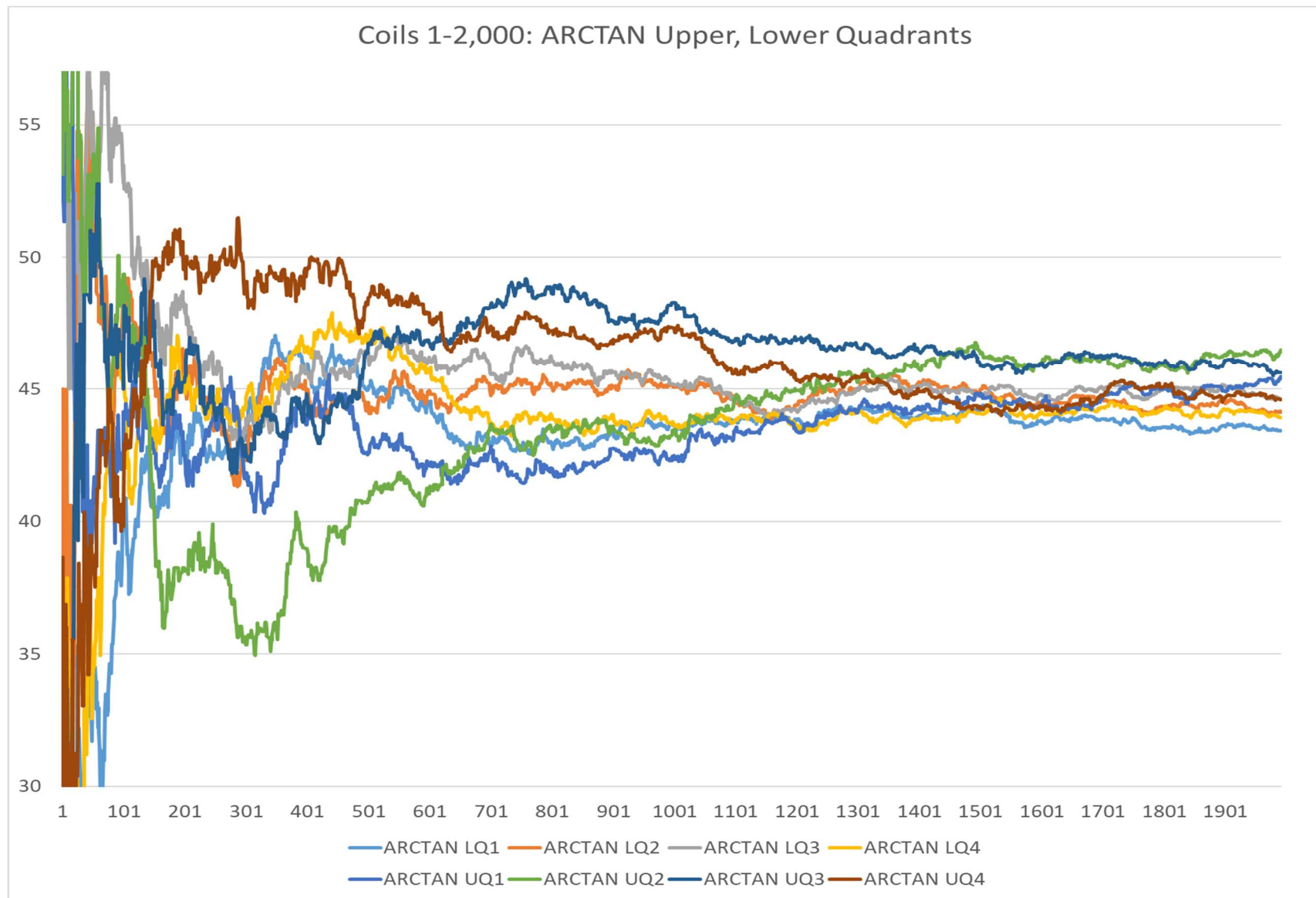


Figure B15 Arctangent versus moving arctangent rotating equilibrium

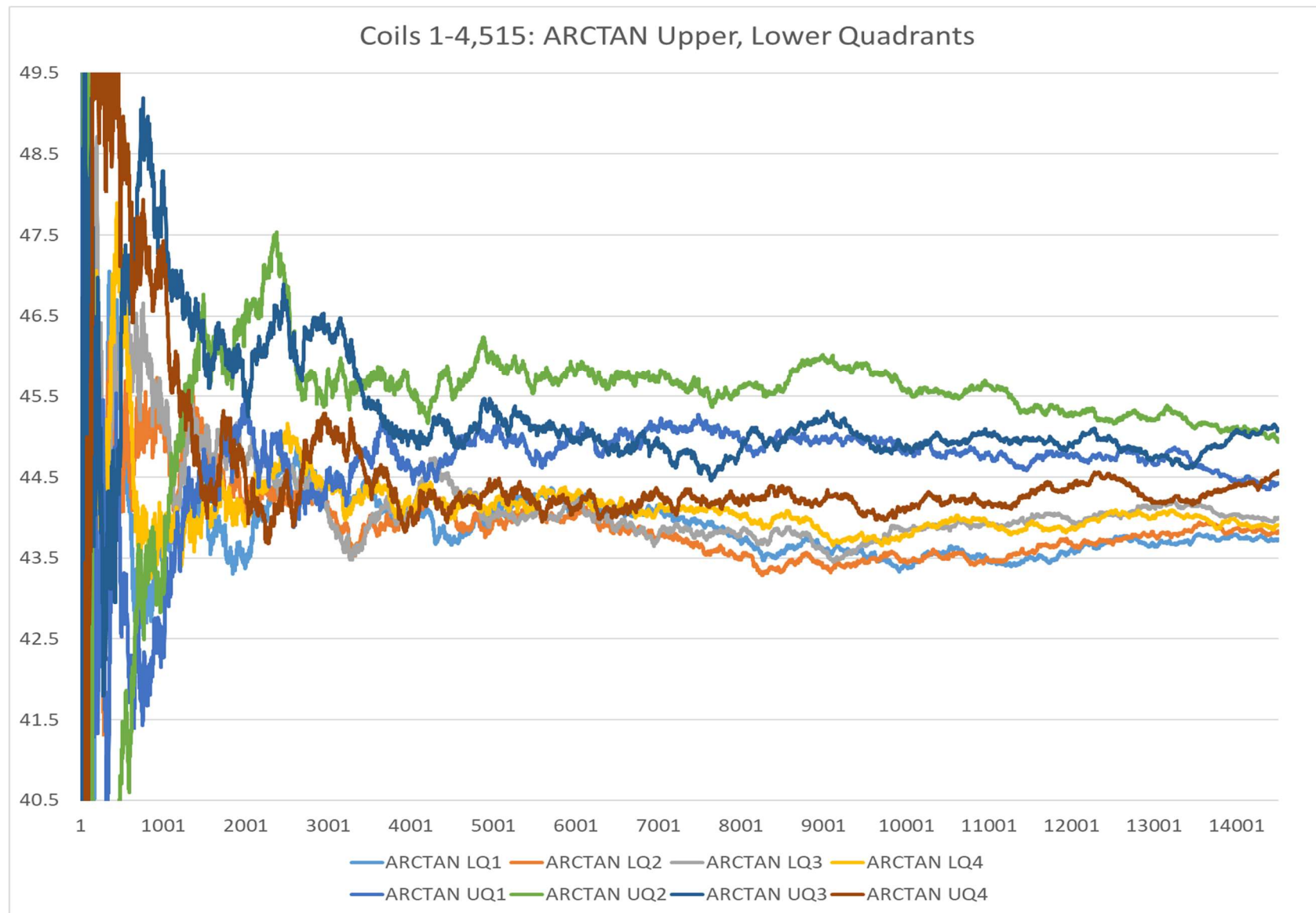


Figure B16 Arctangent versus moving arctangent rotating equilibrium

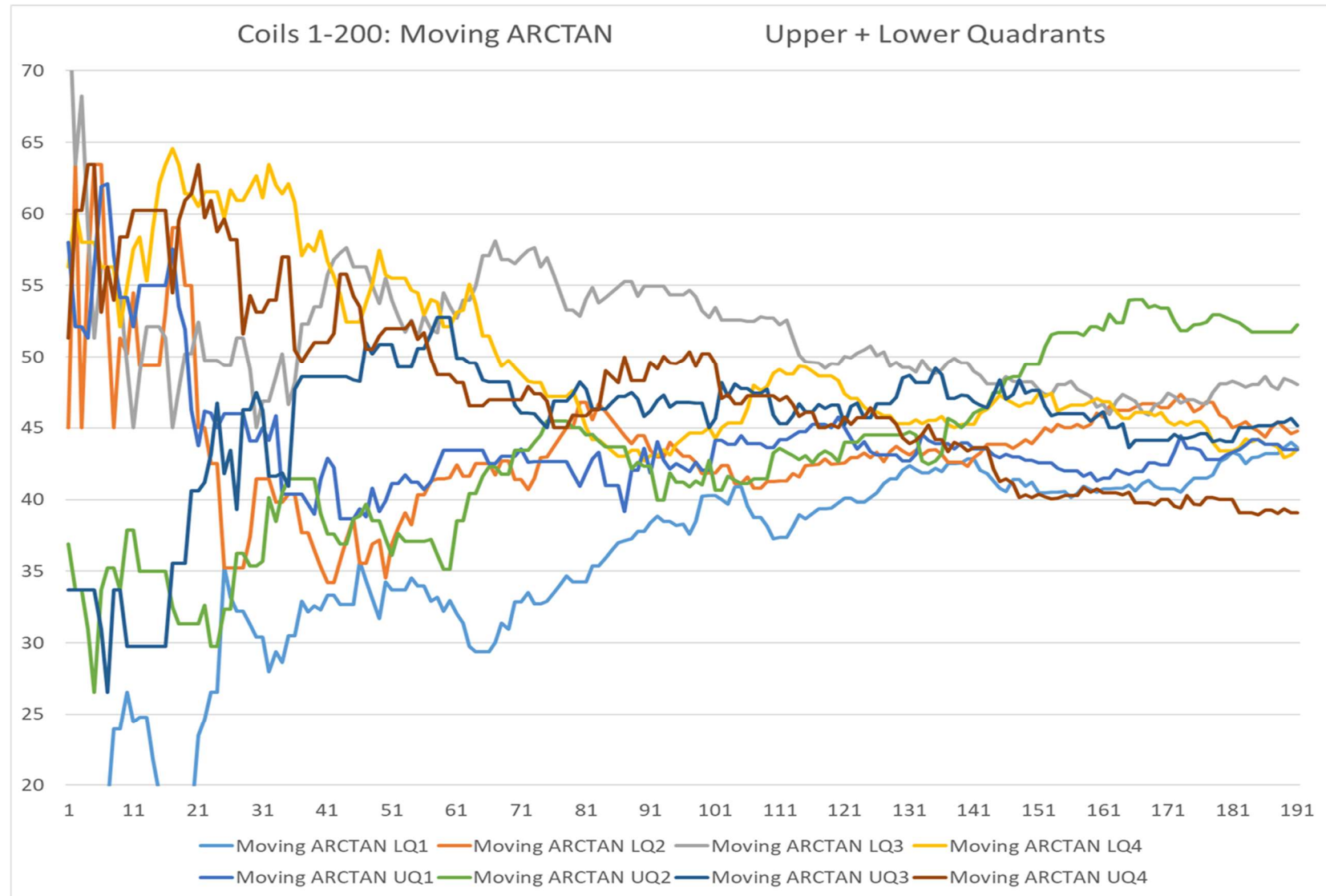


Figure B17 Arctangent versus moving arctangent rotating equilibrium

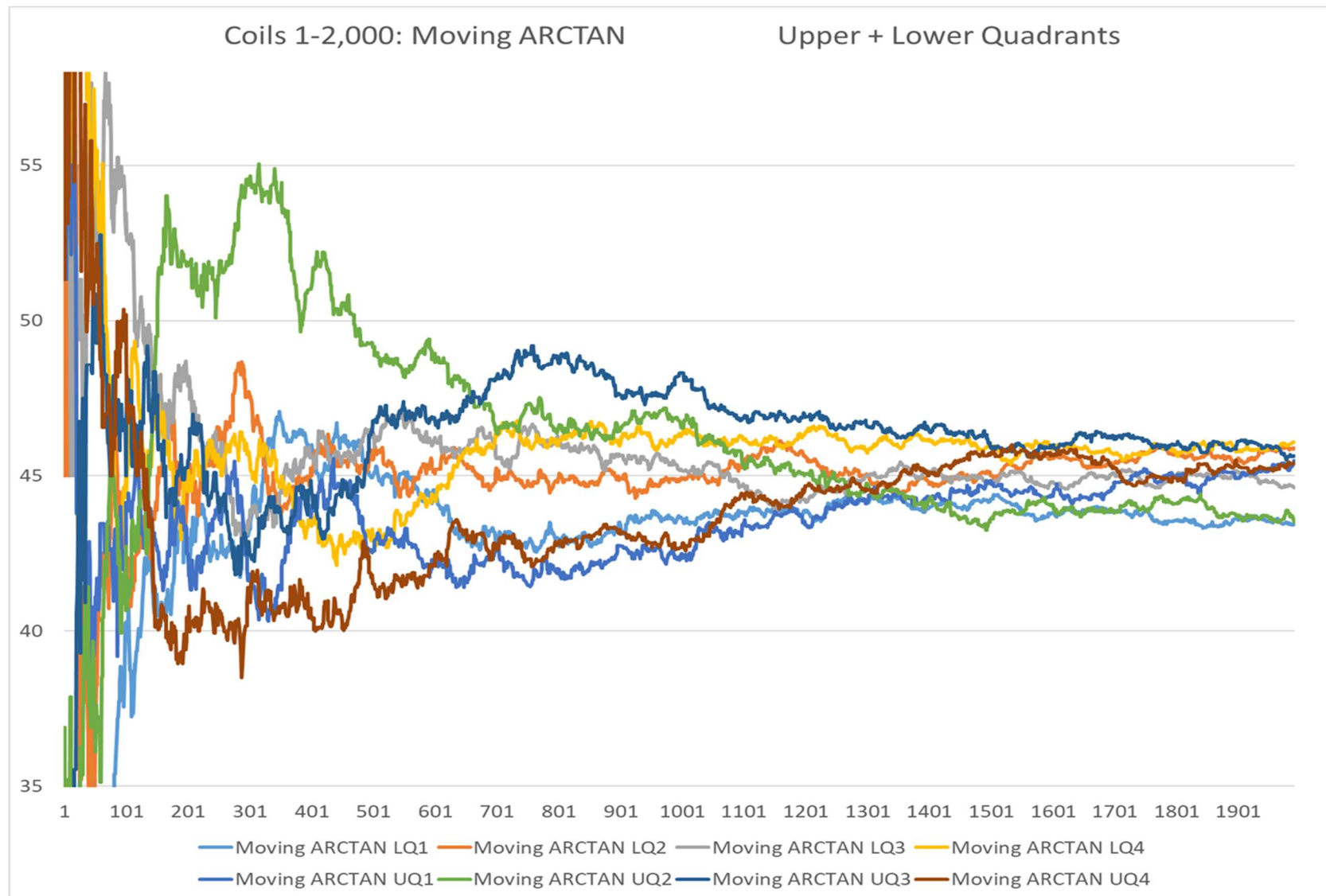


Figure B18 Arctangent versus moving arctangent rotating equilibrium

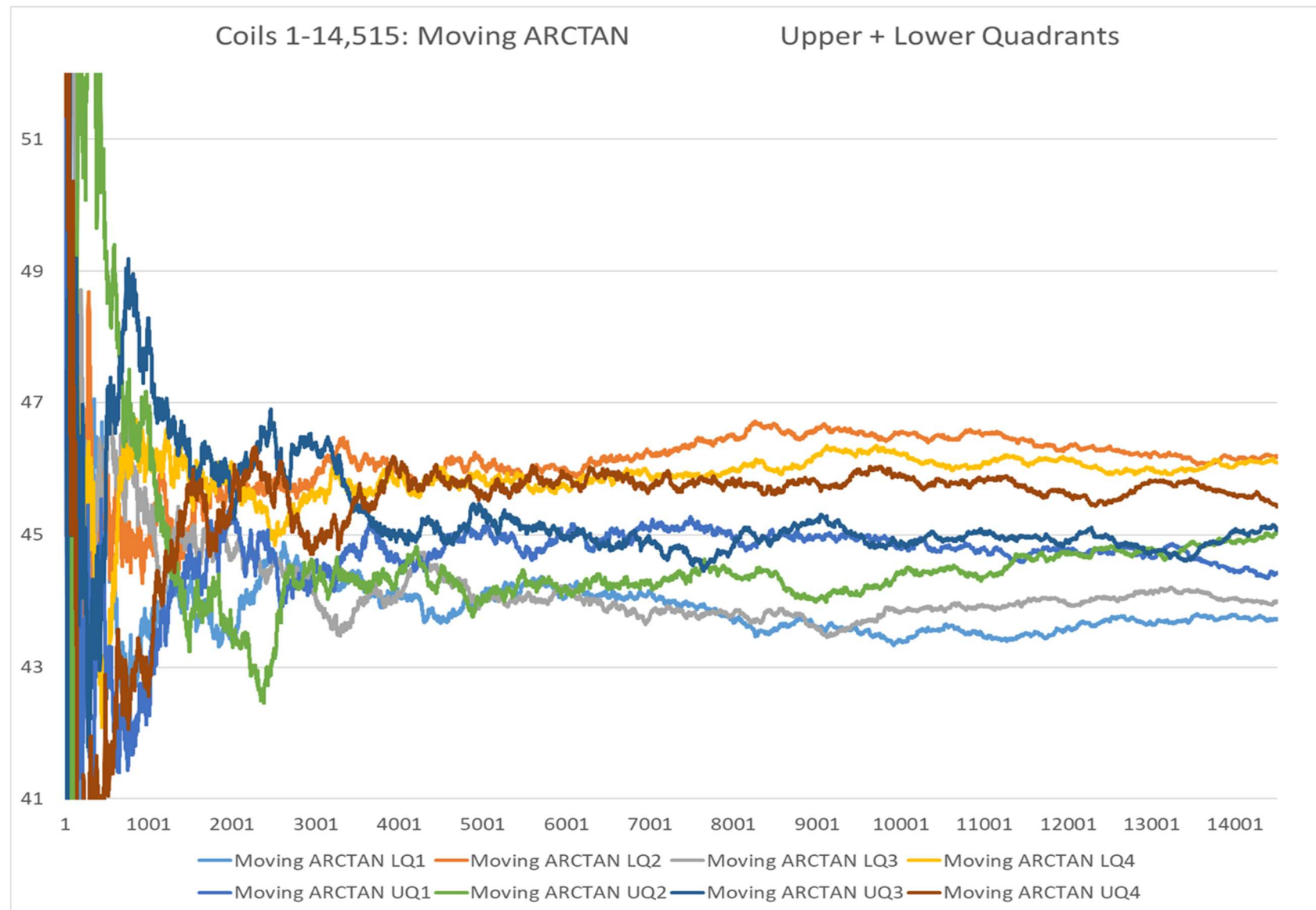


Figure B19 Normal vector tensor products (reciprocals)

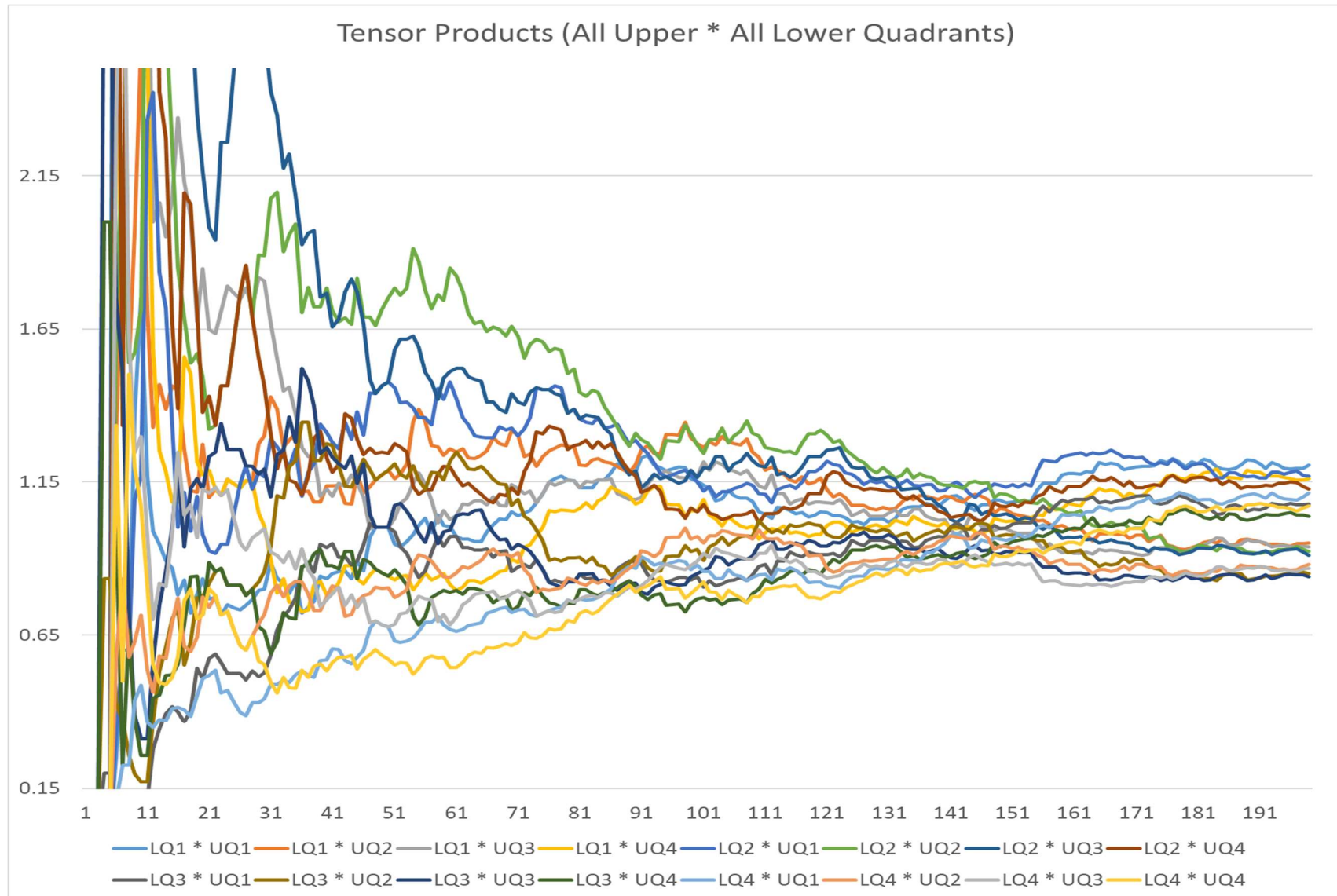


Figure B20 Normal vector tensor products (reciprocals)

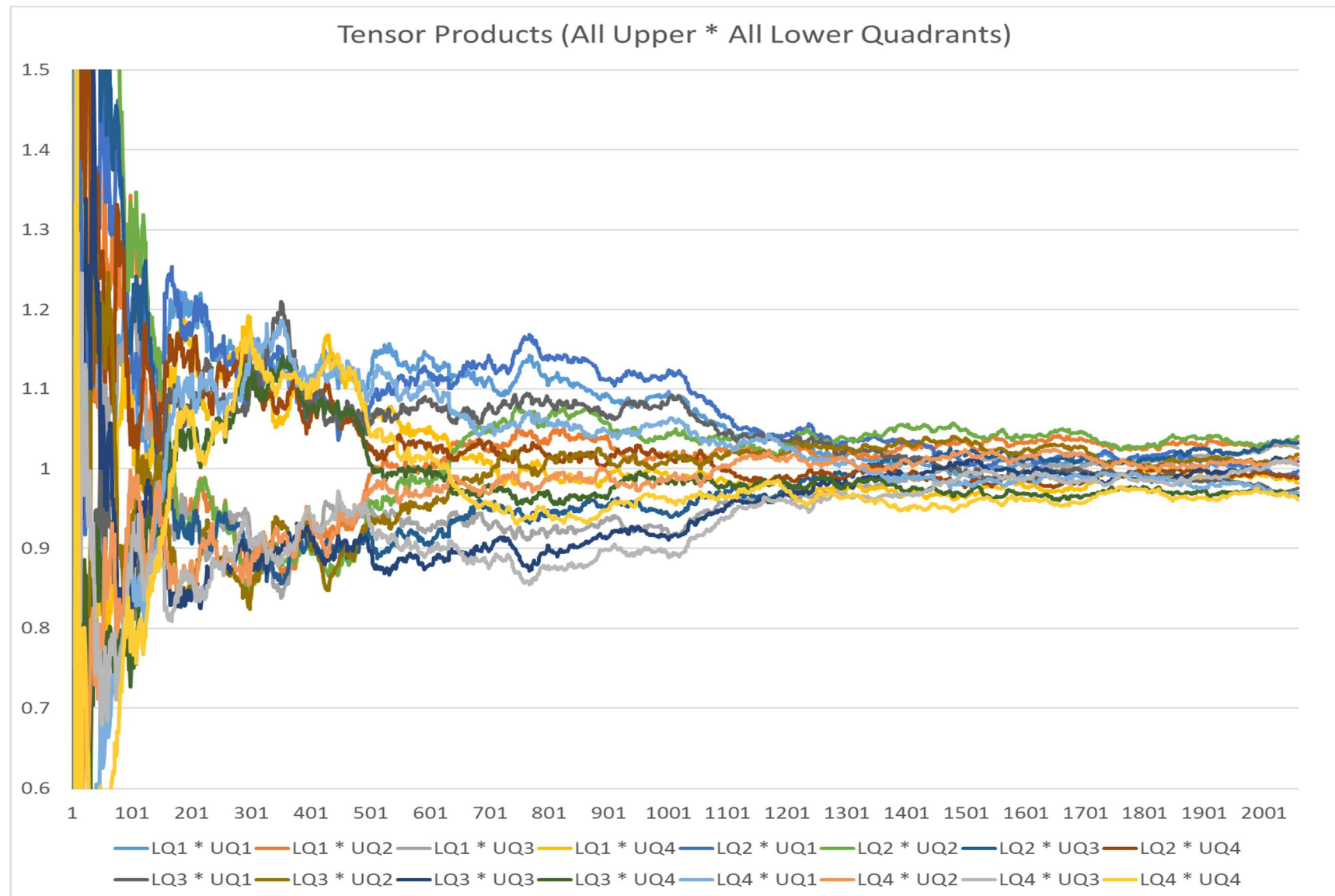


Figure B21 Normal vector tensor products (reciprocals)

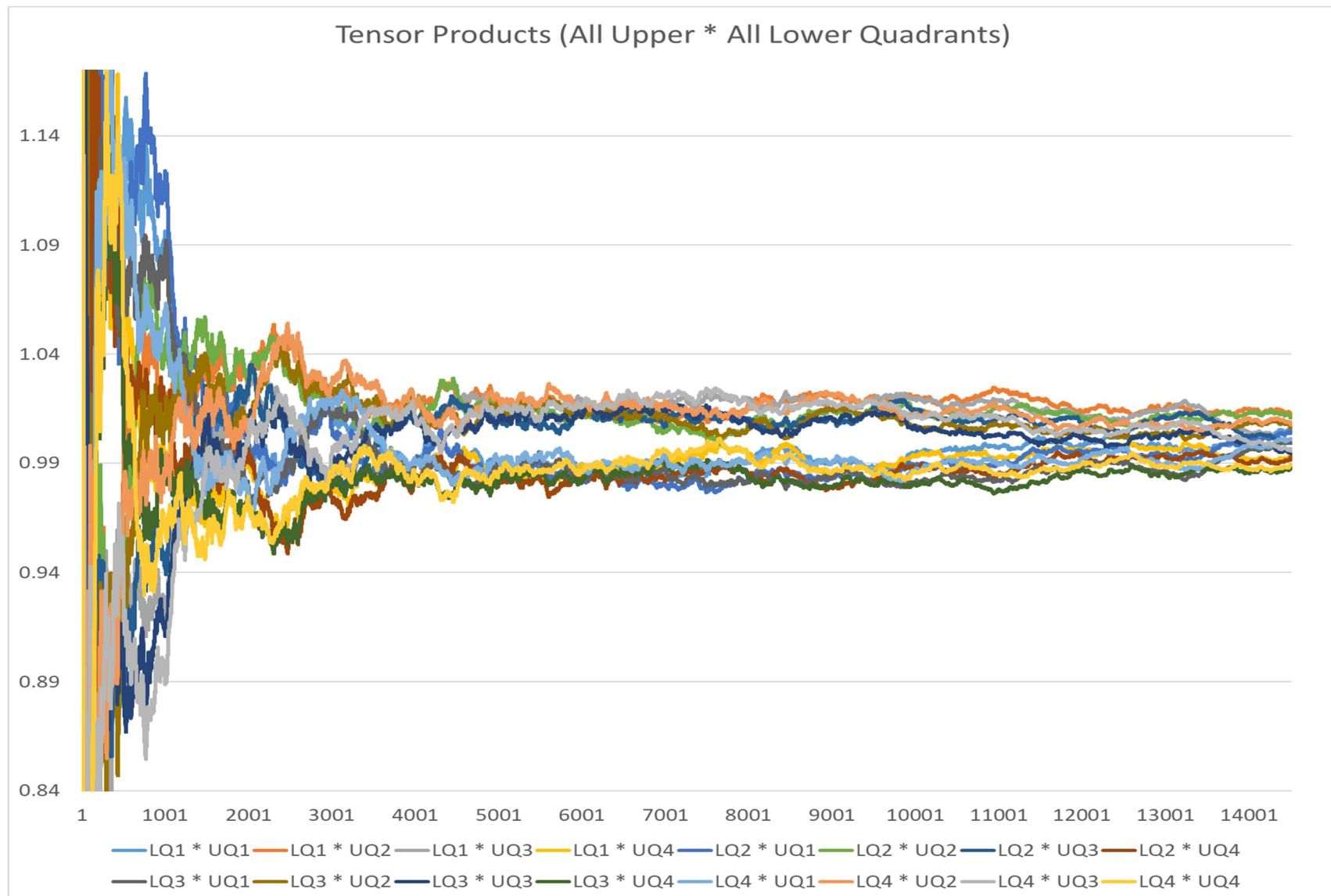


Figure B22 Normal vector tensor products (reciprocals)

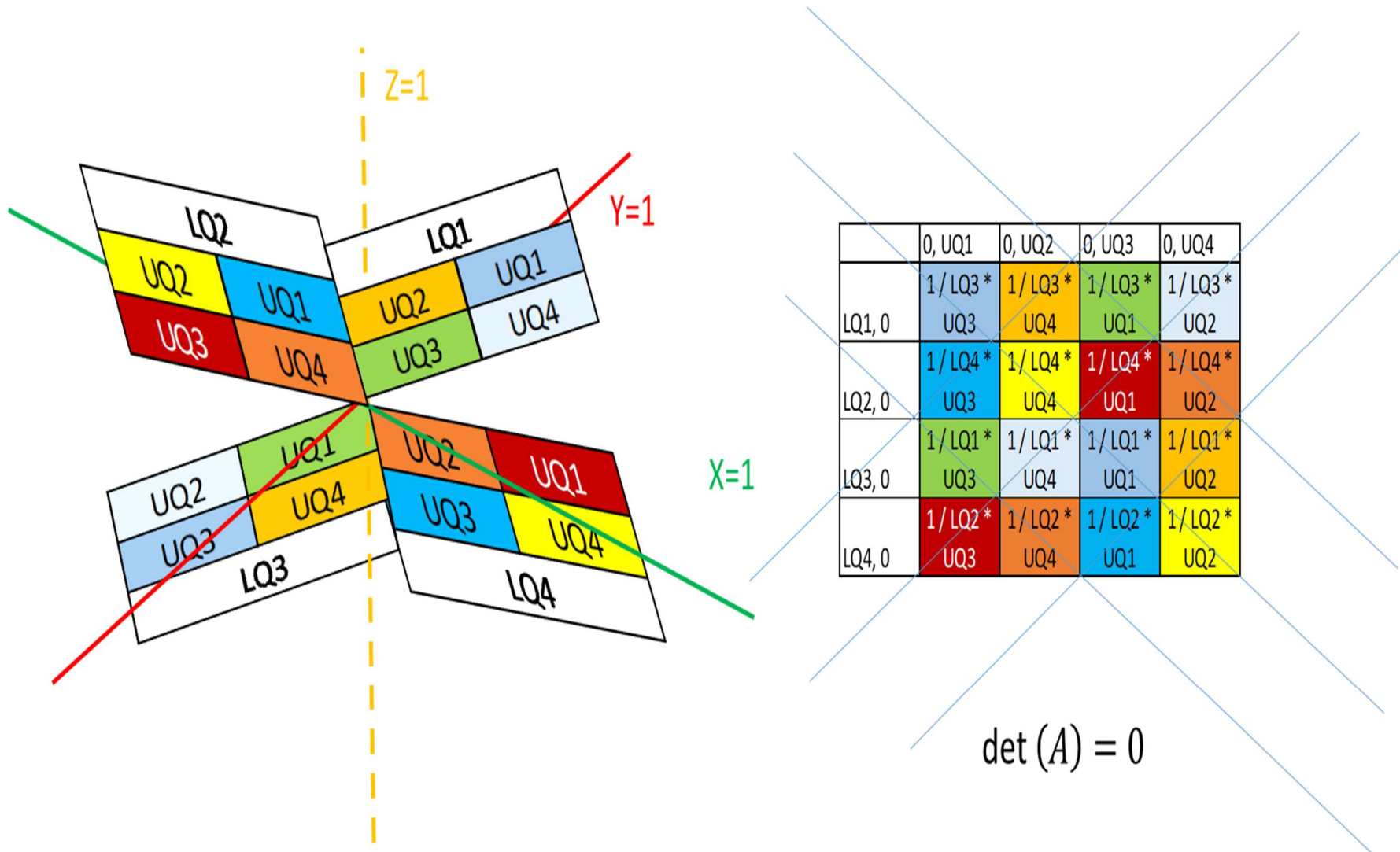
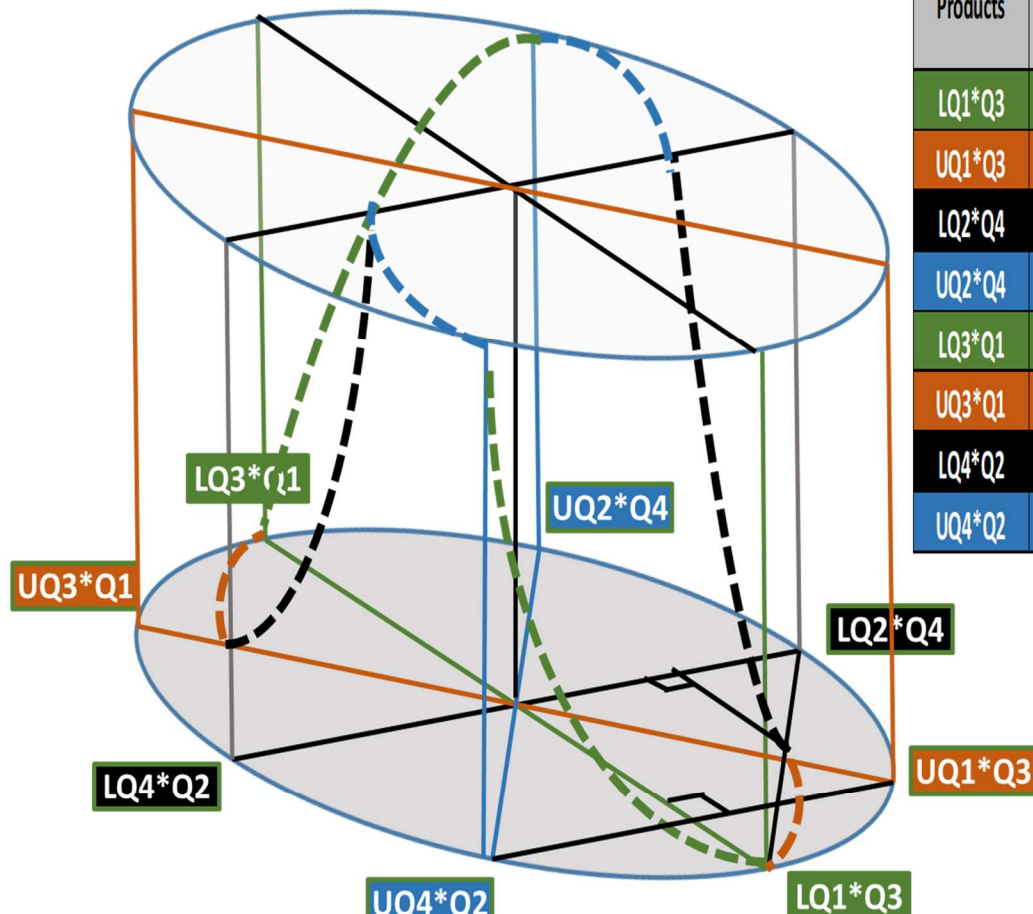
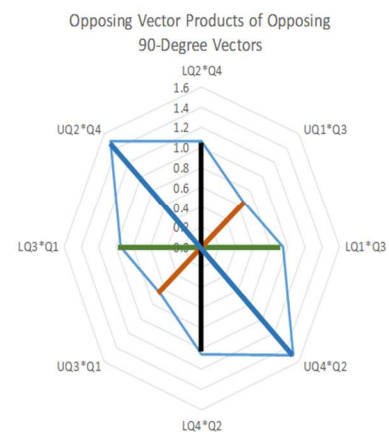


Figure B23 Post zeta normal vector cross products



Vector Products	Value	Location	Next Value from present (p)	Alternating (p, 1/p) every 45	Alternating (0.707, 1/0.707) every 90
$LQ1*Q3$	0.944	0 DEG	$p*(0.707)$	p	0.707
$UQ1*Q3$	0.666	45 DEG	$(0.707)/p$	$1/p$	0.707
$LQ2*Q4$	1.060	90 DEG	$p/(0.707)$	p	$1/0.707$
$UQ2*Q4$	1.502	135 DEG	$1/(0.707 p)$	$1/p$	$1/0.707$
$LQ3*Q1$	0.944	180 DEG	$p*(0.707)$	p	0.707
$UQ3*Q1$	0.666	225 DEG	$(0.707)/p$	$1/p$	0.707
$LQ4*Q2$	1.060	270 DEG	$p/(0.707)$	p	$1/0.707$
$UQ4*Q2$	1.502	315 DEG	$1/(0.707 p)$	$1/p$	$1/0.707$



ProQuest Number: 28968693

INFORMATION TO ALL USERS

The quality and completeness of this reproduction is dependent on the quality
and completeness of the copy made available to ProQuest.



Distributed by ProQuest LLC (2022).

Copyright of the Dissertation is held by the Author unless otherwise noted.

This work may be used in accordance with the terms of the Creative Commons license
or other rights statement, as indicated in the copyright statement or in the metadata
associated with this work. Unless otherwise specified in the copyright statement
or the metadata, all rights are reserved by the copyright holder.

This work is protected against unauthorized copying under Title 17,
United States Code and other applicable copyright laws.

Microform Edition where available © ProQuest LLC. No reproduction or digitization
of the Microform Edition is authorized without permission of ProQuest LLC.

ProQuest LLC
789 East Eisenhower Parkway
P.O. Box 1346
Ann Arbor, MI 48106 - 1346 USA